Energy, Mines and Resources Canada
Énergie, Mines et Ressources Canada

Earth Physics Branch
Direction de la physique du globe

ARCTIC GEOPHYSICAL REVIEW

Edited by J. F. Sweeney

PUBLICATIONS OF THE EARTH PHYSICS BRANCH
PUBLICATIONS DE LA DIRECTION DE LA PHYSIQUE DU GLOBE

OTTAWA, CANADA 1978 **VOLUME 45 — NO. 4**

Energy, Mines and Resources Canada
Earth Physics Branch
1 Observatory Crescent
Ottawa Canada
K1A 0Y3

Énergie, Mines et Ressources Canada
Direction de la physique du globe
1 Place de l'Observatoire
Ottawa Canada
K1A 0Y3

ARCTIC GEOPHYSICAL REVIEW

Edited by J. F. Sweeney

PUBLICATIONS OF THE EARTH PHYSICS BRANCH
PUBLICATIONS DE LA DIRECTION DE LA PHYSIQUE DU GLOBE

OTTAWA, CANADA 1978 **VOLUME 45 — NO. 4**

Available by mail from

Printing and Publishing
Supply and Services Canada,
Ottawa, Canada K1A 0S9

Earth Physics Branch,
Energy, Mines and Resources Canada,
1 Observatory Crescent,
Ottawa, Canada K1A 0Y3

or through your bookseller

Catalogue No. M70-45/4
ISBN 0-660-00711-8
ISSN 0373-4838

Price: Canada: $4.00
Other countries: $4.80

Price subject to change without notice

En vente par la poste:

Imprimerie et Édition
Approvisionnements et Services Canada,
Ottawa, Canada K1A 0S9

Direction de la physique du globe,
Énergie, Mines et Ressources Canada,
1 Place de l'Observatoire,
Ottawa, Canada K1A 0Y3

ou chez votre libraire.

N° de catalogue M70-45/4
ISBN 0-660-00711-8
ISSN 0373-4838

Prix: Canada: $4.00
Autres pays: $4.80

Prix sujet à changement sans avis préalable

TABLE OF CONTENTS

TABLE DES MATIÈRES

Arctic geophysical review — an introduction

J. F. Sweeney and G. V. Haines

Despite many attempts, a consensus of the evolution of much of the Arctic Ocean basin and adjacent landmasses (Fig. 1) has yet to emerge in Arctic literature. In particular, the age of the Amerasia Basin sea-floor is in dispute and there are widely differing views as to its mode of origin. Some workers have argued that parts of this sea-floor could be as old as late Proterozoic or early Paleozoic (Harland, 1966; Churkin, 1969; Dietz and Holden, 1970; Hall, 1970), others believe that it is nowhere older than Late Cretaceous (Vogt and Ostenso, 1970; Ostenso and Wold, 1971; Vogt et al., 1978).

Although it is generally agreed that the Nansen-Gakkel Ridge is currently an active spreading centre (Sykes, 1965; Pitman and Talwani, 1972), the location of this centre and its spreading rate history have not been well defined. The Lomonosov Ridge is considered to be a narrow slice of continental crust (Ostenso, 1962; Wilson, 1963), possibly a fault block (Dietz and Shumway, 1961), but its continental nature has never been unambiguously demonstrated. The Alpha Ridge may be a continental fragment (King et al., 1966), but the Alpha and Mendeleev Ridges have together been called a fossil sea-floor spreading centre (Hall, 1970, 1973; Vogt and Ostenso, 1970; Ostenso and Wold, 1971) and also a fossil subduction zone, an incipient island arc (Herron et al., 1974).

Part of this uncertainty, of course, results from our ignorance of many of the physiographic and morphologic details of the Arctic sea-floor because of the uneven distribution of geophysical measurements over (and within) the Arctic Ocean. Several areas, for example, the Wrangel Plain and much of the Eurasia Basin, have been investigated in reconnaissance fashion only. This limitation is unavoidable at present. A second and avoidable source of ignorance, the subject of this review, is that most of the available geophysical information from the Arctic has not been merged and interpreted on an interdisciplinary basis.

Malgré de nombreuses recherches, la documentation sur l'Arctique est encore loin de présenter un jugement unanime sur l'évolution de la majeure partie du bassin de l'océan Arctique et des masses continentales adjacentes (figure 1). En particulier, l'âge du fond marin du bassin Amérasien est très incertain, et des théories très diverses ont été proposées sur le mode de formation de celui-ci. Certaines régions du fond marin pourraient dater du Protérozoique supérieur ou du Paléozoique inférieur (Harland, 1966; Churkin, 1969; Dietz et Holden, 1970; Hall, 1970), mais certains auteurs pensent que nulle part, son âge ne dépasse le Crétacé supérieur (Vogt et Ostenso, 1970; Ostenso et Wold, 1971; Vogt et al., 1978).

Bien qu'on soit généralement de l'avis que la dorsale de Nansen-Gakkel est un centre d'expansion présentement actif (Sykes, 1965; Pitman et Talwani, 1972), on n'a pas encore pu définir avec précision son emplacement, ni l'évolution de sa vitesse d'expansion. On considère la dorsale de Lomonosov comme une tranche étroite de croûte continentale (Ostenso, 1962; Wilson, 1963), parfois comme un bloc faillé (Dietz et Shumway, 1961), mais on n'a jamais pu démontrer de façon formelle son caractère continental. On a désigné les dorsales Alpha et de Mendeleev comme un axe fossile d'expansion du fond marin (Hall, 1970, 1973; Vogt et Ostenso, 1970; Ostenso et Wold, 1971), et même comme une zone fossile de subduction - et un arc insulaire en formation (Herron et al., 1974).

Cette incertitude résulte en partie de notre ignorance d'un grand nombre des éléments morphologiques et physiographiques du fond marin de l'Arctique; cette ignorance est dû à l'éparpillement des mesures géophysiques effectuées au-dessus de l'océan Arctique (et dans l'océan Arctique). Plusieurs régions, par exemple la plaine Wrangel et une partie du bassin Eurasien, n'ont fait l'objet que de levés de reconnaissance sommaires. Il est actuellement difficile de remédier à cette lacune. Une seconde source d'ignorance, à

For these reasons and also because our knowledge of Arctic continental geology is more complete, the Amerasia Basin evolutionary discussion has, with exceptions (e.g., Hall, 1970, 1973; Vogt and Ostenso, 1970; Ostenso and Wold, 1971; Vogt et al., 1978), been based largely on what is known about geologic events within the bordering landmasses. Evolutionary ideas based on this approach are limited neither by evidence from the sea-floor itself nor by direct evidence of the past relative positions of the tectonic blocks that comprise the present Arctic region. This criticism is not fatal to the ideas in question, but such schemes will remain highly speculative until such time as, for example, detailed investigations of the Amerasia Basin sea-floor are undertaken.

The major purpose here is to assess the nature and evolution of present Arctic Basin features by means of the collection and review of existing Arctic geophysical information. The review is divided into nine subjects: bathymetry (Sobczak and Sweeney), seismicity (Wetmiller and Forsyth), heat flow (Judge and Jessop), magnetotellurics (DeLaurier), geomagnetism (Coles, Hannaford and Haines), gravity (Sobczak), lithospheric structure (Forsyth), topography of the Alpha Ridge (DeLaurier) and the evolution of the Arctic Basin (Sweeney, Irving and Geuer). A final summary paper combines and correlates the collected geophysical information and offers an analysis of Arctic Basin structure and morphology.

Earlier attempts to standardize the nomenclature of major Arctic sea-floor features appear instead to have achieved the opposite, judging from the continuing proliferation of terms in the literature. No two authors have put forward the same nomenclature (e.g., Beal et al., 1966; Hunkins, 1968; Demenitskaya and Hunkins, 1970; Hermon, 1974). Confusion centres around the choice of names for the submarine ridges and the abyssal plains. For example, the terms Fram Basin, Amundsen Basin, Nansen Basin and European Basin have all been used to identify the same Arctic abyssal area. The scheme adopted for this review is shown in figure 1 and some explanations are given below.

The term Lomonosov Ridge is in general use. Present bathymetric data show that the Alpha Cordillera/Alpha-Mendeleev Ridge is probably, in fact, two topographically distinct features. They are therefore separately referred to here as the Alpha Ridge and the Mendeleev Ridge. Mendeleev has

laquelle il est possible de remédier, comme l'indique le présent article, résulte du fait que la majeure partie de l'information géophysique sur l'Arctique n'a pas été rassemblée et interprétée d'un point de vue interdisciplinaire.

Pour ces raisons, et aussi parce que la géologie continentale arctique est beaucoup mieux connue, l'étude de l'évolution du bassin Amérasien est à quelques détails près (par exemple, Hall, 1970, 1973; Vogt et Ostenso, 1970; Ostenso et Wold, 1971; Vogt et al., 1978), largement fondée sur ce que l'on sait des événements géologiques qui ont affecté les masses continentales qui bordent ce bassin. Les théories sur l'évolution du bassin ne sont confirmées ni par l'étude du fond marin lui-même, ni par des indices directs de la position qu'occupaient autrefois les uns par rapport aux autres, les blocs tectoniques qui composent la région arctique actuelle. Cette remarque ne suffit pas à éliminer ces hypothèses, qu'une exploration détaillée du fond marin du bassin Amérasien permettra peut-être de confirmer un jour.

Notre principal objectif est ici d'évaluer la structure et l'âge du bassin Arctique actuel en recueillant et en étudiant l'information géophysique disponible sur l'Arctique. Le présent article est divisé en neuf sujets: la bathymétrie (Sobczak et Sweeney), la séismicité (Wetmiller et Forsyth), le flux thermique (Judge and Jessop), le magnétotellurisme (DeLaurier), le géomagnétisme (Coles, Hannaford et Haines), la gravimétrie (Sobczak), la structure lithosphérique (Forsyth), la topographie de la dorsale Alpha (DeLaurier), et l'évolution du bassin Arctique (Sweeney, Irving et Geuer). Un résumé final combine l'information géophysique recueillie, établit une corélation entre les données, et présente une analyse de la structure et de la morphologie actuelles du bassin arctique.

Il semble que tous les efforts déployés pour normaliser la nomenclature des principales structures du fond marin arctique n'aient pas abouti, si l'on en juge d'après la prolifération des termes employés dans la documentation sur l'Arctique. Aucun schéma terminologique adopté ne s'accorde avec un autre (par exemple, Beal et al., 1966; Hunkins, 1968; Demenitskaya et Hunkins, 1970; Hermon, 1974). C'est surtout la désignation des dorsales sous-marines et des plaines abyssales qui donne lieu à la plus grande confusion. Par exemple, les termes de bassin Fram, bassin Amundsen, bassin Nansen, et de bassin Européen ont tous été employés pour

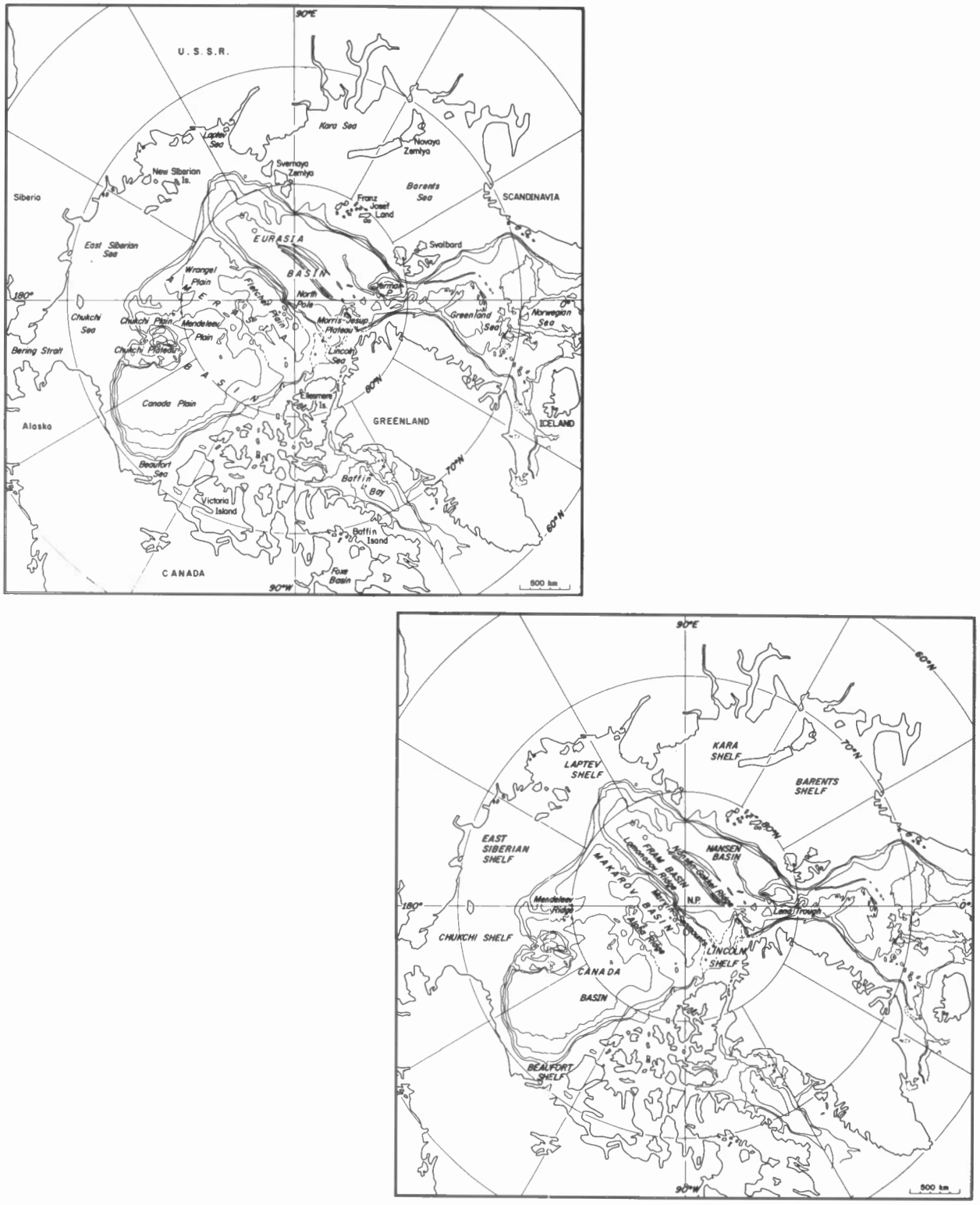

Figure 1. Arctic sea-floor nomenclature. Bathymetric contour interval 1 km. Also shown is 500 m contour.

Nomenclature des fonds marins arctiques. Intervalle des contours bathymétriques 1 km. On donne aussi les contours bathymétriques correspondant à un intervalle de 500 m.

been anglicized to Mendeleyev by some authors, probably as an aid to correct pronounciation. The original Russian form is retained here. Western and Soviet terms are combined for the name of the remaining submarine ridge, hence, Nansen-Gakkel Ridge. For the remaining sea-floor features the Beal et al. (1966) scheme of nomenclature has been used where possible largely because it appears to be the only scheme in which most of the terms have been approved by the U.S. Board of Geographic Names and the International Hydrographic Bureau. This has not guaranteed its wide acceptance in the recent literature, even by some of the authors of the original scheme! In this report several exceptions to the Beal et al. scheme are made based largely on improved bathymetric delineation of the Arctic sea-floor since 1966. The abyssal sea-floor on the Soviet side of the Nansen-Gakkel Ridge, unnamed by Beal et al. (1966) is referred to here as Nansen Basin after Ostenso (1962). That part of the Charlie Gap that is adjacent to the Canada Plain has been renamed the Mendeleev Plain by Hall (1970). The Marvin Spur has been renamed the Marvin Sea Mounts by Sobczak (1977). The term "Rise" as used by Beal et al. (1966) has been replaced by "Plateau" in accordance with definitions provided by the International Oceanographic Commission/International Hydrographic Organization subcommittee on Geographic Names and Nomenclature of Ocean Bottom Features (G.L. Johnson, personal communication, 1977). The term Markarov Basin (Beal et al., 1966) is the anglicized form of Makarov Basin. The latter Russian form, which is in general use, is adopted for this review. The Beaufort Terrace of Beal et al. (1966) was later shown (Beal, 1969) not to exist.

The polar azimuthal equidistant projection is used for the 1:7,500,000 maps (Plates 1-4) presented in this volume. This projection is convenient for locating and plotting information manually because the scale along a meridian is constant. Furthermore, the Link et al. (1960) polar azimuthal equidistant 1:7,500,000 geological map of the Arctic area was used as a guide in the earlier stages of this project.

The exact mathematical representation of the equidistant projection for an ellipsoid involves an infinite series (containing even powers of the ellipsoid's eccentricity), and where the series is truncated is determined by the required map accuracy. Haines (1975) has shown that, with an appropriate radius, a spherical earth representation is adequate for the equidistant maps presented here. The

identifier la même région abyssale de l'Arctique. Le present article choisit la nomenclature de la figure 1 avec quelques explications.

On s'accorde toutefois sur le terme de dorsale de Lomonosov. Les données bathymétriques actuelles montrent que la cordillère Alpha d'une part, et la dorsale Alpha-Mendeleev d'autre part sont probablement deux structures topographiques distinctes. Dans le présent article, celles-ci sont décrites séparement comme la dorsale Alpha et la dorsale de Mendeleev. Certains auteurs ont anglicisé le nom Mendeleev en Mendeleyev, probablement pour permettre de mieux le prononcer. Dans notre article, nous avons conservé la forme russe originale. Nous avons combiné les termes occidentaux et soviétiques, pour dénommer la dorsale sous-marine restante, c'est-à-dire la dorsale de Nansen-Gakkel. Quant aux autres structures du fond marin, nous avons adopté ici le type de nomenclature présenté par Beal et al. (1966) lorsque c'était possible, parce qu'il semble que ce soit la seule nomenclature en majeure partie approuvée par la Commission de la toponymie des Etats-Unis (U.S. Board of Geographic Names) et le Bureau hydrographique international. Toutefois, ceci n'a pas suffi à l'imposer systématiquement à la documentation récente, comme on l'a indiqué plus haut, ni même à certains auteurs de la nomenclature en question! Dans le présent rapport, plusieurs exceptions à la nomenclature de Beal et al. sont largement fondées sur une meilleure délimitation bathymétrique du fond marin Arctique depuis 1966. Le fond marin abyssal, sur le versant soviétique de la dorsale de Nansen-Gakkel, auquel Beal et al. (1966) n'ont pas attribué de nom, est appelé ici bassin Nansen, comme le propose Ostenso (1962). La partie du Passage Charlie adjacente à la plaine canadienne a été redésignée plaine Mendeleev par Hall (1970). L'éperon Marvin a été redésigné guyots de Marvin par Sobczak (1977). Le terme de dorsale, tel qu'utilisé par Beal et al. (1966), a été remplacé par le terme de "plateau", conformément aux définitions énoncées par la Commission océanographique internationale et le Sous-comité de l'Organisation hydrographique internationale chargée de la toponymie et de la nomenclature des structures du fond océanique (G.L. Johnson, communication personnelle, 1977). Le terme de bassin Markarov (Beal et al. 1966) est la forme anglicisée de bassin Makarov. Cette dernière forme, qui est la forme russe généralement utilisée, est celle que l'on a adoptée dans cet article. La Terrase de Beaufort, définie par Beal et al.

error in the 1:7,500,000 maps above latitude 60°N is less than 0.1 mm. For this representation, the map projection is given by $r = R(90 - \lambda)_{rad}$

$$\theta = \phi$$

where λ and ϕ are the geodetic latitude and longitude, and r and θ are polar coordinates on the projected map. The factor R is the spherical earth radius divided by the scale reduction (R = 852.75 mm when the scale reduction is 7,500,000) and the subscript "rad" indicates that the 90-λ must be converted from degrees to radians.

The scale of the map is true along a meridian, whereas the scale along a parallel of latitude λ is larger by a factor $(90 - \lambda)_{rad}/\sin(90 - \lambda)$. The two scales are given in the legend of each map.

The coastline was derived from a digital data-set in latitude and longitude, which was projected according to the above formulas. However, these data are considered to contain inaccuracies of up to 30 km (4 mm on the 1:7,500,000 maps) and so, for higher accuracy, geophysical features should be located by using the latitude-longitude grid rather than the coastline.

As there is no universally accepted SI convention regarding the abbreviation of the term "year", we shall use "a" (for annum) throughout this volume. Millions of years is therefore designated by Ma, and sea-floor spreading rates, for example, are designated by mm/a or cm/a.

The following individuals are thanked for their assistance in the production of this volume: M.J. Berry, M.S. Bradfield, S. Cumyn, M.R. Decosse, R.J. DeLaunais, B.J. Draper, E.J. Gelinas, J.W. Geuer, T.L. Harris, C. Lafleur, J.O. Liard, P.H. Serson, J.G. Tanner and K. Whitham.

(1966) n'existe pas, comme démontré ultérieurement (Beal, 1969).

Les cartes (à l'échelle de 1:7 500 000) inclues dans ce volume, utilisent la projection azimutale équidistante polaire. Ce type de projection est convenable pour localiser et tracer à la main des données, puisque l'échelle est constante le long d'un méridien. En plus, Link et al. (1960) utilisèrent une carte géologique ayant la même échelle et le même type de projection comme référence dans les débuts de ce projet.

L'expression mathématique précise pour la projection équidistante d'un ellipsoide comporte une série infinie (renfermant la valeur de l'eccentricité de l'ellipsoide portée aux puissances de nombres pairs); la précision désirée de la carte se fixe par la troncature de la série. Haines (1975) a démontré qu'une forme sphérique pour la terre (avec un rayon convenable) est suffisante pour les cartes de projection équidistante ci-incluses. A l'échelle de 1:7 500 000, les cartes comportent une erreur de moins de 0.1 mm pour les latitudes supérieures à 60°N. Dans cet exposé, l'équation suivante définie la projection cartographique,

$$r = R(90 - \lambda)_{rad}$$

$$\theta = \phi$$

où λ et ϕ sont les latitudes et longitudes géodésiques, et r et θ, les coordonnées polaires de la carte projetée. Le facteur R est le rayon de la terre sphérique divisé par l'échelle (R = 852.75 mm pour l'échelle 1:7 500 000) et l'indice "rad" signale que l'expression 90-λ en degré doit être convertie en radians.

L'échelle de la carte est exacte le long d'un méridien, tandis qu'elle est augmentée par le facteur $(90-\lambda)_{rad}/\sin(90-\lambda)$ le long d'un parallèle de latitude λ. La légende de chaque carte contient les deux échelles.

Un ensemble de coordonnées sous forme numérique, de latitude et longitude, projeté selon les formules ci-haut, a servi à établir le tracé du littoral. Cependant, comme ces données peuvent être inexactes d'an plus de 30 km (4 mm sur les cartes à l'échelle 1:7 500 000), on devrait utiliser la grille de latitude et de longitude au lieu du littoral, pour trouver l'emplacement de structures géophysiques si l'on désire une plus grande précision.

Puisqu'il n'existe pas de convention universelle dans le Système International en

ce qui a trait au terme "an", nous utiliserons dans cette exposé la lettre "a" (de annum). Donc, un million d'années deviennet 1 Ma, et les vitesses d'expansion sont indiquées par mm/a or cm/a, par exemple.

Nous désirons remercier les personnes suivantes qui ont contribué à l'élaboration de cet exposé: M.J. Berry, M.S. Bradfield, S. Cumyn, M.R. Decosse, R.J. DeLaunais, B.J. Draper, E.J. Gélinas, J.W. Geuer, T.L. Harris, C. Lafleur, J.O. Liard, P.H. Serson, J.G. Tanner and K. Whitham.

REFERENCES

Beal, M.A., 1969. Bathymetry and structure of the Arctic Ocean. Ph.D. thesis, Oregon State Univ., Corvallis, 187 p., Appendix.

Beal, M.A., F. Edvalson, K. Hunkins, A. Molloy and N. Ostenso, 1966. The floor of the Arctic Ocean: Geographic names. Arctic, 19, 215-219.

Churkin, M. Jr., 1969. Paleozoic tectonic history of the Arctic Basin north of Alaska. Science, 165, 549-555.

Demenitskaya, R.M., and K.L. Hunkins, 1970. Shape and structure of the Arctic Ocean. in: The Sea, v.4, Part II, ed. Arthur E. Maxwell, Wiley-Interscience, New York, 223-249.

Dietz, R.S., and J.C. Holden, 1970. Reconstruction of Pangea: Breakup and dispersion of continents, Permian to present. J. Geophys. Res., 75, 4939-4956.

Dietz, R.S., and G. Shumway, 1961. Arctic Basin geomorphology. Geol. Soc. Am. Bull., 72, 1319-1330.

Haines, G.V., 1975. The azimuthal equidistant polar projection. Earth Phys. Br., Div. of Geomag. Internal Rept., 15 p.

Hall, J.K., 1970. Arctic Ocean geophysical studies: The Alpha Cordillera and Mendeleyev Ridge. CU-2-70, Lamont-Doherty Geol. Obs., Palisades, New York, Tech. Rept. 2, 125 p.

Hall, J.K., 1973. Geophysical evidence for ancient sea-floor spreading from Alpha Cordillera and Mendeleyev Ridge. in: Arctic Geology, ed. M.G. Pitcher, Am. Assoc. Petrol. Geol. Mem. 19, 542-561.

Harland, W.B., 1966. A hypothesis of continental drift tested against the history of Greenland and Spitsbergen. Cambridge Res., No. 2, 18-22.

Hermon, Y., 1974. Topography of the Arctic Ocean. in: Marine Geology, and Oceanography of the Arctic Seas, ed. Y. Herman, Springer-Verlag, New York, 73-81.

Herron, E.M., J.F. Dewey and W.C. Pitman III, 1974. Plate tectonics model for evolution of the Arctic. Geology, 2, 377-380.

Hunkins, K.L., 1968. Geomorphic provinces of the Arctic Ocean. in: Arctic Drifting Stations, The Arctic Inst. of N. Am., Washington, D.C., 365-376.

King, E.R., I. Zietz and L.R. Alldredge, 1966. Magnetic data on the structure of the central Arctic region. Geol. Soc. Am. Bull., 77, 619-646.

Link, T.A., J.A. Downing, G.O. Raasch, A.W. Byrne, D.W.R. Wilson and A. Reece, 1960. Geological map of the Arctic. Alberta Soc. Petrol. Geol., Calgary, Alberta.

Ostenso, N.A., 1962. Geophysical investigations of the Arctic Ocean basin. Res. Rept. 4, Geophys. and Polar Res. Center, Univ. of Wis., Madison, 124 p.

Ostenso, N.A., and R.J. Wold, 1971. Aeromagnetic survey of the Arctic Ocean: Techniques and interpretations. Marine Geophys. Res., 1, 178-219.

Pitman, W.C. III, and M. Talwani, 1972. Sea-floor spreading in the North Atlantic. Geol. Soc. Am. Bull., 83, 619-646.

Sobczak, L.W., 1977. Bathymetry of the Arctic Ocean north of 85°N latitude. Tectonophysics, 42, T27-T33.

Sykes, L.R., 1965. The seismicity of the Arctic. Bull. Seism. Soc. Am., 55, 519-536.

Vogt, P.R., and N.A. Ostenso, 1970. Magnetic and gravity profiles across the Alpha Cordillera and their relation to Arctic sea-floor spreading. J. Geophys. Res., 75, 4925-4937.

Vogt, P.R., P.T. Taylor, L.C. Kovacs and G.L. Johnson, 1978. Detailed aeromagnetic investigation of the Arctic Basin. J. Geophys. Res. (in press).

Wilson, J. Tuzo, 1963. Hypothesis of the Earth's behaviour. Nature, 198, 925-929.

Bathymetry of the Arctic Ocean

L. W. Sobczak and J. F. Sweeney

ABSTRACT

A new compilation of available Arctic Ocean bathymetric data has improved the delineation of the position and morphology of several major Arctic sea-floor features shown on previously published charts. Near the North Pole the Lomonosov Ridge pinches to a width of about 20 km with very steep slopes and appears to be dextrally displaced by about 80 km. Close to North America, the Lomonosov Ridge bends toward Ellesmere Island and terminates at about 72°W. The Marvin Spur is actually a series of sea-mounts with 500 m to over 1300 m of relief that lie along the axis of the Fletcher Plain. The Alpha Ridge consists of closed (10 to 40 km wide) elongated (180 to 260 km long) troughs and ridges with over 1000 m of relief. At 140°W the Alpha Ridge appears to be sinistrally offset by about 200 km. The Alpha Ridge is physically separated from the North American polar shelf by a channel approximately 1500 m deep at the base of the continental margin. The Nansen-Gakkel Ridge rises sharply 300 m to 500 m above the adjacent abyssal plains and has an irregular crest composed of a series of peaks and troughs that appear to parallel the ridge. There is as much as 2500 m of relief between the peaks and the troughs which are usually less than 20 km wide. A central rift is over 5100 m deep in places.

RÉSUMÉ

Une nouvelle compilation des données bathymétriques existantes sur l'océan Arctique ont permis de mieux délimiter la situation et la morphologie de plusieurs structures importantes du fond marin arctique, apparaissant sur des cartes déjà publiées. Près du pôle Nord, la dorsale de Lomonsov subit un rétrécissement réduisant sa largeur à 20 km; là, elle est caractérisée par des versants très raides, et semble avoir subi un déplacement dextre d'environ 80 km. Près de l'Amérique du Nord, la dorsale de Lomonosov fait un crochet vers l'île Ellesmere, et se termine à environ 72° de longitude Ouest. L'éperon de Marvin est réellement une série de guyots qui dominent de 500 m à plus de 1 300 m les terrains environnants, et qui sont situés le long de l'axe de la plaine Fletcher. La dorsale Alpha est formée de crêtes et creux fermés (de 10 à 40 km de large), allongées (de 180 à 260 km de long), dominant de plus de 1 000 m les terrains environnants. A 140° de longitude Ouest, la dorsale Alpha semble être décalée vers la gauche d'environ 200 km. La dorsale Alpha est séparée de la plate-forme continentale polaire d'Amérique du Nord par un chenal d'environ 1 500 m de profondeur, à la base de la marge continentale. La dorsale de Nansen-Gakkel s'élève brusquement de 300 à 500 mètres au-dessus des plaines abyssales adjacentes et comporte une crête irrégulière composée d'une série de monticules et creux approximativement parallèles à la crête. Les différences de hauteur entre les monticules et les creux, dont la largeur ne dépasse généralement pas 20 km, peut atteindre 2 500 m. Le rift central a plus de 5 100 m de profondeur en certains endroits.

INTRODUCTION

Accurate and reliable bathymetric information is essential to the interpretation of geophysical data collected over the Arctic Ocean and surrounding landmasses. Although several countries have published progressively more detailed regional bathymetric maps of the Arctic Ocean (Nansen, 1904; Emery, 1949; Link et al., 1960; De Leeuw, 1967; Ritchie, 1969; Heezen and Tharp, 1975) even the most recent of these maps contain significant ambiguities in the position and morphology of major Arctic sea-floor features (Sobczak, 1977). This paper presents a new compilation of existing Arctic bathymetric data which utilizes more combined information than in previous maps (nearly 250,000 digitized water depths, about 7 million values in analog form and several thousand values taken from plotting sheets), removes speculative diagrammatic features, shows the density of control for the various regions and, as a result, gives a more accurate and improved delineation of major Arctic sea-floor features.

DATA COMPILATION

Bathymetric data from several sources were compiled on 22 plotting sheets (Fig. 1). Digitized data were obtained from the gravity libraries of the Earth Physics Branch (EPB), Ottawa, Canada, and the Defense Mapping Agency Aerospace Center (DMAAC), St. Louis, Missouri, USA and soundings were obtained from the Canadian Oceanographic Data Centre (CODC), Ottawa, Canada. This information yielded 30,899 water depths for the area outlined in figure 1 of which 11,299 were plotted (Table 1).

A second major source of 95,100 water depths observed from ice island T-3 (Hunkins, personal communication, 1977) were reduced to about 9,072 plotted values primarily over the Alpha Ridge and the Canada Basin. Additional bathymetry was obtained from GEBCO plotting sheets (De Leeuw, 1967), the North Pole Chart No. 4006 (Ritchie, 1969) and 1:1,000,000 plotting sheets obtained from England (Dixey and Watson, personal communication, 1976) and Germany (Zichwolff, personal communication,

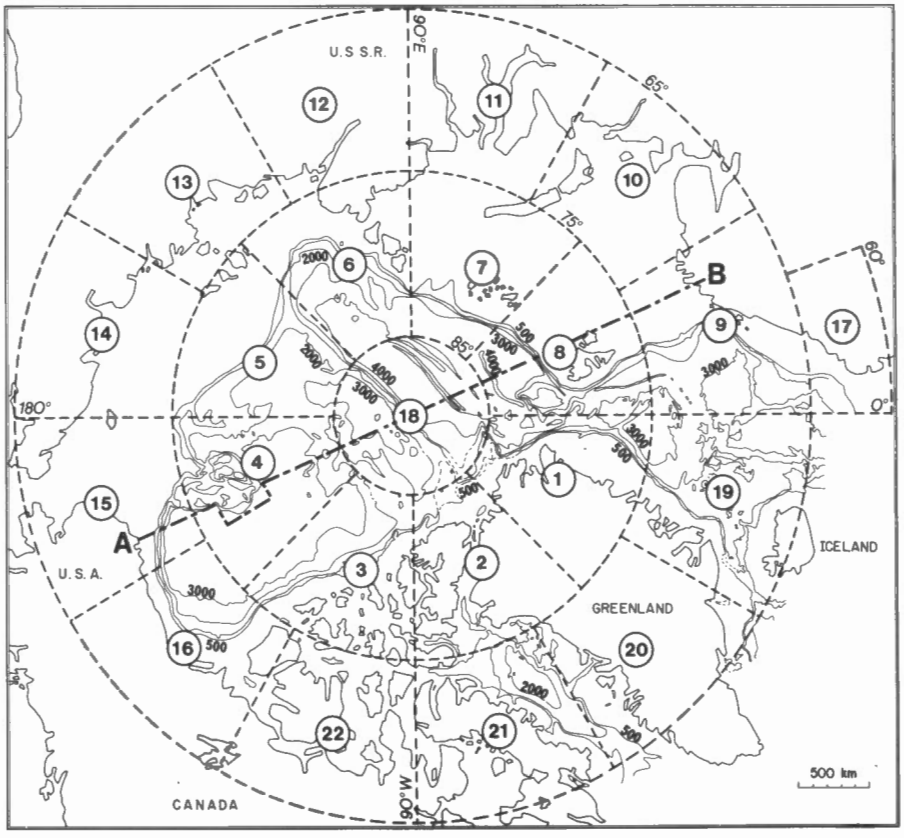

Figure 1. Map of Arctic sea-floor and surrounding regions showing arrangement of the 1:2,000,000 plotting sheets used for compilation of bathymetric data presented on Plate 1. Bathymetric contour interval 1000 m, 500 m contour also shown.

TABLE 1

Summary of Water Depths from the Gravity Libraries of EPB and DMAAC and from the CODC

AREA (FIGURE 1)	DATA POINTS READ IN	OVERPRINTS REMOVED	VALUES PLOTTED
1	584	298	286
2	1284	444	840
3	3416	963	2453
4	696	276	420
5	2291	1823	468
6	---	---	---
7	27	6	21
8	6	0	6
9	6459	5174	1285
10	538	420	118
11	---	---	---
12	---	---	---
13	---	---	---
14	1	1	0
15	1084	381	703
16	8815	5570	3245
17	2438	1754	684
18	3260	2491	769
TOTALS	30,899	19,600	11,299

1976) and Canada (Monahan, personal communication, 1976). Bathymetric contours for the North Atlantic Ocean north of 72°N were taken directly from the map compiled by Perry et al. (1978). Also, 77 water depths obtained for stations where heat flow values were determined (Jessop et al., 1976) and 530 water depths taken during sediment coring programs are included on the map (Marshall, personal communication, 1977).

A third major source of over 92,000 soundings obtained from the Defense Mapping Agency Hydrographic Center, Washington, D.C., (Eaton, personal communication, 1976) were reduced to 17,116 plotted values which provided an additional check of soundings south of 80°N and between about 30°E, westward to about 170°W.

A fourth major source of bathymetric data was collected by submarine traverses in the Arctic Ocean from 1957 to 1962 (Beal, 1969) and represents over seven million soundings (Fig. 2). Because water depths measured on sea ice are more accurately located than those measured from submarines, traverses containing water depths that did not agree with soundings taken in the same area on sea ice were either eliminated or moved slightly in order to get better agreement.

The combined bathymetric sounding data were contoured on each of the 22 plotting sheets (Fig. 1). Station distribution used in plotting is shown in figure 2. Sheets 11, 12 and 13, which cover the innermost parts of the Soviet polar shelf, contain no bathymetric information but the chart by Heezen and Tharp (1975) indicates that water depths for most of this area are less than 200 m. Sheet 18 has been discussed by Sobczak (1977) and is an excellent example of the morphological detail that is available. The map segments were reduced to a scale of 1:7,500,000, and combined to produce the Arctic bathymetric map presented and discussed here (Plate 1).

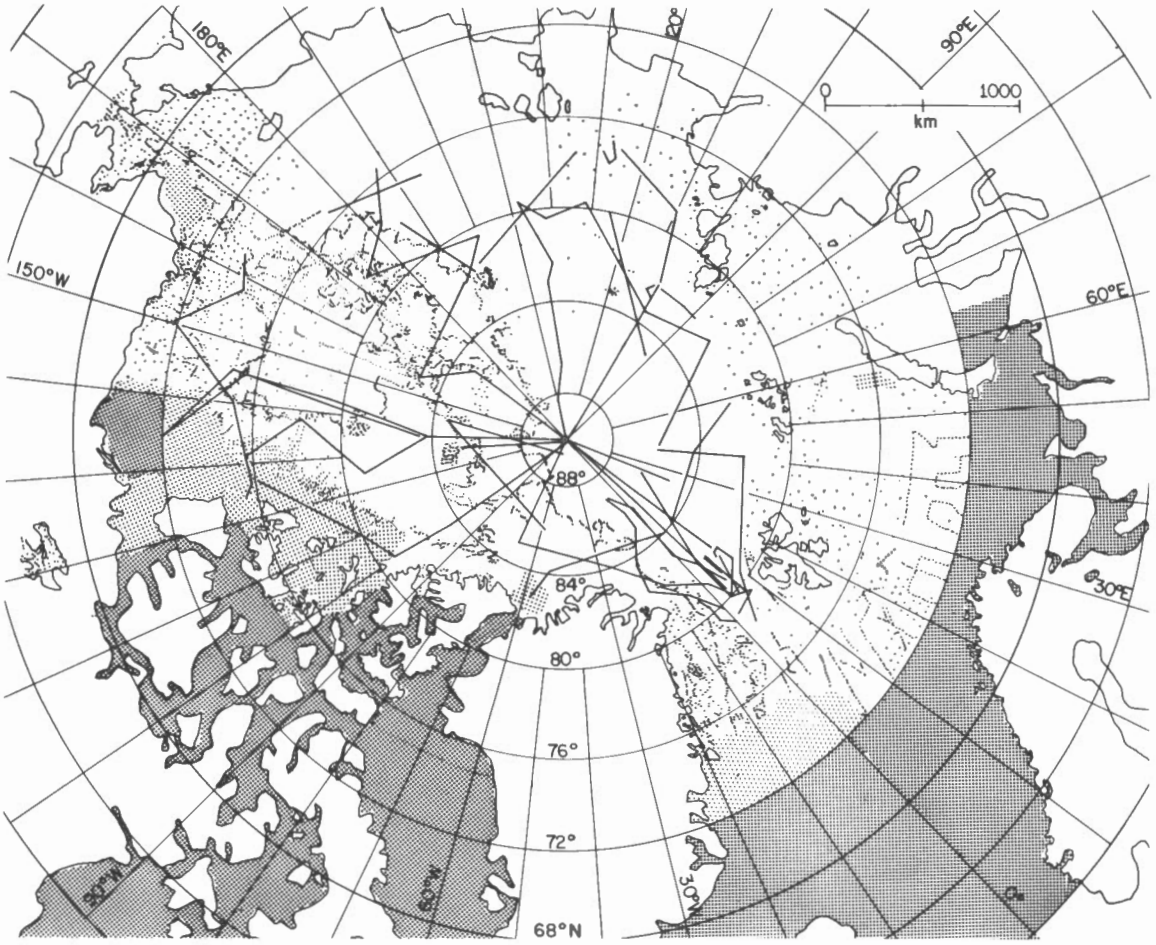

Figure 2. Distribution of bathymetric sounding data in Arctic regions. Solid lines indicate submarine tracks (Beal, 1969). Zones containing closely spaced sounding points are indicated by stipple.

TOPOGRAPHY OF THE FLOOR OF THE ARCTIC OCEAN

The Arctic Ocean floor, covering over 10 million km^2, an area equal to that of Canada, can be separated into continental shelves, continental slopes, submarine ridges and deep basins. Generally, the 500 m and 3000 m contours outline the approximate limits of the continental shelves and the deep basins respectively. Based on planimetric measurements, the shelves underlie about 49 per cent of the ocean surface, the continental slopes and submarine ridges about 30 per cent and the deep basins the remaining 21 per cent. The major submarine ridges (Nansen-Gakkel, Lomonosov, Alpha and Mendeleev Ridges) divide the ocean floor into four large basins (Nansen, Fram, Makarov, and Canada Basins) (Plate 1). Profile AB (Fig. 3) shows the major topographic features of the Arctic sea-floor along a zone well covered by bathymetric sounding data (Fig. 2). The profile is offset from the Chukchi Plateau.

Continental Shelves and Slopes

The Eurasian polar continental shelf is exceptionally broad, with a mean width of about 1000 km, compared to an estimated world-wide average width of about 150 km. The continental shelf break for the Eurasian region occurs at about 200 m depth (the world average, Worzel, 1968) and gradually deepens westward to 500 m. The shelf gradient is usually very flat, about 1 m/km.

The narrow polar shelf of North America varies in width from 20 to 160 km and averages about 110 km. The shelf break deepens eastward from 70 m north of Alaska to 650 m along the Canadian Arctic Archipelago. The shelf gradient varies from 1 to 4 m/km (Sobczak and Weber, 1973).

Gradients of the polar continental slopes of both the Eurasian and North American continents generally vary between 9 m/km to 60 m/km and can change by as much as 45 m/km

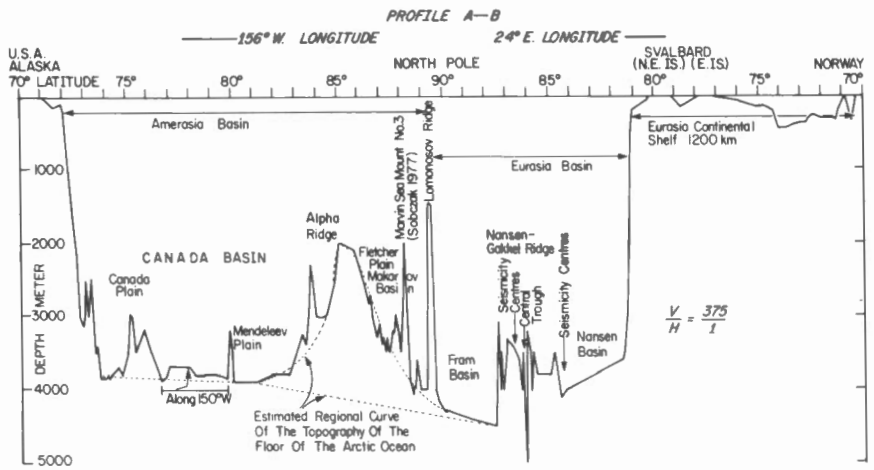

Figure 3. Profile A-B across the Arctic Ocean along 156°W and 24°E Profile location in figure 1.

within 100 km along the slope. A very steep gradient of approximately 250 m/km exists northeast of Greenland at the junction of the North Atlantic and Arctic Oceans between Greenland and Svalbard.

Submarine Ridges

Although definition of polar sea-floor features has improved with the publication of each new bathymetric chart of the Arctic Ocean, the submarine ridges remain only regionally outlined because there are few measurements over most of them. The description here is limited to the morphological and positional refinements of these features indicated by the present compilation (Plate 1). A number of differences noted for sheet 18 (Sobczak, 1977) together with those noted for the other plotting sheets (Fig. 1) are summarized below.

The Lomonosov Ridge was discovered in 1949 by Ya Ya Gakkel of the Soviet Union. It is not well defined toward the Soviet polar margin because very few soundings have been published for this region (Fig. 2). One submarine traverse has been made more or less along the crest of this ridge from the North Pole to the Laptev Shelf.

Existing data show that the Lomonosov Ridge varies from 80 to 100 km in width with 2000 to 3000 m of relief, but at longitude 165°W, about 80 km from the North Pole, the ridge pinches to a width of about 20 km with very steep slopes (Fig. 3). At this location there is an abrupt bend in the ridge. The Eurasian half appears to be dextrally offset by about 80 km relative to the North American half of the ridge at this point.

Close to North America the ridge crest does not strike toward northern Greenland as shown by Heezen and Tharp (1975) but bends westward toward Ellesmere Island as shown by Link et al. (1960), De Leeuw (1967), Ritchie (1969), and Ostenso and Wold (1977). These latter maps show the ridge crest extending to about 82°W. Sounding data from T-3 and the British submarine Sovereign, however, indicate that the ridge crest terminates about 10° further east at about 72°W.

The Alpha Ridge in the Amerasia Basin is, in profile, the most prominent sea-floor feature in the Arctic Ocean (Fig. 3). The adjacent sea-floor slopes gently away from the crest of the Alpha Ridge to a depth of 4500 m adjacent to the Nansen-Gakkel Ridge. The Lomonosov Ridge and Marvin Sea Mounts appear as narrow steep-sided ridges that interrupt an otherwise smoothly declining topography away from the Alpha Ridge. The opposite flank of the ridge in Canada Basin is somewhat steeper, however it is not established that the basement exhibits a similar morphology. Sedimentation patterns may have played a significant role in the construction of the present topography of the flanking basins.

The Alpha Ridge crest varies in depth between 1150 m and about 2440 m. A well outlined ridge crest strikes generally along 85°N between 135°W and 180°W. The ridge itself (as defined by the 2500 m contour, Plate 1) appears to extend to about 165°E, further west than shown on previous maps which show Alpha Ridge bending sharply southward at about 180°W. Between 100°W and 135°W the ridge crest is less clearly defined with as many as three east-west

components at depths of less than 1500 m (a poorly outlined fairly short northern component at about 86°N, and the eastward extension of the main ridge crest which appears to be topographically continuous with a southern component at about 84°N). The crestal complex as a whole, however, appears to be separated from the North American margin by a zone of water depths greater than 1500 m.

This does not seem to be the case with the Mendeleev Ridge, although it is not well defined because very few soundings are available from this area (Fig. 2). Existing information shows that this ridge can be separated from the Alpha Ridge by at least 100 km and by water depths of 2800 m, similar to the depth of the floor of Wrangel Plain. However, data in this region are too sparse to be unambiguously contoured. The Mendeleev Ridge does, however, appear quite different from the Alpha Ridge in morphology; it is narrower and smoother (Plate 1).

Parallel to the Lomonosov Ridge, the Nansen-Gakkel Ridge divides the Eurasia Basin into two sub-basins (Fram and Nansen) with floors at 4000 m and 3000 m respectively (Plate 1). The available sounding data (seven submarine traverses and about 12 soundings) show the ridge to be close to 200 km wide. It rises abruptly about 300 to 500 m above the surrounding abyssal plains (Sobczak, 1977). Its crest is characterized by a series of narrow ridges (maximum heights of 2600 m depth) and troughs (central rift over 5100 m deep) usually less than 20 km wide. The ocean floor to either side of this ridge slopes towards the ridge rather than away from it (Fig. 3). Figure 2, however, indicates that data is sparse over much of the ridge, especially toward the Laptev Shelf where the ridge apparently becomes quite narrow (10 km) at 84° latitude. The Nansen Basin nearly joins the Fram Basin at a depth of about 3700 m at this point. Further southward the ridge changes character and exhibits a single well defined crest that extends about 375 km southward to the Laptev Shelf. This segment of the ridge appears to be aseismic (Plate 2).

Deep Basins

The Canada Basin (over 1 million km^2) contains the Canada, Chukchi and Mendeleev Plains. The Canada Plain is flat bottomed at a depth of about 3800 m and slopes very gently towards the Alpha Ridge (Fig. 3). It differs only in detail from the Heezen and Tharp (1975) map. Its major axis is approximately north-south and is nearly perpendicular to the trends of the other main Arctic basins. To the north a 225 km wide lobe of the Alpha Ridge extends about 300 km southward into the plain.

The Chukchi Plain slopes downward from a depth of about 2200 m to the Mendeleev Plain at about 2500 m. The Mendeleev Plain, in turn, slopes to the northeast towards the Canada Plain. The Chukchi Plateau extends northward nearly 575 km into the Canada Basin and is about 400 km wide. It separates the Chukchi and Canada Plains and is bounded by fairly steep (75 m/km on the west, 133 m/km on the east) escarpments. Its crest is within 300 m of sea-level and is cut by a northeast trending canyon. The canyon floor rises to about 2100 m where it meets the Canada Plain.

Two sea mounts in eastern Canada Basin are shown by Heezen and Tharp (1975). The presence of the more northern sea mount is based on one sounding at a depth of 907 m. This depth is similar to a sounding of 905 m published by De Leeuw (1967), who believed it to be evidence for a large knoll in the Beaufort Sea. However, this latter sounding has not been corroborated by subsequent bathymetric work (Beal, 1969; Sobczak et al., 1973). A submarine traverse (Beal, 1969) over the location of the proposed southern sea mount revealed no topographic irregularities. The existence of these sea mounts is therefore not well established and they are not included in the present chart.

The Makarov Basin lies between the Lomonosov, Alpha and Mendeleev Ridges and contains the Fletcher and Wrangel Plains. The six Marvin Sea Mounts (Sobczak, 1977) rise about 1000 m above the floor of the Fletcher Plain and lie along the axis of the Makarov Basin between 90°W and 180°W. They are parallel to and about 80 km from the Lomonosov Ridge. Their westward extent is uncertain as very few soundings exist beyond 180°W.

The Wrangel Plain appears to be flat bottomed at a depth of about 2800 m and deepens northward at about 85°N into the Fletcher Plain at about 3900 m. The Fletcher Plain deepens somewhat (900 m in 225 km) toward the Lomonosov Ridge (Fig. 3). The deepest part of the Makarov Basin (4100 m) occurs adjacent to the most narrow part of the Lomonosov ridge at 160°W. The basin itself abruptly narrows by about 200 km along this longitude.

The Fram Basin is more or less rectangular in shape (about 300 km by 1500

km), has a relatively smooth bottom floored by an abyssal plain with water depths of 4300 to 4500 m, and it deepens toward the Nansen-Gakkel Ridge (Fig. 3). At the Greenland end of the basin the Morris Jesup Plateau (minimum depth of about 900 m) is shown extending about 300 km northeast from the Greenland polar shelf. Ostenso and Wold (1977) show the Morris Jesup Plateau with a moderate slope on the western side and a very steep slope on the eastern side (550 m/km, a drop of 2750 m over a distance of 5000 m). As bathymetric control in this locality is poor (Fig. 2), the plateau may also extend somewhat northward as well.

The 3500 m to 4500 m deep Lena Trough connects the Fram Basin with the Greenland Sea between 0° and 5°W. It is 10 km to 300 km wide and separates Morris Jesup Plateau and Greenland from Nansen-Gakkel Ridge, Yermak Plateau and Svalbard. Between the Morris Jesup and Yermak Plateaus the trough contains two large sea mounts that have about 1500 m of relief. To the southeast of the Morris Jesup Plateau are two smaller knolls with a relief of about 1100 m.

The Nansen Basin is about 500 km wide bordering the Yermak Plateau north of Svalbard. It extends eastward for about 1000 km where it is truncated by the Nansen-Gakkel ridge and the Kara Shelf. It is floored by an abyssal plain that is between 3600 and 4000 m deep (Fig. 3, Plate 1) and the basin itself is about 500 km shorter than the Fram Basin.

SUMMARY

Although some areas are still not reliably known, large portions of the major physiographic features of the Arctic Ocean floor have been defined in considerable bathymetric detail, and in several instances they have been shown to differ in morphology and location from that given on previously published Arctic bathymetric charts. The four major submarine ridges are morphologically distinct and in some cases unique. The Lomonosov Ridge is narrow (20 km to 200 km wide) with a fairly smooth flat top and has very steep flanks that rise 2 km to 3 km above the surrounding abyssal plains. The ridge crest narrows to about 20 km just west of the North Pole and its crestal axis appears to be dextrally displaced by about 80 km at this location. The ridge extends neither towards north central Greenland (Heezen and Tharp, 1975) nor as far to the west as shown on several charts (Link et al., 1960; De Leeuw, 1967; Ritchie, 1969; Ostenso and Wold, 1977), but trends only slightly towards northeastern Ellesmere Island between 60°W and 70°W.

The Alpha Ridge forms a broad arch with up to 2 km of relief. Between 100°W and about 135°W the Alpha Ridge crest is very broad (up to 300 km wide at 2000 m depth) and can be separated into two and possibly three distinct components. The Mendeleev Ridge is much narrower and smoother than the Alpha Ridge and is approximately perpendicular to it.

The Nansen-Gakkel Ridge appears to be less than 200 km wide. It rises sharply 300 m to 500 m above the adjacent sea floor and is composed of a series of narrow troughs and arches that parallel the ridge with a central rift that is locally over 5100 m deep.

The Marvin Spur is, in fact, a series of six sea mounts named the Marvin Sea Mounts (Sobczak, 1977).

ACKNOWLEDGEMENTS

The senior author (LWS) received a variety of assistance from many people in the form of magnetic tapes, plotting sheets, personal discussions, programming, plotting, drafting and editing and extends his sincere thanks to the following: from the U.S.A., Drs. E.J. Hauer, H.L. Kuykendall and R.O. Seppelin, DMAAC, St. Louis, Mo.; Dr. K. Hunkins and Ms. M. Tharp, Lamont-Doherty Geological Observatory, Columbia Univ.; Dr. M.A. Beal, Arctic Submarine Research Laboratory, San Diego, Calif.; Commander R.H. Eaton, DMAHC, Washington, D.C.; Dr. D.L. Clark, U.S.G.S., Menlo Park, Calif.; Dr. B.V. Marshall, Univ. of Wisconsin; from England, Messrs. D.J. Dixey and R.W.F. Watson, Royal Navy, Taunton; from Germany, Dr. G. Zichwolff, German Hydrographic Institute; from Monaco, Commodore A.H. Cooper, International Hydrographic Bureau; and from Canada, Mr. G.N. Ewing, Canadian Hydrographic Service, Ottawa; Messrs. C. Glennie, R. Pattison and D. Monahan, Canadian Oceanographic Data Centre, Ottawa. The authors thank Drs. R.L. Coles and D. Nagy and Messrs. L. Hampel, J.F. Halpenny, R. Buck, R. Beach, B. Draper, J. Geuer, R.J. Wetmiller, J.M. DeLaurier and D.A. Forsyth, Earth Physics Branch, Ottawa. Special thanks to Dr. G.L. Johnson, Office of Naval Research, Arlington, Va., for a useful discussion of Arctic bathymetry, for providing unpublished maps and for reviewing the manuscript.

REFERENCES

Beal, M.A., 1969. Bathymetry and structure of the Arctic Ocean. Ph. D. thesis, Oregon State Univ., Corvallis, 187 p., Appendix.

De Leeuw, M.M., 1967. New Canadian Bathymetric chart of the western Arctic Ocean, north of 72°. Deep-Sea Res., 14, 489-504.

Emery, K.O., 1949. Topography and sediments of the Arctic Ocean. J. Geol., 57, 512-521.

Heezen, B.C., and M. Tharp, 1975. Am. Geograph. Soc. Map of the Arctic Region. Lamont-Doherty Geol. Obs., Palisades, New York.

Jessop, A.M., M.A. Hobart and J.G. Sclater, 1976. The world heat flow data collection - 1975. Earth Phys. Br. Geothermal Series No. 5, 125 p.

Link, T.A., J.A. Downing, G.O. Raasch, A.W. Byrne, D.W.R. Wilson and A. Reece, 1960. Geological map of the Arctic. Alberta Soc. Petrol. Geol., Calgary, Alberta.

Nansen, F., 1904. The bathymetrical features of the North Polar Seas. in: The Norwegian North Polar Expedition, 1893-1896, v. 4, ed. F. Nansen, Longmans and Green, London, Ch. 13, 1-232.

Ostenso, N.A., and R.J. Wold, 1977. A seismic and gravity profile across the Arctic Ocean basin. Tectonophysics, 37, 1-24.

Perry, R.K., H.S. Fleming, N.Z. Cherkis, R.H. Feden and J.V. Massingill, 1978. Bathymetry of the Norwegian-Greenland and western Barents Seas (map). Geol. Soc. Am. Inc., Boulder, Colo. (in press).

Pitman, W.C. III, and M. Talwani, 1972. Sea-floor spreading in the North Atlantic. Geol. Soc. Am. Bull., 83, 619-646.

Ritchie, G.S., 1969. North Polar Chart, No. 4006. Hydrographer of the Navy, Taunton, England.

Sobczak, L.W., 1977. Bathymetry of the Arctic Ocean north of 85°N latitude. Tectonophysics, 42, T27-T33.

Sobczak, L.W., L.E. Stephens, P.J. Winter and D.B. Hearty, 1973. Gravity measurements over the Beaufort Sea, Banks Island and Mackenzie Delta. Earth Phys. Br. Gravity Map Series No. 151, 16 p.

Sobczak, L.W. and J.R. Weber, 1973. Crustal structure of the Queen Elizabeth Islands and polar continental margin. in: Arctic Geology, ed. M.G. Pitcher, Am. Assoc. Petrol. Geol. Mem. 19, 517-525.

Worzel, J. Lamar, 1968. Advances in marine geophysical research of continental margins. Can. J. Earth Sci., 5, 963-983.

Seismicity of the Arctic, 1908-1975

R. J. Wetmiller and D. A. Forsyth

ABSTRACT

Data are available on more than 3400 earthquakes that have occurred up to the end of 1975 in the Arctic regions including the Arctic Ocean basin and adjacent continental areas of Canada, Alaska and Siberia. The information is derived mainly from published reports and data files of the Earth Physics Branch (Canada), the National Earthquake Information Service (USA) and the Academy of Sciences (USSR). No recomputations of data on Arctic earthquakes are done for this study. Most of the earthquakes covered here have magnitudes less than 5 and have occurred since 1962 in the continental areas of Alaska, Siberia and northern Canada. Prior to 1962, complete detection of Arctic earthquakes varied from those with magnitudes 7 or greater in the early 1900's to those with magnitudes 5 or greater. Since 1962, the threshold of complete detection has been lowered and now includes earthquakes with magnitudes of 3.7 or greater in some continental areas and of about 4.5 or greater in the Arctic Ocean basin. Similarly, the reliability of Arctic earthquake epicentral determinations, which varied from 300 - 100 km prior to 1962, have been improved to between 100 and 50 km since 1962. In the Arctic Ocean basin seismic activity is largely confined to a narrow zone along the Nansen-Gakkel Ridge. The Lomonosov, Alpha and Mendeleev Ridges have no recorded seismic activity associated with them. Small pockets of seismicity along the Canadian Arctic continental slope are possibly related to isostatically uncompensated loads of recent sediments. The active tectonic areas in southern Alaska and eastern Siberia are associated with broad zones of intense seismic activity. In Arctic Canada more subdued seismic activity is associated with older deformational trends in the northern Yukon, Keewatin area, Baffin region and Sverdrup Basin and suggests that at least partial reactivation of such features by contemporary or remnant stresses is possible.

RÉSUMÉ

On dispose de données relatives à plus de 3 400 séismes, ayant eu lieu jusqu'à la fin de 1975 dans les régions arctiques, en particulier dans le bassin de l'océan Arctique et les zones continentales adjacentes du Canada, de l'Alaska et de la Sibérie. Cette information provient principalement de rapports publiés et de fichiers de données appartenant à la Direction de la physique du globe du Canada, au Service national d'information séismique (National Earthquake Information Service) des Etats-Unis, et à l'Académie des sciences de l'URSS. On n'a pas réévalué les données séismiques recueillies dans l'Arctique. La plupart des séismes dont il est question ici ont une magnitude inférieur à 5, et ont eu lieu après 1962 dans les régions continentales de l'Alaska, de la Sibérie et du Nord du Canada. Avant 1962, on n'enregistrait avec précision dans l'Arctique que les séismes dont la magnitude variait entre au moins 5 et un peu plus de 7. Depuis 1962, le seuil de détection complète a été abaissé, et l'on enregistre maintenant les séismes d'au moins 3.7 de magnitude dans certaines régions continentales, et d'au moins 4.7 dans le bassin de l'océan Arctique. De même, depuis 1962, on peut déterminer dans l'Arctique avec un degré de précision plus élevé l'épicentre des séismes (100 à 50 km, au lieu de 300 à 100 km autrefois). L'activité

séismique du bassin de l'océan Arctique se restreint surtout à une bande étroite le long de la dorsale Nansen-Gakkel. Aucune activité séismique enregistrée n'est reliée aux dorsales de Lomonosov, d'Alpha et de Mendeleev. Des charges de sédimentation récentes qui ne sont pas compensées par isostasie peuvent être à l'origine de la séismicité détectée dans des petites régions le long de la peute du plateau continental arctique canadien. L'activité tectonique des régions du sud de l'Alaska et de l'est de la Sibérie est à la source de la séismicité importante trouvée en de grandes zones. Dans les régions arctiques du Canada on associe une activité séismique plus réduite aux regions déformées du nord du Yukon, de Keewatin, de la région de Baffin et du bassin de Sverdrup. Il se peut que la réactivation partielle de telles structures soit dûe aux tensions vestantes ou récentes.

INTRODUCTION

Several reviews of Arctic seismicity have appeared in the literature. These include those of Chapman (1973), Tarr (1970), Barazangi and Dorman (1970), Hodgson et al. (1965), Sykes (1965) and Linden (1961). The aim of this paper is to extend a review of Arctic seismicity to 1975 for the area shown in figure 1 and to discuss the seismicity and its limitations in relation to known Arctic tectonic and structural features. This review includes for the first time much information on the seismicity of Arctic continental areas which has only recently been published, and we draw, in particular, on the results of Basham et al. (1977) for a summary of northern Canadian seismicity.

Figure 1. Arctic regions for which seismicity is shown on Plate 2. Bathymetric contour interval 1 km, 500 m contour also shown.

There are now more than 3400 Arctic earthquakes known for the period between 1908 and 1975, of which more than 80 per cent have been located since 1962 (Fig. 2). The quantity and quality of the Arctic earthquake data have thus improved dramatically with time, but still vary from area to area within the Arctic particularly from the continental to the deep oceanic areas.

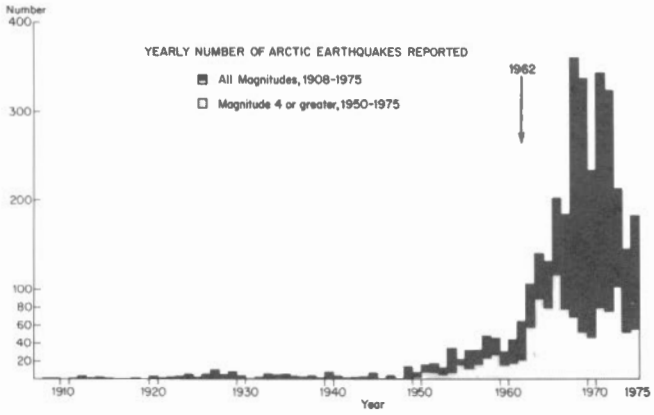

Figure 2. Number of Arctic earthquakes located per year, 1908 - 1975. Only earthquakes plotted on Plate 2 are included.

SOURCES OF DATA

The record of Arctic seismicity discussed in this review has been compiled from several different sources. The first major source is the Earth Physics Branch (EPB) which has provided information on approximately one-half of the earthquakes studied here, all located in northern Canada or adjacent areas. The second major source is the Preliminary Determination of Epicentres (PDE) program operated since 1936 by various U.S. government agencies. Approximately one third of the Arctic earthquakes come from this PDE program via the world-wide seismicity tape of the U.S. National Earthquake Information Service. The PDE earthquakes are distributed generally throughout the Arctic, but with a concentration in south and central Alaska after 1962. The third source for Arctic earthquakes has been the Academy of Sciences of the USSR (MOS) which has published regional earthquake catalogues covering Siberia for the period from 1966 to 1972, providing information on more than 300 earthquakes. All MOS earthquakes are located in northeastern Siberia and in the Arctic Ocean. Similar information for the northwestern USSR was not available at the time this study was completed. The remaining information in this review comes from two groups of sources. The first includes various international agencies such as the International Seismological Centre, the International Seismological Summary and the *Bureau Central International de Séismologie* which are, or have been, responsible for world-wide earthquake determination. The second includes special studies of world-wide and Arctic seismicity which have been published in the literature by Sykes (1965), Gutenberg and Richter (1954) and Linden (1961). These sources have generally provided information on the larger earthquakes prior to 1962.

Many of the larger earthquakes in the Arctic region are reported by more than one agency. When several agencies have reported the same earthquake, often with slightly different parameters, one solution has been selected. For this study EPB and MOS solutions are given preference to those of the PDE or international agencies. No recomputations have been done. No information on focal depths is presented in this study, as these can rarely be calculated with confidence for Arctic earthquakes. However, most Arctic earthquakes are shallow, occurring within the crust; subcrustal earthquakes with focal depths greater than 70 km are only known in southern and central Alaska.

The dramatic increase in the yearly number of Arctic earthquakes reported (Fig. 2) is the result of a significant increase in the sensitivity of the seismograph networks to Arctic earthquakes beginning in 1962. The World-Wide Standard Seismograph Network was installed in the period 1957-1961 and has provided more and better data on Arctic earthquakes and, since 1961, computer processing of data for PDE solutions. Expanded seismograph networks were installed in northern Canada, Alaska and the northeastern USSR in the 1960's. Annual publication of catalogues of smaller magnitude local seismic activity began at the Earth Physics Branch (Canada) in 1961 and the Academy of Sciences (USSR) in 1966.

RELIABILITY AND COMPLETENESS OF THE ARCTIC DATA SET

An understanding of the reliability of epicentral solutions and completeness of the coverage for Arctic earthquakes is important to the interpretation of seismicity patterns

in terms of tectonic processes or structures. The reliability and completeness of the seismicity data set in northern Canada has been discussed extensively by Basham et al. (1977) and Leblanc and Wetmiller (1974). Their conclusions for the continental areas of the Canadian Arctic can be generally applied to other Arctic regions as well including the deep oceanic areas not covered in their studies. For the period prior to 1962, these authors conclude that epicentres are generally uncertain by 100 km, and in some cases by as much as 300 km. These large uncertainties result from the poor and limited data available for early Arctic earthquakes. For completeness of the Arctic data set prior to 1962, Leblanc and Wetmiller (1974) adopt Gutenberg and Richter's (1954) assessment for world-wide seismicity data; that is, detection of all magnitude 7 or greater earthquakes since 1918, and all magnitude 5 or greater since the 1950's. These reliability and completeness figures apply to both the oceanic and continental areas of the Arctic as both were subject to the same generally poor coverage by the world's seismograph networks.

For the period after 1962, a distinction must be made between the oceanic areas and the continental areas of northern Canada, Alaska and northeastern Siberia which contained the expanded seismograph networks. The expanded networks improved the monitoring of seismicity in the oceanic areas but not as dramatically. Basham et al. (1977) suggest that most of the larger earthquakes in continental areas with nearby seismograph stations are located to within 50 km, while some smaller earthquakes which are generally detected by only a few stations may be mislocated by as much as 100 km. For completeness in the continental areas of northern Canada, Leblanc and Wetmiller (1974) suggest that all earthquakes of magnitude 4.5 or greater have been detected since the early 1960's and Basham et al. (1977) suggest that all of magnitude 3.7 or greater have been detected since 1968. For the deep oceanic areas in the period after 1962, the threshold magnitude for complete coverage is necessarily higher than that in the adjacent continental areas; a value of 4.5 would be reasonable for completeness and would represent a gradual improvement in coverage of the deep oceanic areas after 1962. Coverage of oceanic events to magnitudes lower than this could be claimed only in areas along the continental margins close to the seismograph networks. The present epicentral reliability of earthquakes in the deep ocean is difficult to estimate but is probably not worse than the 50 km claimed for the continental earthquakes, mainly because of the higher threshold magnitude required for detection in oceanic areas.

SEISMICITY OF THE ARCTIC REGION

A map of seismicity superimposed on the bathymetry is shown on Plate 2 contained in the back pocket of this report. In plotting seismicity the size of the epicentral symbols is proportional to earthquake magnitude, and the year of occurrence before or after 1962 is distinguished by different symbols. Earthquakes of the same magnitude interval occurring within 75 km of each other have been plotted at the epicentre of the more modern larger magnitude event with the total number of events appended; the plots for the different magnitude symbols are overlaid. The many events for which no formal magnitude has been calculated have been plotted at a minimum spacing of 37.5 km to give a clearer picture of their distribution. These are generally events with magnitudes equal to or lower than the threshold magnitude for their time and location. This overlay scheme results in a simplified map keyed to the distribution of the more recent and reliable earthquakes so that the map shows real patterns of epicentres and real differences in the rate of seismic activity in different areas of the Arctic, subject to the location errors and detection thresholds discussed earlier.

Two points must be kept in mind when viewing this Arctic seismicity. One is that the low detection threshold since 1962 has produced trends that, to a great extent, represent only a 14 year "snapshot" of a region in which the controlling forces are characterized by much longer time scales. The other is the difference in detection thresholds between the continental areas and the deep Arctic Ocean. Thus many smaller earthquakes are shown in the continental areas of northern Canada, Alaska and the northeastern USSR of Plate 2 but the presence or absence of similar events in deep oceanic areas is not known.

Continental Areas

The recent seismicity of northern Canada has been discussed by Basham et al. (1977), and a review of their findings is appropriate before discussing other continental areas. Knowledge of Canadian Arctic seismicity followed the northern expansion of the seismograph network in the 1960's (Fig. 3). A similar upgrading of seismograph networks took place in Alaska following the destructive Prince William Sound earthquake

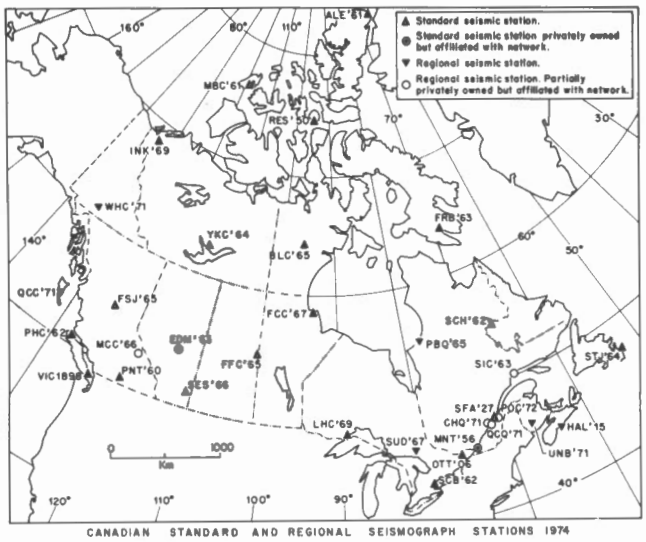

Figure 3. Distribution of seismograph stations in Canada showing their commencement dates.

of March, 1964 (Meyers, 1976) and in northeastern Siberia after 1968 (Chapman, personal communication, 1976) resulting in a similar increase in the number of smaller magnitude events being reported and more reliable determinations for the larger events.

The relatively small number of earthquakes in northern Canada with magnitude greater than 5 (mostly pre-1962) show no strong trend in distribution, as would be expected if there were an active plate margin present, but rather occur in two distinct clusters, one in Baffin Bay and one in northwestern Canada, with a scatter of individual events elsewhere (Plate 2). In contrast, the distribution of smaller magnitude post-1962 seismicity, shows several interesting trends and correlations with other geophysical parameters (Fig. 4).

In north-central Canada a more or less continuous band of epicentres follows the Bell Arch and the Boothia Uplift from south of Baffin Island to the Sverdrup Basin (Fig.

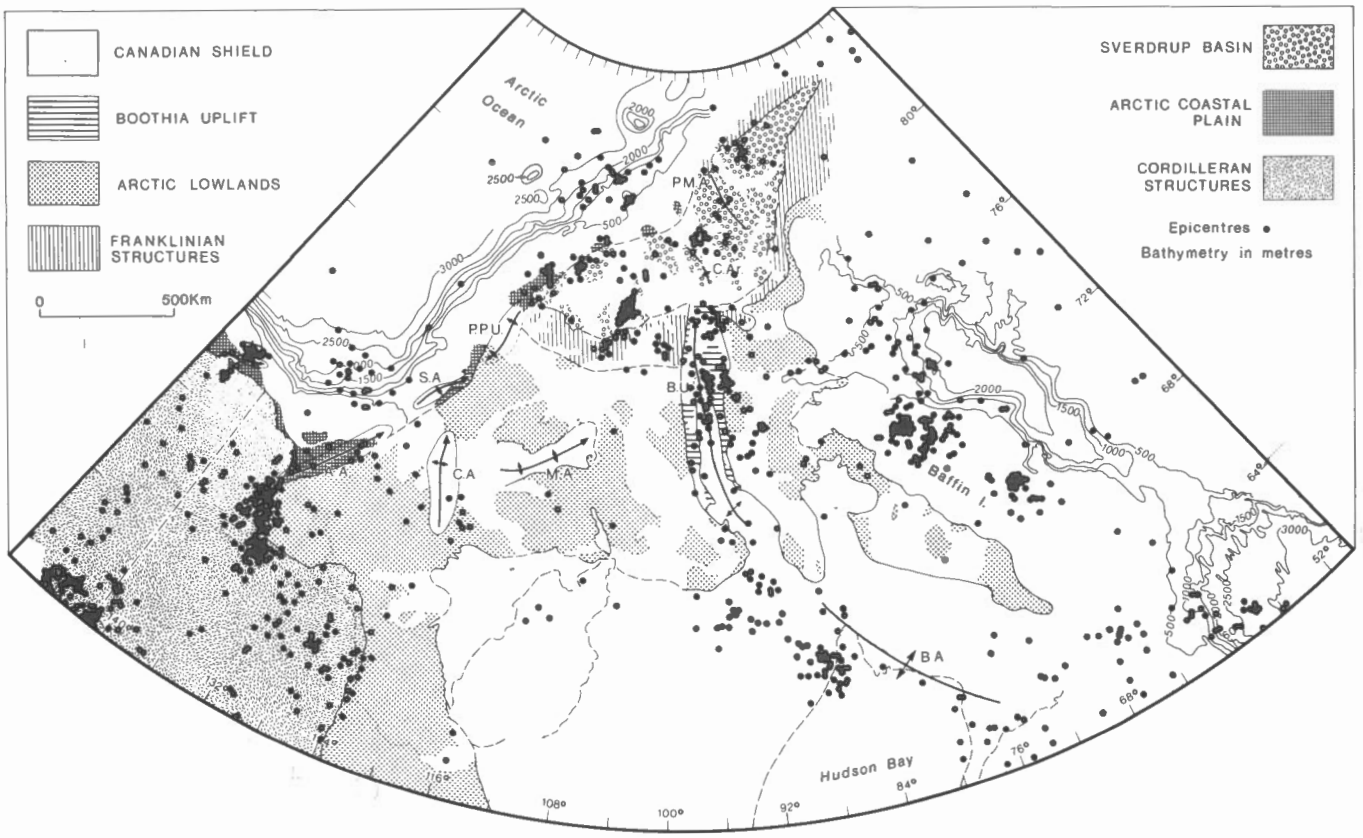

Figure 4. General geological provinces in northern Canada and seismicity for the period 1962-1974 (after Basham et al., 1977); P.M.A.: Princess Margaret Arch, C.Ar.: Cornwallis Arch, B.U.: Boothia Uplift, P.P.U.: Prince Patrick Uplift, S.A.: Storkerson Arch, C.A.: Coppermine Arch, M.A.: Minto Arch, B.A.: Bell Arch.

4). The geological record for the Bell Arch and the Boothia Uplift indicates that these features have been reactivated repeatedly from late Proterozoic to late Paleozoic times (Trettin et al., 1972; Kerr, 1977). The contemporary seismicity apparent in figure 4 suggests that these features are continuing to react. One mechanism which could possibly be triggering this seismicity is glacial rebound. Figure 5 shows Walcott's (1970) smoothed free-air gravity map superimposed on the seismicity. The major gravity lows on this map coincide with regions undergoing isostatic recovery after the removal of the Pleistocene ice sheets. The seismicity through northeastern Keewatin and along northeast Baffin Island appears to correlate with the flanks of the major lows rather than with the lows themselves. The flanks of the anomalies may represent hinge zones in the rebound process which could be sites of maximum regional stress gradients within the crust and may therefore be capable of triggering seismic activity. The Franklinian structures and the Cornwallis Arch (Fig. 4) are other examples of Paleozoic tectonic features in northern Canada which are presently associated with contemporary seismic activity.

In the Baffin region earthquakes are concentrated over the shelf in northwest Baffin Bay, in two areas of northeast Baffin Island and to the southeast of Baffin Island (Fig. 4). The epicentres on northeastern Baffin Island are distributed mainly over the region of dykes thought by Fahrig et al. (1971) to possess a component of magnetization induced during the early Cenozoic opening of Baffin Bay. This suggests that the seismic activity on Baffin Island may be controlled by structures, not necessarily the dykes themselves, created or reactivated during the opening of Baffin Bay.

In Baffin Bay it is tempting to correlate the several earthquakes with magnitude greater than 5 (Plate 2) with the trend of a possible Cenozoic spreading centre responsible for the opening of the Bay (Keen et al., 1972). Such a correlation must be considered with caution because most of the larger earthquakes in Baffin Bay occurred prior to 1962 and therefore may have epicentral uncertainties as large as 100 to 300 km. An epicentral trend down central Baffin Bay is not evident in the distribution of the more reliable and numerous post-1962 seismicity (Fig. 4). Most recent activity

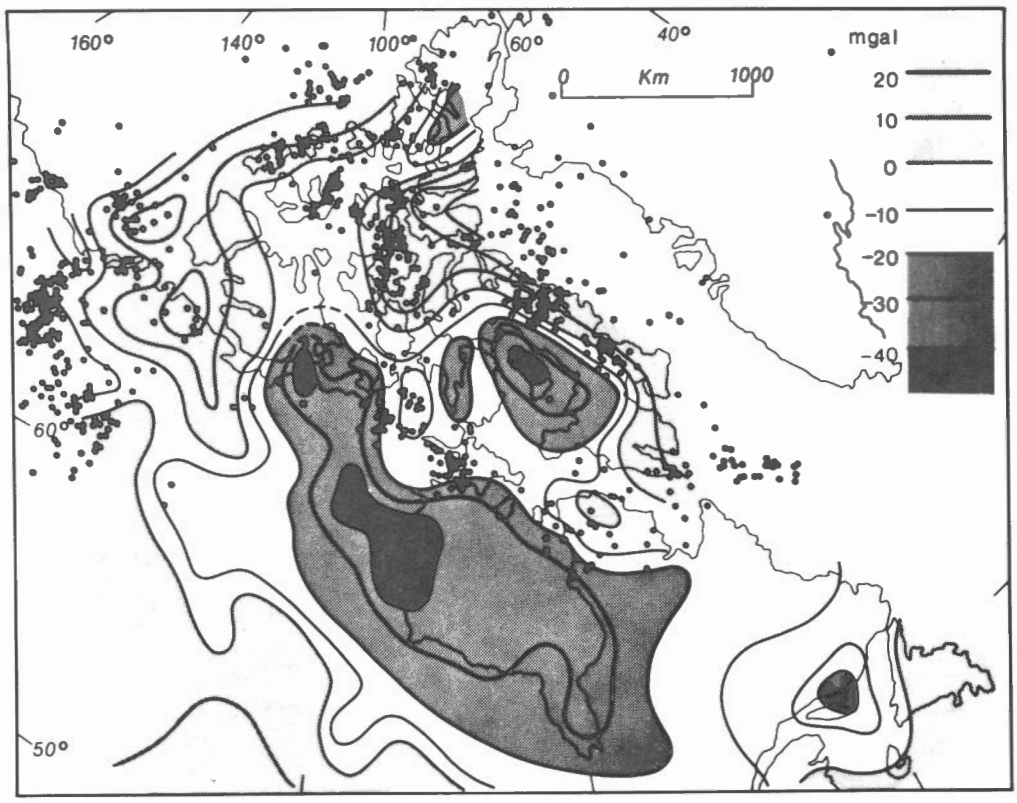

Figure 5. Smoothed free-air gravity map by Walcott (1970) and Canadian seismicity north of 60°N for the period 1962-1974 (after Basham et al., 1977).

has been concentrated in the northern portion of the bay and it is only rarely that earthquakes are located beneath 2000 m or deeper waters of the bay.

In northwestern Canada (Fig. 6) seismic activity is concentrated along the major deformational trends of the northern Cordillera while adjacent areas of the western Canadian Shield and the Arctic Coastal Plain (Fig. 4) show a more diffuse pattern. The implication is again that deformational structures of past tectonic regimes may be reactivated by the contemporary stress field although in northwestern Canada little information is available on the distribution of stress within the crust.

The record of earthquakes in northern Canada since 1962 shows that earthquake

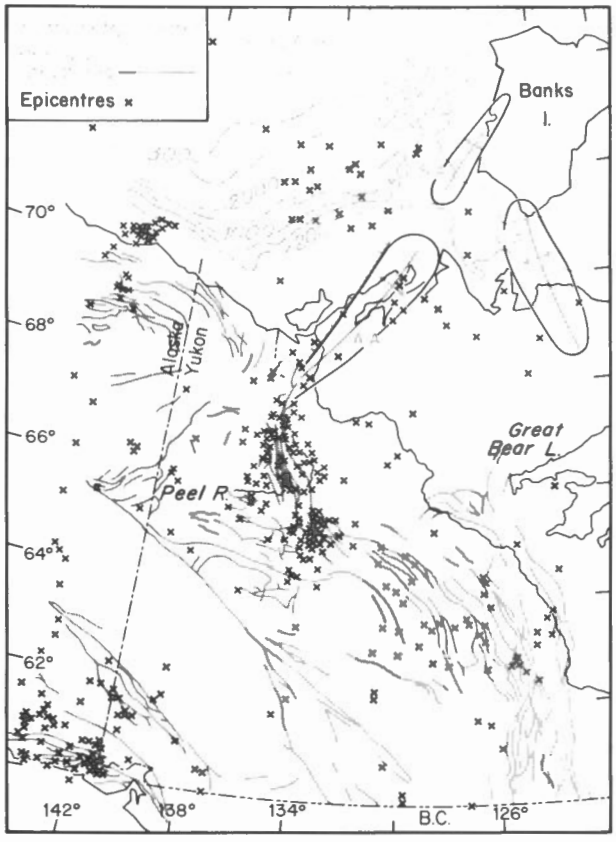

Figure 6. Major structural features in the Yukon-Beaufort Sea region and seismicity for the period 1962-1974 (after Basham et al., 1977). The seismicity shown in Alaska is not representative for this period; S.A.: Storkerson Arch, A.A.: Aklavik Arch, C.A.: Coppermine Arch.

swarms are a relatively frequent phenomena. Three known swarms deserve mention. In a 30-day period in 1965 a swarm of about 2000 microearthquakes (magnitude less than 3) occurred along the southeast coast of Prince Patrick Island (Smith et al., 1968). This swarm is spatially coincident with, and suggests recent movement on, structures associated with the Prince Patrick Uplift (Fig. 4). In 1972, swarm activity commenced in the Byam Martin Channel within the Sverdrup Basin and included, in a two month period, several hundred earthquakes, four with magnitude equal to 5, in an area which previously had shown very little evidence of seismic activity (Basham et al., 1977). The proposed (Hasegawa, 1977) triggering mechanism for this activity is attributed to remanent stresses acting upon a source region that is weakened by reactivated localized intrusions. Swarm activity occurred in 1968 on the Alaskan continental shelf near Martin Point northwest of the Yukon-Alaska border (Stevens et al., 1976). The epicentral distribution correlates with a mapped anticline-syncline sequence traversing the continental shelf from the Alaska mainland (Grantz et al., 1975) and also correlates with the landward flank of an elliptical free-air gravity anomaly (Fig. 7).

Sobczak (1975) suggests that such gravity anomalies may be caused by uncompensated loads of recent sediments. These loads may provide sufficient deviatoric stress to trigger seismic activity along basement structures. The distribution of seismic activity would depend on the particular relationship of the load to the underlying stuctures. The existence of suitable structures by themselves would not be sufficient for associated seismic activity to occur. As an example, on the Canadian continental shelf east of the epicentral area of the Alaskan shelf swarm and to the northwest of the Aklavik Arch (A.A. in Fig. 6), deformational structures to a depth of 3 km have been mapped, and a major fault zone that crosses the continental shelf has been proposed (Yorath and Norris, 1975; Young et al., 1976). No related seismic activity has been observed, however (Fig. 7).

No swarms, such as the one on the Alaskan continental shelf, have been detected on the Canadian Arctic continental shelf, but clusters of seismic activity do occur on the continental slope north of Canada (Fig. 7). These again correlate with the flanks of elliptical free-air gravity anomalies although in this case it is with the seaward flank and not with the landward flank as seen with the Alaska shelf swarm. For the

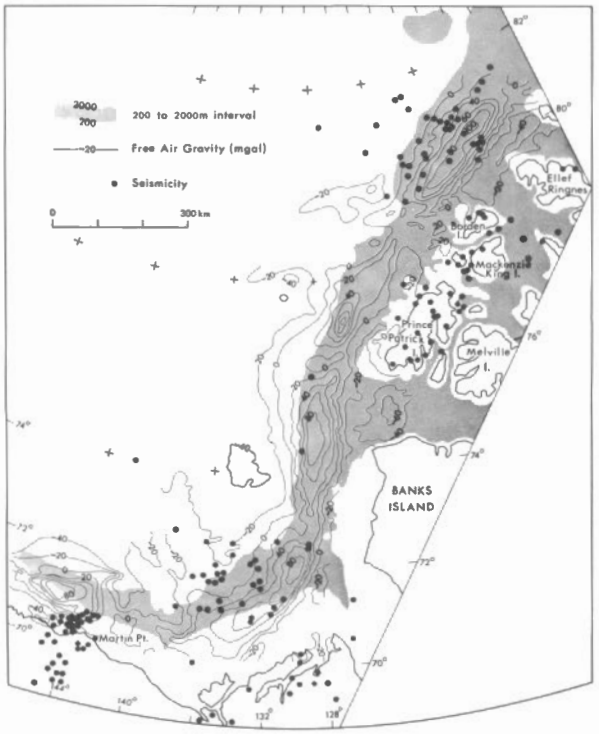

Figure 7. Free-air gravity along the Canadian Arctic coast and seismicity for the period 1962-1974 (after Basham et al., 1977). Continental slope is shaded and free-air gravity is shown in 20 mgal contours.

clusters of Canadian continental slope seismicity, no major deformational trends have been mapped, although the change in slope gradient at these two locations (Plate 2) may indicate the presence of major structures.

The relationship between seismicity and the major deformational trends in the northern Yukon Territory, the Arctic Archipelago, the Boothia Uplift and Baffin Island suggests that deformational features formed or reactivated by mid-Paleozoic or younger orogenic phases may respond to contemporary stress fields by exhibiting seismic activity. The result in northern Canada is a scatter of small magnitude shallow focus seismic activity in many areas even though northern Canada occupies a relatively stable part of the North American plate, and no active plate boundaries are known to traverse the area. Such a reactivation phenomenon may equally be expected to occur in other continental areas, and in such regions as Alaska or northeastern Siberia where active tectonic zones do occur, reactivation of old structures might be expected to broaden the seismic trends associated with contemporary tectonism. In Alaska, for example, the intense seismic activity in southern Alaska (Plate 2) is surrounded by a wide band of loosely connected more subdued seismicity including that of the northern Yukon which was discussed earlier as an example of the reactivation of older deformational trends. On the other hand, the distribution of subcrustal earthquakes (Tarr, 1970) is confined to south and central Alaska and suggests a much more restricted extent to the presently active tectonic zone. In northeastern Siberia, Chapman and Solomon (1976) comment on the breadth of the active seismic zone (up to 600 km in some areas) and suggest that it may be controlled by older deformational trends. With the absence of subcrustal earthquakes in northern Siberia, it is more difficult to precisely determine the active tectonic zone through Siberia. Chapman and Solomon (1976) believe that the Siberian seismic zone represents an extension of the Nansen-Gakkel Ridge plate boundary through northeastern Siberia. However, as in southern Alaska, the extent of the active tectonic zone in northeastern Siberia may be relatively restricted compared to the extent of the seismicity.

Oceanic Areas

The seismicity of the Arctic oceanic areas is dominated by the continuous chain of epicentres which follows the northern portion of the Mid-Atlantic Ridge in the North Atlantic Ocean and the Nansen-Gakkel Ridge across the Arctic Ocean and represents the boundary between the North American and Eurasian crustal plates. The locus of this boundary is well defined by the trace of the multiple epicentres on Plate 2. In the North Atlantic Ocean the seismicity follows a broad arc south from Svalbard, with considerable scatter of seismicity on both sides of the central trend. From Svalbard to the Laptev Shelf the seismicity follows a remarkably linear trend with no offsets of more than 100 km evident. There is little scatter of seismicity on either side of this central trend in the Arctic Ocean, certainly much less than in the North Atlantic.

Fault plane solutions showing predominantly normal faulting presented by Sykes (1967) and Chapman and Solomon (1976) support the idea that the Nansen-Gakkel Ridge is a spreading centre, and a continuation of the Mid-Atlantic Ridge. Lazareva and Misharina (1965) quote, but do not show,

fault plane solutions which suggest compressive stress associated with the eastern extension of the ridge across the Laptev Shelf. The tectonics of this continental shelf area are undoubtedly more complex than in the adjacent oceanic area.

Other oceanic areas including the Lomonosov, Alpha and Mendeleev Ridges appear to be largely aseismic. Although the occurrence of small magnitude earthquakes in the remote oceanic areas may go undetected, no larger earthquakes, similar to those on the Nansen-Gakkel Ridge, are located in these regions. The stress concentration mechanism due to wedges of recent sediments, suggested as causing clusters of seismicity on the northern Canadian continental slope, may also explain some of the seismicity along continental slopes elsewhere in the map area such as at the Eurasian continental margin in the Laptev Sea.

Several studies of surface wave propagation through the Arctic region have shed some light on the gross structure of the Arctic Basin. These include Hunkins (1963) and Oliver et al. (1955). Both of these studies find no evidence of continental crustal structure in the Arctic Ocean basin; Hunkins (1963) concludes that the Arctic Ocean crust had an average thickness of between 6 and 15 km. Chapman (1973) in a more recent study of Rayleigh Wave propagation concludes that the deep parts of the Arctic Ocean have an average sediment layer of 2 km and a crustal thickness of 15 km overlying an oceanic mantle. The Nansen-Gakkel Ridge is interpreted by Chapman (1973) to be a typical spreading centre on the basis of the surface wave observations. Studies such as these are restricted to sampling of gross crustal structure of the Arctic region and are not sensitive enough to determine the detailed structure of individual features within the Arctic Basin such as the Lomonosov, Alpha and Mendeleev Ridges.

ACKNOWLEDGEMENTS

We thank W.E. Shannon for assistance in preparing computer data files on Arctic earthquakes, and P.W. Basham for valuable discussions and critical appraisal of the manuscript.

REFERENCES

Barazangi, M.W., and J. Dorman, 1970. Seismicity map of the Arctic. Bull. Seism. Soc. Am., 60, 1741-1743.

Basham, P.W., D.A. Forsyth and R.J. Wetmiller, 1977. Seismicity of northern Canada. Can. J. Earth Sci., 14, 1646-1667.

Chapman, E.D., 1973. Structure and tectonics of the Arctic region. MSc. thesis, Massachusetts Inst. of Technol., Cambridge, 119 p.

Chapman, M.E., and S.C. Solomon, 1976. North American - Eurasian plate boundary in northeast Asia. J. Geophys. Res., 81, 921-930.

Fahrig, W.F., E. Irving and G.D. Jackson, 1971. Paleomagnetism of the Franklin Diabases. Can. J. Earth Sci., 8, 455-467.

Grantz, A., M.L. Holmes and B.A. Kososki, 1975. Geological framework of the Alaska continental terrace in the Chukchi and Beaufort Seas. in: Canada's Continental Margins, eds. C.J. Yorath, E.R. Parker and D.J. Glass, Can. Soc. Petrol Geol. Mem. 4, 669-700.

Gutenberg, B., and C.F. Richter, 1954. Seismicity of the Earth and Associated Phenomena. Princeton Univ. Press, Princeton, 273 p.

Hasegawa, H., 1977. Focal parameters of four Sverdrup Basin, Arctic Canada, earthquakes in November and December of 1972. Can. J. Earth Sci., 14, 2481-2494.

Hodgson, J.H., M. Bath, H. Jenson, A. Kvale, N.A. Lindne, L.M. Murphy, N.V. Shebalin, E. Tryggvason and E. Vesanen, 1965. Seismicity of the Arctic. Ann. Internat. Geophys. Year 30, 33 p.

Hunkins, K., 1963. Submarine structure of the Arctic Ocean from earthquake surface waves. in: Proceedings of the Arctic Basin Symposium, October 1962. The Arctic Inst. of N. Am., Washington, D.C., 3-8.

Keen, C.E., D.L. Barrett, K.S. Manchester and D.I. Ross, 1972. Geophysical studies in Baffin Bay and some tectonic implications. Can. J. Earth Sci., 9, 239-256.

Kerr J.W., 1977. Cornwallis Fold Belt and the mechanism of basement uplift. Can. J. Earth Sci., 14, 1374-1401.

Lazareva, A.P., and L.A. Misharina, 1965. Stresses in earthquake foci in the Arctic seismic belt. Izy. Akad. Sci. USSR Phys. Solid Earth, English Transl. 2, 84-87.

Leblanc, G., and R.J. Wetmiller, 1974. An evaluation of seimological data available for the Yukon Territory and Mackenzie valley. Can. J. Earth Sci., 11, 1435-1454.

Linden, N.A., 1961. Seismicity of the Arctic region. Ann. Internat. Geophys. Year, 1, 375-387.

Meyers, H., 1976. An historical summary of earthquake epicenters in and near Alaska. NOAA Tech. Memo., EDS NGSDG-1, 57 p.

Oliver, J., M. Ewing and F. Press, 1955. Crustal structure of the Arctic region from the Lg Phase. Bull. Geol. Soc. Am., 66, 1063-1074.

Smith, W.E.T., K. Whitham and W. Piché, 1968. A microearthquake swarm in 1965 near Mould Bay, N.W.T., Canada. Bull. Seism. Soc. Am., 53, 1991-2012.

Sobczak, L.W., 1975. Gravity anomalies and passive continental margins, Canada and Norway. in: Canada's Continental Margins, eds. C.J. Yorath, E.R. Parker and D.J. Glass, Can. Soc. Petrol. Geol. Mem. 4, 743-761.

Stevens, A.E., W.G. Milne, R.B. Horner, R.J. Wetmiller, G. Leblanc and G.A. McMechan, 1976. Canadian Earthquakes - 1968. Earth Phys. Br. Seism. Series No. 71, 39 p.

Sykes, L.R., 1965. The seismicity of the Arctic. Bull. Seism. Soc. Am., 55, 501-518.

Sykes, L.R., 1967. Mechanism of earthquakes and nature of faulting on the mid-oceanic ridges. J. Geophys. Res., 72, 2131-2153.

Tarr, A.C., 1970. New maps of polar seismicity. Bull. Seism. Soc. Am., 60, 1745-1747.

Trettin, H.P., T.O. Frisch, L.W. Sobczak, J.R. Weber, L.K. Law, J. DeLaurier and K. Whitham, 1972. The Innuitian Province. in: Variations in Tectonic Styles in Canada, eds. R.A. Price and R.J.W. Douglas, Geol. Assoc. Can. Sp. Paper 11, 83-179.

Walcott, R.I., 1970. Isostatic response to loading of the crust in Canada. Can. J. Earth Sci., 7, 716-726.

Yorath, C.J., and D.K., Norris, 1975. The tectonic development of the southern Beaufort Sea and its relationship to the origin of the Arctic Ocean basin. in: Canada's Continental Margins, eds. C.J. Yorath, E.R. Parker and D.J. Glass, Can. Soc. Petrol. Geol. Mem. 4, 589-611.

Young, F.G., D.W. Myhr and C.J. Yorath, 1976. Geology of the Beaufort-Mackenzie Basin. Geol. Survey Can. Paper 76-11, 65 p.

Heat flow north of 60° N

A. S. Judge and A. M. Jessop

ABSTRACT

The terrestrial heat flow data base north of 60°N has been analyzed and subdivided on the basis of physiographic and tectonic setting. Although 329 observations spread over 34 x 10^6 km^2 does not constitute a good data base from which to draw major conclusions, some interesting conclusions do emerge. As observed elsewhere the highest mean heat flow values are associated with the active ocean-spreading centres (121 mWm^{-2}) and the lowest with exposed areas of Precambrian shields (40 mWm^{-2}). Continental platform areas, ocean basins and inactive ridges lie intermediate between these values (60 mWm^{-2}, 57 mWm^{-2}, and 52 mWm^{-2} respectively). These averages are similar to those observed on similar features in other parts of the world. A detailed examination of individual features reveal some important contrasts between similar features. Whereas, for example, the Nansen-Gakkel ridge system exhibits a typical heat flow distribution for an active spreading centre, the North Atlantic system exhibits an unusually high heat flow for the age of the oceanic crust. The mean heat flow differs by 13 mWm^{-2} between the two inactive ridge systems in the Arctic Ocean, the Alpha and Lomonosov Ridges; a fact which may reflect their different origins.

RÉSUMÉ

On a analysé et subdivisé, en fonction de la physiographie et de la configuration tectonique, la base de données relatives au flux thermique terrestre au nord de 60° de latitude. Bien que 329 observations réparties sur 34 x 10^6 km^2 ne constituent pas une base de données suffisante pour tirer des conclusions définitives, on peut quand même en déduire quelques faits intéresants. Comme on l'a ailleurs constaté, les valeurs maximales du flux thermique moyen sont associées aux centres actifs d'expansion du fond marin (121 mWm^{-2}), et les valeurs minimales aux affleurements des boucliers précambriens (42 mWm^{-2}). Les plates-formes continentales, les bassins océaniques et les dorsales inactives sont caractérisés par des valeurs intermédiaires (60 mWm^{-2}, 57 mWm^{-2}, et 52 mWm^{-2} respectivement). Ces moyennes sont semblables à celles constatées dans le cas de structures similaires situées en d'autres point du globe. Un examen détaillé des structures individuelles met en évidence de profondes différences entre celles-ci. Par exemple, alors que le réseau de dorsales de Nansen-Gakkel est caractérisé par une distribution du flux thermique typique pour un centre d'expansion actif, celui du réseau de l'Atlantique Nord est caractérisé par un flux thermique anomalement élevé, par rapport à l'âge de la croûte océanique. Le flux thermique diffère en moyenne de 13 mWm^{-2} entre les deux dorsales inactives de l'océan Arctique, les dorsales Alpha et de Lomonosov; cet écart reflète peut-être leur différence d'origine.

SOURCES OF DATA

The World Heat Flow Data Collection - 1975 (Jessop et al., 1976) contains 223 individual heat flow values north of 60°N. In addition Lachenbruch and Marshall (1969) have published summary heat flow data for a further 106 sites situated primarily in the sediments of the Canada Basin and the Alpha Ridge. Because of the incomplete nature of these further data (lack of individual heat flows, temperature gradients and thermal conductivities) the latter were excluded from the world listing. The complete data set (329 heat flow values of which 221 are in the Arctic Ocean proper) has been divided on the basis of physiographic setting as summarized in Table 1 and figure 1. All heat flow values are expressed in mWm^{-2} (41.8 mWm^{-2} equals 1 HFU).

DISCUSSION OF DATA

Continental Heat Flow Data

Although considerable geothermal data in the form of underground temperatures have become available for the land areas in the past several years (Gavlina and Makarenko, 1975; Kehle et al., 1970; Taylor and Judge, 1976) only 86 measurements of heat flow on land have been published. Of these determinations 53 are in the USSR (Lubimova et al., 1973), 9 of which are in the shield terrain of the Karelia Peninsula (Lubimova et al., 1972) and are consequently combined in Table 1 with data from the shield of the rest of Scandinavia (Puranen et al., 1968; Swanberg et al., 1974). These results and those from Greenland (Sass et al., 1972) reflect the well-known low heat flow of shield areas as summarized by Rao and Jessop (1975) although the mean is marginally higher than the 35 mWm^{-2} previously reported for the Baltic Shield alone (Puranen et al., 1968; Swanberg et al., 1974). The Siberian data (Fotiadi et al., 1969; Sergiyenko et al., 1972) have an average of 60 ± 6 mWm^{-2} which is near the world average of 62 mWm^{-2} for continental areas (Jessop et al., 1976) and is consistent with a basement of upper Paleozoic age (Polyak and Smirnov, 1968). The very small number of Canadian and Alaskan data are scattered, one in the Churchill Province of the Canadian Shield (Beck and Sass, 1966), one in the Rocky Mountain Front (Garland and Lennox, 1962), two on the Arctic coastal plain of Alaska (Lachenbruch and Brewer, 1959; Lachenbruch et al., 1965) and one on the Paleozoic Arctic Platform (Misener, 1955) of Canada. This latter result at Resolute Bay on Cornwallis Island (121 mWm^{-2}) was found to be much higher than normal (Judge, 1973 suggested a range of 50 to 67 mWm^{-2}) for the tectonic setting leading to some speculation about the earth's interior in high latitudes. However, the value is uncorrected for the complex surface history of the site and provides an excellent example of the very large near surface distortions to the earth's thermal field that occur in northern land and continental shelf regions as a consequence of the recent history of deglaciation, the dynamic shoreline history resulting from eustatic sea-level changes and isostatic readjustments of the landmass, and the widespread distribution of high ice content permafrost to depths of as much as 700 m (Lachenbruch, 1957; Lachenbruch and Gold, 1973; Balobaev et al., 1973; Judge, 1973; Hunter et al., 1976). Lachenbruch (1957) calculated that as a result of the shoreline recession history at the Resolute site the apparent heat flow was over 100 per cent greater than the equilibrium flux (a transient flux equivalent to the earth's equilibrium flux is being derived from adjacent water bodies). The statistics for Canada and Alaska have been calculated with and without the Resolute result although they probably have little significance for such a widely scattered group of measurements from such varied geological settings.

The 13 heat flow determinations for Iceland (Palmason, 1967, 1973) reflect the young volcanic nature of the island astride the Mid-Atlantic Ridge. The average (139 mWm^{-2}) is high, with individual values ranging from intermediate to very high (63 to 310 mWm^{-2}). Palmason (1973) has related the heat flow distribution primarily to dyke injection at the ridge axis and to surface subsidence. Hydrothermal circulation in the highly permeable lavas will also play a very significant role in determining the pattern of heat flow (Lister, 1977).

Oceanic Heat Flow Data

Heat flow values in the Arctic Ocean show both some predictable results and some unexpected patterns. With the exception of the ship-gathered data from the North Atlantic, the Bering Sea and Baffin Bay, (e.g., Horai et al., 1970; Foster, 1962; Pye and Hyndman, 1972) the ocean data have been primarily gathered from drifting ice stations such as NP-15 (Tomara, 1973) by the USSR, T-3 (Lachenbruch and Marshall, 1966) and Arlis 2 (Lachenbruch and Marshall, 1968) by the USA. In general the rate of drift of the sea-ice is slower by an order of magnitude than that of a ship on the open sea thus permitting

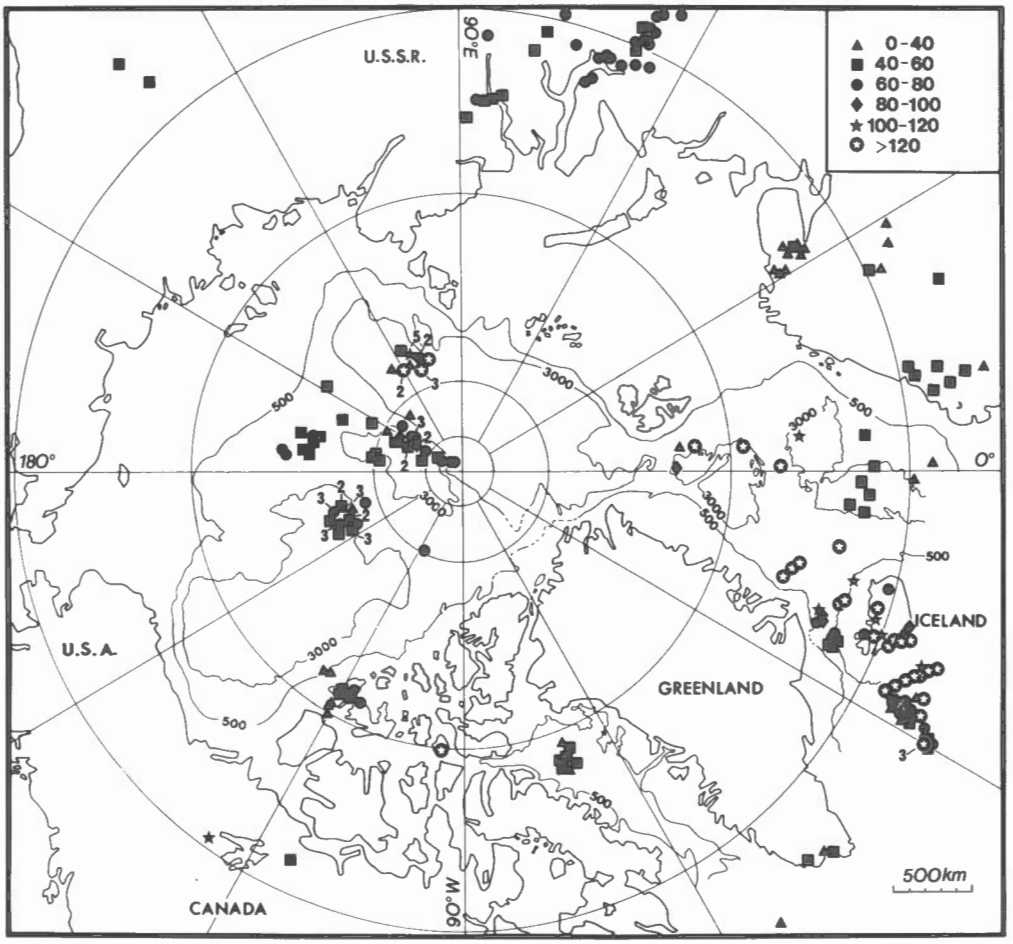

Figure 1. Distribution of heat flow observations north of 60°N. Many sites are too close to allow individual representation. Russian oceanic data as revised by Lubimova et al. (1976).

very closely spaced detailed observations. The direction of drift of the ice is generally less predictable however, and subject to the vagaries of wind and current, resulting in the irregular spatial distribution of some of the heat flow sites. Some heat flow measurements have been made with the help of aircraft to position the equipment on the ice (Law et al., 1965; Lubimova et al., 1976).

Data from the coastal waters of the westernmost Canadian Arctic and preliminary unpublished data from the Arctic Islands show a definite trend of increasing heat flow towards the northeast and the interior of the Sverdrup Basin (Law et al., 1965; Paterson and Law, 1966; Niblett and Whitham, 1970). This phenomenon has been related to a local geomagnetic variation anomaly and a seismic 'time-delay' in the region but now appears to reflect a more general thermal transition between regions of different tectonic history (Judge, 1973). The 122 measurements in the Canada Basin and the adjacent uplands of the Alpha Ridge and the Chukchi Sea (Lachenbruch and Marshall, 1966; 1969) show very distinct variations between the value of 57 ± 3 mWm^{-2} for the 46 measurements in the basin areas of water depth greater than 3500 m and the value of 50 ± 7 mWm^{-2} for the 76 observations in shallower water, i.e., the heat flow in the deep basin is roughly 15 per cent greater and much more uniform than in the surrounding areas. These data thus suggest an average heat flux from the mantle beneath the basin that exceeds the average heat flow in the surrounding upland areas and, hence, they also imply differences between the two areas that are derived partially from the mantle. In addition, Lachenbruch and Marshall (1966) studied in

detail the transition at 83°N, 160°W between the Canada Basin and the Alpha Ridge. The abrupt change in heat flow measured over a distance of 60 km requires a lateral discontinuity of thermal conductivity throughout the crust. Of the two plausible explanations the first requires that the lower conductivity crust of the ridge project out tens of kilometres under the adjacent basin. The second requires the intrusion of a deep dyke parallel to the ridge. Neither of these interpretations is inconsistent with an anomaly caused by an accumulation of basalt from an extinct mid-ocean ridge. The low heat flow values suggest, however, that the thermal anomaly has dissipated, and because the topographic highs associated with active spreading centres are generally attributed to temperature induced effects (Sclater and Francheteau, 1970), the existence of present topographic relief of over 2000 m (Plate 1) is difficult to explain. Pitman and Herron (1974) have suggested that the Alpha and Mendeleev Ridges are, in fact, an island arc behind a subduction zone. Present thermal data alone are insufficient to resolve the origin of these ridges.

The measurements north of Iceland in the Denmark Strait confirm a high heat flow near the mid-ocean rift, which drops to normal values over distances of 100 km (Lachenbruch and Marshall, 1968). In addition, the measurements reveal temperature changes on the ocean floor with periods of several hours to weeks, and with a wavelength of several hundred kilometres. These variations were interpreted in terms of masses of cold water moving across the bottom of the Denmark Strait. Results from the Mohns (155 ± 83 mWm^{-2}) and Reykjanes Ridges (105 ± 83 mWm^{-2}) show high average heat flows and large standard deviations, reflecting very low and very high individual values, typical of active ocean spreading centres (Horai et al., 1970; Langseth et al., 1970; Talwani et al., 1971; Langseth et al., 1972; Langseth and Zielinski, 1974; Haenel, 1974).

Seven heat flow measurements over a distance of 50 km across the Nansen-Gakkel Ridge range in value from 40 to 142 mWm^{-2} (Lubimova et al., 1969b), averaging 97 ± 51 mWm^{-2}. The average is lower than that for the Reykjanes (105 mWm^{-2}) or Mohns Ridges (155 mWm^{-2}), but not significantly so given the low number of data points. Lubimova et al. (1976) point out that the lowest value, which they attribute to refraction effects, was recorded 50 km from the ridge axis. Langseth and Zielinski (1974) have shown that the heat flow in the Norwegian and Greenland Seas is higher than that for ocean crust of the same age in the North Pacific (Sclater and Francheteau, 1970). In general, this area of anomalously high heat flow and abnormally high shallow temperatures stretches from 53°N to at least 80°N. There are too few results from the Nansen-Gakkel Ridge to determine if its heat flow is similarly anomalous.

Heat flow in the vicinity of the Lomonosov Ridge (Lubimova, 1968; Lubimova et al., 1969a; Alexandrov et al., 1972; Tomara, 1973; Lubimova et al., 1973) averages 76 ± 15 mWm^{-2}, an average including several distinct physiographic units. Subdividing the 28 measurements into four units, the average heat flows are 77 ± 17 mWm^{-2} for the Lomonosov Ridge, 76 ± 12 mWm^{-2} for the Makarov Basin, 86 mWm^{-2} for two determinations in the Fram Basin and 66 ± 7 mWm^{-2} for the Mendeleev Ridge. In a more recent paper Lubimova et al. (1976) have revised downwards without explanation the thermal conductivity results for the sea-bottom sediments in this region. The thermal conductivity determinations were based on moisture content, an approach that Lachenbruch and Marshall (1966) have shown to have limited validity for the Alpha Ridge. Using the revised heat flow values the averages become 63 ± 13 mWm^{-2} for the Lomonosov Ridge, 57 ± 4 mWm^{-2} for the Makarov Basin, 66 mWm^{-2} for two determinations in the Fram Basin and 53 ± 11 mWm^{-2} for the Mendeleev Ridge. Because of the present uncertainties in the actual heat flow, the Mendeleev Ridge results have not been included with the averages for the Alpha Ridge, although their revised average of 53 ± 11 mWm^{-2} is much closer to the 50 ± 7 mWm^{-2} average (Table 1) for the latter. These revised averages are used in Table 1 and in figure 1. Lubimova et al. (1976) have attributed the wide variation of results on the Lomonosov Ridge to topographic effects caused by the "strong dissected relief" of the ridge. In the vicinity of the geographic north pole a single profile was established as ice station NP-15 drifted from the Makarov Basin, across the Lomonosov Ridge to the Fram Basin. This profile, contrary to the average heat flows just discussed, reveals a disparity of 12 mWm^{-2} between the ridge and the flanking basins.

Heat flow measurements have been made in several of the marginal seas bordering the Arctic Ocean. Foster (1962) and Erickson et al. (1975), the latter as part of the Deep-Sea Drill Holes Program, determined heat flow in the southern Bering Sea. The low values, ranging from 38 to 54 mWm^{-2}, are

TABLE 1

Heat Flow Statistics North of 60°N in mWm^{-2}

AREA	NUMBER MEASUREMENTS	AVERAGE	STANDARD DEVIATION	MINIMUM	MAXIMUM
Continental					
Greenland	3	43	8	36	51
Scandinavia and Karelia	21	39	9	20	54
Canada and Alaska	5	77	24	54	121
(without Resolute)	4	66	11	54	83
Canadian Coastal Arctic	10	44	20	18	68
Siberia	44	60	6	45	71
Iceland	13	139	74	63	310
Oceanic					
Baffin Bay	9	55	6	41	64
Norwegian Sea	6	54	3	50	59
Bering Sea*	6	44	5	38	54
Denmark Strait	9	77	21	54	112
Canada Basin	46	57	3	48	65
Makarov Basin	6	57	4	53	64
Fram Basin	2	66	-	65	67
Alpha Ridge	76	50	7	31	77
Mendeleev Ridge	8	53	11	38	66
Lomonosov Ridge	15	63	13	50	88
Nansen-Gakkel Ridge	8	97	51	13	155
Reykjanes Ridge	33	105	83	2	325
Mohns Ridge	15	155	83	14	268
TOTAL	329	69	55	2	325

*South of 60°N and omitted from statistics.

typical of the region of submerged continental crust. The nine heat flow determinations in Baffin Bay and the Labrador Sea (Pye, 1971; Pye and Hyndman, 1972) yield average heat flows of 56 ± 6 mWm^{-2} and 55 ± 6 mWm^{-2} respectively. Heat flow in the centre of the Baffin Bay basin is only slightly higher, by 8 mWm^{-2}, than that measured in marginal areas and indicates that there has been no recent spreading activity in Baffin Bay.

SUMMARY

In summary the heat flow results north of 60°N generally behave in a predictable way in the gross sense. A total of 329 sites unevenly distributed over 34 x 10^6 km does not constitute a good data base from which to draw major conclusions. However, accepting these spatial limitations and the uncertainties present in some of the data, particularly that from the USSR, some

tentative summary statements and conclusions may be drawn.

The average heat flow for the Arctic Ocean is 64 mWm^{-2}, which includes a mean of 57 ± 4 mWm^{-2} for 54 determinations in the basins, (Canada, Makarov and Fram Basins). This average heat flow for the Arctic basins lies between those for the Atlantic Ocean basins of 54 mWm^{-2}, the Indian Ocean basins of 59 mWm^{-2} and the Pacific Ocean basins of 61 mWm^{-2}. While the Canada and Makarov Basins exhibit very uniform heat flow, the few measurements at the margin of the Fram Basin exhibit a 15 per cent higher average. The Fram Basin is, of course, associated with a spreading centre and is probably of younger age.

Of the 69 heat flow determinations associated with the active spreading centres (Reykjanes, Mohns and Nansen-Gakkel Ridges and Iceland), all but 8 are associated with the North Atlantic ridge system. Their mean heat flow of 121 ± 85 mWm^{-2} compares with means of 69 for active ridges in the Indian Ocean and 129 for those in the Pacific. If the measurements from the Nansen-Gakkel Ridge are treated separately, their average heat flow is 97 mWm^{-2}, compared with 72 mWm^{-2} for active ridges in the Atlantic Ocean as a whole, but 124 mWm^{-2} for the Mid-Atlantic Ridge north of 53°N. As well as exhibiting very high mean heat flow, the spreading centres also show very wide variations in heat flow as a result of the very complex associations of volcanism and hydrothermal circulation of water. The abnormally high heat flow for a given age of ocean crust exhibited by the North Atlantic ridge system indicates very high temperatures at the base of the lithosphere. This does not appear to be true for the Nansen-Gakkel Ridge, however, where the mean heat flow appears to be 20 per cent lower, but is admittedly based on very little data. However, the heat flow at the edge of the Fram Basin coincides with the heat flow-age relationship for the North Pacific Ocean at 40 Ma rather than with that for the North Atlantic Ocean. Of course, if the Nansen-Gakkel system is much older than 40 Ma, its present thermal situation would be even more anomalous.

For 99 determinations of heat flow associated with the inactive ridge systems, the average heat flows are 63 ± 15 mWm^{-2} (15 measurements) on the Lomonosov Ridge and 50 ± 8 mWm^{-2} (84 measurements) on the Alpha and Mendeleev Ridges. In comparison aseismic ridges in the Atlantic, Indian and Pacific Oceans exhibit mean heat flows of 50, 52 and 57 respectively. A variety of reasons can be responsible for lower heat flow through aseismic ridges than through the ocean floor; e.g., thickening of the lithosphere or deficiency in heat producing materials in the lithosphere beneath the ridges, conductivity contrasts and the thermal blanketing effect of the ridges or, indeed, simply the reflection of a transient thermal situation. Similarly, if the asthenosphere and the lithosphere are coupled in their motions, the origin of the differences may be much deeper. Although a spatial variation of heat flow between the margins of the Canada Basin and the Alpha and Mendeleev Ridges is consistent with a simple thermal conductivity contrast, the contrast could not explain the differences in average heat flow between the entire basin and the two ridges. The difference in heat flow of 13 mWm^{-2} between the Lomonosov Ridge and the Alpha and Mendeleev ridge system may result from their different positions within the Arctic Ocean; whereas the latter lies astride two basins of similar heat flow, the former lies between one of those basins and a perhaps much younger basin containing an active spreading centre. Alternatively, if surrounding thermal conditions in the ocean basins are similar and each ridge possesses a crustal thickness of 10 to 20 km, the heat generation of the Lomonosov crust must be 1.5 to 3 times that of the Alpha and Mendeleev Ridges. If, as has been proposed, the latter are a pile of basaltic rocks, then the Lomonosov crust may well be composed of a Precambrian basement, including gneisses or granodiorites, and covered with sediments.

Detailed heat flow surveys similar to that of Lachenbruch and Marshall (1966) combined with other geophysical surveys would explain the nature and origin of many of these features and thus unravel the plate tectonic history not only of the Arctic Ocean but also of the surrounding continental landmasses.

The 96 determinations of heat flow on land and on the associated continental shelves encompass a very wide range of tectonic styles and ages, from the Precambrian shields to the young volcanic island of Iceland. Iceland itself has been included in the discussion of the mid-ocean ridge system. The average shield heat flow of 40 ± 9 mWm^{-2}, primarily from 21 measurements in Scandinavia and Karelia, contrasts strongly with the value of 60 ± 6 for 44 determinations in the Siberian Platform. In general, the Baltic Shield exhibits, at 40 mWm^{-2}, the same heat flow as that on the Superior Province of the Canadian Shield (Jessop and Lewis, 1978), but

a considerably lower heat flow than the South African (47 mWm^{-2}) and the Indian (57 mWm^{-2}) shields. Coupled with heat generation measurements on surface rocks and reasonable models for the distribution of radioactivity and conductivity in the crust, calculated temperatures at the base of the crust range from 200° to 350°C for the Baltic Shield, and from 350° to 500°C for the Canadian Shield (Rao and Jessop, 1975). The Siberian heat flows appear quite consistent with those measured on other platforms with relatively undeformed Paleozoic sediments overlying Precambrian shields.

The difference in heat flow between exposed shields and their Paleozoic platform cover is a relatively common phenomenon, possibly attributable to the preservation, within the platform succession, of shield-derived sediments which, because they were eroded from higher levels within the Precambrian crust, possess a higher heat generation.

Over the next few years considerably more heat flow determinations in the northern regions, particularly of North America, should be published as work already underway reaches completion.

REFERENCES

Alexandrov, A.L., E.A. Lubimova and G.A. Tomara, 1972. Heat flow through the bottom of the inner seas and lakes in the USSR. Geothermics, 1, 73-80.

Balobaev, V.T., V.N. Dyviatkin and I.M. Kutasov, 1973. Contemporary geothermal conditions of the existence and development of perenially frozen rocks. in: Proc. of 2nd Internat. Permafrost Conference, Moscow, 1, 11-19.

Beck, A.E., and J.H. Sass, 1966. A preliminary value of heat flow at the Muskox intrusion near Coppermine, N.W.T., Canada. Earth Planet. Sci. Lett., 1, 123-219.

Erickson, A.J., R.P. Von Herzen, J.G. Sclater, R.W. Girdler, B.V. Marshall and R. Hyndman, 1975. Geothermal measurements in deep-sea drill holes. J. Geophys. Res., 80, 2515-2528.

Foster, T.D., 1962. Heat-flow measurements in the northeast Pacific and in the Bering Sea. J. Geophys. Res., 67, 2991-2993.

Fotiadi, E.E., U.I. Moissenko and L.S. Sokolova, 1969. The heat field of the West Siberian Platform. Dokl. Akad. Nauk. SSSR, 189, 385-388 (Am. Geol. Inst. English Transl., 189, 50-53).

Garland, G.D., and D.H. Lennox, 1962. Heat flow in western Canada. Geophys. J.R. Astr. Soc., 6, 245-262.

Gavlina, G.B., and F. A. Makarenko, 1975. Geothermal map of the USSR. in: Proc. 2nd United Nations Symposium on the Development and Use of Geothermal Resources, San Francisco, 2, 1013-1017.

Haenel, R., 1974. Heat flow measurements in the Norwegian Sea. Meteor. Forsch., C, 17, 74-78.

Horai, K., M. Chessman and G. Simmons, 1970. Heat flow measurements on the Reykjanes Ridge. Nature, 225, 264-265.

Hunter, J.A., A.S. Judge, H.A. MacAuley, R.M. Gagné, R.A. Burns and R.L. Good, 1976. The occurrence of permafrost and frozen sub-seabottom materials in the southern Beaufort Sea. Beaufort Sea Project Tech. Rept. No. 22, Dept. of Environment, Victoria, 176 p.

Jessop, A.M., M.A. Hobart and J.G. Sclater, 1976. The world heat flow data collection - 1975. Earth Phys. Br. Geothermal Series No. 5, 125 p.

Jessop, A.M., and T.L. Lewis, 1978. Heat flow and heat generation in the Superior Province of the Canadian Shield. Tectonophysics (in press).

Judge, A.S., 1973. The prediction of permafrost thickness. Can. Geotech. J., 10, 1-11.

Judge, A.S., 1974. The occurrence of offshore permafrost in northern Canada. in: The Coast and Shelf of the Beaufort Sea, The Arctic Inst. of N. Am., Washington, D.C., 427-437.

Kehle, R.O., R.J. Schoeppel and R.K. Deford, 1970. The A.A.P.G. geothermal survey of North America. Geothermics, 1, 358-367.

Lachenbruch, A.H., 1957. Thermal effects of the ocean on permafrost. Geol. Soc. Am. Bull., 68, 1515-1529.

Lachenbruch, A.H., and M.C. Brewer, 1959. The dissipation of the temperature effect in drilling a well in Arctic Alaska. U. S. Geol. Survey Bull. 1083-C, 73-109.

Lachenbruch, A.H., and L.W. Gold, 1973. Thermal conditions in permafrost - a review of North American literature in permafrost. in: North American Contributions to the 2nd Internat. Conf., Nat. Acad. Sci., Washington, D.C., 3-26.

Lachenbruch, A.H., G.W. Green and B.V. Marshall, 1965. Permafrost and the geothermal regimes. in: Environment of the Cape Thompson Region, Alaska 1966, USAFC Div. of Tech. Info., Washington, D.C., 149-164.

Lachenbruch, A.H., and B.V. Marshall, 1966. Heat flow through the Arctic Ocean floor, the Canada Basin-Alpha Rise boundary. J. Geophys. Res., 71, 1223-1248.

Lachenbruch, A.H., and B.V. Marshall, 1968. Heat flow and water temperature fluctuations in the Denmark Strait. J. Geophys. Res., 73, 5829-5842.

Lachenbruch, A.H., and B.V. Marshall, 1969. Heat flow in the Arctic. Arctic, 22, 300-311.

Langseth, M.G., I. Malone and D. Berger, 1970. Sea floor geothermal measurements from Vema cruise 23. 2-CU-2-70, Lamont-Doherty Geol. Obs., Palisades, New York, Tech. Rept. 4, 168 p.

Langseth, M.G., I. Malone and D. Berger, 1972. Sea floor geothermal measurements from Vema cruise 25. 4-CU-4-72, Lamont-Doherty Geol. Obs., Palisades, New York, Tech. Rept. 4, 163 p.

Langseth, M.G., and G.W. Zielinski, 1974. Marine heat flow measurements in the Norwegian-Greenland Sea and in the vicinity of Iceland. in: Geodynamics of Iceland and the North Atlantic Area, ed. L. Kristjansson, Reidel, Dorecht-Holland, 227-296.

Law, L.K., W.S.B. Paterson and K. Whitham, 1965. Heat flow determinations in the Canadian Arctic Archipelago. Can. J. Earth Sci., 2, 59-71.

Lister, C.R.B., 1977. Qualitative models of spreading-centre processes, including hydrothermal penetration. Tectonophysics, 37, 203-218.

Lubimova, E.A., 1968. Thermal conditions of the earth and moon. Nauka, Moscow, 217-219, (in Russian).

Lubimova, E.A., G.A. Tomara and A.L. Aleksandrov, 1969a. Heat flow through the floor of the Arctic Basin in the vicinity of the Lomonosov Ridge. Dokl. Akad. Nauk. SSSR, 184, 403-405 (in Russian).

Lubimova, E.A., G.A. Tomara, R.M. Demenitskaya and A.M. Karasik, 1969b. Measurement of heat flow across the Arctic Ocean floor in the vicinity of the median Hakkel Ridge. Dokl. Akad. Nauk. SSSR, 186, 1318-1821 (Am. Geol. Inst. English Transl. 186, 22-24).

Lubimova, E.A., E.V. Kutas, F.V. Firsov, G.N. Starikova, V.K. Vlasov, L.N. Lyusova and E.R. Koperbach, 1972. Terrestrial heat flow on the Precambrian shields in the USSR. Geothermics, 1, 81-89.

Lubimova, E.A., B.G. Polyak, Y.B. Smirnov, R.I. Kutas, F.V. Firsov, S.I. Sergienko and L.N. Lutsova, 1973. Heat flow on the USSR territory catalogue of data. Geophys. Committee Acad. Sci., USSR, Moscow, 63 p.

Lubimova, E.A., V.N. Nikitina and G.A. Tomara, 1976. Thermal fields of the inland and marginal seas of the USSR. 43-52, in: Geological and Geophysical Studies and the Results of Heat Flow Determinations, Nauka, Moscow, 43-52 (in Russian).

Misener, A.D., 1955. Heat flow and depth of permafrost at Resolute Bay, Cornwallis Island, N.W.T., Canada. Trans. Am. Geophys. Union, 36, 1055-1060.

Niblett, E.R., and K. Whitham, 1970. Multi-disciplinary studies of geomagnetic variation anomalies in the Canadian Arctic. J. Geomagn. Geoelectr., 22, 99-111.

Palmason, G., 1967. On heat flow in Iceland in relation to the mid-Atlantic Ridge. in: Iceland and Mid-Ocean Ridges, 40, Soc. Sci. Islandica, Reykjavik, 111-127.

Palmason, G., 1973. Kinematics and heat flow in a volcanic rift zone with application to Iceland. Geophys. J.R. Astr. Soc., 33, 451-481.

Palmason, G., 1977. Heat flow and hydrothermal activity in Iceland. in: Geodynamics of Iceland and the North Atlantic Area, ed. L. Kristjansson, Reidel, Dorecht-Holland, 297-306.

Paterson, W.S.B., and L.K.Law, 1966. Additional heat flow determinations in the area of Mould Bay, Arctic Canada. Can. J. Earth Sci., 3, 237-246.

Pitman, W.C. III, and E.M. Herron, 1974. Continental drift in the Atlantic and the Arctic. in: Geodynamics of Iceland and the North Atlantic Area, ed. L. Kristjansson, Reidel, Dorecht-Holland, 1-16.

Polyak, B.G., and Y.A.B. Smirnov, 1968. Relationship between terrestrial heat flow and the tectonics of continents. Geotectonics, 4, 205-213.

Puranen, M., P. Jarvimaki, U. Hamalainen and S. Lehtinen, 1968. Terrestrial heat flow in Finland. Geoexploration, 6, 151-162.

Pye, G.D., 1971. Heat flow measurements in Baffin Bay and the Labrador Sea. MSc. thesis, Dalhousie Univ., Halifax, 41 p.

Pye, G.D., and R.D. Hyndman, 1972. Heat flow measurements in Baffin Bay and the Labrador Sea. J. Geophys.Res., 77, 938-944.

Rao, R.U.M., and A.M. Jessop, 1975. A comparison of the thermal character of shields. Can. J. Earth Sci., 12, 347-360.

Roy, R.F., E.R. Decker, D.D. Blackwell and F. Birch, 1968. Heat flow in the United States. J. Geophys. Res., 73, 5207-5221.

Sass, J.H., B.L. Nielsen, H.A. Wollenberg and R.J. Munroe, 1972. Heat flow and surface radioactivity at two sites in south Greenland. J. Geophys. Res., 77, 6435-6444.

Sclater, J.G., and J. Francheteau, 1970. The applications of terrestrial heat flow observations on current tectonic and

geochemical models of the crust and upper mantle of the earth. Geophys. J.R. Astr. Soc., 20, 509-542.

Sergiyenko, S.I., Ya.B. Smirnov and B.P. Stavitski, 1972. Heat flow in western Siberia. Geotectonics, 12, .

Swanberg, C.A., M.D. Chessman, G. Simmons, S.B. Smithson, G. Gronlie and K.S. Heier, 1974. Heat flow - heat generation studies in Norway. Tectonophysics, 23, 31-48.

Talwani, M., C.C. Windisch and M.G. Langseth, 1971. Reykjanes Ridge crest - a detailed geophysical study. J. Geophys.Res., 76, 473-517.

Taylor, A.E., and A.S. Judge, 1976. Geothermal data collection - northern wells 1975. Earth Phys. Br. Geothermal Series No. 6, 142 p.

Tomara, G.A., 1973. The analysis of records of the geothermal gradient on the floor of the Arctic Basin. in: Heat flows from the crust and upper mantle of the earth, results of researchs on the International Geophysical Project, ed. V.E. Vlokavich and E.A. Lubimova, Nauka, Moscow, 12, 145-149 (in Russian).

Arctic Ocean sediment thicknesses and upper mantle temperatures from magnetotelluric soundings

J. M. DeLaurier

ABSTRACT

Published Arctic Ocean magnetotelluric soundings (periods <7200 s) are used to determine electrical conductances of sub-bottom materials (presumably sediments) under Wrangel Plain, Chukchi Plateau, Lomonosov Ridge, East Siberian Shelf and Nansen-Gakkel Ridge. From these conductances, sediment thicknesses are determined using a model for the electrical conductivity profile of conducting sub-bottom materials. The conductivity profile is obtained by combining Magara's empirical porosity-depth relation with Archie's Law and with a linear relation to describe the increase in seawater (filling pores) conductivity with temperature. From this model, up to 4 km of conducting materials are inferred beneath the Chukchi Plateau and Wrangel Plain locations. These thicknesses are consistent with determinations from seismic studies. Between 1 km and 4 km of sub-bottom conducting materials are derived for two East Siberian Shelf locations. Lomonosov Ridge, displaying a relief of 2.9 km, is believed to be wholly composed of conducting materials (sediments? volcanics?) since about 3.7 km of these materials are estimated for the axial portion of the Ridge. The Nansen-Gakkel Ridge has less than 0.5 km of conducting materials. Four-layer conductivity models which fit the observed long-period (> 7200 s) apparent resistivity curves of Trofimov and Fonarev have provided a range of depths to and conductivities of an upper mantle conductor. They reported depths of 165 km, 320 km and 325 km, and conductivities of 0.32 S/m, 0.43 S/m and 0.59 S/m respectively for Chukchi Plateau, Lomonosov Ridge and Wrangel Plain. The models studied here provide an uncertainty in estimating these depths (about ± 15 per cent) and conductivities (factor of 10). Temperatures in the upper mantle between depths of 100 km and 400 km are expected to be within 1100°C and 2000°C. It is not possible to derive upper mantle temperatures more precisely than this because of the large uncertainty in estimating the electrical conductivity and in assuming an ionic intrinsic conduction mechanism for an olivine upper mantle. No upper mantle conductor could be detected beneath the Nansen-Gakkel Ridge location.

RÉSUMÉ

Les résultats publiés de sondages magnétotelluriques effectués dans l'océan Arctique (avec périodes <7200 s) ont servi à déterminer les conductances électriques de matériaux du sous-sol marin (en principe sédimentaires), de la plaine Wrangel, de la dorsale de Chukchi, de la dorsale de Lomonosov, de la plate-forme Sibérienne orientale, et de la dorsale de Nansen-Gakkel. Une fois les conductances obtenues, on peut déterminer l'épaisseur des sédiments en utilisant un modèle comportant le profil de conductivité électrique des matériaux conducteurs du sous-sol marin. On obtient le profil de conductivité en combinant la relation empirique de Magara (1976) entre la porosité et la profondeur, avec la loi d'Archie et une relation linéaire qui donnent l'augmentation de la conductivité de l'eau de mer (eau de remplissage des pores) en fonction de la température. De ce modèle, on déduit qu'entre 1 km et 4 km de matériaux conducteurs composent le sous-sol de la dorsale de Chukchi et de la plaine Wrangel. Cette épaisseur

concorde avec les déterminations basées sur des études séismiques. On a ainsi évalué à 1 km - 4 km l'épaisseur des matériaux conducteurs du sous-sol de deux emplacements du plateau Sibérien oriental. On pense que la dorsale de Lomonosov, qui forme un relief de 2.9 km, est entièrement composée de matériaux conducteurs (sédiments? roches volcaniques?), puisque la portion axiale de la dorsale comporte environ 3.7 km de ces matériaux. La dorsale de Nansen-Gakkel a moins de 0.5 km de matériaux conducteurs. Des modèles de conductivité composés de quatre couches, qui concordent avec les courbes de la résistivité apparente en fonction de la longue période observée (>7200 s), établies par Trofimov (1976), nous ont donné une gamme de résultats pour la profondeur et la conductivité d'un niveau conducteur du manteau supérieur. On a obtenu pour la profondeur 165 km, 320 km et 325 km, et la conductivité 0.32 S/m, 0.43 S/m et 0.59 S/m respectivement pour la dorsale de Chukchi, la dorsale de Lomonosov, et la plaine Wrangel. Les modèles étudiés ici nous donnent avec un certaine marge d'erreur la profondeur (envion ± 15 %) et la conductivité (facteur de 10). Dans le manteau supérieur, entre 100 km et 400 km, les températures se situent probablement entre 1100°C et 2000°C. Il n'est pas possible de déduire les températures du manteau supérieur avec une plus grande precision, parce que l'evaluation de la conductivité électrique et l'hypothèse d'un mécanisme intrinsèque de conduction ionique dans le manteau supérieur riche en olivine contiennent une importante marge d'erreur. On n'a pu déceler aucun niveau conducteur du manteau supérieur au-dessous de la dorsale de Nansen-Gakkel.

INTRODUCTION

It is difficult to infer a probable evolutionary history for the Arctic Ocean basins and rises if present sub-bottom geophysical parameters have not been determined. For example, if 1 km of sediments accumulated at a rate of 10 mm/1000 a, then the sediment accumulation time is 100 Ma. Hence, the underlying basement (oceanic layer 2, for instance) cannot be younger. Such simple computations can provide a valuable constraint in the development of Arctic Ocean evolutionary models. Sediment thickness is a required parameter. This paper will show that magnetotelluric experiments (M-T soundings), conducted on the frozen Arctic Ocean surface, are capable of deducing thicknesses of sub-bottom conducting materials (presumably sediments). Although several M-T soundings have been reported in the literature (Swift and Hessler, 1964; Trofimov et al., 1973; Trofimov and Fonarev, 1972, 1974, 1976; Deniskin and Lipskaya, 1967), with one exception (Deniskin and Lipskaya, 1967), sediment thicknesses have not been determined from them. The difficulty is that the electrical conductivity of sub-bottom sediments is not precisely known. This paper proposes a conductivity profile for sub-bottom sediments and, from it, deduces sediment thicknesses from the published Arctic Ocean data.

Another geophysical parameter of interest is the temperature distribution in the upper mantle beneath the Arctic Ocean. Upper mantle temperatures could be derived from conductivity models fitting the long-period (>7200 s) apparent resistivity measurements, although no such derivations have been published. In this paper, depths and electrical conductivities of a possible upper mantle conductor are redetermined from the apparent resistivity curves of Trofimov and Fonarev (1976). Possible upper mantle temperatures under the Arctic Ocean are inferred from these conductivities.

ARCTIC OCEAN MAGNETOTELLURIC SURVEY PROCEDURES

At each ice station, magnetotelluric surveys measure transient variations in four components of the earth's electromagnetic field: namely, two magnetic components, H_x and H_y, and two potential gradients (telluric components), E_x and E_y. The subscripts, x and y, refer to geographic north and east positive directions respectively. The electromagnetic response of an earth (and ocean) to an external inducing field arising from electric currents in the ionosphere is determined by the frequency dependence of the impedance (E_x/H_y or E_y/H_x), or equivalently of the apparent resistivity (ρ_α). Appendix 1 outlines the relation that these functions have with the electrical conductivities and thicknesses of a presumed multilayered earth.

For an oceanic model, the first layer consists of seawater and sub-bottom sediments, and its total conductance, or

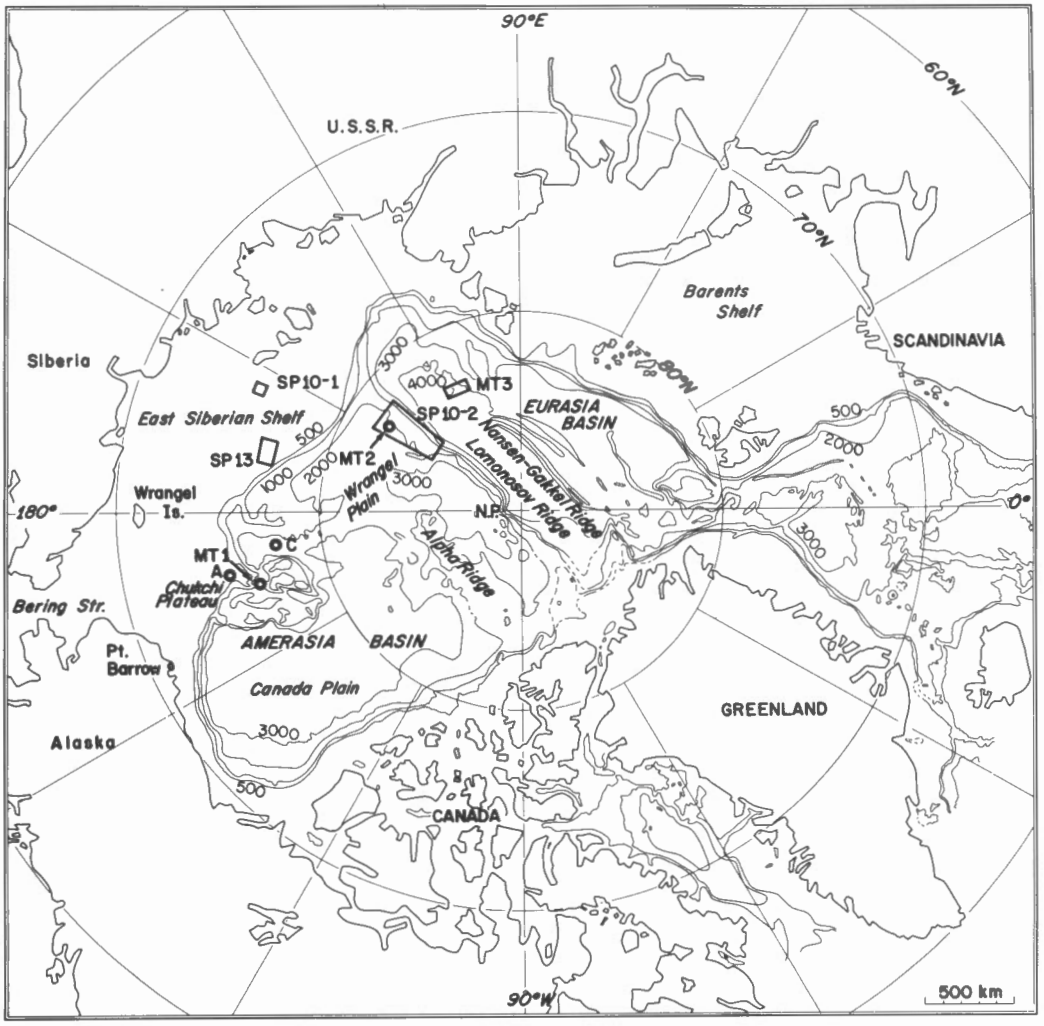

Figure 1. Generalized map of the Arctic Ocean showing locations of magnetotelluric studies at ice stations Charlie (C), Arlis 1 (A), Chukchi Plateau (MT1), Lomonosov Ridge (SP 10-2), Wrangel Plain (MT2), Nansen-Gakkel Ridge (MT3), and East Siberian Shelf (SP 10-1, SP 13).

conductivity-thickness product (see Appendix 1 for derivation) is computed directly from the observed short-period (< 7200 s) response. Since ocean depths can be determined by acoustic sounding, and seawater conductivity can be estimated from salinity-temperature profiles (discussed below) under each station, sub-bottom sediment conductance can be determined by subtracting seawater conductance from total conductance (Deniskin and Lipskaya, 1967; Trofimov and Fonarev, 1972). Sediment thickness can therefore be deduced if sediment conductivity is either known or assumed.

The drifting ice pack of the Arctic Ocean provides an excellent platform on which Soviet and American scientists have conducted magnetotelluric experiments. However, there are obvious difficulties. For example, summer thawing usually restricts operations to the winter months in which the consequent cold and harsh weather affects both personnel and instrumentation. The drifting ice precludes observations at a fixed site so that all surveys discussed below represent a spatial average. Deniskin and Lipskaya (1967) mentioned 10 to 15 km as the drift for their short period (< 1000 s) results.

Swift and Hessler (1964) discussed magnetotelluric recordings obtained on ice islands Charlie (C in Fig. 1) and Arlis 1 (A in Fig. 1). These ice islands drifted over

and near the Chukchi Plateau during the winters of 1959-1960 (Charlie) and 1960-1961 (Arlis). The magnetic field components were measured with an Askania magnetometer (Wienert, 1970, p. 149); the telluric components were obtained using two pairs of lead electrode strips (244 cm long by 5 cm wide) spaced 1.082 km apart on Charlie (Hessler, 1960) and 0.20 km apart on Arlis (Swift and Hessler, 1964), and suspended under ice in seawater. A simple voltmeter or potentiometer measured the potential differences. Swift and Hessler (1964) confirmed that their data were consistent with a simple two-layer oceanic model for variations with periods between 600 s and 3600 s. From their impedances, sediment thicknesses have been derived (Table 1) from the conductivity-depth model proposed in this paper.

Novysh and Fonarev (1966) summarized their experimental procedures in measuring the magnetic and telluric components on ice station North Pole 10. This ice station drifted from the shallow (80-260 m) East Siberian Shelf (SP 10-1 in Fig. 1) in 1962 to Makarov Basin and Lomonosov Ridge in 1963 (SP 10-2 in Fig. 1; Novysh and Fonarev, 1963, 1966; Fonarev and Novysh, 1965). A Bobrov (1964) magnetometer recorded the magnetic variations. Potentiometers measured potential differences between two pairs of non-polarizing silver chloride electrodes, immersed (through ice) to a depth of 7 m in seawater, and spaced 120 m and 153 m apart. When necessary the component orientations were corrected for ice floe rotations or magnetic declination changes.

These Soviet authors confirmed the predictable dependence of impedance on seawater depth at short-periods (< 600 s), pointed out the excellent (and predictable, Appendix 1) correlation between the orthogonal component pairs, $E_x - H_y$ and $E_y - H_x$, and classified a wide range (1 s to 86,400 s) of telluric field variations. Trofimov and Fonarev (1972, 1974, 1976) and Trofimov et al. (1973) plotted the SP 10-2 M-T sounding data as a sediment conductance map (Fig. 2) over the Lomonosov Ridge and as apparent resistivity curves (Figs. 3b,c) for two selected observing drift regions (precise locations and size not disclosed). Trofimov and Fonarev (1974, 1976) plotted magneto-telluric data obtained over and near the Chukchi Plateau (MT1 in Fig. 1) and the Nansen-Gakkel Ridge (MT3 in Fig. 1) as apparent resistivity curves (Figs. 3a, d), but they did not publish experimental procedures or collection dates. These data are re-examined in the following sections.

Deniskin and Lipskaya (1967) reported results of magnetotelluric observations collected over shallow (250 m to 330 m) water depths in the East Siberian Sea (SP 13 in Fig. 1). They measured the four field components with several instruments (types not disclosed) which covered a period range of 0.2 s to 100,000 s but apparent resistivity curves were published only for periods between 1 s and 1000 s. Each of Deniskin and Lipskaya's (1967) four apparent resistivity curves represented a 10 to 15 km

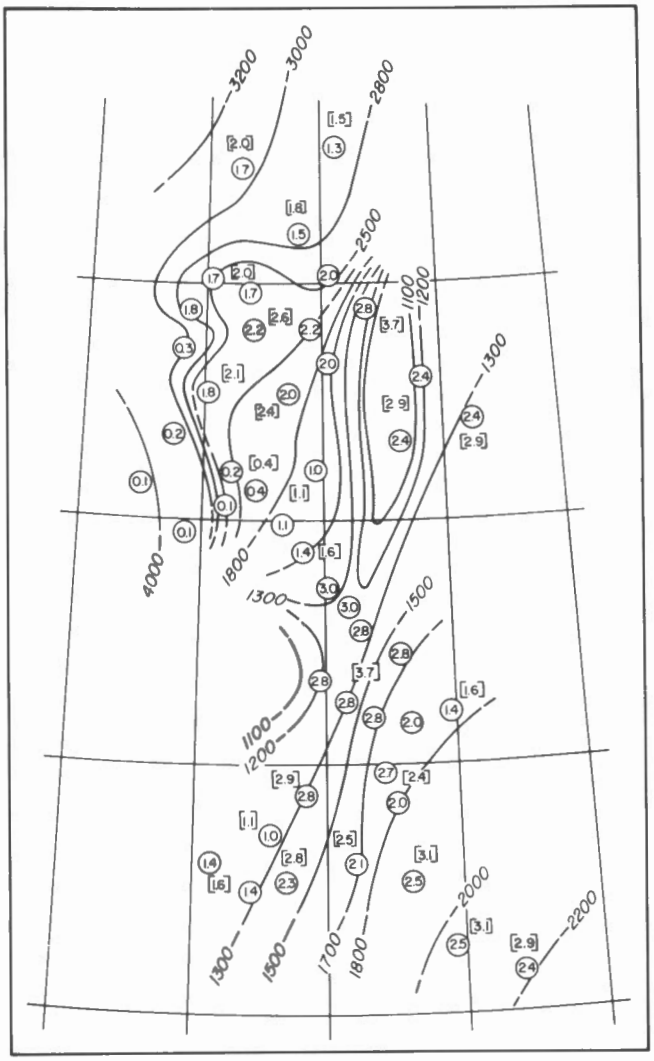

Figure 2. Observed sub-bottom integrated conductivity (in 1000 S, circles) and bathymetry (in m) over Lomonosov Ridge - SP 10-2 in figure 1 (after Trofimov et al., 1973). Sediment thicknesses (km) enclosed in square brackets are derived from figure 4b using the 60°C/km profile.

area with constant water depths (exact values not published), with distances between these areas of 50 to 80 km within the SP 13 drift region (Fig. 1). They deduced sediment thicknesses under the East Siberian Shelf drift regions of North Pole 13 and North Pole 10 (SP 10-1 in Fig. 1). From these data, sediment thicknesses are redetermined in Tables 1 and 2 using the model proposed in this paper.

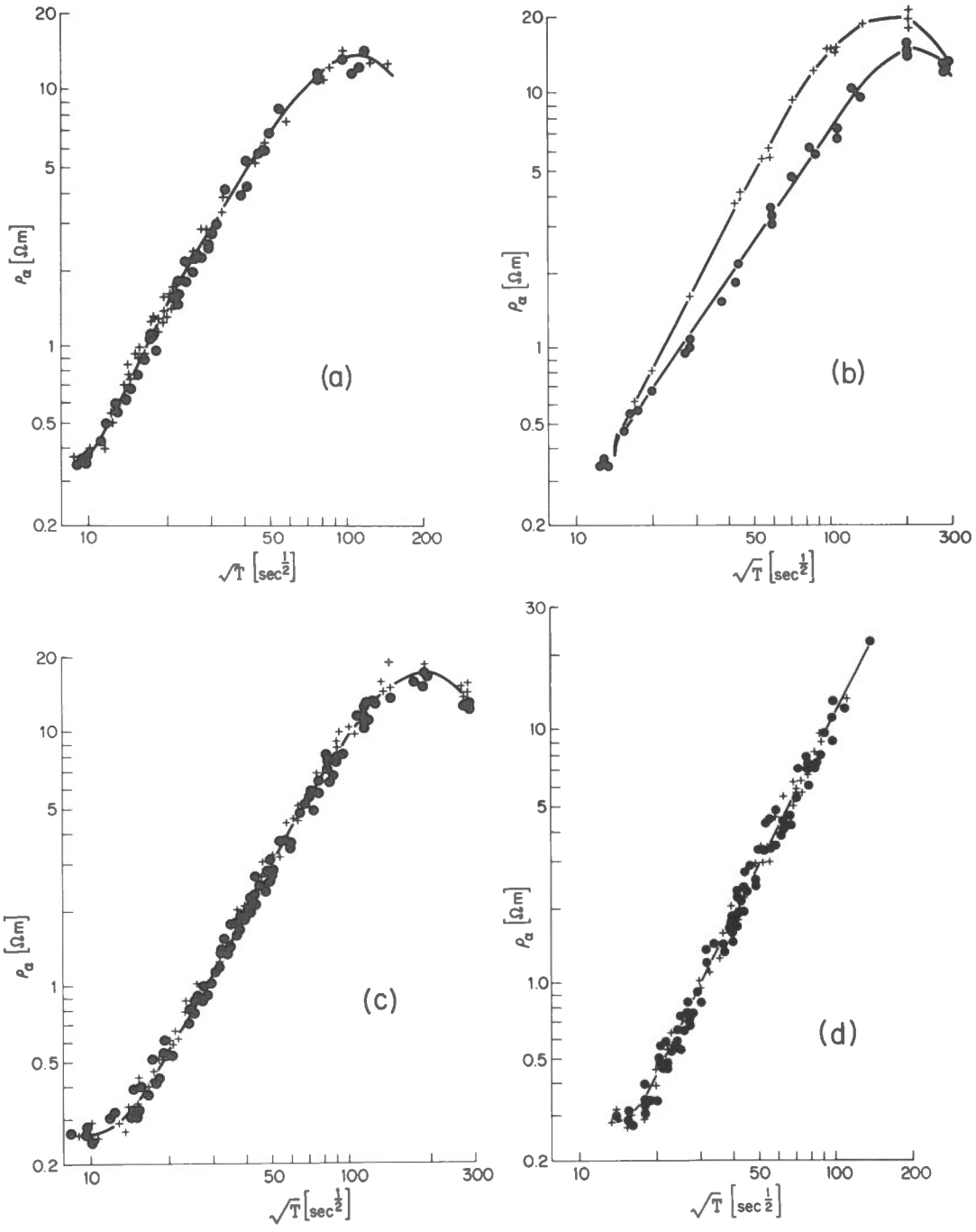

Figure 3. Observed apparent resistivity, ρ_α , measured in two orthogonal directions (+,-): (a) near Chukchi Plateau - MT1 in figure 1, (b) over Lomonosov Ridge - only the curve with plus signs interpreted, (c) over Wrangel Plain - MT2 in figure 1, (d) over Nansen-Gakkel Ridge - MT3 in figure 1 (from Trofimov and Fonarev, 1976).

TABLE 1

LOCATION	TOTAL CONDUCTANCE σh siemen (1)	WATER DEPTH D metre	PREDICTED DEPTH h metre	SEAWATER CONDUCTANCE σD siemen (2)	SEDIMENT CONDUCTANCE siemen	SEDIMENT THICKNESS metre $60^{o}C/km$	SEDIMENT THICKNESS metre $120^{o}C/km$ (3)
Charlie	7720±22%	2250	2660	6530	1190	1350	950
Arlis 1	3160±22%	425	1090	1230	1930	2250	1450
SP10-1	1330	130	460	380	950	1080	700
	1770	240	610	700	1070	1230	870

Notes: 1. Total conductance for Charlie and Arlis 1 obtained from the mean of 6 (Arlis 1) and 3 (Charlie) impedances in Swift and Hessler (1964; Table 1); for SP 10-1, the data here are those of Deniskin and Lipskaya (1967; Table 1).
2. Seawater conductivity taken to be 2.9 S/m.
3. Sediment thickness scaled from figure 4b for these two thermal gradients.

TABLE 2

LOCATION	PERIOD $\sqrt{s}$ (1)	TOTAL CONDUCTANCE siemen	WATER DEPTH metre	SEAWATER CONDUCTANCE siemen (3)	SEDIMENT CONDUCTANCE siemen	SEDIMENT THICKNESS metre $60^{\circ}C/km$	SEDIMENT THICKNESS metre $120^{\circ}C/km$ (4)
SP 13	15±10% (2)	5340	330	960	4380	-	3180
	11±10%	3910	300	870	3040	4300	2210
	8.5±10%	3020	250	730	2290	2780	1680
Chukchi Plateau	17±12%	6050	1100	3190	2860	3830	2070
Wrangel Plain	29±10%	10320	2550	7400	2920	3990	-
Lomonosov Ridge	22±10%	7830	2000	5800	2030	2400	-
Nansen-Gakkel Ridge	30±10%	10680	3500-4000	10150-11600	530-0	-	450-0

Notes:
1. SP 13 periods and water depths from Deniskin and Lipskaya (1967); for remaining locations, the periods and the water depths are obtained from Trofimov and Fonarev (1976).
2. Relative error is percent scatter about smooth apparent resistivity curves in figure 3 in text.
3. Seawater conductivity is taken to be 2.9 S/m.
4. Sediment thicknesses scaled from conductance profile of figure 4b for the adopted thermal gradients for Wrangel Plain, Lomonosov Ridge and Nansen-Gakkel Ridge.

ERRORS

The scatter of 10 to 20 per cent observed about the smooth apparent resistivity curves (Figs. 3a,b,c,d) and reported for the sediment conductances of figure 2 (Trofimov and Fonarev, 1972) is a measure of error for these M-T soundings. Contributions to this scatter include errors in determining event amplitudes and periods from the wide-band, highly irregular wiggly traces on the recordings (Deniskin and Lipskaya, 1967); possible large (10 to 20 per cent) deviations from the ideal condition of uniform water depths in regions of drift (10 to 15 km), important at short-periods (< 7200 s); and potentials induced at long-periods by motions due to tides and ice drift that strongly affect the earth potentials. Novysh and Fonarev (1963) corrected their telluric components using the measured ice drift velocities of SP 10 (data and procedure not disclosed). None of the papers discussed tidal contributions.

ARCTIC OCEAN SEAWATER CONDUCTIVITIES

Magnetotelluric experiments should be able to measure seawater conductivity* directly if field fluctuations of 1 to 240 s can be obtained reliably; none however have been reported. Estimates can be obtained from a knowledge of the temperature, salinity and pressure profiles within Arctic seawater.

Within the Eurasia and Canada Basins, for depths greater than 300 m, water temperatures are between -1°C and 1°C, and salinities are uniform between 34 ppt and 35 ppt (Coachman and Aagaard, 1974). Surface water (< 300 m) salinities can be as low as 33 ppt for the Eurasia Basin and 27 ppt for the Canada Basin (Coachman and Aagaard, 1974) with temperatures of -1°C to -2°C in ice-covered regions and up to 2°C (locally 6°C) in ice-free regions.

For deep (> 300 m) Arctic seawater within the above salinity and temperature range, electrical conductivities are between 2.66 S/m and 3.16 S/m (interpolated and extrapolated from Bullard and Parker, 1971, Table II, p. 723). Locally, seawater conductivity may be 2.29 S/m (0°C, 27 ppt salinity). Hence, for computation purposes in this paper, a constant value of 2.9 S/m has been adopted for deep (>300 m) Arctic seawater.

*S.I. units used: conductivity unit is 1 siemen per metre (1 S/m).

Swift and Hessler (1964) used a seawater conductivity of 3 S/m. Deniskin and Lipskaya (1967) used an average value of 2.5 S/m (no details disclosed) for the seawater over the East Siberian Shelf. Trofimov and Fonarev (1972) derived a seawater conductivity of 2.7 S/m from measurements of salinity and temperature (no details or references given).

A PROPOSED SUB-BOTTOM CONDUCTIVITY AND CONDUCTANCE PROFILE

Sediments with conductivities near or much less than 0.1 S/m contribute only a small amount to the total conductance of the seawater-sediment layer. For example, if a 4 km seawater-sediment layer has a total conductance of 7300 S, an additional 2 km sediment section of conductivity 0.1 S/m will add only 3 per cent to this total conductance. Since the scatter about the smooth apparent resistivity curves (Figs. 3a,b,c,d) is 10 to 20 per cent, Arctic Ocean surface M-T soundings cannot resolve this additional 2 km of sediments. Further, from Appendix 1 it can be shown that the conductivity of the layer beneath seawater and sediments must be much less than 0.15 S/m if straight lines of slope 2 are to be obtained on apparent resistivity curves. Because the observed apparent resistivity curves do have slopes of approximately 2, 0.1 S/m can be considered to be a lower bound for sediment conductivity at depth within the sediment section.

Boyce (1968) measured (at 25°C, 101.3 kPa) electrical conductivities of 46 samples from 7 cores (< 3 m long) recovered from the basin floor south of Bering Sea and from the adjacent Alaskan shelf. Values averaged 2.86 S/m for basin samples and 1.96 S/m for shelf samples (Boyce, 1968). Measured porosities were between 58 and 89 per cent. A reduction of about 40 per cent to these measured conductivities is predicted at a sea bottom temperature of 0°C (Keller, 1966, p. 555). Hence, a conductivity of 1.7 S/m can be considered to be an upper bound for saturated sediments near the sea-floor.

An upper bound of 1.7 S/m near the sea-floor and a lower bound of 0.1 S/m at depth within the sediment section suggest that sediment conductivity decreases with depth of burial. Sediment bulk conductivity (σ_b) is the product of pore fluid conductivity (σ_w) and porosity (μ) squared ($\sigma_b = \sigma_w \mu^2$, Archie's Law, Brace et al., 1965). Porosity is known to decrease rapidly in the first few hundred metres of silty or clayey deposits until the increasing grain to grain contact

supports the compacting load (Rieke and Chilingarian, 1974). For saturated sub-bottom sediments, pore pressure is hydrostatic. Electrical conductivity of saturated crustal rocks depends on effective pressure, that is, total overburden pressure less pore pressure (Brace, 1971). Increasing the effective pressure tends to close connections between pores and thereby removes conduction paths for electric current. Thus the bulk sediment conductivity decreases with depth of burial.

Hence, if the pore fluid (seawater) conductivity variation with depth can be determined (see below), the empirical shale porosity-depth relation of Magara (1976) combined with Archie's law generates a conductivity-depth profile. Integrating this profile gives sediment conductance for any sediment thickness. Figure 4 displays both the conductivity and conductance profiles for four thermal gradients (details in Appendix 2).

Pore fluid (seawater) conductivity increases with temperature. Quist and Marshall (1968) have measured electrical conductances of prepared 0.01 M and 0.1 M NaCl solutions over a large range of temperatures (0-800°C) and pressures ($0-4 \times 10^5$ kPa). Extrapolating their data to a 0.5 M NaCl solution (seawater with salinity of 30 ppt) and for a thermal gradient of 50° C/km, seawater conductivity increases at the rate of 5×10^{-3} S/m^2. An assumed linear function with depth (Appendix 1) is consistent with Quist and Marshall (1968) data provided temperatures do not exceed 250°C.

Heat flow data from the Arctic Ocean (Jessop et al., 1976) indicate mean thermal gradients of 69 ± 13°C/km for Lomonosov Ridge, 67 ± 10°C/km for Makarov Basin and 120 ± 57°C/km for Nansen-Gakkel Ridge. The choice of 60°C/km and 120°C/km in Tables 1 and 2 is certainly within these large standard deviations and within the 10-12 per cent relative error for sediment conductances. Since geothermal gradients have not been measured at the remaining locations of Tables 1 and 2, sediment thicknesses are given for both 60 and 120°C/km gradients.

ARCTIC OCEAN SEDIMENT THICKNESSES

Either impedance or apparent resistivity can be used to determine sub-bottom sediment conductance (Appendix 1). For a seawater layer of conductivity, σS/m, and of thickness, h m, the impedance (ohm) is

$$\frac{E_x}{H_y} = \frac{1}{\sigma h}$$

Under ice island Charlie, h agreed within 16 per cent with the measured depth (2.3 km), but under Arlis 1 h was more than double the actual water depth (~ 425 m). Swift and Hessler (1964) interpreted this discrepancy to be the influence of electric currents within the deep Canada Basin-Beaufort Sea to the east of Arlis. However, a thick section of highly conducting sediments under Arlis easily explains the discrepancy between apparent and observed water depths (Deniskin and Lipskaya, 1967). Table 1 gives an estimated sub-bottom sediment thickness of about 1.0 km under Charlie and about 2.3 km under Arlis 1. Deniskin and Lipskaya (1967) gave a smaller section (1.84 km) under Arlis but, unlike the model proposed in this paper, they presumed a constant sediment conductivity (1.25 S/m).

Table 2 gives the total estimated sediment thicknesses for the SP 13 locations (two of the curves of Deniskin and Lipskaya, 1967, have been combined). Large sediment thicknesses are deduced for the East Siberian Shelf. Note in Table 2 that a high thermal gradient (120°C/km) is required to explain the high sediment conductance of 4380 S if pore fluids have the seawater salinity assumed here (30 ppt).

Sediment conductances at 45 sites over Lomonosov Ridge (Fig. 2) give up to 3.7 km of sediments from the model in figure 4. Lomonosov Ridge, having a relief of 2.9 km (Fig. 2), is therefore totally composed of highly conducting materials (sediments? volcanics?).

Total conductances are obtained from the four apparent resistivity curves given in figures 3a,b,c,d. Note in figure 4b that sediment conductances for the Chukchi Plateau and Wrangel Plain locations can only be explained for thermal gradients greater than 50°C/km, assuming 30 ppt salinity for pore fluids. Large thicknesses (2-4 km) of conducting materials (sediments presumably) have been detected for the Chukchi Plateau, Wrangel Plain and Lomonosov Ridge locations, but less than 0.5 km cover the Nansen-Gakkel Ridge.

DISCUSSION

The conductivity-depth model presented here depends on porosity, the geothermal gradient, and seawater salinity and is independent of sediment lithology. In any conductivity-depth model for saturated rocks

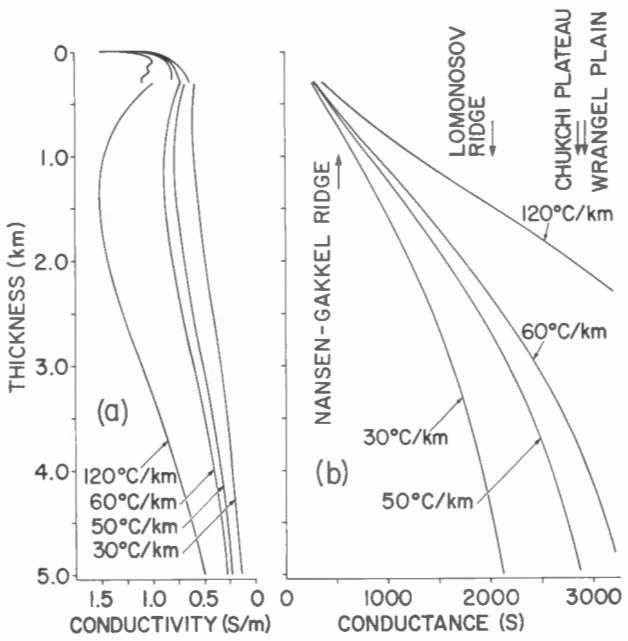

Figure 4. Sediment conductivity profiles (a) and sediment conductance profiles (b) versus depth for four thermal gradients. Observed sediment conductance for the four Arctic locations are indicated with arrows in (b).

an expression is required to control the volume content of seawater (in pores) with depth. Magara's (1976) empirical shale porosity-depth relation is used here.

For the Chukchi Plateau location (MT1 in Fig. 1), about 3.8 km of conducting sediments can be inferred (Table 2) from figure 4b. This is near the maximum thickness which can be detected with M-T soundings (for a 60°C/km geothermal gradient and salinity of 30 ppt) as seawater conductivity decreases rapidly for temperatures much higher than 250°C, or below 4.1 km for a 60°C/km gradient (Quist and Marshall, 1968, Fig. 11). Shaver and Hunkins (1964), however, interpreted their Chukchi Plateau magnetic anomaly in terms of a model which includes 12 km of non-magnetic materials. If their model is correct and the 12 km of non-magnetic materials are sediments, then M-T soundings have detected only 30 per cent of the section under the Chukchi Plateau.

To the south of the Chukchi Plateau at the Arlis 1 position Table 1 indicates either 2.3 km or 1.5 km of sediments. No heat flow measurements have been made at this location. Hunkins (1965) inferred 6 km of sediments (3 km/s velocity) from a reversed seismic refraction profile between Arlis 1 and Point Barrow, Alaska. A thermal gradient less than 30°C/km is required in order to deduce this thickness from the conductance profile in figure 4b.

At the Wrangel Plain location (MT2 in Fig. 1), about 4 km of sediments have been estimated using a 60°C/km thermal gradient which is near the measured values (see above). Kutschale (1966) reported at least 3.5 km of sediments over central Wrangel Plain based on seismic reflection studies.

Table 2 lists 2.4 km of sediments present at the unstated Lomonosov Ridge location where the apparent resistivity curve (Fig. 3b) was measured. Figure 2 shows that a maximum of 3.7 km (square brackets) of conducting sediments occur beneath the ridge crest. These sediment thicknesses (Fig. 2) are consistent with seismic results of Kiselev (1970) and Gramberg and Kulakov (1975), namely, a unit 0.1 - 1.0 km thick covering an undulating topography of a second deeper unit 2.5 - 3.0 km thick. Hence, the maximum of 3.7 km of conducting materials adequately accounts for the relief of 2.9 km displayed in figure 2.

For the Nansen-Gakkel Ridge drift region (MT3 in Fig. 1) ocean water depths between 3.5 km and 4.0 km were given by Trofimov and Fonarev (1976). Using the 3.5 km depth, Table 2 lists a sediment thickness of 0.45 km, consistent with the 0.3 to 0.4 km of sediments present as a discontinuous veneer (Rassokho et al., 1967; Demenitskaya and Karasik, 1969; Deminitskaya and Hunkins, 1970).

UPPER MANTLE CONDUCTOR

Few long-period (>7200 s) M-T soundings are published in the literature. This is surprising since reliable measurements of the electrical conductivity of the upper mantle can determine in principle its temperature distribution (Tozer, 1959). Consequently, the long-period apparent resistivity data (Fig. 3) of Trofimov and Fonarev (1976) are most welcome. However, difficulties in obtaining reliable M-T data are numerous, some of which are long term instrumentation stability, electrode polarization, tidal influences and non-uniqueness in practical inversion techniques. It is presumed that some of these difficulties have been resolved but Trofimov and Fonarev (1976) do not discuss this.

A four-layer conductivity model of the earth is assumed. For this model, the seawater and sub-bottom conducting sediments are the first two layers, the underlying layer is resistive and the fourth layer is a conducting half-space. The sum of seawater and sediment conductances is, however, a constraint in generating the apparent resistivity curves for such models. For computation purposes, the conductivity of the sediment layer is determined by dividing sediment thickness into the corresponding sediment conductance of Table 2.

Trofimov and Fonarev (1976) reported depths of 165 km, 320 km and 325 km, and conductivities of 0.32 S/m, 0.43 S/m and 0.59 S/m for an upper mantle conductor beneath the Chukchi Plateau, Lomonosov Ridge and Wrangel Plain locations respectively. The rectangles (CD and TL) of figure 5 provide a range of depths (about ± 15 per cent) and of conductivities (factor of ~10) that give satisfactory fits (within 20 per cent) to the observed ρ_α curves (Figs. 3a,b,c). The conductivity profiles of Banks (B2, 1972), Parker (P, 1970) and Larsen (L, 1975) are also included in figure 5. Obviously, greater precision (by an order of magnitude) in measuring apparent resistivity

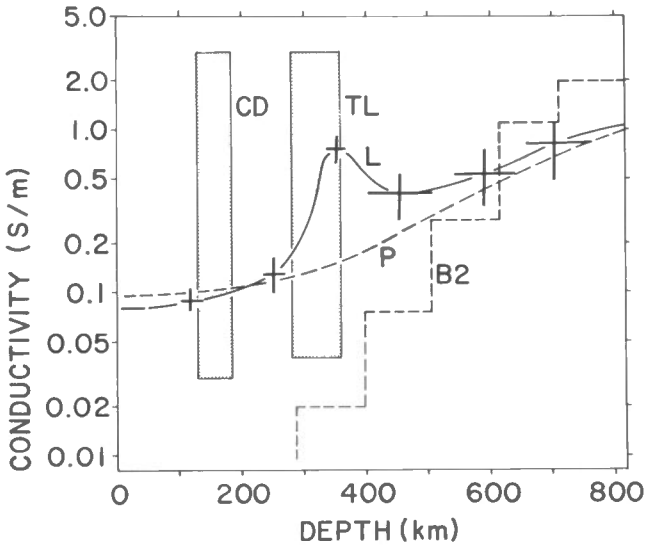

Figure 5. Conductivity profiles of Larsen (L,1975), Parker (P,1970) and Banks (B2, 1972). Rectangles are the range of conductivities and depths for Chukchi Plateau (CD) and Wrangel Plain - Lomonosov Ridge (TL).

is required to significantly reduce the uncertainties indicated in figure 5.

Upper mantle temperatures are estimated from the conductivity data of figure 5. A mineral composition for the upper mantle must, however, be assumed. Olivine (90 per cent forsterite, Fo90) is a major component (60-70 per cent) of lherzolite which occurs as nodules in kimberlite pipes; hence, Ito and Kennedy (1967) concluded that their lherzolite sample probably represents the composition of the upper mantle. The laboratory results of Duba et al. (1974) provide electrical conductivity versus temperature (to 1660°C) and pressure (to 8 x 10^5 kPa) for an olivine (Fo91) from the Red Sea area. It is further assumed that the ionic intrinsic conduction mechanism prevails throughout the upper mantle and that the pressure coefficient for conductivity is negligible (Duba et al., 1974). Therefore, these data are used to derive (following Duba, 1972) the temperature profiles of figure 6 from the conductivity data of figure 5.

For upper mantle depths between 100 km and 400 km, temperatures are expected to be within 1100°C and 2000°C (profiles TO, CR, L,P in Fig. 6). Trofimov and Fonarev (1976) ρ_α data (Fig. 3) give temperatures consistent with this expectation but the obvious uncertainty in estimating mantle conductivity (CD and TL in Fig. 5) precludes a more precise determination of upper mantle temperatures. Another source for uncertainty is the simplifying assumption of an ionic intrinsic conduction mechanism for an olivine dominant mantle. Other mechanisms such as ionic extrinsic conduction or electronic conduction may predominate within the mantle. Further, laboratory results (Duba, 1976) show that a high conductivity could be the result of the order-disorder state of the mineral and of time. Duba (1976) discusses these and other insufficiently studied mechanisms. The simplifying assumption used here (ionic intrinsic conduction) could therefore have resulted in temperatures about 300°-500°C too high. It is possible, to conclude only that upper mantle temperatures are within 1100°C to 2000°C between 100 km and 400 km.

At the Nansen-Gakkel Ridge location, no mantle conductor can be detected with the observed curve (Fig. 3d). Trofimov and Fonarev (1976) stated that a mantle conductor, if present, could not be at a depth less than 400 km. However, the Nansen-Gakkel Ridge has been considered to be a spreading centre (Pitman and Talwani,

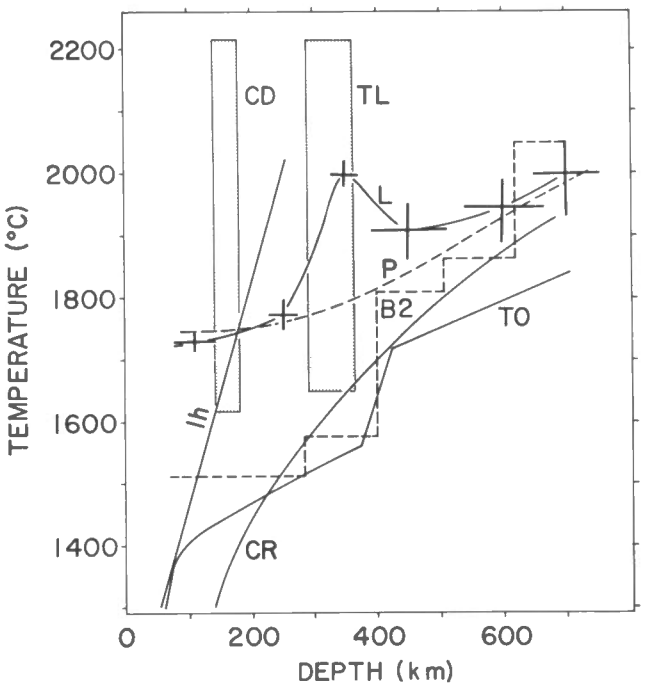

Figure 6. Temperature profiles L, P and B2 determined from the corresponding conductivity profiles of figure 5 using Duba et al. (1974) parameters: $\log \sigma_x = 6.82$ and $A_x = 3.13$, for their Red Sea olivine (Fo91). Temperatures within rectangles correspond to the conductivities observed for Chukchi Plateau (CD) and Wrangel Plain - Lomonosov Ridge (TL) of figure 5, CR is Clark and Ringwood (1964) oceanic geotherm; TO is Turcotte and Oxburgh (1969) oceanic geotherm; also shown is the lherzolite (lh) solidus extrapolated from Ito and Kennedy (1967).

1972), a concept strongly supported by the epicentre and focal mechanism studies of Sykes (1965, 1967) and Chapman and Solomon (1976). The Oxburgh and Turcotte (1968) model for a presumed ascending plume beneath a spreading ridge has temperatures near 1800°C at depths between 100 km and 200 km depths. Using the data of Duba et al. (1974) the corresponding conductivity at these depths could be near 0.2 S/m and such a conductor should be detected with M-T soundings. It is unfortunate that Trofimov and Fonarev (1976) could not publish more than one long-period (at 140 $s^{\frac{1}{2}}$) ρ_α value. Hence, their data cannot detect an expected upper mantle conductor at shallow depths beneath the Nansen-Gakkel Ridge.

CONCLUSIONS

The available M-T sounding data over the Arctic Ocean has been re-examined and interpreted in order to show that certain geophysical parameters of the Arctic Ocean sub-bottom crust and mantle can be inferred. Sediment thicknesses and upper mantle temperatures are two geophysically important properties which have been considered in this paper.

Sediment thicknesses are derived using a proposed profile for the electrical conductivity of conducting sub-bottom materials (usually sediments). This conductivity profile is obtained by combining Magara's (1976) empirical porosity-depth relation with Archie's Law and with a linear relation to describe the increase of seawater conductivity with temperature. The Wrangel Plain, the Chukchi Plateau and the Lomonosov Ridge have 1 to 4 km of conducting materials, equivalent to the thicknesses estimated for the East Siberian Shelf. The lithology of these conducting materials has not been determined but a sedimentary origin has been presumed. Hence, short-period (<7200 s) M-T sounding is a useful tool to infer sediment thicknesses from the frozen Arctic Ocean surface provided geothermal gradients are known.

A large uncertainty (two orders in magnitude) exists in estimating upper mantle conductivity from the observed apparent resistivity curves; greater precision (by at least an order in magnitude) is required in measuring long-period apparent resistivities. The simplifying assumptions used in deriving temperatures from these conductivity estimates may not be valid for upper mantle conditions and hence the derivations above could have grossly overestimated in situ temperatures. At present it can only be concluded that the upper mantle between depths of 100 km and 400 km beneath the Arctic Ocean could have temperatures between 1100°C and 2000°C.

ACKNOWLEDGEMENTS

I am indebted to Dr. P.A. Camfield for his editing of a first draft.

REFERENCES

Banks, R.J., 1972. The overall conductivity distribution of the Earth. J. Geomag. Geoelectr., 24, 337-351.

Berdichevskiy, M.N., 1965. Electrical prospecting with the telluric current method. Quart. Col. School of Mines, 60,

No. 1, (Translated by Mr. G.V. Keller) 216 p.

Bobrov, V.N., 1964. Three-component magnetic variation station IZMIRAN-1. Geomag. and Aeron., 4, 884-886 (Am. Geophys. Union English Transl.).

Boyce, R. E., 1968. Electrical resistivity of modern marine sediments from the Bering Sea. J. Geophys. Res., 73, 4739-4766.

Brace, W.F., 1971. Resistivity of saturated crustal rocks to 40 km based on laboratory measurements. in: The Structure and Physical Properties of the Earth's Crust, ed. J.G. Heacock, Am. Geophys. Union Geophys. Mono. 14, 243-255.

Brace, W.F., A.S. Orange and T.M. Madden, 1965. The effect of pressure on the electrical resistivity of water-saturated crystalline rocks. J. Geophys. Res., 70, 5669-5678.

Brace, W.F., and A.S. Orange, 1968. Further studies of the effects of pressure on electrical resistivity of rocks. J. Geophys. Res., 73, 5407-5420.

Bullard, E.C., and R.L. Parker, 1971. Electromagnetic induction in the Oceans. in: The Sea, v. 4, Part 1, ed. Arthur E. Maxwell, Wiley-Interscience, New York, 695-750.

Cagniard, L., 1953. Basic theory of magnetotelluric method of geophysical prospecting. Geophysics, 18, 605-635.

Chapman, M., and S.C. Solomon, 1976. North American-Eurasian plate boundary in northeast Asia. J. Geophys. Res., 81, 921-930.

Clark, S.P. Jr., and A.E. Ringwood, 1964. Density distribution and constitution of the mantle. Rev. Geophys., 2, 35-88.

Coachman, L.K., and K. Aagaard, 1974. Physical oceanography of Arctic and subarctic seas. in: Marine Geology and Oceanography of the Arctic Seas, ed. Y. Herman, Springer-Verlag, New York, p. 1-72.

Demenitskaya, R.M. and K.L. Hunkins, 1970. Shape and structure of the Arctic Ocean. in: The Sea, v. 4, Part II, ed. Arthur E. Maxwell, Wiley-Interscience, New York, 233-249.

Demenitskaya, R.M., and A.M. Karasik, 1969. The active rift system of the Arctic Ocean. Tectonophysics, 8, 345-351.

Deniskin, N.A., and N.V. Lipskaya, 1967. Results of magnetotelluric probing in the station Severnyy Polyus 13 drift area. Dokl. Akad. Nauk. SSSR, 177, 1320-1323 (Am. Geol. Inst. English Transl. 177, 28-30).

Duba, A., 1972. The electrical conductivity of olivine. J. Geophys. Res., 77, 2483-2495.

Duba, A., 1976. Are laboratory electrical conductivity data relevant to the earth? Acta Geodaet., Geophys. et Montonist., 11, 485-495.

Duba, A., H.C. Heard and R.N. Schock, 1974. Electrical conductivity of olivine at high pressure and under controlled oxygen fugacity. J. Geophys. Res., 79, 1667-1673.

Fonarev, G.A., and V.V. Novysh, 1965. Some results of telluric current measurements at station North Pole 10 in 1963. Dokl. Akad. Nauk. SSSR, 160, 332-333 (Am. Geol. Inst. English Transl., 160, 1-2).

Gramberg, I.S., and Yu. N. Kulakov, 1975. General geological features and possible oil and gas provinces of the Arctic Basin. in: Canada's Continental Margins, eds. C.J. Yorath, E.R. Parker, and D.J. Glass, Can. Soc. Petrol. Geol. Mem. 4, 525-529.

Hamilton, E.L., 1959. Thickness and consolidation of deep-sea sediments. Bull. Geol. Soc. Am., 70, 1399-1424.

Heezen, B.C., and M. Ewing, 1961. The mid-oceanic ridge and its extension through the Arctic Basin. in: Geology of the Arctic, v. 1, ed. G.O. Raasch, Univ. Toronto Press, Toronto, 622-642.

Hessler, V.P., 1960. Telluric current micropulsations on Arctic drifting station Charlie. Nature, 188, 567-568.

Hunkins, K.L., 1965. The Arctic continental shelf north of Alaska. in: Continental Margins and Island Arcs. ed. W.H. Poole, Geol. Survey Can. Paper 66-15, 196-205.

Ito, K., and G.C. Kennedy, 1967. Melting and phase relations in a natural periodotite to 40 kilobars. Am. J. Sci., 265, 519-538.

Jessop, A.M., M.A. Hobard and J.G. Sclater, 1976. The world heat flow data collection - 1975. Earth Phys. Br. Geothermal Series No. 5, 125 p.

Keller, G.V., 1966. Electrical properties of rocks and minerals. in: Handbook of Physical Constants. ed. Sydney P. Clark Jr., Geol. Soc. Am. Mem. 97, 553-577.

Kiselev, Yu.G., 1970. Some of the features of the present morphotectonic structure of the Lomonosov Ridge based on seismic data. Morskaya Geol. i Geofiz., 1, 123-128 (in Russian).

Kutschale, H.W., 1966. Arctic Ocean geophysical studies - the southern half of the Siberian basin. Geophysics, 31, 682-710.

Larsen, J.C., 1975. Low frequency (0.1-6.0 cpd) electromagnetic study of

deep mantle electrical conductivity beneath the Hawaiian Islands. Geophys. J. R. Astr. Soc., 43, 17-46.

Magara, K., 1976. Water explusion from elastic sediments during compaction-directions and volumes. Am. Assoc. Petrol. Geol. Bull., 60, 543-553.

Novysh, V.V., and G.A. Fonarev, 1963. Telluric currents in the Arctic Ocean. Geomag. and Aeron., 3, 919-921 (Am. Geophys. Union English Transl.).

Novysh, V.V., and G.A. Fonarev, 1966. Some results of electromagnetic investigations in the Arctic Ocean. Geomag. and Aeron., 6, 325-327 (Am. Geophys. Union English Transl.).

Oxburgh, E.R., and D.L. Turcotte, 1968. Mid-ocean ridges and geotherm distribution during mantle convection. J. Geophys. Res., 73, 2643-2661.

Parker, R.L., 1970. The inverse problem of electrical conductivity in the mantle. Geophys. J. R. Astr. Soc., 22, 121-138.

Pitman, W.C. III and M.Talwani, 1972. Sea-floor spreading in the North Atlantic. Geol. Soc. Am. Bull., 83, 619-646.

Price, A.T., 1962. The theory of magnetotelluric methods when the source field is considered. J. Geophys. Res., 67, 1907-1918.

Quist, A.S., and W.L. Marshall, 1968. Electrical conductance of aqueous sodium chloride solutions from 0 to 800° and at pressures to 4000 bars. Jour. Phys. Chem., 72, 684-703.

Rassokho, I.I., L.I. Senchura, R.M. Demenitskaya, A.M. Karasik, Yu. G. Kiselev and N.K. Timoshenko, 1967. The central submarine Arctic Ridge and its place in the ridge system of the Arctic Ocean. Doklady Akad. Nauk. SSSR, 172, 659-662 (Transl. 379, U.S. Naval Oceano. Office).

Rieke, H.H. III and G.V. Chilingarian, 1974. Compaction of Argillaceous Sediments. Developments in Sedimentology, Series 16, Elsevier, New York, 424 p.

Schmucker, V., 1970. Anomalies of geomagnetic variations in the southwestern United States. Bull. Scripps Inst. Oceanography, 13, La Jolla, Calif., 165 p.

Shaver, R., and K. Hunkins, 1964. Arctic Ocean geophysical studies: Chukchi Cap and Chukchi Abyssal Plain. Deep-Sea Res., 11, 905-916.

Swift, D.W., and V.P. Hessler, 1964. A comparison of telluric current and magnetic field observations in the Arctic Ocean. J. Geophys. Res., 69, 1883-1893.

Sykes, L.R., 1965. The seismicity of the Arctic. Bull. Seism. Soc. Am., 55, 501-518.

Sykes, L.R., 1967. Mechanism of earthquakes and nature of faulting on the mid-oceanic ridges. J. Geophys. Res., 72, 2131-2153.

Tozer, D.C., 1959. The electrical properties of the Earth's interior. in: Physics and Chemistry of the Earth, v. 3, Pergamon Press, New York, 414-436.

Trofimov, I.L., and G.A. Fonarev, 1976. Deep magnetotelluric surveys in the Arctic Ocean. in: Geoelectric and Geothermal Studies, KAPG Geophys. Mono., ed. A. Adam, Academiai Kiodo, Budapest, 712-715.

Trofimov, I.L., and G.A. Fonarev, 1974. Some results of magnetotelluric sounding in the Arctic Ocean. Izv., Earth Phys., 89-92 (Am. Geophys. Union English Transl.).

Trofimov, I.L., and G.A. Fonarev, 1972. Some results of magnetotelluric profiling in the Arctic Ocean. Izv., Earth Phys., 81-82 (Am. Geophys. Union English Transl.).

Trofimov, I.L., G.A. Fonarev and V. S. Shneyer, 1973. Some results of magnetotelluric research in the central Arctic. J. Geophys. Res., 78, 1398-1400.

Turcotte, D.L., and E.R. Oxburgh, 1969. Convection in a mantle with variable physical properties. J. Geophys. Res., 74, 1458-1474.

Wienert, K.A., 1970. Notes on geomagnetic observatory and survey practice. UNESCO, Paris, 217 p.

APPENDIX 1

Derivation of Total Conductance

From the solution of Maxwell's electromagnetic equations (Price, 1962; Berdichevskiy, 1965; Schmucker, 1970) for two or more horizontal layered earth models, the following ratios are the geophysically measurable quantities:

$$\frac{H_z}{H} = -i\nu G(o)$$

$$\frac{E_x}{H_y} = \frac{E_y}{H_x} e^{i\pi} = i\mu_o \omega G(o)$$

where H is vertical magnetic component and H $=(H_x^2 + H_y^2)^{\frac{1}{2}}$ and remaining components are defined in the text. G(0) is a function of the conductivities (σ_i) and the thicknesses (h_i) of each layer, of wave number (ν) and of frequency ($f = \omega/2\pi$). The magnetic permeability ($\mu_o = 4 \times 10^{-7}$ H/m) is a constant for all space.

The function G(0) can be evaluated for any number (n) of layers from the expression:

$$G_n(0) = -\frac{1}{\theta_1} \coth \left[\theta_1 h_1 + \operatorname{argcoth} \left(\frac{\theta_1}{\theta_2} \coth \ldots + \operatorname{argcoth} \frac{\theta_{n-1}}{\theta_n}\right)\ldots\right]$$

where $\theta_i^2 = \nu^2 + i\mu_o \omega \sigma_i$

If the conductivity of the first layer (seawater-sediments) is much larger than that of the second layer, the impedance for this two-layer oceanic model is

$$\frac{E_x}{H_y} = \frac{E_y}{H_x} e^{i\pi} = \frac{1}{\sigma_1 h_1}$$

(Swift and Hessler, 1964) where $\sigma_1 h_1$ is the integrated conductivity, or total conductance of the first layer. A 4 km deep ocean, conductivity 2.9 S/m, has a total conductance

$$\sigma_1 h_1 = 11{,}600 \text{ S}$$

The apparent resistivity is defined to be (Cagniard, 1953)

$$\rho_\alpha = \frac{1}{\mu_o \omega} \left|\frac{E_x}{H_y}\right|^2 \text{ (in ohm metre)}$$

On substituting for impedance this becomes

$$\rho_\alpha = \frac{T}{2\pi\mu_o} \cdot \frac{1}{(\sigma_1 h_1)^2}$$

or

$$\log \rho_\alpha = \log \frac{1}{2\pi\mu_o (\sigma_1 h_1)^2} + 2 \log \sqrt{T}$$

which is a straight line having a slope +2. The intercept with the $\rho_\alpha = 1$ line results in the evaluation of conductance

$$\sigma_1 h_1 = \left(\frac{T}{2\pi\mu_o}\right)^{\frac{1}{2}}$$

which is therefore an observable geophysical parameter.

It can be shown that slopes of +2 are obtained whenever the condition

$$\frac{\sigma_2 T}{2\pi\mu_o (\sigma_1 h_1)^2} \ll 1 \text{ holds.}$$

For a 4 km ocean, $\sigma_1 = 2.9$ S/m and T = 7200 s, the second layer conductivity (σ_2) must be much less than 0.15 S/m.

APPENDIX 2

Conductivity - Depth Relation

For pore pressure equal to hydrostatic pressure the empirical shale porosity-depth relation of Magara (1976, Fig. 7, p. 548) is

$$\mu(z) = 0.39\ e^{-0.31z}, \text{ for } z \geq 0.3 \text{ km},$$

μ porosity

This expression is applicable for sub-bottom depths greater than 300 m, since the clay to shale transition occurs near this depth (Hamilton, 1959; Rieke and Chilingarian, 1974). Then,

$$\frac{1}{\mu}\frac{d\mu}{dz} = -\ 0.31\ \text{km}^{-1}$$

But Archie's Law is $\sigma_b = \sigma_w \mu^2$, where σ_b is wet bulk conductivity and σ_w is the conductivity of the interstitial fluid (seawater). Taking derivatives of the latter with respect to the effective pressure, P, (temperature fixed) and substituting the above porosity derivative, then,

$$\frac{\sigma_w}{\sigma_b}\frac{d(\sigma_b/\sigma_w)}{dP} = -\frac{0.62}{dP/dz}\ \text{kPa}^{-1}$$

An estimate of the order of change in conductivity with depth of burial can therefore be obtained, and for this purpose the effective pressure gradient is near 1.44×10^4 kPa/km for the first few km of a sediment section. This value was obtained using the Brace (1971) relation $(\rho_s - \rho_w)\ gz$ with $\rho_s = 2500$ kg/m and $\rho_w = 1024$ kg/m (g is acceleration due to gravity). Hence,

$$\frac{\sigma_w}{\sigma_b}\ \frac{d(\sigma_b/\sigma_w)}{dP} = -\ 4.3 \times 10^{-5}\ \text{kPa}^{-1}$$

Since the data of Quist and Marshall (1968) indicate that ρ_w is independent of pressure ($< 2 \times 10^5$ kPa), this equality predicts a decrease in σ_b by about a factor of 10 for a 0.54×10^5 kPa increase in effective pressure, equivalent to an increase of 3.7 km in burial depth. This change in conductivity with pressure is of the same order as reported for a wide variety of crustal rocks (Brace et al. 1965; Brace and Orange, 1968; Brace, 1971) in which cracks were easily closed for pressures between 0 and 1-2 $\times 10^5$ kPa (at room temperatures). Thus Magara's porosity-depth relation gives results consistent with laboratory measurements.

For temperatures less than 250°C, the data of Quist and Marshall (1968) indicate that a linear function with depth is valid for the conductivity of saline solutions; namely

$$\sigma_w(z) = \sigma_1 + az,\ z \geq 0.3 \text{ km}$$

where a is the conductivity gradient. For a 0.5 M NaCl solution (equivalent to a seawater salinity of about 30 ppt) the conductivity increases with temperature at the rate $\alpha = 0.1$ S/m°C (extrapolated from Quist and Marshall, 1968), so that on assuming appropriate thermal gradients, a in S/m^2 is determined. If, however, pore space contains seawater equivalent to a 1 M NaCl solution, then rate (α) is doubled, and each curve in figure 4 is obtained with half the indicated geothermal gradient.

Hence, using Archie's law and the above relations for $\sigma_w(z)$ and $\mu(z)$, the conductivity profile can be computed from the relation

$$\sigma(z) = (\sigma_1 + az)\ (0.39\ e^{-0.31z})^2$$

and on integrating, the conductance profile in figure 4b, for suitable geothermal gradients, is obtained.

The conductivity and conductance profile for the 300 m clay section can be determined from the porosity-depth data of Hamilton (1959, Table 1, p. 1404) using the relation

$$\sigma(z) = \sigma_o + az \qquad \text{, for } z \leq 0.3 \text{ km}$$

The conductivity discontinuity at 300 m in figure 4 is a result of the different methods used in determining porosities. However, the effect on conductances at 300 m is less than 20 per cent for the profiles labelled 30, 50 and 60°C/km in figure 4b.

Magnetic anomalies and the evolution of the Arctic

R. L. Coles, W. Hannaford and G. V. Haines

ABSTRACT

Extensive magnetic surveys have been made over the Arctic Ocean during the past 30 years, but it is very difficult to interrelate data sets, and even conclusions, from different surveys. Many uncertainties present in the data sets preclude a full compilation of the data in a single format at this time. This paper summarizes the information available and discusses the various interpretations made from the data sets. The many ambiguities in interpretation result in considerable uncertainties regarding present Arctic Basin structure, and therefore its evolution. Magnetic anomaly data over the Eurasia Basin have indicated possible spreading rates, however, and an analysis of Earth Physics Branch high-level airborne magnetic data over the Greenland end of the Nansen-Gakkel Ridge suggests rates of 8 mm/a from 0 to 3 Ma and 5 mm/a from 3 to 20 Ma. There is no persistent anomaly pattern associated with the Lomonosov Ridge, the evidence suggesting that the Ridge is of continental character. The magnetic pattern over the Alpha and Mendeleev Ridges is quite different from that over the Nansen-Gakkel Ridge. The amplitudes and character of the anomalies over the Alpha Ridge are similar in some respects to continental shield anomalies. A strongly positive, very long wavelength anomaly characterizes the Alpha Ridge, whereas the Nansen-Gakkel and most active spreading ridges have associated weak positive or negative very long wavelength anomalies. On the other hand, the magnetic pattern of the Alpha Ridge might be a result of a series of imbricate subduction zones and associated island arcs. Although many thousands of line-kilometres of magnetic survey data exist, the general understanding of the magnetic anomalies and their significance is still at a rudimentary level.

RÉSUMÉ

Des relevés du champ magnétique ont été effectués au-dessus de l'océan Arctique pendant les trentes dernières années, cependant il est très difficile de comparer les données des différents relevés, et encore plus leurs conclusions. Les incertitudes des données empêchent actuellement une compilation complète dans un format unique. Cette étude résume les informations disponibles et discute des interprétations diverses que l'on en a fait. Les ambiguités d'interprétation ont implantées des incertitudes considérables quant à la structure actuelle du bassin Arctique, et par conséquent de son évolution. Néanmoins, les anomalies magnétiques du bassin Eurasie ont indiqué des vitesses possibles d'expansion. Par une étude des données aéromagnétiques recueillies à haute altitude par la Direction de la physique du globe au-dessus de l'extrémité de la crête Nansen-Gakkel près du Groenland, on estime des vitesses de 8 mm/a de 0 à 3 Ma et 5 mm/a de 3 à 20 Ma. Il n'y a pas d'arrangement défini des lignes magnétiques parmis les anomalies associées avec la crête Lomonosov; l'évidence suggère que la crête a un character continental. L'arrangement des anomalies magnétiques des crêtes Alpha et Mendeleev est tout différent de celui de la crête Nansen-Gakkel. Les amplitudes et le caractère des anomalies au-dessus de la crête Alpha sont pareils aux anomalies des boucliers continentaux sous quelques rapports. Une anomalie très positive de très grande longueur d'onde caractérise la crête

Alpha, tandis que la crête Nansen-Gakkel et la plupart des crêtes d'expansion actives ont des anomalies de très grande longueur d'onde qui ne sont que faiblement positives ou négatives. Par contre, l'arrangement des anomalies magnétiques de la crête Alpha pourrait être un résultat d'une série de zones de subduction imbriquées et d'arcs insulaires associés. Bien qu'il existe des millieurs de ligne-kilomètres de relevés magnétiques, la compréhension générale des anomalies magnétiques et leur signification restent à un niveau rudimentaire.

INTRODUCTION

Extensive magnetic surveys have been made over the Arctic Ocean since about 1946. The survey techniques have varied considerably, as have the methods and forms of data presentation. In fact, it is difficult to interrelate data sets, and even conclusions, from different surveys. This review tries to place into perspective the various sets of magnetic anomaly data in the Arctic which have been published. Some new surveys are currently in progress; discussion of their results is not possible here, but the locations of these surveys, along with locations of earlier surveys, are indicated.

A discussion of interpretations of the magnetic anomalies and the uncertainties therein is also given, and some new information and concepts are introduced.

SURVEY PROBLEMS

Magnetic surveying is considerably more difficult in the Arctic regions than at lower latitudes. The vast areas of frozen ocean, the low temperatures and severe weather conditions, the restricted availability of airbases, all contribute to the logistics problems in operating an airborne survey in the Arctic. Shipborne magnetic surveying is restricted to marginal seas, because of the ice conditions. Some scattered and irregular profiles have been obtained from magnetometers operated on drifting ice stations.

Until recently, there have been major difficulties with navigation. The small number of radio beacons and the great distances involved placed much emphasis on celestial fixes and dead reckoning. Recently, more sophisticated navigational aids (such as very low frequency radio, satellite, and inertial navigation systems) have become available.

In addition, the temporal variations in the magnetic field present complex, and not well-understood, perturbations in the measured signal, which are considerably greater than the perturbations at mid-latitudes. Storm and diurnal activities are particularly high in the auroral oval, although these effects are somewhat smaller in the polar cap region. There are major difficulties in removing these effects from the data because of the scarcity of magnetic observatories, and because of the lack of spatial correlations in many of the temporal variations.

An airborne survey is commonly designed so that flight lines are roughly normal to major structural trends. In the Arctic Ocean, no geological information is available to suggest these trends. Bathymetric data alone can indicate possible directions. Once a preferred flight direction is chosen, this acts as an automatic directional filter for short wavelength magnetic anomalies, and tends to suppress features which are parallel to the flight lines. Thus, the planning of a survey may to a certain extent depend on an *a priori* hypothesis for the nature and evolution of a region, with the possible result that information supporting other hypotheses is suppressed. This is a danger anywhere, but it is particularly acute in the Arctic, where many conflicting hypotheses and very little data exist. This latter fact has also resulted in assumptions and in mathematical artifices being used to change the directions and/or positions of profiles for comparison purposes.

AIRBORNE SURVEYS

Several early reconnaissance airborne surveys were conducted by Soviet agencies from 1946 onward.

The first major airborne survey in the central Arctic was made by the U.S. Air Force and U.S. Coast and Geodetic Survey (USCGS) (1950-52). The data from this survey were discussed by King et al. (1966). The survey was restricted to the western half of the Arctic region and consisted of widely spaced lines roughly parallel to the 0-180° meridian and lines roughly radial from the North Pole. The flight altitudes were about 6 km above sea level. Vector magnetic

measurements were made every 5 minutes, primarily for use in compiling world magnetic charts for 1955, and continuous total field measurements provided anomaly data. The navigation was based mainly on celestial fixes, with an estimated accuracy of ±8 km.

During 1955, a series of reconnaissance survey flights was made in the Canadian Arctic Archipelago (Gregory et al., 1961). Total field measurements were taken at a nominal terrain clearance of 250 m. Track location was by continuous film-strip photography.

In the period 1960 through 1963, several flights were made by Project Magnet aircraft in the Arctic region. Vector measurements were taken at 5 minute intervals, with continuous total field measurements. Flight altitudes were between 2.5 and 3 km, typically. Navigational control was primarily by celestial fixes.

In 1961, 1963, and 1964, surveys were conducted by the University of Wisconsin Polar Research Institute over much of the central Arctic, at altitudes of about 450 m (Ostenso and Wold, 1971). Total field measurements were taken. The flight lines, although scattered and widely spaced, attempted to cover in reconnaissance fashion most of the Arctic region. Navigation used some radio aids, celestial fixes and dead reckoning, an accuracy of ±15 km being quoted by Ostenso and Wold (1971).

Surveys were conducted in 1963, 1965, 1970 and 1972 by the Earth Physics Branch (EPB), Ottawa. The 1963 survey consisted of widely spaced lines over the Canada Basin and Canadian Arctic Islands (Haines, 1967). The 1965 survey covered the region north of Greenland and Svalbard, the Norwegian and Greenland Seas, and Greenland on a wide line spacing, and Scandinavia and Iceland on closer line spacing. Flight altitudes were between 3.5 and 5 km; navigation was primarily by celestial fixes (Haines et al., 1970; Hannaford and Haines, 1969). A more detailed survey over the Canadian Arctic, part of the Nansen-Gakkel Ridge, and part of Greenland was flown in 1970; line spacing was approximately 70 km, at 3.5 km altitude (Haines and Hannaford, 1974). The northern section of the 1972 survey, at 3.5 km altitude and 20 km spacing, covered some Arctic mainland regions of Canada (Haines and Hannaford, 1976). In these EPB surveys continuous vector measurements were made, using fluxgate magnetometers. In the 1965, 1970, and 1972 surveys, a proton precession magnetometer also recorded total field intensity. Data were presented as averages over 30 seconds of flight time (about 3.5 km distance). Navigational equipment included a Doppler drift and ground speed unit, radar, and Loran units. Probable errors in position were quoted as ±5 km for the navigational fixes. Further discussions have been given by Riddihough et al. (1973) and Coles et al. (1976a).

During the 1960's surveys by the Canadian Polar Continental Shelf Project (PCSP) were flown over the outer Canadian Arctic Islands and the continental shelf, at 300 m altitude. The lines were typically 2 to 3 km apart, with radio navigational control. Total field intensity was measured. Maps of the data at scales of four miles to one inch and two miles to one inch were published by the Geological Survey of Canada, Ottawa. An analysis of some of these data was given by Bhattacharyya (1968).

A reconnaissance survey was conducted by the Geological Survey of Canada (GSC) and National Aeronautical Establishment (NAE), Ottawa, in 1975 (Hood and Bower, 1976). Total field intensity measurements at 300 m altitude were made on two lines between Ellesmere Island and the North Pole, a series of lines over part of the Alpha Ridge, and a series of lines over the polar continental shelf. Navigation used a GNS-VLF system and Doppler radar.

Karasik et al. (1972) discussed in some detail the Soviet aeromagnetic surveying techniques used in the Arctic. The large-area compilation maps were derived from a combination of data from reconnaissance flights tied together by data from a number of more detailed and systematic survey areas. The authors emphasized the need for overlap between surveys, and they discussed the problems inherent in the use of drifting ice as bases for the aircraft support stations and radio navigational beacons. Although specific details of individual surveys were not given, it is inferred from Karasik et al. (1972) that flight altitudes were between 300 and 600 m. Over shelf areas, the authors claimed a positional accuracy of 1 to 2 km using radio navigation. Where radio navigational installations were used on drifting ice, an accuracy of 1 to 2 km was again claimed for small survey areas (this accuracy may, however, be only relative). For much of the area covered by Soviet surveys, radio aids were not available, and rms errors of 10-20 km were quoted. By using comparisons among

reconnaissance flights and detailed surveys, Karasik et al. (1972) claimed that many navigational inadequacies were removed from the reconnaissance data.

DRIFTING ICE STATIONS

Although most magnetic field measurements in the Arctic basin have been made by airborne magnetometers, some useful measurements have been made from drifting ice stations. The inclement weather conditions, low temperatures, high magnetic disturbance and diurnal fields, and navigation inaccuracies are still present, but in addition the lack of control over the path of the ice station presents problems in data interpretation. To a considerable degree, the specific region surveyed is a matter of chance.

Hunkins et al. (1962) described the magnetic and other measurements over the Chukchi Plateau taken from drifting station Charlie. The path of this station was particularly fortunate. Distinctive magnetic anomalies were observed, but unfortunately several magnetic storms interrupted an otherwise continuous profile over the Chukchi Plateau. Hunkins et al. interpreted the data as indicating a magnetic basement ridge under the western slope of the Plateau.

Heirtzler (1967) demonstrated a gradiometer technique for defining crustal magnetic anomalies with measurements from Fletcher's Ice Island. He showed that magnetic anomalies can be detected in the presence of large time variations using this technique.

Hall (1970, 1973) discussed magnetic and other data obtained from Fletcher's Ice Island (Station T-3) during the period 1962 to 1970. During this time, the Ice Island traversed the Chukchi Plateau, portions of the Alpha and Mendeleev Ridges, and the Chukchi, Mendeleev, and Canada Plains. Hall concluded that the data, along with data from other investigations (including some magnetic data obtained by the British Trans-Arctic Expedition (1968-69) on an ice flow 140 km from Station T-3), supported the idea that the Alpha and Mendeleev ridge system is an inactive centre of sea-floor spreading. He inferred a series of parallel fractures across the ridge, which he attributed to transform faults. The magnetic data from this study are certainly considerable, and demonstrate the changing character of the field in the different regions, but suffer from a common problem of drifting station data - that the traverses are irregular and anomaly closures are generally ill-defined.

ARCTIC MARGINAL SEAS

Much of the Arctic waters overlie the anomalously wide Eurasian polar continental shelf. Airborne magnetic coverage of much of this shelf appears to be fairly complete (Demenitskaya and Karasik, 1971). Vogt and Ostenso (1973) reported reconnaissance shipborne magnetic surveys in the Barents and Kara Seas. They considered that the subdued magnetic field over the Barents Sea does not indicate a continuation of Caledonian or Precambrian basement structures at shallow depth. Deep sedimentary basins were suggested. In the northern and central Kara Sea the field is more irregular, and a shallow magnetic basement was inferred; to the south, the magnetic field is subdued and smooth.

Bassinger (1968) described a shipborne magnetic survey in the northeast Chukchi Sea. He outlined a prominent north-trending magnetic high between 166° and 167°W which he related to structures in northwestern Alaska. To the east of this feature, there is little magnetic relief as far as longitude 163°W.

Several shipborne surveys over the Beaufort Sea have produced data yet to be fully compiled and interpreted, although they suggest considerable depths to magnetic basement.

DATA COMPILATION

It has not been possible to assemble the published airborne data sets over the central Arctic into a unified compilation. Some of these data sets were not available, and those that were presented major problems.

Figure 1 shows flight track positions for data sets for which information is available in digital form (Haines et al., 1970; Haines and Hannaford, 1974, 1976; King et al., 1966; Project Magnet, 1966; Hood and Bower, 1976; PCSP data) and, in addition, shows the area covered by Soviet surveys (e.g., Karasik, 1974; Demenitskaya and Karasik, 1971; Rassokho et al., 1967). Figure 2 shows tracks from Ostenso and Wold (1971) and approximate regions recently surveyed by U.S. agencies (H. Eppert, P.R. Vogt, G.L. Johnson, personal communications, 1976, 1977).

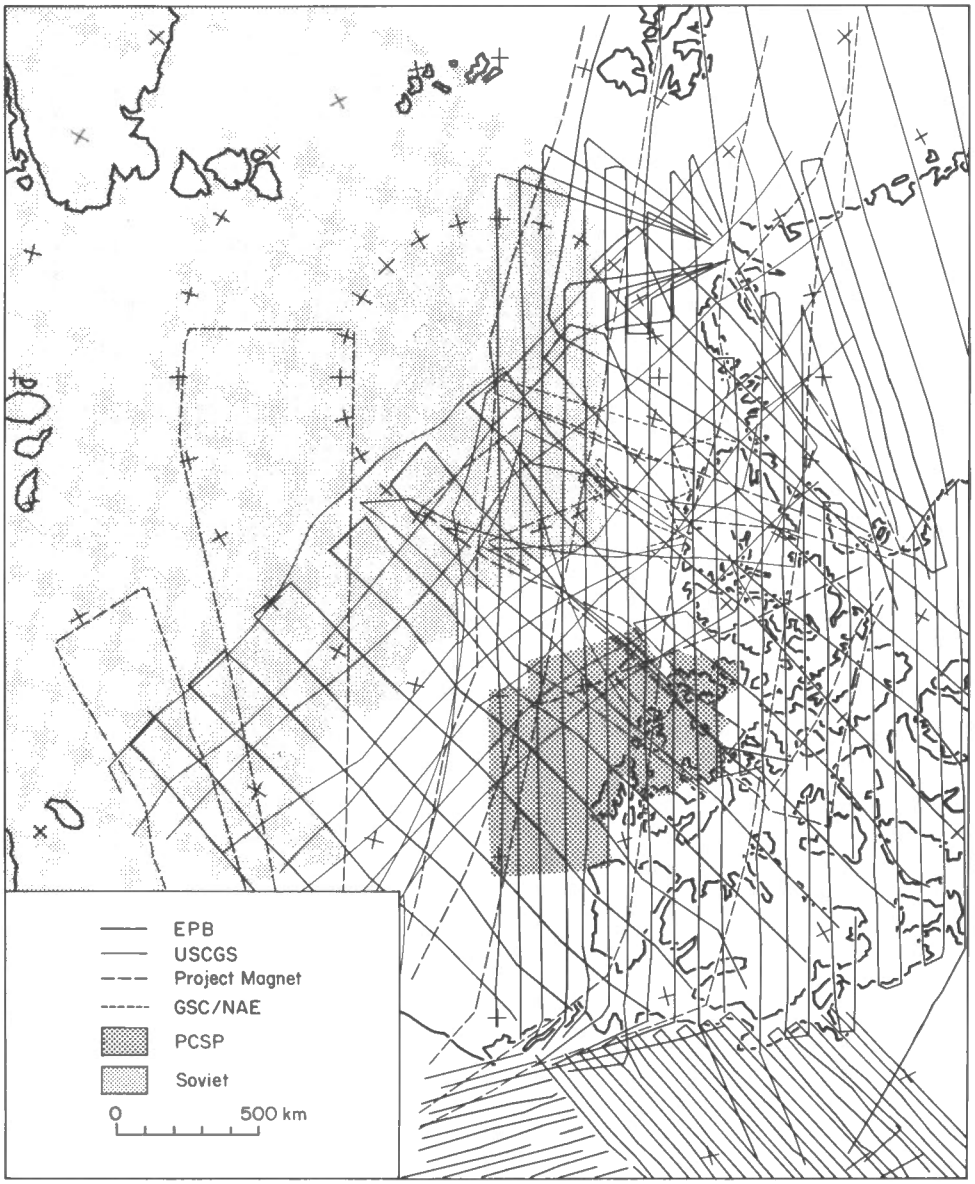

Figure 1. Arctic airborne magnetic surveys. Digital position data are plotted for surveys of the Earth Physics Branch (EPB), U.S. Coast and Geodetic Survey (USCGS), Project Magnet, and Geological Survey of Canada/National Aeronautical Establishment (GSC/NAE). The Polar Continental Shelf Project (PCSP) surveys had tracks too closely spaced to show here. Individual track data are not available for Soviet surveys.

In close examination, there were some internal inconsistencies within available data sets, both in terms of magnetic level and of navigation. Some, but by no means all, of these errors were removed or reduced. Different data sets agreed in some areas, but again there were major disagreements. Many of the problems appeared to stem from the navigational difficulties. Although in some cases navigation data of one survey were obviously in error, the correct solution was indeterminate. In other cases, locations of flight lines of both intersecting surveys may have been in error by unknown amounts. Compounded with these problems were the effects of time variations

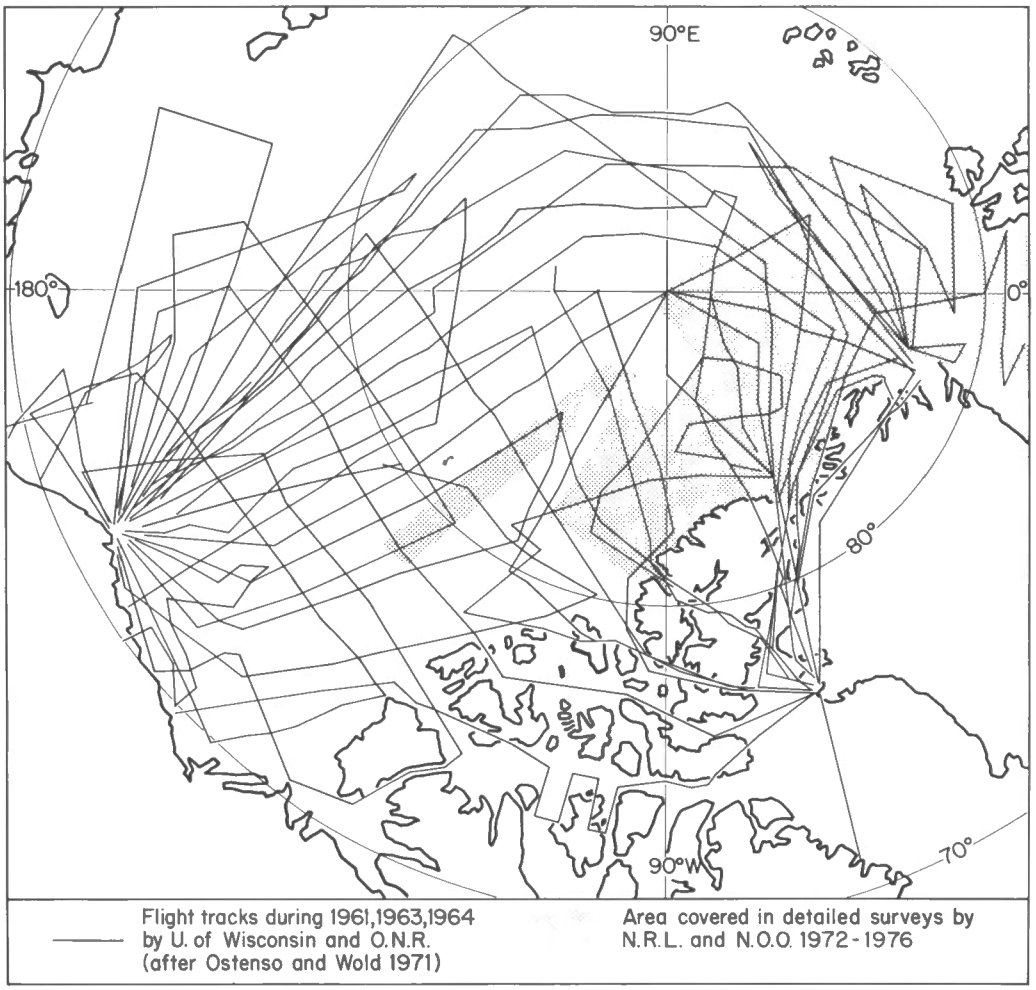

Figure 2. The chart shows approximate positions of tracks described by Ostenso and Wold (1971). Stippled areas show recent coverage by low-level surveys at close line spacing.

in the magnetic field. Suspected disturbance effects on a number of flights produced apparently false anomalies. In some cases, no amount of reasonable adjustment of flight line positions could resolve major differences, not only of field level but also of apparent anomaly structure. Secular changes from year to year were accommodated by working with data-derived regional fields; any deficiencies in these fields appear minor when compared with the other discrepancies.

Because of these uncertainties, and because of the non-availability of several major data sets, it was considered that a useful compilation of anomaly amplitude data could not be achieved with the presently available information. However, a generalized overview of the several magnetic patterns characterizing the Arctic region has been produced (Fig. 3), primarily indicating zero-contours.

A series of zero-contour maps (i.e. showing positive and negative anomalous field areas) over the eastern parts of the Arctic has been presented by Soviet authors. The maps are too small for accurate positioning, and give no information on amplitudes of anomalies, but are useful for indicating the gross patterns of anomalies. A preliminary chart was given by Rassokho et al. (1967); it included much of the Eurasia Basin, the Lomonosov Ridge, Mendeleev Ridge, and the Eurasian polar continental shelf. Karasik (1973) showed a chart of part of this region

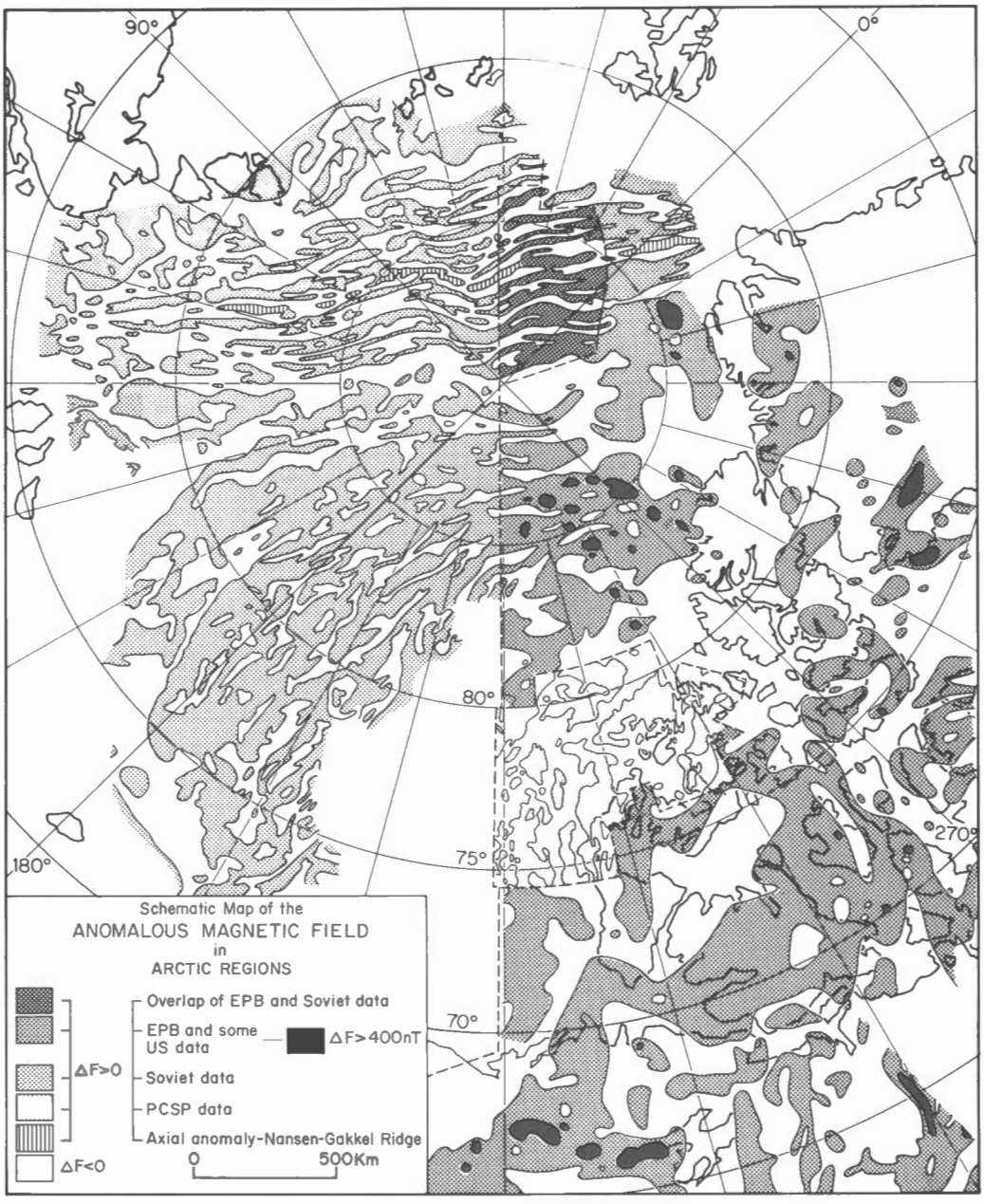

Figure 3. Schematic map of the anomalous magnetic field in Arctic regions. The contours on the right side of the map are based on digital data. To the left, north of 70°N, they are derived from Soviet zero-contour charts.

and, later (Karasik 1974), produced another chart which includes most of the Alpha, Mendeleev and Lomonosov Ridges and the Eurasia Basin. There are many differences in detail among these zero-contour charts, presumably as revised compilations were made with additional data, but the same general features persist.

It was possible to graphically and photographically combine the zero-contour chart of Karasik (1974), for the eastern half

of the Arctic, with similar charts derived from Earth Physics Branch data (available in original digital form) and Polar Continental Shelf Project data (digitized from large-scale published maps), with some input from data of King et al. (1966; digitized from large-scale profiles) and from Project Magnet profiles used in analog form.

The form of presentation used in figure 3 is, of course, limited in its information content, as noted earlier. However, in the western sector, where amplitude information is available, those large regions with anomaly amplitudes greater than 400 nanoteslas (at 3.5 km average altitude) are also indicated. Even with this chart, problems were encountered.

Cross-checks between the several Soviet charts and the EPB data, showed that the latitude-longitude grid on the map of Karasik (1974) was distorted and displaced. The distortion and displacement were adjusted in the compilation of figure 3, although anomaly positions on the Soviet side of the Amerasia Basin are not well defined. The overall pattern is, however, basically transcribed from Karasik (1974).

In the area of overlap between EPB and Soviet data over the Eurasia Basin, the positions of the zero contours were constrained by the EPB profiles, but were guided by the Soviet map between the EPB profiles. Individual regional trends were removed from the EPB profiles in this area; the zero crossovers were generally in good agreement with those in the adjusted Soviet chart, within the limits of resolution of the chart.

Elsewhere, the EPB anomalies were relative to a 3rd degree polynomial surface fitted by a least-squares method (Haines, 1968) to the data set. The data of King et al. (1966) were relative to regional fields applied to individual profiles. The Project Magnet profiles were used in analog form, basically as cross checks in positioning where possible. The PCSP data were relative to best-fit polynomial surfaces applied to the several individual surveys.

INTERPRETATIONS

Eurasia Basin - Nansen-Gakkel Ridge

It has been generally agreed that the Nansen-Gakkel Ridge is an accreting plate margin, possibly a continuation of the North Atlantic spreading ridge (Vogt and Ostenso, 1970; Vogt et al., 1970; Karasik 1973, 1974; Feden et al., 1974; and others). The pattern of anomalies over the Nansen-Gakkel Ridge and much of the Eurasia Basin is very similar to that over other mid-oceanic ridges and adjacent ocean-floor (e.g., Reykjanes Ridge: Talwani et al., 1971; Haines et al., 1970) which have been interpreted as regions of lithospheric spreading. A major difference is that magnetic anomaly amplitudes are much lower over the Nansen-Gakkel Ridge than those over other active spreading ridges (Vogt et al., 1970; and others). The relatively intense axial anomaly which is so characteristic of other ridges is not present over the full length of the Nansen-Gakkel Ridge (Haines and Hannaford, 1974; Feden et al., 1974). However, comparisons between the Soviet maps which indicate the location of an axial anomaly (e.g., Karasik, 1973) and the EPB data do show an anomaly which appears essentially continuous, though of very low amplitude in places - particularly between latitudes 84°30'N and about 86°30'N in the western half of the ridge. Two Project Magnet profiles, tracks 637 and 638, show anomalies which also confirm the position of an 'axial' anomaly.

Vogt et al. (1970) showed several profiles over the Nansen-Gakkel Ridge, which they aligned on the basis of several bathymetric profiles, and concluded that there was no prominent axial anomaly. However, it is significant that all the profiles across the ridge shown in Soviet papers display a prominent central anomaly. Comparisons with the seismicity chart (Plate 2; Wetmiller and Forsyth, 1978) confirm that a relatively intense magnetic anomaly corresponds with high seismicity, apparently at the spreading axis.

Estimates of the spreading rate from the ridge axis vary. Karasik (1973) gave a figure of 11 mm/a as an average total rate. Vogt et al. (1970), interpreting a profile taken from Rassokho et al. (1967), estimated a half-rate of less than 9 mm/a in the axial region (the actual position of this axial region along the ridge was not defined). Vogt et al. (1970), interpreting the profiles of Ostenso (1968), suggested half-rates less than 10 mm/a, but their interpretation of the location of the spreading axis does not appear to be borne out by other data sets. More recently, Karasik (1974) estimated half-rates for the main Eurasia Basin of 5 mm/a over the last 10 Ma, with lower values (around 3 mm/a) back to 38 Ma and faster rates prior to this time. The spreading has certainly been slow, and may be the cause of the relatively low anomaly amplitudes, since extruded lavas on the ridge may be intermixed

with sediments, and may overlap one another sufficiently to distort the 'striping signal'. Off-axial dike injection would also be a distorting factor, and reheating resulting from burial may destroy the remanent magnetization by viscous decay or hydrothermal alteration (e.g., Vogt and Avery, 1974).

Vogt and Ostenso (1970) suggested that spreading on the Nansen-Gakkel Ridge began about 40 Ma. Feden et al. (1974), however, suggested that, in the region near Greenland, spreading began about 65 Ma. Karasik (1973) refers to complex zoning of the anomaly field, reflecting a multistage development of the basin.

Figure 4 shows an analysis of EPB profiles over the Nansen-Gakkel Ridge and adjacent regions. The flight altitudes were between 2.4 and 3 km above sea level (1970 survey) except for two flights at 5 km altitude (1965 survey). Thus, the magnetic anomalies are smoother than anomalies observed by Ostenso and Wold (1971) and by other low altitude surveys. In addition to the set of near-parallel survey lines, several sections of ferry flights along which measurements were made are shown. No corrections for diurnal field variations have been incorporated; no magnetic storm disturbances occurred during the profile sections shown in figure 4. The reference field used was a 3rd degree polynomial surface fitted to the entire 1970 survey data set, and is not optimized for the area shown here. In addition, diurnal and interplanetary magnetic field variations result in mismatches in profile levels.

A number of inferred fracture zones are shown in figure 4. The two marked V are taken from figure 10a of Vogt et al. (1970). The ridge crest as inferred by Vogt et al. agrees in position with the prominent 'axial' anomalies seen on profiles 2 and 3 in figure 4, which were at 2.4 km altitude, and with a fourth profile which shows the 'axial' anomaly (between profiles 2 and 3; flown at 5 km altitude in the 1965 survey). The position of the 'axial' anomaly on profile 1 is displaced from the inferred ridge crest of Vogt et al. (1970).

A small scale chart of recent more closely-spaced aeromagnetic profiles obtained by the U.S. Naval Research Laboratory is part of a bathymetric chart for the Norwegian-Greenland and west Barents Seas (Perry et al., 1978). Though difficult to examine in detail, these profiles appear to confirm the anomalies recorded by the earlier EPB survey.

Using the general trend indicated by the Vogt et al. fracture zones, a series of additional fracture zones are postulated (marked P in figure 4). Possible anomaly correlations between the profiles, including sections of the ferry lines, are shown. North of profile 3, the prominent 'axial' anomaly is not seen, but there are indications that the flanking anomalies persist. One possibility is that spreading has not occurred north of profile 3 during the last 2 or 3 million years, although slight seismic activity persists.

Several fracture zones (marked S in figure 4) were taken from Soviet work (Demenitskaya and Karasik, 1969). An interesting observation is that one of these fracture zones passes through a bathymetric deep (spot sounding) marked D. By analogy, two of the inferred fracture zones P were constrained to pass through other known deeps D (from echogram profiles in Beal, 1969; L. Sobczak, personal communication, 1977). However, offsets on the inferred fracture zones would appear to be only a few kilometres. The frequency of fracture zones is comparable with that inferred over the Soviet end of the Eurasia Basin (Demenitskaya and Karasik, 1969).

By considering model profiles based on the polarity reversal time scale of Heirtzler et al. (1968), modified by Talwani et al. (1971), a correlation of anomalies was made (Fig. 5). Although there are many uncertainties in the identification of anomalies, figure 5 suggests a spreading rate in the region of profiles 1, 2 and 3 of 8 mm/a over the past 3 Ma and 5 mm/a from 20 to 3 Ma. It should be noted that an alternate possibility is that most of the anomaly pattern might be much older, followed by a period of inactivity, with a resurgence of spreading in the south during the past 3 Ma. This possibility is suggested by the apparent continuity of the flanking anomalies on the profiles to the northeast of profile 3. The half-rates quoted above are consistent with rates obtained from other segments of the North Atlantic - Nansen-Gakkel spreading system, for a pole of rotation near 65°N, 139°E (Karasik, 1974).

The present separation of 1000 metre isobaths (representing the limits of oceanic-type crust), perpendicular to the mean direction of the spreading ridge, is about 280 km. At the rates interpreted in figure 5, this total spreading would have taken about 26 Ma. Thus, prior to about 26 Ma, the Morris Jesup Plateau and Yermak Plateau would have been in contact. If,

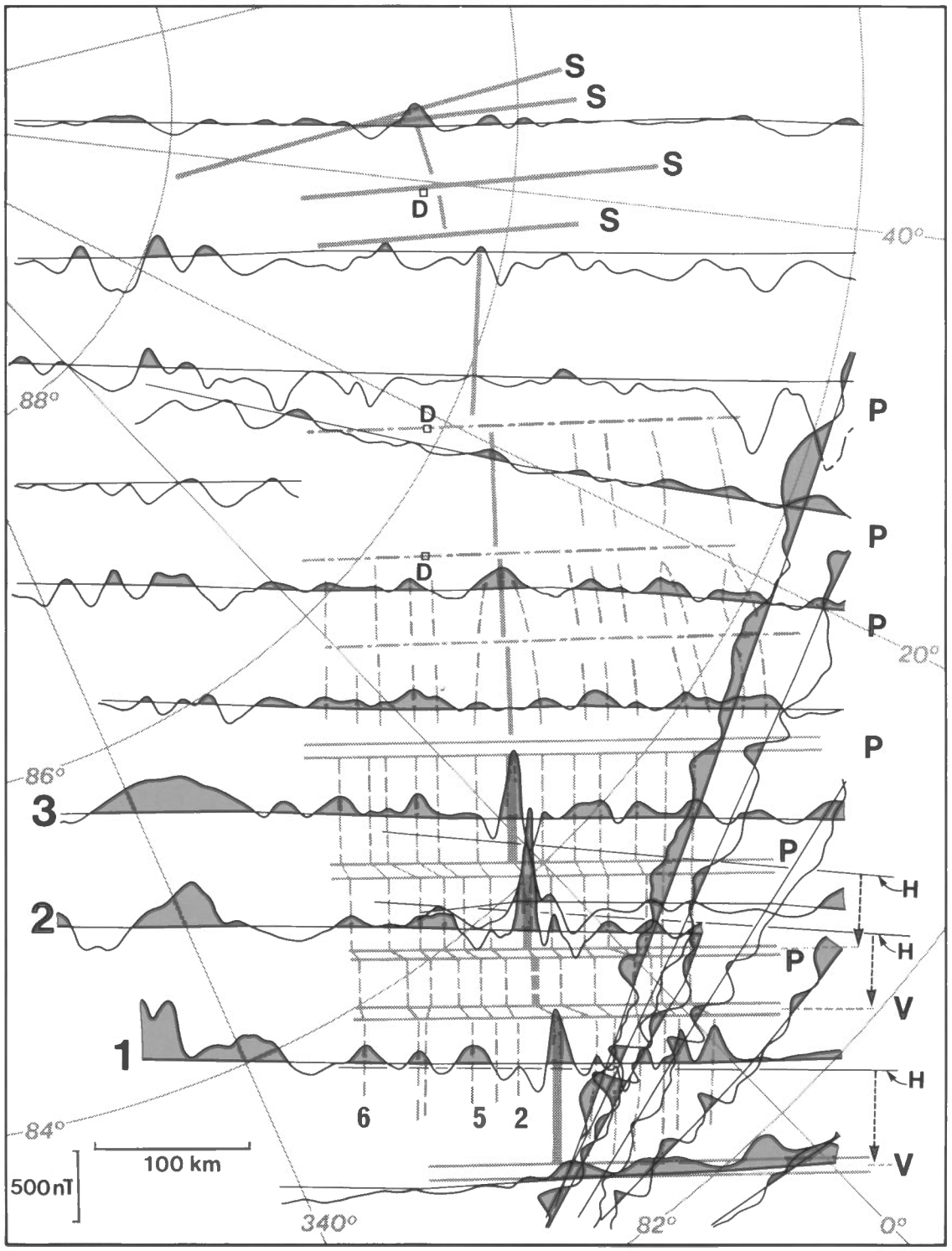

Figure 4. An interpretation of EPB magnetic profiles over part of the Nansen-Gakkel Ridge. The thick solid lines represent the inferred ridge crest, and short dashed lines represent suggested anomaly correlations. Double solid lines, long dashed lines, and solid heavy lines represent inferred fracture zones (S- from Soviet work; V- from Vogt et al. (1970); P- postulated in this study). Points marked D represent deep points from two echogram profiles and a spot sounding. The three lines marked H indicate the positions of three supposed fractures from the map of bathymetry by Heezen and Tharp (1975).

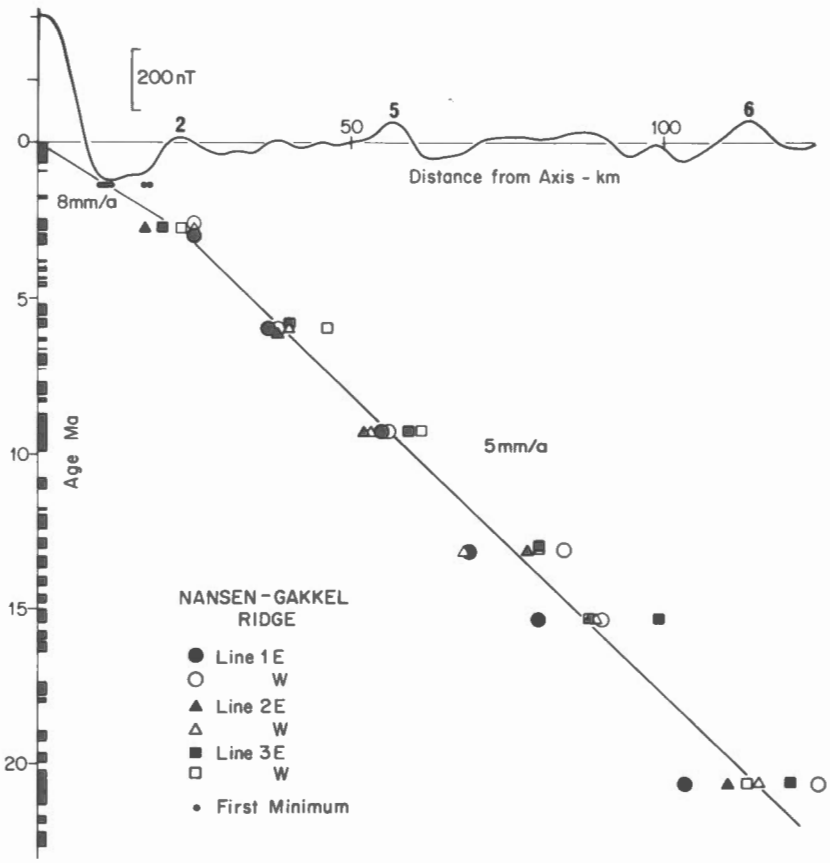

Figure 5. An interpretation of spreading on the Nansen-Gakkel Ridge near Greenland, using the time scale of Heirtzler et al. (1968), modified by Talwani et al. (1971). Line locations given in figure 4.

indeed, spreading occurred in the main part of the Eurasia Basin before this time, any movement between the Greenland block and the Eurasian block must have been taken up by a transcurrent fault movement. The postulated fracture zone immediately north of profile 3 could be a major discontinuity decoupling the earlier spreading.

Lomonosov Ridge

The magnetic character of the Lomonosov Ridge is very different from that of the Eurasia Basin. Anomalies are typically broader, and irregular in form. Although in places anomalies tend to follow the trend of the ridge, elsewhere magnetic features show no particular orientation. Near the North Pole, a broad positive anomaly lies on the Amerasian flank of the ridge, with a deep low on the Eurasian flank. King et al. (1966) claimed that a persistent anomaly of moderate size is associated with the ridge. The EPB data show that although there are small highs over the ridge, there is no truly persistent anomaly. Ostenso and Wold (1971) pointed out that over most of the ridge there is no significant anomaly, but that there is more magnetic relief over the part of the ridge profiled by King et al. (1966). The Soviet data (Karasik et al., 1971; Karasik, 1974; and Fig. 3) show a discontinuous anomaly pattern over the ridge.

It is generally agreed that the Lomonosov Ridge is continental in character. The low amplitude magnetic anomalies over much of the ridge could indicate a considerable thickness of sediment, but may also indicate a weakly magnetic crystalline basement. Ostenso and Wold (1971) calculated fifteen depth estimates, the bulk of which indicated sources at or near the surface of the ridge. King et al. (1966) suggested that the higher anomalies observed over part of the ridge were caused by volcanic rocks with magnetic susceptibility of 0.09 SI (0.007 emu). Ostenso and Wold (1971) pointed out that this value is more typical of continental mafic rocks.

Alpha and Mendeleev Ridges

Whereas the magnetic field over the Eurasia Basin and Lomonosov Ridge is subdued, that over the Alpha Ridge and adjacent regions is characterized by high intensity, apparently sublinear anomalies but with many irregularities. For example, figure 6 shows the 1970 EPB survey data profiles.

King et al. (1966), Ostenso and Wold (1971), and Vogt and Ostenso (1970) attempted correlations between profiles across the Alpha Ridge and suggested a system of linear anomalies. King et al. (1966) concluded that anomalies over the ridge were too irregular in height and frequency to correspond with oceanic type anomalies, and they associated them with continental type features, i.e., with a sunken continental block. Vogt and Ostenso (1970), however, concluded that the data support the idea of a fossil mid-ocean spreading ridge, on the basis of profile correlations with Mohns Ridge and Reykjanes Ridge in the North Atlantic. As these authors admit, these correlations are not very convincing, but could be interpreted to be a result of spreading during 40-60 Ma.

The tracks in these earlier data sets were not well oriented with respect to the axis of the ridge, and were widely spaced. The later EPB tracks over the Alpha Ridge were along parallel lines, almost perpendicular to the ridge axis, but again were widely spaced (about 70 km; Fig. 6). The EPB data do suggest sublinear features on the ridge, but also indicate much irregularity as the ridge approaches the continental shelf near Ellesmere Island (Riddihough et al., 1973; Coles et al., 1976a).

Hood and Bower (1976) found little evidence of symmetry in their profiles over the Alpha Ridge, but these short profiles were near the Canadian end of the ridge. Hood and Bower found intense anomalies to the south of the ridge proper (also seen in the EPB data).

The Soviet data cover most of the Alpha and Mendeleev Ridges (Karasik, 1974; and Fig. 1); the density of coverage is not given, however. The anomaly pattern certainly appears anisotropic, but is markedly different from the pattern in the Eurasia Basin (Nansen-Gakkel Ridge). Karasik (1974) favours the interpretation of the ridge as a fossil spreading centre, but emphasizes the paucity of the data.

Hall (1970, 1973) has interpreted bathymetric, gravity and magnetic data to show the existence of a number of fracture zones parallel to longitude 142°W. He concludes that these fractures are transform faults from the now-inactive spreading, and that the Alpha and Mendeleev Ridges owe their present form to the many offsets along these transform faults. The irregularity of the magnetic anomaly field may perhaps be related to these fracture zones. A noteworthy point is the subparallelism of Hall's fractures to some of the fractures inferred on the Nansen-Gakkel Ridge by Demenitskaya and Karasik (1969).

The absence of a dominant central axial anomaly over the Alpha Ridge has been attributed to viscous decay of magnetization since the cessation of spreading (Vogt and Ostenso, 1970). The relatively intense anomaly pattern continues from the Alpha Ridge into the basins on each side.

Herron et al. (1974) interpreted the Alpha and Mendeleev Ridges as a result of subduction. The anomaly pattern does not have the character of present island arcs or active continental regions (e.g., the Aleutians, Japan), but if the ridge results from a series of imbricate subduction zones, it is possible that a complex magnetic signature, such as that in the Canadian Cordillera (Haines et al., 1971; Coles et al., 1976a; Coles and Currie, 1977), could have developed.

Langel et al. (1975) produced a magnetic anomaly map north of 50°N based on specially selected quiet-time data from POGO satellites. This map shows a prominent positive anomaly over the Alpha Ridge, confirmed by an upward continuation of EPB airborne data (Coles et al., 1976b). Regan et al. (1975) showed a similar satellite-derived magnetic anomaly map for latitudes 50°S to 50°N. Mid-ocean spreading ridges are not characterized by similar major positive anomalies, with the exception of the ridge west of Peru in the Pacific. However, high positive anomalies do occur over small continental shields, such as western Australia, India, southern Africa, northern Greenland, and the Kolyma region, and around the edges of some larger shields such as the Siberian and North American. Whereas the field over the Alpha Ridge, north Greenland, and the Barents Shelf is relatively high, that over the Eurasia Basin and southern Canada Basin is low. Thus, in terms of its very long wavelength magnetic character, the

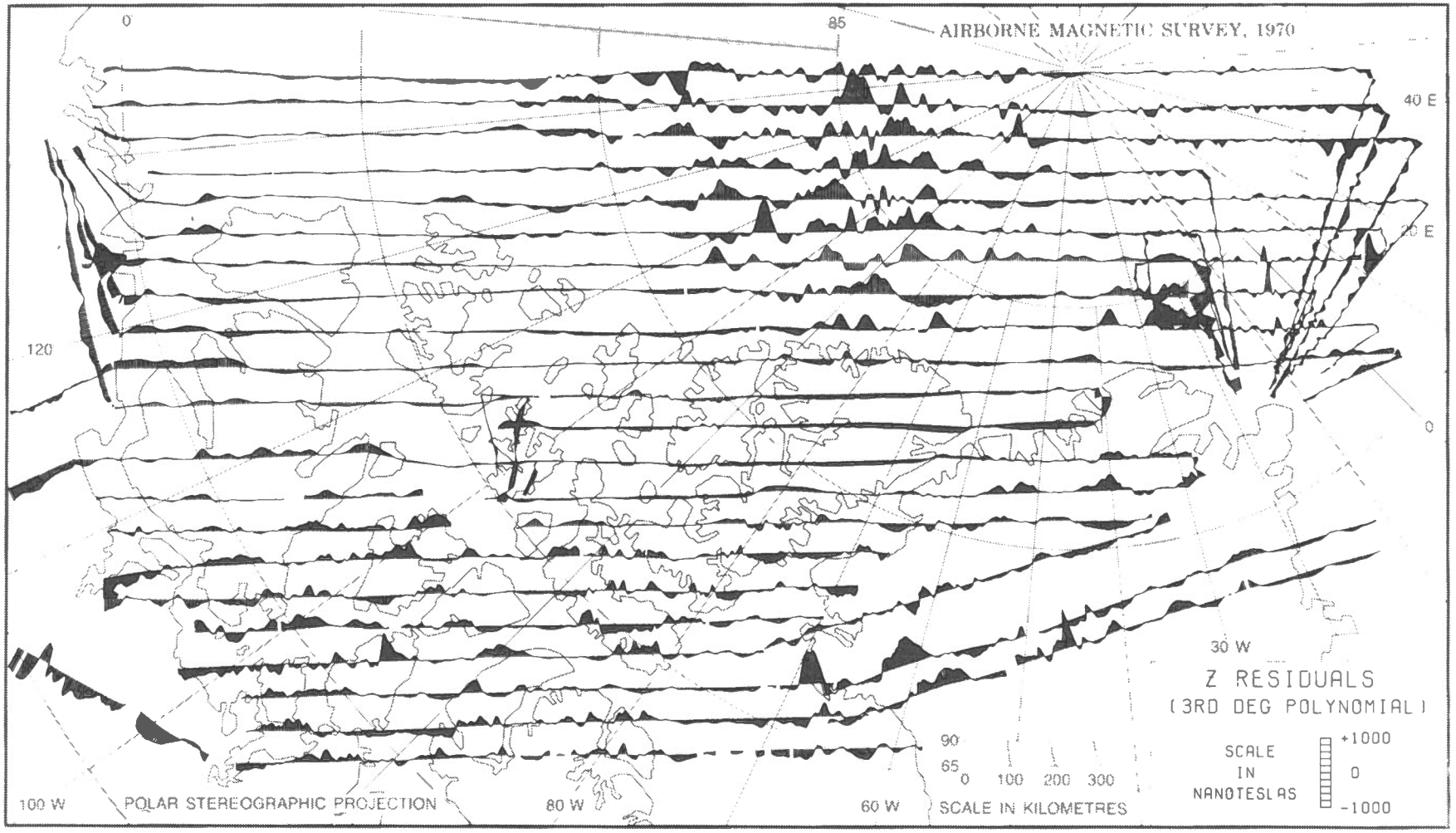

Figure 6. Some EPB magnetic profiles over the Arctic, to demonstrate the various anomaly amplitude regions.

Alpha Ridge is more akin to continental shield areas than to oceanic spreading ridges. This is, of course, a return to the notions held some years ago by Soviet scientists, and also expressed by King et al. (1966).

Canada Basin

The Canada Basin is perhaps the most enigmatic region of the Arctic. Diverse opinions are held regarding its origin and age. It may be young, or it may be one of the oldest segments of oceanic crust remaining. In the northern part of the basin, the magnetic field has high amplitude, irregular but rather sublinear, anomalies, similar to those over the adjacent Alpha Ridge. In the southern part of the basin, the field is subdued, with no discernible linear patterns.

CONCLUSIONS

This review has attempted to give an overview of the state of magnetic data in the Arctic, as available in the scientific literature. It could not discuss data which, for one reason or another, are held confidential or are unavailable to the authors.

Although many thousands of line-kilometres of magnetic surveying have been flown, drifted, or sailed, in the Arctic, the state of the scientific community's understanding of the magnetic anomalies, and their significance for Arctic structure and evolution, is still at a rudimentary level. It is not until data are freely exchanged, or published in more usable formats, that prejudices and biasses in the interpretation of the data can be avoided.

It cannot be overemphasized that all published evolutionary scenarios for the Arctic, and in particular for the Amerasia Basin, are extremely tentative, on the basis of the available magnetic data. There are insufficient data, of all kinds, for any definitive models to be made at this stage.

ACKNOWLEDGEMENTS

We are grateful to those individuals and agencies, referred to in the paper, who have provided information. We wish to thank our colleagues in the Earth Physics Branch who have helped us considerably by way of discussions and constructive comments. In particular, we thank Dr. P.H. Serson, Dr. J.F. Sweeney, and Dr. K. Whitham for their reviews of the manuscript.

REFERENCES

Bassinger, B.G., 1968. Marine magnetic study in the northeast Chukchi Sea. J. Geophys. Res., 73, 683-687.

Beal, M.A., 1969. Bathymetry and structure of the Arctic Ocean. Ph. D. thesis, Oregon State Univ., Corvallis, 187 p., Appendix.

Bhattacharyya, B.K., 1968. Analysis of aeromagnetic data over the Arctic Islands and continental shelf of Canada. Geol. Survey Can. Paper 68-44, 14 p.

Coles, R.L., and R.G. Currie, 1977. Magnetic anomalies and rock magnetizations in the southern Coast Mountains, British Columbia: Possible relation to subduction. Can. J. Earth Sci., 14, 1753-1770.

Coles, R.L., G.V. Haines and W. Hannaford, 1976a. Large scale magnetic anomalies over western Canada and the Arctic: A discussion. Can. J. Earth Sci., 13, 790-802.

Coles, R.L., R.A. Langel, M. Kempa and M. Mayhew, 1976b. Comparisons between POGO satellite magnetic data and airborne magnetic data over Canada, 50°N-85°N, 100°W-140°W (abs). EOS, Trans. Am. Geophys. Union, 57, 908.

Demenitskaya, R.M., and A.M. Karasik, 1969. The active rift system of the Arctic Ocean. Tectonophysics, 8, 345-351.

Demenitskaya, R.M., and A.M. Karasik, 1971. Problems of the genesis of the Arctic Ocean. in: Istoriya Mirovogo Okeana, Nauk. SSSR, Moscow. 58-76 (in Russian).

Feden, R.H., H.S. Fleming, J.D. Phillips, J.V. Massingill and R.K. Perry, 1974. Aeromagnetic survey over the Eurasian Basin, Arctic Ocean (abs). Geol. Soc. Am. Bull., 6, 730.

Gregory, A.F., M.E. Bower and L.W. Morley, 1961. Geological interpretation of aerial magnetic and radiometric profiles, Arctic Archipelago, Northwest Territories. Geol. Survey Can. Bull. 73, 148 p.

Haines, G.V., 1967. A Taylor expansion of the geomagnetic field in the Canadian Arctic. Pub. Dom. Obs., 35, 115-140.

Haines, G.V., 1968. Polynomial estimation of certain geomagnetic quantities, applied to a survey of Scandinavia. Pub. Dom. Obs., 37, 75-112.

Haines, G.V., and W. Hannaford, 1974. A three-component aeromagnetic survey of the Canadian Arctic. Pub. Earth Phys. Br., 44, 209-228.

Haines, G.V., and W. Hannaford, 1976. A three-component aeromagnetic survey of Saskatchewan, Alberta, Yukon and the District of Mackenzie. Earth Phys. Br. Geomag. Series No. 8, 34 p.

Haines, G.V., W. Hannaford and P.H. Serson, 1970. Magnetic anomaly maps of the Nordic countries and the Greenland and Norwegian Seas. Pub. Dom. Obs., 39, 121-149.

Haines, G.V., W. Hannaford and R.P. Riddihough, 1971. Magnetic anomalies over British Columbia and the adjacent Pacific Ocean. Can. J. Earth Sci., 8, 387-391.

Hall, J.K., 1970. Arctic Ocean geophysical studies: The Alpha Cordillera and Mendeleyev Ridge. CU-2-70, Lamont-Doherty Geol. Obs., Palisades, New York, Tech. Rept. 2, 125 p.

Hall, J.K., 1973. Geophysical evidence for ancient sea-floor spreading from Alpha Cordillera and Mendeleyev Ridge. in: Arctic Geology, ed. M.G. Pitcher, Am. Assoc. Petrol. Geol. Mem. 19, 542-561.

Hannaford, W., and G.V. Haines, 1969. A three-component aeromagnetic survey of the Nordic countries and the Greenland Sea. Pub. Dom. Obs., 37, 113-164.

Heezen, B.C., and M. Tharp, 1975. Am. Geograph. Soc. Map of the Arctic Region. Lamont-Doherty Geol. Obs., Palisades, New York.

Heirtzler, J.R., 1967. Measurements of the vertical geomagnetic field gradient beneath the surface of the Arctic Ocean. Geophys. Prosp., 15, 194-203.

Heirtzler, J.R., G.O. Dickson, E.M. Herron, W.C. Pitman III and X. Le Pichon, 1968. Marine magnetic anomalies, geomagnetic field reversals, and motions of the ocean floor and continents. J. Geophys. Res., 73, 2119-2136.

Herron, E.M., J.F. Dewey and W.C. Pitman III, 1974. Plate tectonics model for the evolution of the Arctic. Geology, 2, 377-380.

Hood, P.J., and M.E. Bower, 1976. Arctic Ocean: Low-level aeromagnetic profiles obtained in 1975. Geol. Survey Can. Paper 76-1A, 421-424.

Hunkins, K., T. Herron, H. Kutschale and G. Peter, 1962. Geophysical studies of the Chukchi Cap, Arctic Ocean. J. Geophys. Res., 67, 235-247.

Karasik, A.M., 1973. Anomalous magnetic field of the Eurasian Basin of the Arctic Ocean. Dokl. Akad. Nauk. SSSR, 211, 86-89 (in Russian).

Karasik, A.M., 1974. The Euro-Asian Basin of the North Polar Ocean from the standpoint of plate tectonics. in: Problems of the Geology of the polar regions of the Earth, Leningrad, 23-31 (in Russian).

Karasik, A.M., N.I. Guerevich, V.N. Masolov and V.G. Shchelovanov, 1971. Some features of the deep structure and genesis of the Lomonosov Ridge based on data of airborne magnetic surveys. Geofiz. Metody razvedki v Arktike, 6, 9-19 (in Russian).

Karasik, A.M., V.N. Masalov and V.G. Shchelovanov, 1972. Methodological problems of aerial magnetic mapping in the Arctic Ocean. Geofiz. Metody razvedki v Arktike, 7, 74-79 (in Russian).

King, E.R., I. Zietz and L.R. Alldredge, 1966. Magnetic data on the structure of the central Arctic region. Geol. Soc. Am. Bull., 77, 619-646.

Langel, R.A., S.J. Bensusen, R.D. Regan, W.M. Davis and J.C. Cain, 1975. High latitude magnetic anomaly maps (abs). EOS, Trans. Am. Geophys. Union., 56, 356.

Ostenso, N.A., 1968. Geophysical studies in the Greenland Sea. Geol. Soc. Am. Bull. 79, 107-132.

Ostenso, N.A., and R.J. Wold, 1971. Aeromagnetic survey of the Arctic Ocean: Techniques and interpretations. Marine Geophys. Res., 1, 178-219.

Perry, R.K., H.S. Fleming, N.Z. Cherkis, R.H. Feden and J.V. Massingill, 1978. Bathymetry of the Norwegian-Greenland and western Barents Seas (map). Geol. Soc. Am. Inc., Boulder, Colo. (in press).

Project Magnet, 1966. Geomagnetic Surveys 1953-1965. U.S. Naval Oceanographic Office, Magnetics Div., Brochure 3.

Rassokho, I.I., L.I. Senchura, R.M. Demenitskaya, A.M. Karasik, Yu. G. Kiselev and N.K. Timoshenko, 1967. The Central Submarine Arctic Ridge and its place in the ridge system of the Arctic Ocean. Dokl. Akad. Nauk. SSSR, 172, 659-662 (in Russian).

Regan, R.D., J.C. Cain and W.M. Davis, 1975. A global magnetic anomaly map. J. Geophys. Res., 80, 794-802.

Riddihough, R.P., G.V. Haines and W. Hannaford, 1973. Regional magnetic anomalies of the Canadian Arctic. Can. J. Earth Sci., 10, 147-163.

Talwani, M., C.C. Windisch and M.G. Langseth, 1971. Reykjanes Ridge crest: A detailed geophysical study. J. Geophys. Res., 76, 473-517.

Vogt, P.R., and O.E. Avery, 1974. Tectonic history of the Arctic basins: Partial solutions and unsolved mysteries. in: Marine Geology and Oceanography of the Arctic Seas, ed. Y. Herman, Springer-Verlag, New York, 83-117.

Vogt, P.R., and N.A. Ostenso, 1970. Magnetic and gravity profiles across the Alpha Cordillera and their relation to Arctic sea-floor spreading. J. Geophys. Res., 75, 4925-4938.

Vogt, P.R., and N.A. Ostenso, 1973. Reconnaissance geophysical studies in Barents and Kara Seas - summary. in: Arctic Geology, ed. M.G. Pitcher, Am. Assoc. Petrol. Geol. Mem. 19, 542-561.

Vogt, P.R., N.A. Ostenso and G.L. Johnson, 1970. Magnetic and bathymetric data bearing on sea-floor spreading north of Iceland. J. Geophys. Res., 75, 903-920.

Wetmiller, R.J., and D.A. Forsyth, 1978. Seismicity of the Arctic, 1908-1975. in: Arctic Geophysical Review, ed. J.F. Sweeney, Pub. Earth Phys. Br. (this volume).

Gravity from 60° N to the North Pole

L. W. Sobczak

ABSTRACT

Three free-air gravity anomaly maps for the Arctic region north of 60°N are presented. The maps show the gravity field derived from mean values based on observed and predicted data, the field based on calculated satellite gravity data, and the residual gravity field derived by removing the satellite gravity field from the observed field. The satellite map shows regional gravity anomalies with widths of 1000 km or more. The residual anomaly map and the map compiled from observed and predicted data outline gravity anomalies with widths ranging from 100 km to 1000 km. The smaller wavelength of the latter provides information on the locations of anomalous sub-surface structures and major density - lithological variations within the crust and mantle. Gravity highs straddle the polar continental breaks of North America, Svalbard, Scandinavia, and Greenland and are present over submarine ridges (Lomonosov, Alpha and Mid-Atlantic) and plateaus (Chukchi, Morris Jesup and Yermak). Many of these highs are simply a reflection of positive sea-bottom topography, but those along the continental margins are believed to indicate regions of uncompensated sediments. Extensive gravity lows which correlate with regions of generally high relief, such as northern Greenland and southeastern Alaska and adjacent Yukon, probably indicate that these regions are overcompensated by either a thicker crust or less dense crust and mantle than normal. Gravity lows over the Canada, Makarov, and Fram Basins may be indicative of the thick low density sediments present there. Over central Greenland a belt of steep gradients separates a relatively negative region of anomalies to the north from a more positive gravity field to the south and suggests significant changes in either the thickness of the crust or in the lithologies and densities of the crust and mantle in this region.

RÉSUMÉ

On présente ici trois cartes d'anomalies gravimétriques à l'air libre, pour la région Arctique au nord de 60° de latitude. Les cartes représentent le champ gravitationnel déterminé d'après les valeurs moyennes basées sur des observations et simulations, le champ gravitationnel basé sur des données gravimétriques issues d'orbites de satellites, et enfin le champ gravitationnel résiduel, obtenu en soustrayant le champ gravitationnel du satellite du champ mesuré. La carte issue des données orbitales, nous donne une vue d'ensemble des anomalies gravimétriques régionales possédant des largeurs d'au moins 1000 km. La carte des anomalies résiduelles et la carte compilée à partir des données basées sur les observations et simulations mettent en relief les anomalies gravimétriques de 100 à 1000 km de largeur. Les anomalies de faible longueur d'onde de ces dernières nous renseignent sur la configuration des structures proches de la surface qui engendrent ces anomalies et sur les variations densimétriques et lithologiques importantes de la croute et du manteau. Les maxima gravimétriques parcourent les ruptures de pente de la plate-forme continentale polaire d'Amérique du Nord, du Groenland, du Svalbard et de la Scandinavie ainsi qu'au-dessus des dorsales sous-marines

(Lomonosov, Alpha et le milieu de l'Atlantique) et des plateaux (Chukchi, Morris Jesup et Yermak). On recontre aussi des maxima gravimétriques au-dessus des crêtes et plateaux sous-marins. Un grand nombre de ces maxima gravimétriques ne font que refléter la topographie positive du fond marin, mais ceux qui longent les marges continentales peuvent correspondre à des zones sédimentaires n'ayant pas subi de compensation isostatique. Les vastes minima gravimétriques qui correspondent à des régions de relief généralement élevé, comme le nord du Groenland, ainsi que le sud-est de l'Alaska et le Territoire du Yukon avoisinant, semblent indiquer que ces régions subissent probablement une compensation démesurée due à un épaississement inhabituel de la croûte, ou à l'existence d'une zone de croûte et manteau moins denses que la normale. Les minima gravimétriques enregistrés dans les bassins du Canada, de Makarov et de Fram peuvent indiquer la présence de couches épaisses de sédiments de faible densité. Dans le centre du Groenland, une zone de fort gradient gravimétrique, séparant une région nord d'anomalies relativement négatives, d'un champ gravitationnel de caractère plus positif au sud pourrait correspondre à une forte variation, soit de l'épaisseur de la croûte, soit de la lithologie et de la densité de la croûte et du manteau dans cette région.

INTRODUCTION

Most gravity data in Arctic regions have been acquired over the last two decades and have been made available to the public by the Earth Physics Branch (EPB) Ottawa, Canada, and the Defense Mapping Agency Aerospace Centre (DMAAC), St. Louis, Missouri, USA.

Field procedures and the accuracy of measurements for gravity surveys have been discussed in Canada by Sobczak and Weber (1970), Stephens et al. (1972), Sobczak et al. (1973), Sobczak and Stephens (1974) and in the USA by Barnes (1969), Wold et al. (1970), Wold and Ostenso (1971), Talwani and Eldholm (1972), Wold (1973), Wilcox et al. (1975) and Ostenso and Wold (1977). In this report a compilation of available gravity data over the Arctic Ocean and the surrounding landmasses is presented, the quality of the data is assessed, and major features of the free-air gravity maps are discussed. The first map (Plate 3) shows mean free-air anomalies ($\frac{1}{2}^{o}$ latitude x 2^{o} longitude) calculated from over 119,000 gravity observations that cover about 60 per cent of the area (Fig. 1) together with predicted mean free-air anomalies (1^{o} x 1^{o}) determined by DMAAC for about 30 per cent of the area (Fig. 1). The remaining 10 per cent of the region (blank area on Fig. 1) in the Eurasia Basin is covered only by satellite gravity. The second map (Fig. 2) shows 5^{o} x 5^{o} mean free-air gravity anomalies for the entire region, calculated from satellite observations and represented by spherical harmonic coefficients to degree and order 25. The third map (Plate 4) shows residual free-air anomalies defined as differences between the calculated and predicted mean free-air anomalies (Plate 3) and the satellite derived anomalies (Fig. 2).

CALCULATED MEAN FREE-AIR ANOMALIES

The DMAAC and EPB provided about 60 per cent and 40 per cent of the gravity observations respectively. A cursory check of a listing of these data sorted by degree square revealed 1641 erroneous gravity values which were deleted from the tapes. The accepted data (119,326 observations) were recomputed using Geodetic Reference System 1967 (GRS 67) and the datum was provided by the International Gravity Standardization Net 1971 (IGSN 71, Morelli et al., 1971); these data are concentrated over the Canadian, north Alaskan, Icelandic and Scandinavian regions (Fig. 3).

This area was divided into 3102 compartments of $\frac{1}{2}^{o}$ latitude by 2^{o} longitude and the mean value of gravity observations within each compartment was then determined.

Mean anomaly values have been determined using from 1 to nearly 1000 gravity observations per geographic block with a total range within a block in some instances of more than 200 mgal (2000 $\mu m/s^2$) for land stations and about 100 mgal for stations over water. Thus, if very few observations are available for a particular block, a non-representative mean may be obtained. This does not appear to be a serious problem, however, because the mean values contoured at

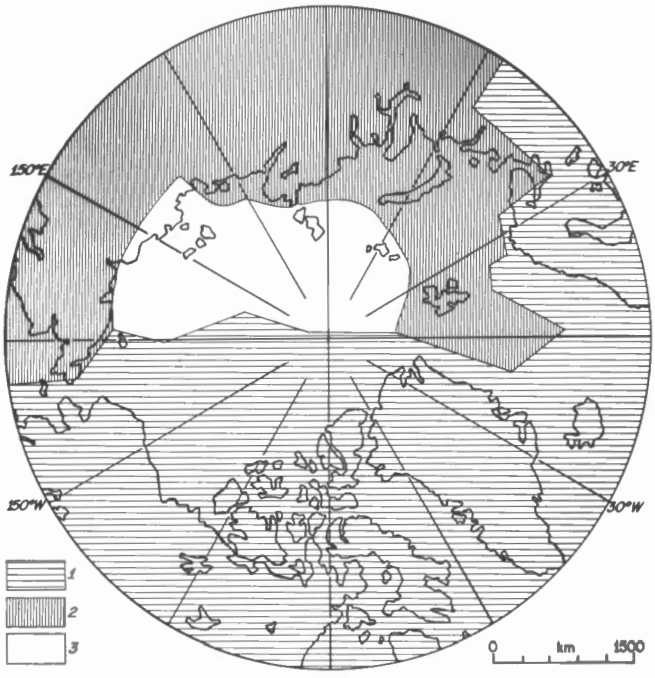

Figure 1. Distribution of gravity information used to compile Plate 3. The gravity field in area 1 is derived from calculated (½° latitude x 2° longitude) mean free-air anomalies, and that in area 2 from predicted (1° x 1°) mean free-air anomalies. There are no gravity data available in area 3.

20 mgal intervals show a smoothly changing gravity field. The map (Plate 3) based on arithmetic means gives a reasonable representation of the major regional gravity anomalies when compared with maps based on individual observations. For example, comparison between Plate 3 and Sobczak's (1977b) map contoured using observed values for the prominent belt of free-air highs over much of the North American polar continental break shows that the amplitude of the highs based on arithmetic means is reduced according to the aerial extent of the anomaly; about 25 per cent reduction for the more extensive anomalies and about 50 per cent for the smaller ones. Therefore, computing mean anomaly values has the effect of flattening the peaks of the shorter wavelength observed anomalies and is, in effect, a low pass filter.

The average value of all calculated means is near zero (1.9 mgal) and individual means have a range of about 236 mgal, from -129 mgal over northwestern Greenland to 107 mgal over east-central Greenland. Belts of gravity highs are observed along the continental breaks, continental areas of high relief, structural uplifts, and submarine ridges, including an extensive high centered over Iceland. There are two major lows, one over northern Greenland and central Ellesmere Island and the other over the northeastern Canadian mainland. In addition lows usually are found over major sedimentary basins and over abyssal plains.

A belt of steep gradients (0.6 mgal/km) trends eastwards across central Greenland separating a region of relatively negative anomalies to the north from a more positive region to the south. It is a very pronounced change and suggests drastic changes in either the thickness of the crust or in the lithologies and densities of the crust and mantle in this region.

Two northwest trending regional gravity lows separated by a positive anomaly belt are present over the northeastern Canadian mainland and the western part of Baffin Island. Belts of prominent positive free-air gravity anomalies are found along the polar

Figure 2. Free-air gravity anomaly map produced from a combination of satellite tracking data using Goddard Earth Model 8 (GEM 8) and surface gravity data. Contour interval 10 mgal.

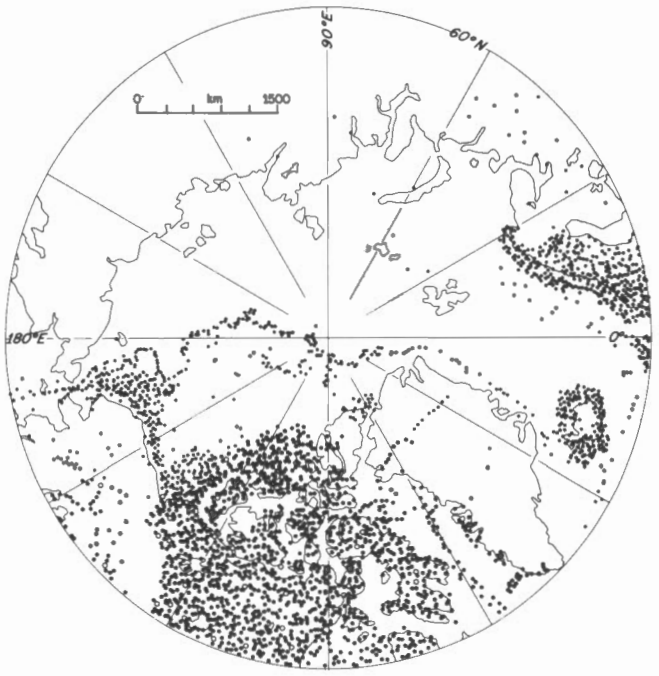

Figure 3. Distribution of gravity observations north of 60°N. Each dot represents 20 gravity observations.

continental margins of North America and Scandinavia-Svalbard. Another interesting gravity lineament is the series of free-air highs more or less along the central axis of Baffin Bay. Towards the north, these anomalies split into Greenland and into the Canadian Arctic Archipelago. More local gravity lows are noted adjacent to the southeastern margin of the Beaufort Sea and the southeastern periphery of the Canada Basin.

PREDICTED MEAN FREE-AIR ANOMALIES

A total of 5,386 predicted mean free-air anomalies were determined by DMAAC and were used primarily over the USSR, Barents Sea, Svalbard and the Greenland Sea (Fig. 1) where few observed gravity data are available. As with the calculated means, these data are referenced to the IGSN 71 (Morelli et al., 1971) and the gravity anomalies are computed using the GRS 67. Wilcox (1974) explained the methods used in predicting the 1° x 1° mean free-air gravity anomaly values and discussed their accuracy. The procedures take into consideration the earth's structure, composition, and surficial rock type distributions by means of observed or computed correlations between gravity and other geophysical parameters. Prediction functions (see Appendix) are used to describe relationships between gravity and elevation within structurally homogenous regions. The gravity effects of local structural variations, terrain, tectonic features, etc., can also be included. Wilcox (1974) estimated that gravity predictions for 1° x 1° areas have an accuracy range of 5 to 20 mgal where little or no measured gravity data exist, and in areas with adequate amounts of measured data, accuracies of 1 to 2 mgal can be achieved. Comparison of predicted anomalies adjacent to observed anomalies (Plate 3) shows that over the Greenland and Norwegian Seas the two sets of data merge well but over the Ural mountains there is a marked discrepancy of 40 to 50 mgal. Predicted values form a positive belt along 58°E but adjacent observed anomalies are primarily negative. This difference demonstrates that either the effects of isostasy have not been considered or that insufficient compensation has been assumed in predicting the gravity values for the Ural region. Thus, predicted anomalies are only as reliable as the assumptions that are made.

Predicted free-air anomaly values range from -62 to 126 mgal. Over the western part of the USSR a very broad negative anomaly (about 3700 km wide) extends eastwards from the polar Ural mountains to the Verkhoyansk mountains and overlies several basins and troughs and a shield area. Within and to the north of this regional low there is a belt of gravity highs east of the West Siberian Basin (between 80°E and 90°E) and another around the northwestern edge of the Central Siberian Platform centred at about 70°N.

Over the northeastern part of the USSR an extensive region (about 2600 km wide) of positive anomalies overlies several basins, troughs and mountainous regions; these anomalies are predicted to extend eastwards from the Verkhoyansk mountains to the Bering Sea.

Two pronounced parallel belts of highs, one over the Svalbard - Scandinavian continental shelf break and the other primarily over the east side of the Lena Trough and Mohns Ridge, are extensions of observed positive anomaly belts that are associated respectively with the polar continental margin of North America and Scandinavia and the Mid-Atlantic Ridge.

CALCULATED SATELLITE FREE-AIR ANOMALIES

The United States National Geodetic Satellite Program (NGSP) has, since the mid-1960's, produced eight solutions (identified as Goddard Earth Models, GEM 1-8) for the geoid and the earth's gravity field based on a combination of satellite tracking data and surface gravity measurements using mean gravity anomalies for 5° x 5° areas. New solutions, calculated in pairs, are periodically determined as more gravity data become available. The odd-numbered solutions use only satellite tracking data and provide long wavelength gravity information. The even-numbered solutions also take into account gravity data measured on the surface of the earth and thus more truly represent the fine structure of the earth's field.

The GEM 8 solution is complete to degree and order 25. A more detailed account of solutions for the geopotential coefficients and tracking station coordinates is described by Smith et al. (1976) and Wagner et al. (1976). The rms errors for GEM 8 are such that its calculated gravitational field is accurate to within ±4 mgal for wavelengths of 1000 km or larger (Smith et al., 1976). Using GEM 8, free-air gravity values were determined for 5° x 5° compartments north of 60°N. The resulting anomaly pattern (Fig. 2) generally correlates well with the previously discussed pattern of Plate 3. For example, there is a high (about 45 mgal, 3750 km wide) centred over south-central Greenland that extends northward to the North Pole and covers parts of the Lomonosov and Alpha Ridges. A second high (about 25 mgal) covers all of eastern USSR east of the Verkhoyansk mountains. A third high (about 27 mgal) overlies southern Alaska and the western interior of North America. An extensive low (about -48 mgal, 3700 km wide) lies over the northeastern Canadian mainland and the southern part of the Canadian Arctic Archipelago between the highs of Greenland and Alaska. This low extends westwards across the Beaufort and Chukchi Seas to the New Siberian Islands. Another regional low (about -23 mgal, 3700 km wide) overlies central USSR.

CALCULATED RESIDUAL FREE-AIR ANOMALIES

Residual anomalies were determined by subtracting the satellite field (Fig. 2) from the calculated and predicted compilation (Plate 3). On a broad scale the residual field (Plate 4) is quite flat and generally varies between 20 mgal and -20 mgal. The anomaly values range from about 115 mgal south of Svalbard to about -134 mgal in northern Greenland.

Plate 4 is similar in many respects to Plate 3. A more or less continuous lineament of positive elliptical anomalies (up to 115 mgal) straddles the polar continental break west of Svalbard and Scandinavia and also staddles the North American break from Greenland to north of the Bering Strait. There are also gravity highs over the Chukchi Plateau and over the centre of the Canada Plain. The broad and relatively flat Chukchi Shelf has four positive anomalies associated with it. Generally, the positive anomalies over the Canadian Arctic Archipelago and the USSR coincide with areas of high relief.

Residual gravity highs are observed over the central part of the Alpha Ridge, over part of the Lomonosov Ridge, Mohns Ridge, Jan Mayan Island and Iceland. An arcuate positive belt of anomalies extends from Iceland into southeastern Greenland. Positive anomalies are also observed over the Boothia Uplift (68°-74°N, 90°-96°W) and the Coppermine Arch (120°W, 68°N) in northern Canada.

Gravity lows are observed over the southern and eastern peripheral regions of the Canada Basin, over the Fletcher Plain and over the Nansen Basin. Belts of negative anomalies are observed over the mountainous west coast of Scandinavia and over the western part of Baffin Island, along the southern rim of the Arctic Archipelago and along the north coast of western Canada and Alaska. The latter extends southward over the Brooks Range and the Bering Strait. Extensive lows also dominate the mountainous and ice covered regions of the north and west half of Greenland and the mountainous part of southern Alaska and adjacent parts of Canada.

SUMMARY

Available gravity data in the form of observed and predicted free-air anomalies and satellite information have been compiled to produce preliminary gravity maps of the Arctic region north of 60°N. Although the amplitudes of some of the shorter wavelength anomalies have been reduced by as much as 50 per cent, Plate 3 provides a first approximation of the free-air gravity field for anomaly widths of 100 km or more over the Arctic Ocean and surrounding landmasses.

The regional field (Fig. 2) derived from satellite gravity data (GEM 8) is subtracted from Plate 3 to remove anomalies with widths of 1000 km or more. The result (Plate 4) is

a preliminary residual free-air anomaly field for about half of the Arctic Ocean and the surrounding landmasses that can be used for a qualitative analysis of the density variation within the crust as well as for the location of anomalous sub-surface structures.

A major characteristic of the gravity field is the widely observed correlation between gravity and topography; gravity highs are observed over positive areas such as mountains, icecaps, and submarine ridges (Ellesmere Island, southeastern Greenland, the Verkhoyansk mountain range, the Alpha and Lomonosov Ridges, the Chukchi and Morris Jesup Plateaus), while gravity lows are observed over sedimentary basins and abyssal plains (the mainland south of the Beaufort Sea, the Canada and Fletcher Plains). This gravity-elevation relationship (high relief-positive anomalies and low relief-negative anomalies) may indicate that these topographic features are, at least in part, isostatically undercompensated. In contrast to this are broad areas of high elevation that display negative anomalies (northwestern Alaska, much of southern Alaska, and northern Greenland) that probably relate to isostatically overcompensated areas, and basinal areas with positive anomalies (the Canada and Baffin Bay Basins) that may be produced by dense sub-surface structures.

Some anomalies are completely unrelated to topography; an example is a high on the mainland southeast of Beaufort Sea which has been explained by a mafic intrusion within the Precambrian basement (Stacey, 1971; Riddihough and Haines, 1972). An extensive high over northern Baffin Bay, an elongated high over the west Greenland continental break and one spur of a high trending towards the central western coast of Greenland probably relate in part to exposed basalts (Ross, 1973). A free-air anomaly map of Baffin Bay (Ross, 1973) shows a ring of negative gravity values encircling a central high over Baffin Bay basin, and the map also shows highs more or less straddling the continental break within Baffin Bay. Gravity highs and flanking lows also straddle the North American and Svalbard-Scandinavian continental breaks. One explanation for these anomaly patterns may be the presence of Cenozoic sediments acting as an uncompensated load on the outer part of the continental shelf (Sobczak, 1975a,b). With the exception of the western coastline of Scandinavia, where Precambrian felsic crystalline rocks are exposed, thick basins of sediments may be the cause of gravity lows over the inner zones of the Beaufort Shelf and over adjacent areas to the north of northwestern Alaska.

ACKNOWLEDGEMENTS

The author is particularly grateful to Drs. E.J. Hauer, H.L. Kuykendall and R.O. Seppelin, all of the Defense Mapping Agency Aerospace Centre, for the magnetic tapes of digitized principal facts gravity data. The author is also indebted to Messrs. L. Hampel, J.F. Halpenny and Dr. D. Nagy of the Gravity and Geodynamics Division, Earth Physics Branch, for programming and plotting of the data, to the drafting office for the drawings completed and to all contributors to this volume for comments and editing of this report.

REFERENCES

Barnes, D.F., 1969. Progress on a gravity map of Alaska. EOS, Trans. Am. Geophys. Union, 50, 550-552.

Basham, P.W., D.A. Forsyth, and R.J. Wetmiller, 1977. Seismicity of northern Canada. Can. J. Earth Sci., 14, 1646-1667.

Defense Mapping Agency Aerospace Centre, 1973. Computational methods for determining 1^{o} x 1^{o} mean gravity anomalies and their accuracies. St. Louis Air Force Station, Mo., Rept. No. 73-00001, 30 p.

Geodetic Reference System, 1967. Internat. Assoc. Geodesy, Sp. Pub. No. 3, 1-116.

Morelli, C., C. Gantar, T. Honkasalo, R.K. McConnell, J.G. Tanner, B. Szabo, U. Uotila and C.T. Whalen, 1971. The International Gravity Standardization Net 1971 (IGSN71). Internat. Assoc. Geodesy, Sp. Pub. No. 4, 1-194.

Ostenso, N.A., and R.J. Wold, 1977. A seismic and gravity profile across the Arctic Ocean basin. Tectonophysics, 37, 1-24.

Riddihough, R.P., and G.V. Haines, 1972. Magnetic Measurements over Darnley Bay, N.W.T. Can. J. Earth Sci., 10, 972-978.

Ross, D.I., 1973. Free air and simple Bouguer gravity maps of Baffin Bay and adjacent continental margins. Geol. Survey Can. Paper 73-37, 11 p.

Smith, D.E., F.J. Lerch, J.G. Marsh, C.A. Wagner, R. Kolenkiewiez, and M.A. Khan, 1976. Contribution to the National Geodetic Satellite Program by Goddard Space Flight Center. J. Geophys. Res., 81, 1006-1026.

Sobczak, L.W., 1975a. Gravity and deep structure of the continental margin of Banks Island and Mackenzie Delta. Can. J. Earth Sci., 12, 378-394.

Sobczak, L.W., 1975b. Gravity anomalies and passive continental margins, Canada and Norway. in: Canada's Continental Margins, eds. C.J. Yorath, E.R. Parker and D.J. Glass, Can. Soc. Petrol. Geol. Mem. 4, 743-761.

Sobczak, L.W., 1977a. Bathymetry of the Arctic Ocean north of 85°N latitude. Tectonophysics 42, T27-T33.

Sobczak, L.W., 1977b. Discussion on "The tectonic development of the southern Beaufort Sea and its relationship to the origin of the Arctic Ocean basin by Yorath and Norris, 1975". Bull. Can. Petrol. Geol., 25, 698-703.

Sobczak, L.W., and L.E. Stephens, 1974. The gravity field of northeastern Ellesmere Island, part of Northern Greenland and Lincoln Sea with map. Earth Phys. Br. Gravity Map Series No. 114, 9 p.

Sobczak, L.W., L.E. Stephens, P.J. Winter and D.B. Hearty, 1973. Gravity measurements over the Beaufort Sea, Banks Island and Mackenzie Delta. Earth Phys. Br. Gravity Map Series No. 151, 16 p.

Sobczak, L.W., and J.R. Weber, 1970. Gravity measurements in the Queen Elizabeth Islands with maps. Earth Phys. Br. Gravity Map Series No. 115 and 116, 14 p.

Stacey, R.A., 1971. Interpretation of the gravity anomaly at Darnley Bay, N.W.T. Can. J. Earth Sci., 8, 1037-1042.

Stephens, L.E., L.W. Sobczak, and E.S. Wainwright, 1972. Gravity measurements on Banks Island, N.W.T. with map. Earth Phys. Br. Gravity Map Series No. 150, 4 p.

Talwani, M., and O. Eldholm, 1972. Continental margin off Norway: A geophysical study. Geol. Soc. Am. Bull., 83, 3575-3608.

Wagner, C.A., J.E. Lerch, J.E. Brown, and J.A. Richardson, 1976. Improvement in the geopotential derived from satellite and surface data (GEM 7 and 8). Document X-921-76-20, NASA Goddard Space Flight Center, Greenbelt, Md.

Wilcox, L.E., 1974. An analysis of gravity prediction methods for continental areas. Defense Mapping Agency Aerospace Centre, St. Louis Air Force Station, Mo., Rept. 74-001, 284 p.

Wilcox, L.E., J.T. Voss, and P.F. Pals, 1975. Regional gravity and elevation maps of Greenland. Defense Mapping Agency Aerospace Centre, St. Louis Air Force Station, Mo., 8 p.

Wold, R.J., 1973. Gravity surveys of the Arctic Ocean basin. Dept. of Geol. Sci., Univ. of Wisconsin, Milwaukee, 222 p.

Wold, R.J., and N.A. Ostenso, 1971. Gravity and bathymetry survey of the Arctic and its geodetic implications. J. Geophys. Res., 76, 6253-6264.

Wold, R.J., T.L. Woodzick and N.A. Ostenso, 1970. Structure of the Beaufort Sea continental margin. Geophysics, 35, 849-861.

Woollard, G.P., and K.I. Daugherty, 1973. Investigations on the prediction of gravity in oceanic areas. Defense Mapping Agency Aerospace Centre, St. Louis Air Force Station, Mo., Part 1, 1-127, Part 2, 1-42.

APPENDIX

The Normal Gravity Anomaly Prediction Method (NOGAP) as given by the following formula is the one most frequently used for land areas where very few gravity measurements exist.

$\overline{\Delta g_F} = \overline{\Delta g_B} + 0.1119\bar{h}$ where

$\overline{\Delta g_F}$ = predicted $1^o \times 1^o$ mean free-air anomaly

$\bar{h}$ = $1^o \times 1^o$ mean elevation taken from topographic charts

$\overline{\Delta g_B}$ = BP + $\overline{g_R}$ + $\overline{g_L}$ where

Δg_B = predicted $1^o \times 1^o$ mean Bouguer anomaly

BP = basic predictor

$\overline{g_R}$ = regional correction

$\overline{g_L}$ = local geologic correction

The basic predictor is the equation of linear regression between $1^o \times 1^o$ mean Bouguer anomaly values and the corresponding mean elevation values where the gravity anomaly field is known (control region)

BP = $\alpha_R + \beta_R \bar{h} = \overline{\Delta g_B}$ where

$\overline{\Delta g_\beta}$ = a $1^o \times 1^o$ mean Bouguer anomaly

$\bar{h}$ = the $1^o \times 1^o$ mean elevation corresponding to Δg_B

α_R and β_R are determined by a linear regression of point elevation and point Bouguer anomalies within the $1^o \times 1^o$ area represented by $\overline{\Delta g_B}$ and $\bar{h}$. This BP is applied to predict basic regional gravity anomaly values in an adjacent region which contains few or no gravity measurements. Both the control and prediction regions should be contained within the same geologic/tectonic province. The basic predictor contains that portion of the regional component of mean Bouguer anomalies which is constant with respect to the mean elevation but does not control the gravitational effects of any long period changes in crust-mantle structure within the same geologic/tectonic province. Hence, a regional correction $\overline{g_R}$, is sometimes added to the BP.

There are many techniques for determining these corrections. Most common is a correlation between mean Bouguer anomalies and crustal thickness. The local geologic correlation $\overline{g_L}$ accounts for variations in the Bouguer gravity field caused by uncompensated mass distributions in a local geologic structure. Various techniques can be used to determine $\overline{g_L}$ and several examples are given (Wilcox, 1974). Various other corrections can be made to NOGAP depending on circumstances and various other methods can also be used (Wilcox, 1974).

The predicted anomalies shown on Plate 3 are based on the methods outlined by Wilcox (1974) and Woollard and Daugherty (1973). It is not known, however, which methods were used and what assumptions were made in specific areas.

Review of Arctic crustal studies

D. A. Forsyth

ABSTRACT

The Arctic areas north of 60°N latitude most extensively surveyed by deep seismic sounding techniques are the northern and offshore Baltic Shield, Scandinavia and the Canadian Arctic Islands. The average crustal velocity of 6.6 - 6.7 km/s for central Norway and Sweden is perhaps the highest yet measured for areas north of 60°N. A major fracture zone of at least crustal extent has been mapped in the continental-oceanic transition zone north of the Baltic Shield. Shallower results from Canada's polar continental margin suggest the presence of a major basement ridge along the north edge of the Sverdrup Basin and also a faulted margin in the Beaufort Sea. Recent seismic results show the Soviet map of average crustal velocities based upon mainly non-seismic geophysical and geological parameters is in need of revision. To date there has been no program of deep seismic sounding completed over the Arctic Ocean basins and therefore much work remains in mapping regional differences in crustal properties.

RÉSUMÉ

Les zones Arctiques, situées au nord de 60° de latitude, qui ont été explorées en détail par prospection séismique à grande profondeur, sont la partie septentrionale et le plateau continental du bouclier Baltique, de la Scandinavie et de l'archipel Arctique canadien. La vitesse moyenne des ondes séismiques dans la croûte (6.6 - 6.7 km/s dans la partie centrale de la Norvège et de la Suède), est probablement la vitesse la plus élevée mesurée jusqu'à présent dans les régions situées au nord de 60° de latitude. On a cartographié une importante zone de fractures, dont la profondeur est à l'échelle de la croûte terrestre, dans la zone de transition qui sépare les terrains continentaux des terrains océaniques au nord du bouclier Baltique. Des résultats de sondages moins profonds, obtenus sur la marge continentale polaire du Canada, suggèrent l'existence d'une importante dorsale océanique le long du rebord septentrional du bassin Sverdrup, ainsi que celle d'une marge continentale faillée dans la mer de Beaufort. Les résultats d'études séismiques récentes montrent qu'il faut corriger la carte soviétique qui donne la vitesse moyenne des ondes séismiques dans la croûte, parce qu'elle est surtout basée sur des paramètres géophysiques et géologiques non déterminés par prospection séismique. Jusqu'à présent, dans les bassins de l'océan Arctique, aucun programme de prospection séismique à grande profondeur n'a été complété, et il reste par conséquent beaucoup à faire pour cartographier à l'échelle régionale les divers caractères de la croûte terrestre.

INTRODUCTION

This review describes the results of deep seismic sounding (DSS) surveys in the Arctic continental and coastal areas and discusses some of the interpretations. While considerable DSS work has been done north of 60°N, the results are yet too sparse to draw conclusions about regional differences in lithospheric structure. Because all of the northern deep crustal surveys have been done since 1950 and most have been completed within the last decade there is an approximate uniformity with respect to the accuracy of recording equipment. Measurement of calculated velocities and depths assumes plane layering and homogeneous layers in all cases. Given these restrictions, the works described herein show that an average crustal or upper lithospheric structure may be described with velocities known to within ±0.2 km/s and depths known generally to better than ±5 km.

The nature of the terrain, weather conditions and associated logistic costs probably account for the paucity of deep reflection-refraction results north of 60°N. Scandinavia is probably the best surveyed area. Based on the relationship between extensive DSS results, geological structures and geophysical parameters south of 60°N, Soviet scientists have constructed a map predicting average crustal velocities

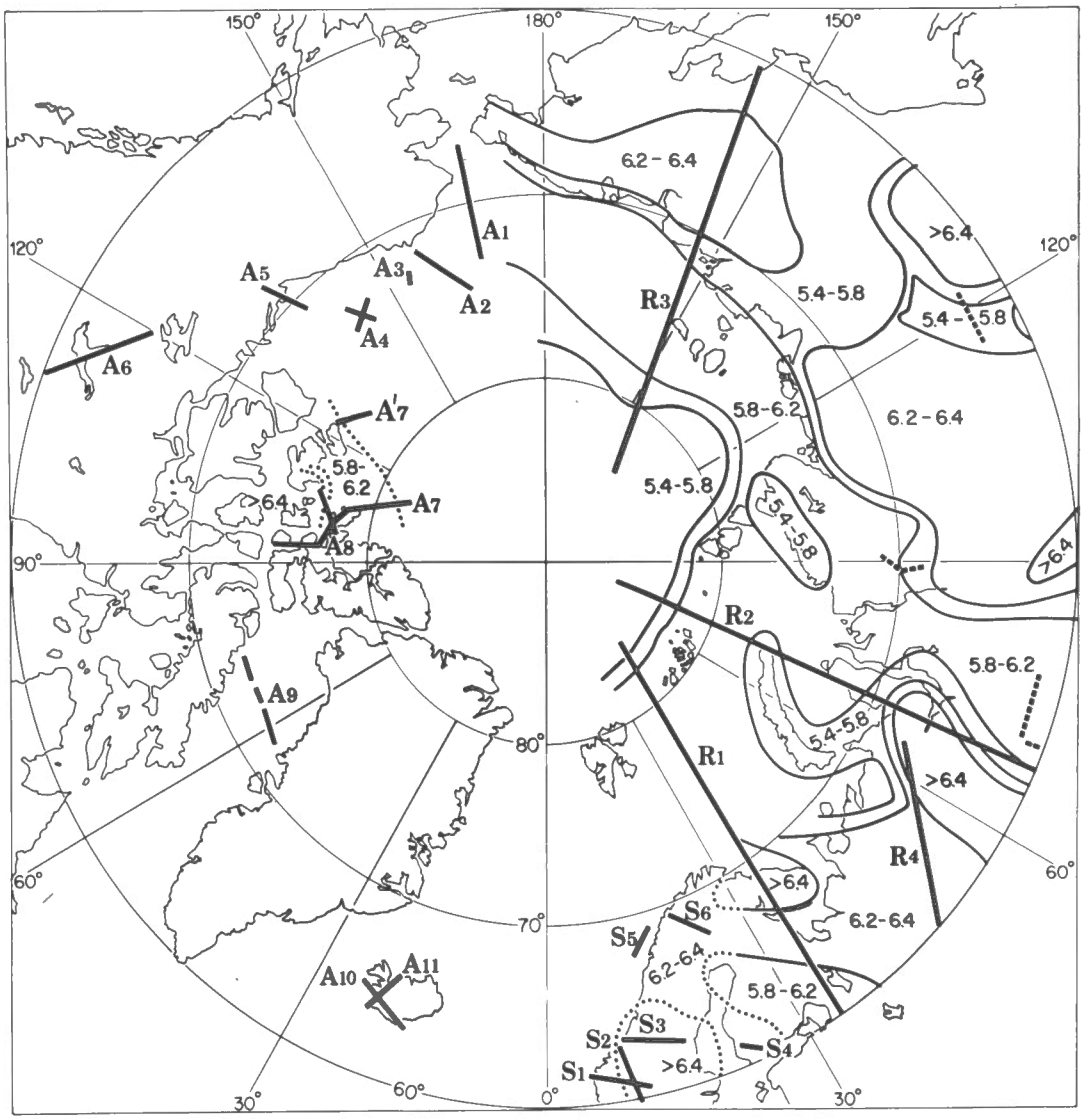

Figure 1. Polar map showing location of crustal sections and the Arctic portion of the Soviet map (Vol'vovskii, 1973) of average crustal velocities in km/s.

for the area of the USSR north of 60°N (Fig. 1). Recent DSS results indicate that this map is in need of revision. For Arctic regions, the location of crustal profiles is shown on figure 1, the place names mentioned are shown on figure 2 and details of the sections are described in the text that follows.

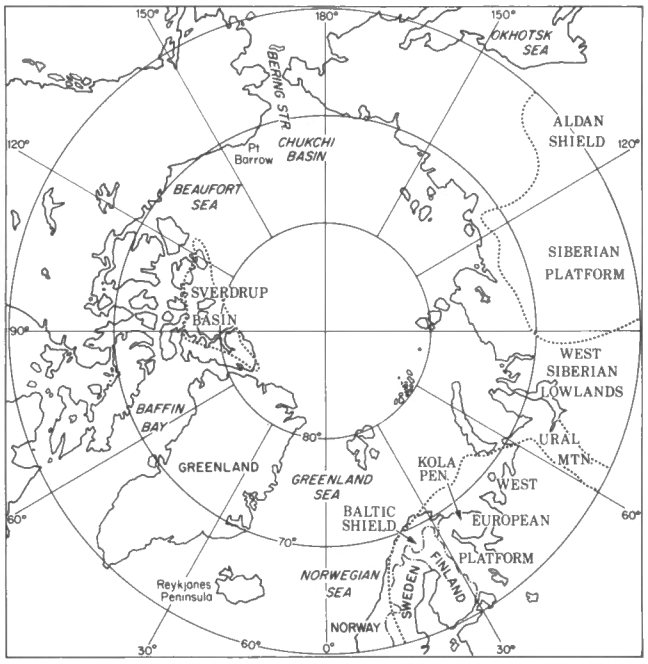

Figure 2. Polar map showing place names referred to in text.

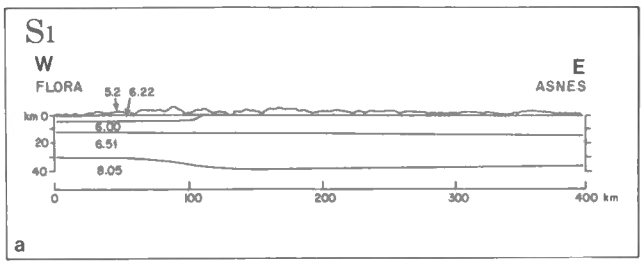

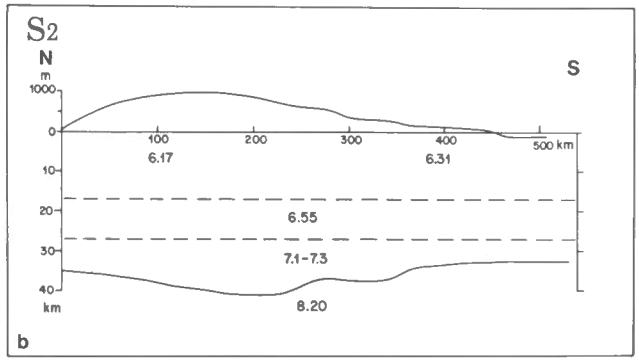

Figure 3. a) Section S_1 from Flora to Asnes across southern Norway (Kanestrom, 1971).
b) Section S_2, a north-south profile across southern Norway (Kanestrom and Haugland, 1971).

SCANDINAVIA

The area most intensely studied by DSS techniques north of 60°N is probably the area of Norway, Sweden, Finland and neighboring offshore areas. The work done to 1969 on the continent is summarized in Vogel and Lund (1971). The offshore work is summarized in Johnston et al. (1975), Eldholm and Talwani (1977) and Houtz and Windisch (1977).

In southern Norway and Sweden relief on the Mohorovicic discontinuity correlates well with the topography of the Caledonian mountains, the major geological features and regional gravity anomalies (Figs. 3a and 3b). The average crustal velocity for central Norway and Sweden, at 6.6 - 6.7 km/s, is perhaps the highest yet measured for areas north of 60°N latitude (Fig. 4a).

In Finland the mean thickness of the crust is 42 km. In the region of the Gulf of Bothnia, separating Finland and Sweden, the Conrad discontinuity lies at about 18 km. It increases in southern Finland to 19 - 21 km, in eastern Finland to 22 - 23 km and in northern Finland to 23 km. The granitic surface layer appears to thin from east to west as in figure 4b but the largest variations in thickness occur in the underlying basaltic layer (Penttila, 1971a).

In Norway the crust varies in thickness from 32 km in the south to 41 km in the central part and is approximately 30 km thick beneath the northwestern coastal structures (Figs. 5a and 5b). The observed surface velocity at the west coast of Norway is very high (6.3 km/s) compared with surface velocities observed elsewhere in Scandinavia.

USSR

Excluding earthquakes, there is little deep seismic information north of 60°N from the Soviet Union. The available deep seismic sounding sections are too sparse to be regionally descriptive. The contours of average crustal velocity, V, shown for the

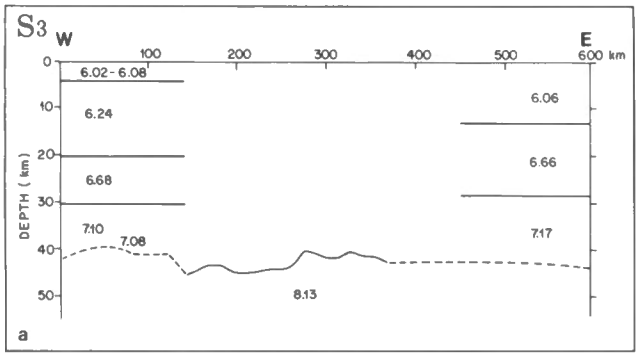

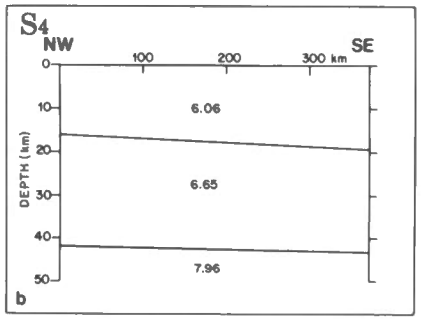

Figure 4. a) Section S_3, an east-west section across central Norway and Sweden (Vogel and Lund, 1971). b) Section S_4, a northwest-southeast section across southern Finland (Penttila, 1971b).

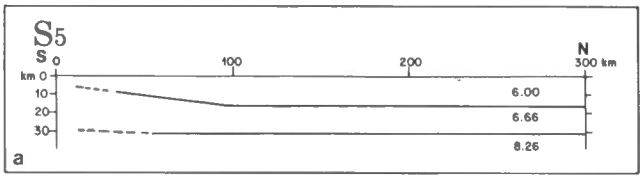

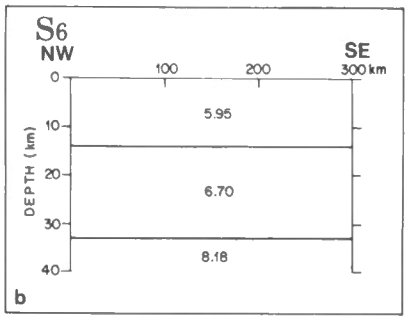

Figure 5. a) Section S_5, a northeast-southwest profile along the northwest continental margin of Norway (Sellevoll, 1969). b) Section S_6, a section from northwest Norway to northwest Finland (Kanestrom, 1971).

USSR in figure 1, although controlled by seismic data where possible, are based on the "topography of the consolidated basement", large scale tectonic generalizations, inferences from the distribution of metamorphic facies, physical properties of rocks, outcrops of intrusive complexes and intrusions hidden by the sedimentary cover (Belyaevskiy et al., 1972, Vol'vovskii, 1973). For example, the region of 5.4 - 5.8 km/s velocity in figure 1 is bordered in part by velocities of 6.2 - 6.4 km/s associated with the Siberian Platform and the Aldan Shield. The lower velocity region includes the Ural mountains and appears to be derived mainly from the great thicknesses (25 - 30 km) of Paleozoic deposits present within the zone (Nalivkin, 1957). Therefore, the velocity contours are only significant in so far as the above properties may be used to infer average velocities. There are several studies which suggest such inferences may be reasonable.

For the Canadian landmass, Goodacre (1972) showed that regional variations in the Bouguer gravity field are caused mainly by changes in crustal thickness, and that there is an approximately linear relationship between the measured compressional velocities and depth within the crust.

Based on a study in the Okhotsk region, Demenitskaya et al. (1973) suggest that beneath the polar shelf north of Eurasia, seismic discontinuities within the lithosphere are coincident with the upper and lower boundaries of anomalous magnetic bodies and are indicative of zones where the magnetization changes rapidly in the vertical direction.

By comparing the structure of the Baltic Shield with the Ukranian Shield, Sollogub et al. (1973) suggest that areas of thick crust (50 - 65 km) seem to be associated with Early Proterozoic geosynclinal zones, and regions of thinner crust (30 - 40 km) may be associated with median massifs and ancient (Early Proterozoic?) platform areas.

In categorizing average crustal velocity values, Belyaevskiy et al. (1972) suggest that higher V values (6.3 - 6.4 km/s) are characteristic of:

a) shields or flanks of shields such as the East European and Siberian Platforms,
b) platforms with thin sedimentary cover, particularly where the basalt layer is

thick, such as the Kola Peninsula on the Baltic Shield, and

c) areas of large concentrations of granulite facies rocks, such as the Aldan Shield.

Relatively high V values are also associated with the Paleozoic fold region of the Ural mountains due to a greatly increased thickness of the "basalt layer". Average crustal velocities of about 6.2 km/s are considered typical of areas with a larger proportion of lower velocity granitic material relative to basaltic material, e.g., the Baltic Shield. The Paleozoic rocks of the West Siberian Lowlands exhibit lower V values (5.8 - 6.0 km/s) due to a thick unconsolidated sediment cover. Low V values are also considered typical of Alpine and Mesozoic fold regions because of their great sediment thicknesses. The Soviet polar continental shelf is considered to be an area of low V values (6.0 km/s) by analogy with the eastern marginal Sea of Okhotsk.

Thus for the USSR in figure 1 the measurements of average crustal velocities for the Arctic are contoured by extrapolating

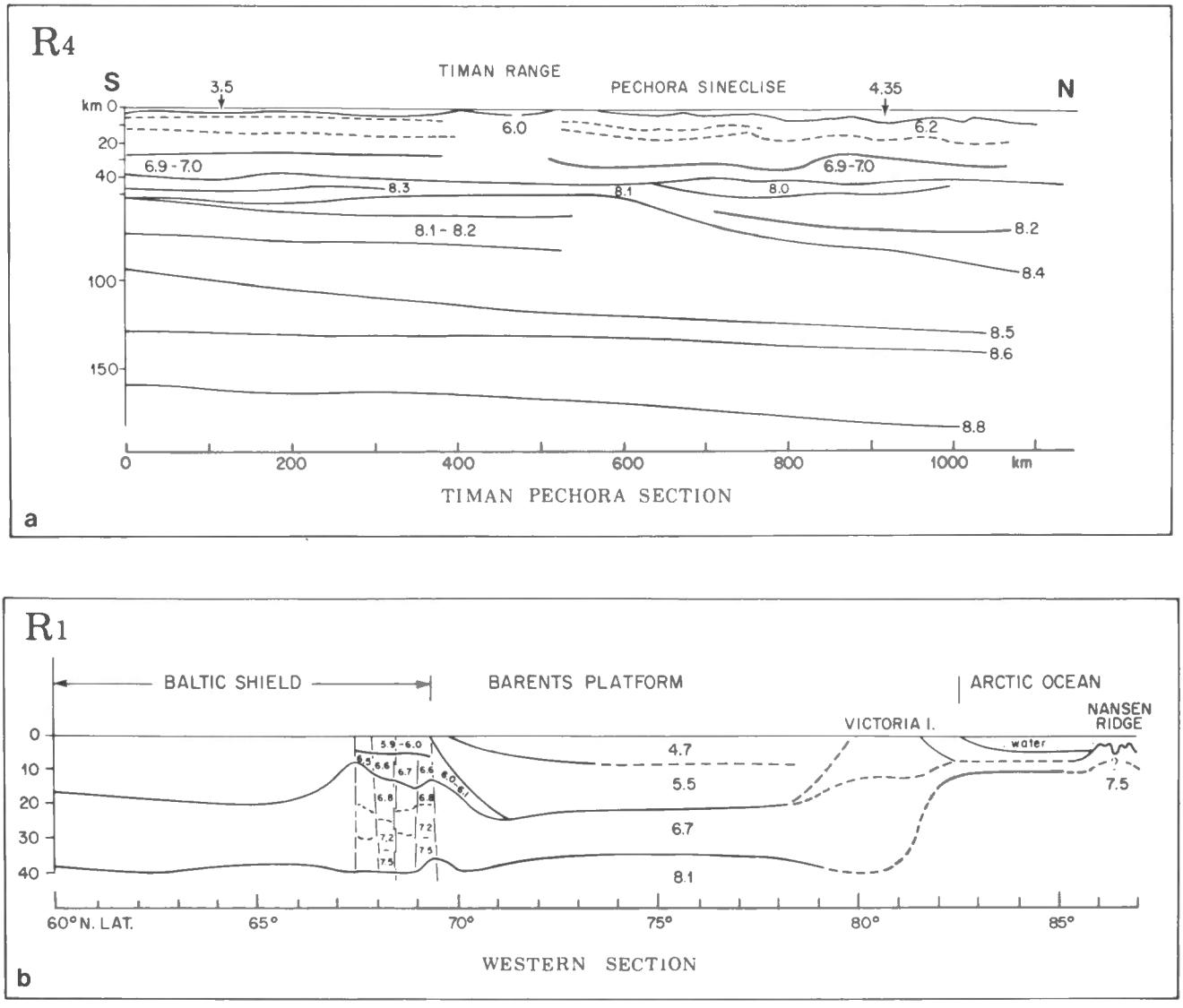

Figure 6. a) Section R_4. The northern portion of a profile running from the Black Sea to the polar Urals (Belyaevskiy et al., 1976).
b) Section R_1. A generalized section from the Baltic Shield to the Arctic Ocean (Belyaevskiy et al., 1968).

the results found south of 60°N latitude using geological and other, mainly non-seismic, geophysical data. The contours of constant velocity are therefore suggestive, but cannot be taken to seismically identify tectonic features in those areas not yet studied by DSS techniques. The only Arctic area covered extensively by DSS studies is the Baltic Shield and the associated northward transition to oceanic crust (Demenitskaya et al., 1968; Sollogub et al., 1973).

Recent work indicates that the general contours shown in figure 1 are approximately correct but will change in detail as more DSS results become available. For example, from profile R_4 (Fig. 6a) which runs from the southeast to the polar Urals, Belyaevskiy et al. (1976) determined an average crustal velocity of 6.45 - 6.55 km/s in the area immediately south of 60°N. The northern part of this profile is described as having a "slightly lower average crustal velocity". The velocity contours indicate a velocity of 6.2 to 6.4 km/s for this region.

With the exception of the southern half of section R_1 through the Baltic Shield, which is supported by extensive DSS work, the Arctic portion of sections R_1, R_2, R_3 (Figs. 6b, 7a and 7b) must also be regarded as predictive. The section R_1 shows that the Baltic Shield-Barents Sea transition is characterized by a major fracture pattern which extends to the Moho.

NORTH AMERICA

The positions of deeper crustal sections for North America are shown in figure 1. While considerable shallow seismic profiling has been done along the Canadian-American Arctic shelf (e.g., Grantz et al., 1975, p. 671) the deep seismic sounding results are too sparse to be correlated regionally.

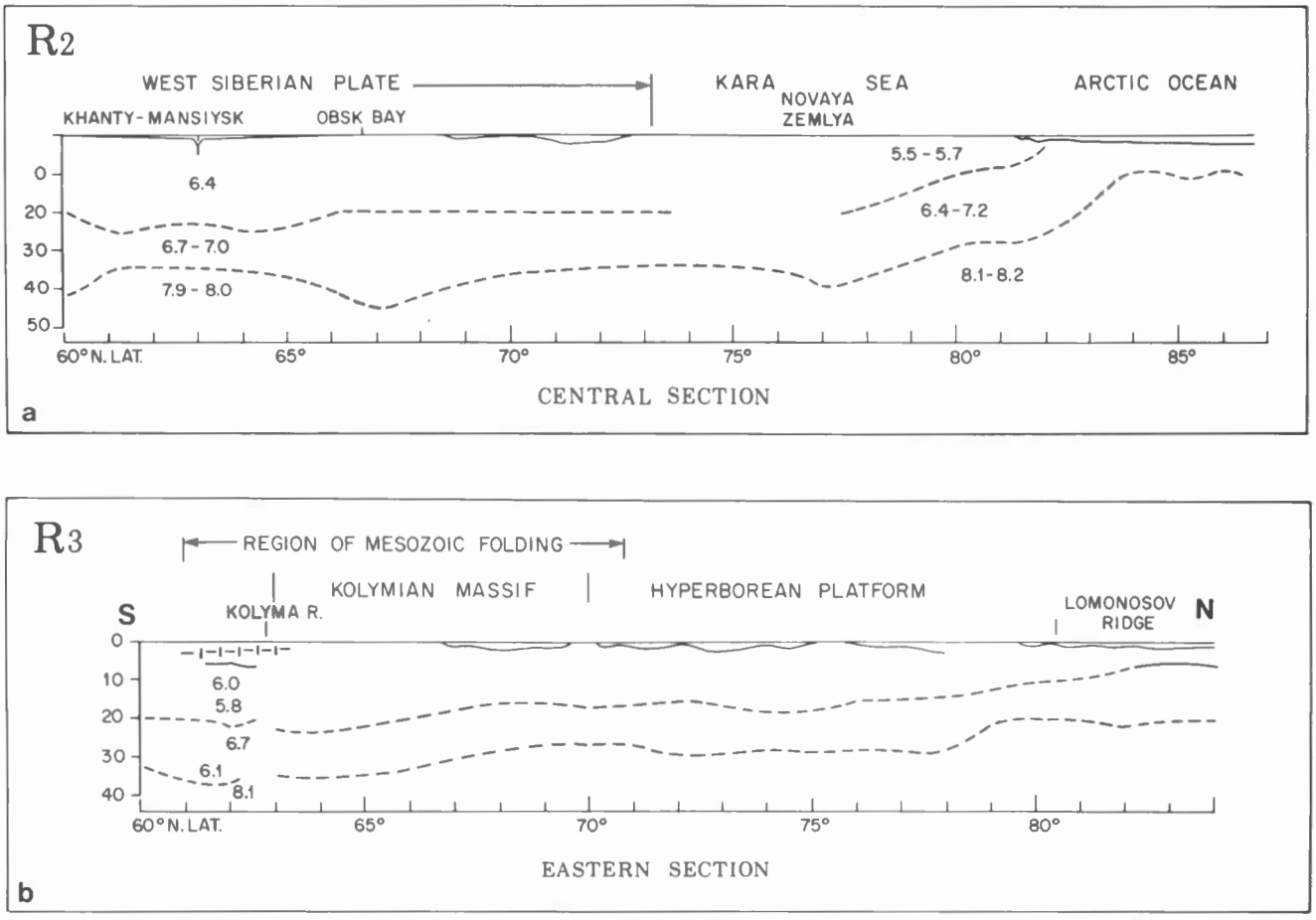

Figure 7. a) Section R_2, a north-south generalized section from the West Siberian Lowlands to the Arctic Ocean (Belyaevskiy et al., 1968). b) Section R_3, a north-south generalized section across the eastern USSR. (Belyaevskiy et al., 1968).

Section A_1 (Fig. 8a), although not truly a deep seismic profile, indicates that the large scale crustal structure northwest of Alaska consists of three major sedimentary basins separated by structural highs. The

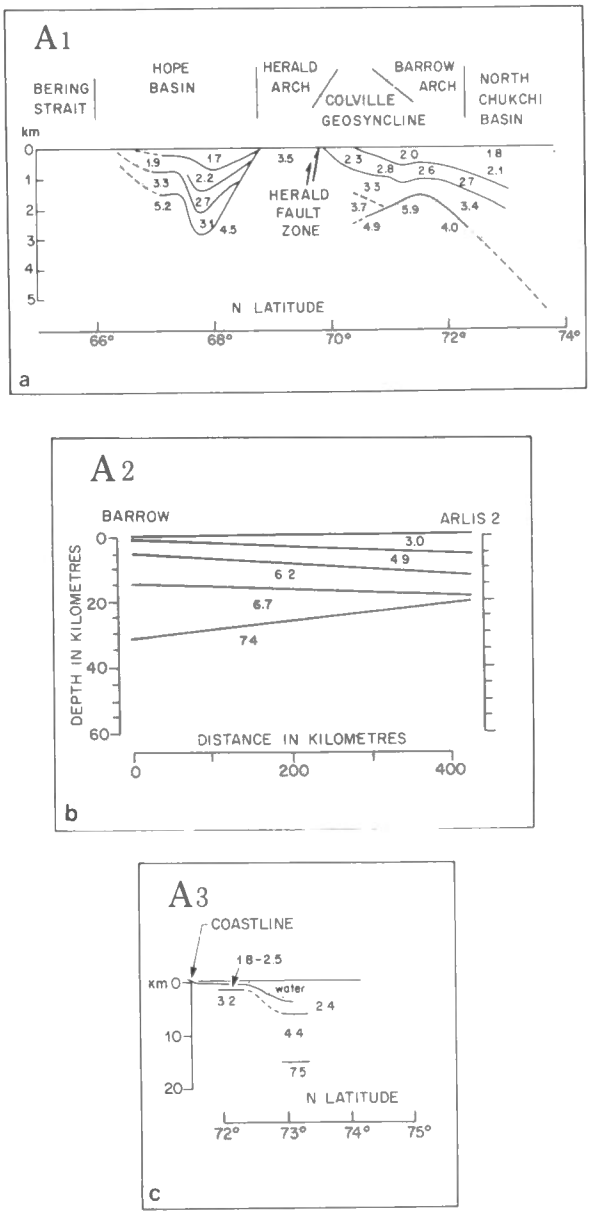

Figure 8. a) Section A_1, a shallow north-south section from the Bering Strait to the North Chukchi Basin (Grantz et al., 1975).
b) Section A_2, a crustal section from Point Barrow to the Arctic Ocean (Hunkins, 1965).
c) Section A_3 from the Alaskan shelf to the western Canada Basin after Grantz et al. (1975) and Milne (1966).

basins trend west to northwest and their enclosed sediments become more marine from south to north (Grantz et al., 1975). To the northwest a reversed refraction profile A_2 (Fig. 8b) shows that the crust thins from 32 km at Point Barrow to about 20 km near the edge of Chukchi Shelf. The average crustal velocity near Point Barrow is 6.5 km/s and at the northwest end V is 4.8 km/s. These measurements do not follow the trends predicted by Belyaevskiy et al. (1976), and are further evidence that the average velocity contours of figure 1 are in need of revision. An unreversed profile by Milne (1966) suggests the oceanic crust of the Canada Basin northeast of Point Barrow is, at 15 km, thicker than normal (Fig. 8c). There has been no other published work on the southern Canada Basin, however, to confirm this finding. A reversed refraction profile (A_4, Fig. 1) consisting of crossed 200 km lines done as part of the AIDJEX project in 1976 (Mair et al., in preparation) may provide more information on the basin's deep structure.

Although DSS studies have yet to be done in the Beaufort Sea, Section A_5 (Fig. 9a), based on shallow profiling across the continental shelf, depicts the block faulted margin of early Mesozoic and older rocks overlain by a clastic Tertiary sequence which thickens rapidly towards the Canada Basin.

The only large scale refraction-reflection surveys on the Canadian Shield north of 60°N were reported by Barr (1971) and Clee et al. (1974). The results of these works are shown on section A_6 (Fig. 9b). The results indicate that the crust thickens from about 30 km beneath Aphebian rocks in the northwest to about 35 km beneath Archean rocks to the southeast. The crust thickens significantly beneath the East Arm of Great Slave Lake which separates the Churchill province from Aphebian rocks to the northwest. The average crustal velocity along the whole profile is in the 6.2 - 6.4 km/s range. In the area immediately beneath Yellowknife figure 9b shows that there is good correlation between the local geology and the seismic interpretation.

SVERDRUP BASIN

Perhaps the area of the North American Arctic best studied by DSS techniques is the Canadian Arctic Archipelago. The details of the work are described in papers by Hobson (1962), Sander and Overton (1965), Hobson and Overton (1967), Overton (1970), Sobczak and Weber (1973) and Berry and Barr (1971). An east-west refraction profile (A_8, Fig. 1)

across the basin was conducted in 1972 and 1973. The interpretation of these data is in progress at the Earth Physics Branch (Mair et al., in preparation).

The south end of Section A_7 (Fig. 10) shows surface layer velocities of 6 km/s produced by high velocity Paleozoic sediments and Precambrian basement. Lower velocity sediments thicken to a depth of at least 10 km to the north, then thin dramatically over a major basement ridge along the northern edge of the Sverdrup Basin. The basement ridge structure is taken from the study by Hobson and Overton (1967) which covers the seaward transition zone more completely than does the study by Sander and Overton (1965) from which the southern half of section A_7 is taken.

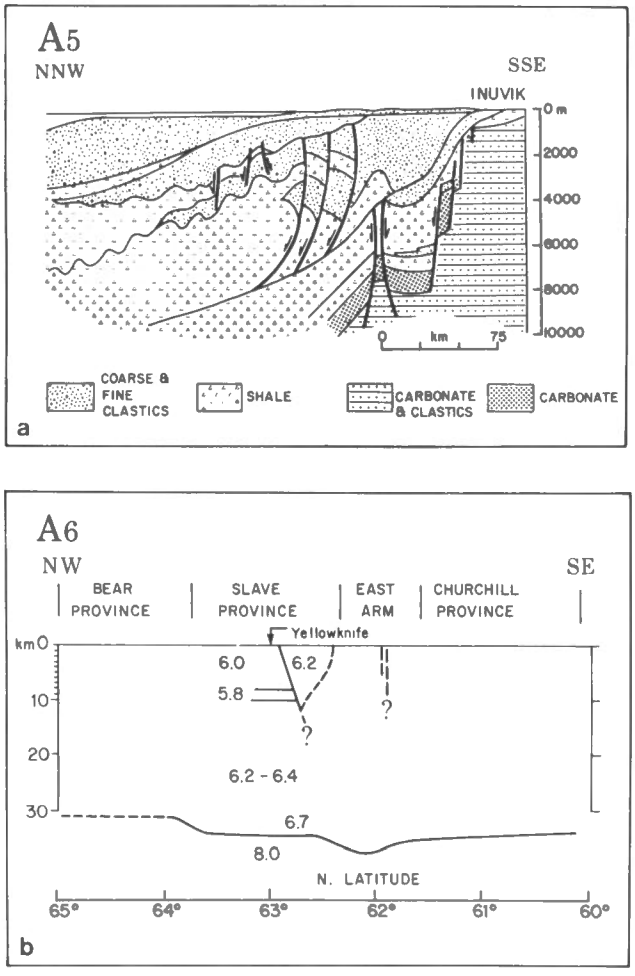

Figure 9. a) Section A_5, a generalized shallow section across the northwest continental margin of Canada (Hawkings and Hatlelid, 1975).
b) Section A_6, a profile across Proterozoic provinces of the northwest Canadian Shield (Clee et al., 1974).

A_7' on figure 1 indicates the position of a refraction profile by Berry and Barr (1971). Although beset with navigational difficulties, this is the only profile which was designed to cross the Arctic continental margin of North America. The better resolved data show an oceanic crustal structure not significantly different from the Arctic Ocean end of section A_7 (Fig. 10).

BAFFIN BAY

An important tectonic link in the chain of events which led to the present relationship between the North Atlantic spreading ridge and the Canadian Arctic Archipelago lies in the history of Baffin Bay. Explanations of the bay's evolution have been somewhat hampered by the fact that, despite the implications of data recorded in the Labrador Sea (Srivastava, 1978) or other areas of the North Atlantic (Eldholm and Talwani, 1977), clear geophysical evidence from within Baffin Bay has yet to be found which would indicate separation of Baffin Island from Greenland by sea-floor spreading. In fact, the distribution of oceanic crust in northern Baffin Bay still remains to be settled (Keen et al., 1972; Wetmiller, 1974). Keen et al. (1972, Fig. 11) indicate a relatively featureless 10 km thick crust below the central region of the bay that has an average velocity of 4.49 km/s. Other geophysical results from Baffin Bay are summarized in papers by Grant (1975), Hood and Bower (1975), Jackson et al. (1977) and Srivastava (1978).

NORTH ATLANTIC AND ICELAND

The Greenland and Norwegian Seas have been studied by numerous, shallow profiling, refraction-reflection experiments (e.g., Johnson et al., 1975; Sundvor and Nysaether, 1975). However, with the exception of the Iceland area, most of these profiles have retrieved information from depths of less than 5 km. The crustal structure of Iceland and the shelf to its southwest has been outlined to a depth of about 20 km by many refraction surveys (e.g., Palmason, 1971). Four principal layers overlying a thick lower crustal or upper mantle layer have been detected (Fig. 12). Layer 0 represents a surface layer everywhere within the Neovolcanic zone. Its greatest thickness (1.0 km) occurs on the southern Reykjanes

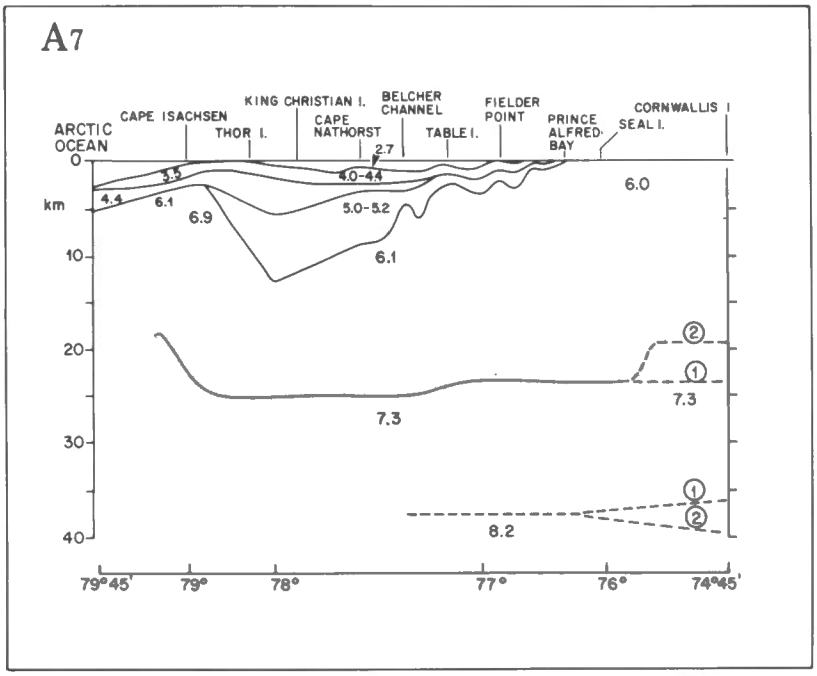

Figure 10. Section A7 across the Sverdrup Basin adapted from Sander and Overton (1965) and Hobson and Overton (1967). Circled numbers indicate alternative interpretations.

Peninsula. Layers 1 and 2 are mainly Tertiary flood basalts. Layer 1 occurs at the surface in western, northern and eastern Iceland while layer 2 is exposed in the southeast. Layer 2 is missing as a first arrival seismic event on the Reykjanes Peninsula. The existence of layer 3 has been recorded everywhere except under the central northwest peninsula. The average apparent P-wave velocities are shown below from Palmason (1971).

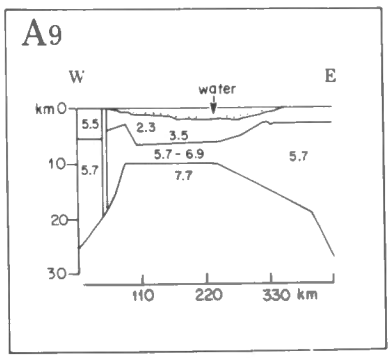

Figure 11. Section A9, an east-west section across Baffin Bay (Keen et al., 1972).

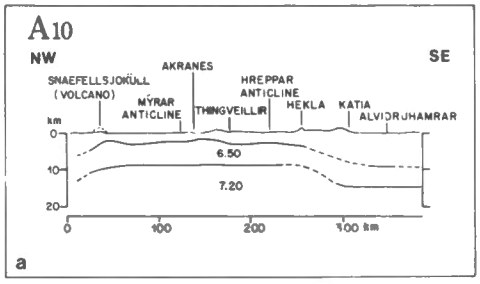

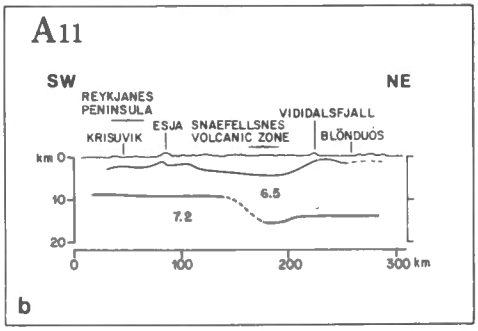

Figure 12. a) Section A_{10}, a northwest-southeast profile across Iceland (Palmason, 1971).
b) Section A_{11}, a profile across Iceland extending to the northeast from the Reykjanes Peninsula (Palmason, 1971).

Layer	P-velocity km/s
0	2.75
1	4.14
2	5.08
3	6.35
4	7.2

The sections shown in figures 12a and b for Iceland criss-cross the area of the Reykjanes Ridge in southwest Iceland. In figure 12a, layers 0, 1 and 2 are shown as a single layer. Tryggvason (1961) indicates an increase to 8.2 km/s at a depth of about 140 km.

SUMMARY

This report has attempted to collect and discuss the available results of deep seismic sounding surveys in Arctic continental and coastal areas. The only regions which have been extensively studied by DSS techniques are the Baltic Shield and associated offshore areas, Scandinavia and the Canadian Arctic Islands. While the number of DSS studies in Arctic regions has been limited, some major crustal structures have been detected. Examples are the major crustal arch beneath the northern Canadian Archipelago, the major vertical faults extending to the Moho beneath the Baltic Shield continental shelf and the long wavelength features of the Bering Strait - North Chukchi Basin area.

REFERENCES

Barr, K.G., 1971. Crustal refraction experiment: Yellowknife, 1966. Can. J. Earth Sci., 8, 1929-1947.

Belyaevskiy, N.A., A.A. Borisov, I.S. Vol'vovskii and Yu. K. Schukin, 1968. Transcontinental crustal sections of the USSR and adjacent areas. Can. J. Earth Sci., 5, 1067-1078.

Belyaevskiy, N.A., I.S. Vol'vovskii, M.I. Razinkova and V.Z Ryaboy, 1972. Average crustal velocities of longtudinal seismic waves in the USSR. Dokl. Akad. Nauk. SSSR, 198, 32-34.

Belyaevskiy, N.A., I.S. Vol'vovskii, A.V. Yegorkin, M.K. Polshkov, Ye. A. Popov, M.M. Chernyshev and Yu. G. Yurov, 1976. Lithospheric structure along a profile from the Black Sea to the polar Urals. Tectonophysics, 33, 359-378.

Berry, M.J., and K.G. Barr, 1971. A seismic refraction profile across the polar continental shelf of the Queen Elizabeth Islands. Can. J. Earth Sci., 8, 347-360.

Clee, T.E., K.G. Barr and M.J. Berry, 1974. Fine structure of the crust near Yellowknife. Can. J. Earth Sci., 11, 1534-1549.

Demenitskaya, R.M., A.M. Karasik, Yu. G. Kiselev, I.V. Litvinenko and S.A. Ushakov, 1968. The transition zone between the Eurasian continent and the Arctic Ocean. Can. J. Earth Sci., 5, 1125-1129.

Demenitskaya, R.M., S.S. Ivanov and V.E. Volk, 1973. Crust of the Arctic seas of Eurasia. Tectonophysics, 20, 97-104.

Eldholm, O., and M. Talwani, 1977. Sediment distribution and structural framework of the Barents Sea. Geol. Soc. Am. Bull., 88, 1015-1029.

Goodacre, A.K., 1972. Generalized structure and composition of the deep crust and upper mantle in Canada. J. Geophys. Res., 77, 3146-3161.

Grant, A.C., 1975. Geophysical results from the continental margin off southern Baffin Island. in: Canada's Continental Margins, eds. C.J. Yorath, E.R. Parker, and D.J. Glass, Can. Soc. Petrol. Geol. Mem. 4, 411-431.

Grantz, A., A.L. Holmes and B.A. Kososki, 1975. Geologic framework of the Alaskan continental terrace in the Chukchi and Beaufort Seas. in: Canada's Continental Margins, eds. C.J. Yorath, E.R. Parker, and D.J. Glass, Can. Soc. Petrol. Geol. Mem. 4, 669-700.

Hawkings, T.J., and W.G. Hatlelid, 1975. The regional setting of the Taglu field. in: Canada's Continental Margins, eds. C.J. Yorath, E.R. Parker and D.J. Glass, Can. Soc. Petrol. Geol. Mem. 4, 633-647.

Hobson, G.D., 1962. Seismic exploration in the Canadian Arctic Islands. Geophysics, 27, 253-273.

Hobson, G.D., and A. Overton, 1967. A seismic section of the Sverdrup Basin, Canadian Arctic Islands. in: Seismic Refraction Prospecting, ed. A.W. Musgrave, Soc. Explor. Geophys. Tulsa, Okla., 550-562.

Hood, P., and M. Bower, 1975. Aeromagnetic reconnaissance of Davis Strait and adjacent areas. in: Canada's Continental Margins, eds. C.J. Yorath, E.R. Parker, and D.J. Glass, Can. Soc. Petrol. Geol. Mem. 4, 433-451.

Houtz, R., and C. Windisch, 1977. Barents Sea continental margin and sonobuoy data. Geol. Soc. Am. Bull., 88, 1030-1036.

Hunkins, K.L., 1965. The Arctic continental shelf north of Alaska. in: Continental Margins and Island Arcs, Geol. Survey Can. Paper 66-15, 197-205.

Jackson, H.R., C.E. Keen and D.L. Barrett, 1977. Geophysical studies on the continental margin of Baffin Bay and in Lancaster Sound. Can. J. Earth Sci., 14, 1991-2001.

Johnson, G.L., N.J. McMillan, and J. Egloff, 1975. East Greenland continental margin. in: Canada's Continental Margins, eds. C.J. Yorath, E.R. Parker and D.J. Glass, Can. Soc. Petrol. Geol. Mem. 4, 205-224.

Kanestrom, R., 1971. Seismic investigations of the crust and upper mantle in Norway. in: Proc. Colloquium on Deep Seismic Sounding in Northern Europe, ed. A. Vogel, Swedish Natural Sci. Res. Council, Stockholm, 17-27.

Kanestrom, R., and K. Haugland, 1971. Profile Section 3-4. in: Proc. Colloquium on Deep Seismic Sounding in Northern Europe, ed. A. Vogel, Swedish Natural Sci. Res. Council, Stockholm, 76-91.

Keen, C.E., D.L. Barrett, K.S. Manchester and D.I. Ross, 1972. Geophysical studies in Baffin Bay and some tectonic implications. Can. J. Earth Sci., 9, 239-256.

Milne, A.R. 1966. A seismic refraction measurement in the Beaufort Sea. Bull. Seism. Soc. Am., 56, 775-779.

Nalivkin, D.V., 1957. The geology of the USSR a short outline. The Academy of Sciences USSR, (English translation by S.I. Tomkeieff, 1960), ed. J.E. Richey, Permagon Press, London, 170 p.

Overton, A., 1970. Seismic refraction surveys, western Queen Elizabeth Islands and polar continental margin, Canada. Can. J. Earth Sci., 7, 346-365.

Palmason, G., 1971. Crustal Structure of Iceland from Explosion Seismology. Snaebjorn Jonsson and Co., Reykjavik, 187 p.

Penttila, E., 1971a. Seismic investigations on the Earth's crust in Finland. in: Proc. Colloquium on Deep Seismic Sounding in Northern Europe, ed. A. Vogel, Swedish Natural Sci. Res. Council, Stockholm, 9-13.

Penttila, E., 1971b. Profile section 1-2. in: Proc. Colloquium on Deep Seismic Sounding in Northern Europe, ed. A. Vogel, Swedish Natural Sci. Res. Council, Stockholm, 58-61.

Sander, G.W., and A. Overton, 1965. Deep seismic refraction investigations in the Canadian Arctic Archipelago. Geophysics, 30, 87-96.

Sellevoll, M.A., 1969. Crustal studies in Norway. Geofysiikan paivat, Ed. P. Tuomikoski. Physical Dept., Oulo Univ., Finland. AF 61 (052)-859, Seismological Obs., Univ. of Bergen 1967.

Sellevoll, M.A., and R.E. Warrick, 1971. A refraction study of the crustal structure in southern Norway. Bull. Seism. Soc. Am., 61, 457-471.

Sobczak, L.W., and J.R. Weber, 1973. Crustal structure of Queen Elizabeth Islands and polar continental margin, Canada. in: Arctic Geology, ed. M.G. Pitcher, Am. Assoc. Petrol. Geol. Mem. 19, 517-522.

Sollogub, V.B., E.V. Litvinenko, A.V., Chekunov, S.A. Ankudinov, A.A. Ivanov, L.T. Kalyuzhnaya, L.K. Kokorina and A.A. Tripolsky, 1973. New DSS data on the crustal structure of the Baltic and Ukranian shields. Tectonophysics, 20, 67-84.

Srivastava, S.P., 1978. Evolution of the Labrador Sea and its bearing on the early evolution of the North Atlantic. Geophys. J.R. Astr. Soc., 52, 313-357.

Sundvor, E., and E. Nysaether, 1975. Geological outline of the Norwegian continental margin between 60° and 68° north. in: Canada's Continental Margins, eds. C.S. Yorath, E.R. Parker and D.J. Glass, Can. Soc. Petrol. Geol. Mem. 4, 267-281.

Tryggvason, E., 1961. Wave velocity in the upper mantle below the Arctic-Atlantic Ocean and northwest Europe. Annali di Geofisica, 14, 379-392.

Vogel, A., and C. Lund, 1971. Profile section 2-3. in: Proc. Colloquium on Deep Seismic Sounding in Northern Europe, ed. A. Vogel, Swedish Natural Sci. Res. Council, Stockholm, 62-75.

Vol'vovskii, J.S., 1973. Seismic wave velocities within the crust and the upper mantle in the USSR. in: Deep Seismic Sounding, ed. L.F. Egorova, (translated from Glubinnoe Seismicheskoe Zondirovanie, Izdatel'stvo "Nauka" Kazakhkoi SSR, Alma-Ata, 1973), 254 p.

Wetmiller, R.J., 1974. Crustal structure of Baffin Bay from the earthquake generated Lg phase. Can. J. Earth Sci., 11, 123-130.

Young, F.G., D.W. Myhr and C.J. Yorath, 1976. Geology of the Beaufort-Mackenzie Basin. Geol. Survey Can. Paper 76-11, 65 p.

The Alpha Ridge is not a spreading centre

J. M. DeLaurier

ABSTRACT

A sediment-corrected mean water depth profile across the Alpha Ridge is obtained using water depths from four submarine echograms and an assumed sediment distribution. The sediment-corrected relief of the Alpha Ridge is 2900 ± 500 m. This relief is of the same order as that observed for 70 - 80 Ma old oceanic crust about currently active spreading ridges in other oceans. Lack of present seismic activity along Alpha Ridge indicates that it is not a centre of active sea-floor spreading. If it represents a former spreading ridge that has been inactive over the past 40 - 70 Ma, then simple thermal cooling models predict that the relief of the ridge should have decayed by 2200 - 2900 m since that time. That is, the Alpha Ridge should display little present relief (500 m or less). Active accretion along the ridge within the past few million years is also unlikely judging from the presence of marine Maastrichtian (65 - 70 Ma) fossils near the ridge crest and the 380 - 1200 m thicknesses of pelagic sediments present over the ridge. It is therefore concluded that the spreading ridge hypothesis cannot explain the origin of the Alpha Ridge.

RÉSUMÉ

On a obenu un profile bathymétrique transversal, de part et d'autre de la dorsale Alpha, avec correction de puissance des sédiments, en utilisant les relevés bathymétriques transmis par quatre échogrammes sous-marins, et en supposant que les sédiments ont une répartition uniforme. Avec correction de puissance des sédiments, on évalue le relief de la dorsale Alpha à 2900 ± 500 m. Le relief est du même ordre que celui de la croûte océanique de 70 à 80 millions d'années d'âge, située aux abords des dorsales océaniques actuellement actives dans les autres océans. L'absence actuelle d'activité séismique le long de la dorsale Alpha indique que celle-ci n'est pas un centre d'expansion actif du fond marin. Au cas où il s'agirait d'une ancienne dorsale océanique, inactive depuis 40 à 70 millions d'années, de simples modèles de refroidissement thermique indiquent que le relief de la dorsale rait dû diminuer de 2200 à 2900 m depuis cette époque. C'est-à-dire que la dorsale Alpha devrait actuellement avoir un relief très modéré (500 m au plus). Si l'on en juge par la présence de fossiles marins du Maastrichtien près de la crête de la dorsale, et l'épaisseur des sédiments pélagiques (380 à 1200 m) à proximité de la crête, il semble peu probable qu'aient eu lieu des processus actifs d'accrétion le long de la dorsale ces derniers millions d'années. On en conclut que pour expliqué l'origine de la dorsale Alpha, on ne peut faire appel à l'hypothèse selon laquelle il s'agirait d'une dorsale océanique.

INTRODUCTION

Recently, Herron et al. (1974) have suggested that the Alpha Ridge (Fig. 1) is the result of a subduction zone of Laramide age. Their suggestion arose because the ridge's elevation above the surrounding abyssal plains precludes it from being a fossil spreading centre. This paper presents a depth profile for the Alpha Ridge and concludes that it was not a spreading centre in pre-Tertiary time. Further, the age and thickness of sediments now present on the Alpha Ridge precludes a more recent history of spreading activity as well. The Alpha Ridge, therefore, did not originate as an accreting margin.

ALPHA RIDGE BATHYMETRIC PROFILE

Only four of the submarine echograms of Beal (1969) are relevant in providing a water depth profile for the Alpha Ridge. The submarine tracks chosen (Fig. 1) are within 15° of the azimuth 141°W and hence are almost normal to the strike of this ridge. Two echograms provide simultaneous soundings about 4 km apart paralleling track B (Fig. 1). Water depths (scaled every 37.5 km) are displayed in figure 2 between 80°N to 89°N latitude. Errors in reproducing the echograms of Beal (1969) are estimated to be 25 km in horizontal distance and 50 m in depth. The mean depths (Fig. 2) give a smooth profile for the Alpha Ridge. Measured water depths are within ± 500 m of the mean (1750 m) near the ridge crest and within ± 110 m of the mean (3780 m) in the Canada Plain near 80°N. The large scatter (Fig. 2) is probably the result of the small sample size and the lack of parallelism between the submarine tracks in figure 1. Nevertheless, this profile is consistent with the bathymetry for Alpha Ridge (Plate 1).

The mean water depths (Fig. 2) are corrected for sediment thickness and the load which it produces. Sediment cores at least 10 m thick have been recovered from the Alpha Ridge and Canada Plain (Clark, 1975). Three

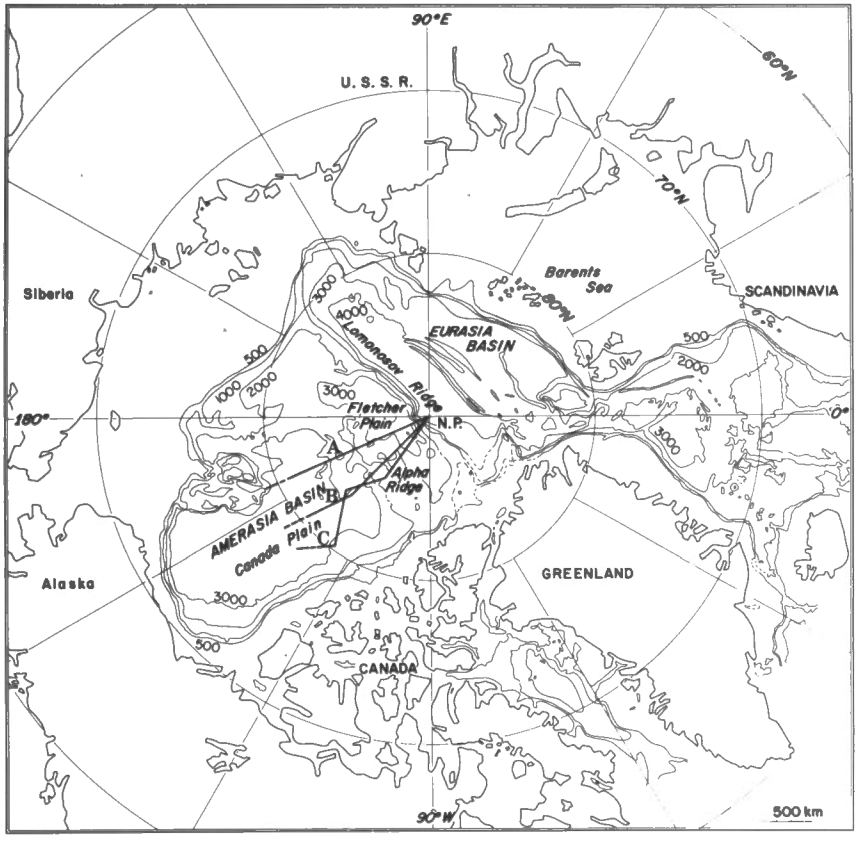

Figure 1. Generalized map of the Arctic Ocean. The lines labelled A, B, C are submarine tracks from Beal (1969); A - 156°W (track No. 3, 4, his figure 20); B - 135°W (track No. 5 in his figures 30, 32 are combined); C - 126°W (track No. 1, his figure 28).

unreversed refraction profiles over a small area of the Alpha Ridge suggested a greater thickness - about 380 m (at 2.0 km/s velocity) of unconsolidated sediments (Hunkins, 1961). Hall (1973), using seismic reflection records obtained on ice island T-3, reported up to 1.2 km of sediments (2.0 km/s velocity) filling the valleys of the Alpha Ridge. Also, gently sloping multiple reflectors from the ridge flanks that become subhorizontal beneath the Canada Plain are interpreted (Hall, 1973) as indicating at least 2 km of sediments under the Canada Plain. Up to 1.5 km of sediments are reported for the Fletcher Plain (Crary and Goldstein, 1957; Ostenso and Wold, 1977). A smooth increase in sediment thickness from 500 m at the ridge crest to 2000 m in the flanking basins is therefore assumed. The sediment-corrected mean water depths are easily obtained by removing the assumed overburden and the Alpha Ridge displays a sediment-corrected relief of 2900 ± 500 m (Fig. 2).

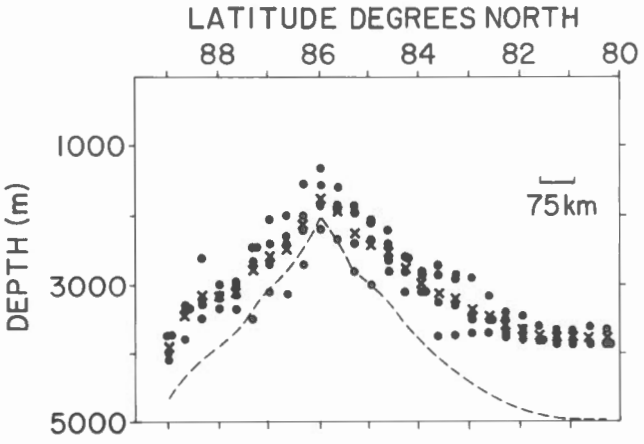

Figure 2. Water depth profile over the Alpha Ridge. Dots are depths scaled at 37.5 km intervals from four submarine echograms taken along the tracks shown in figure 1. Crosses are the average of these depths. Dashed line is a corrected mean depth profile for the Alpha Ridge after removal of sediment (ρ = 2000 kg/m^3).

DISCUSSION

Measured relative to 70 to 80 Ma old oceanic crust, the sediment-corrected relief of the North Pacific spreading ridge is 2900 ± 200 m, of the southeast Indian 2700 ± 200 m and of the South Atlantic 3100 ± 500 m (Sclater et al., 1971). For the North Atlantic spreading ridge south of 31°N, a relief of 3100 ± 600 m is measured with respect to 72 Ma old crust (Parsons and Sclater, 1977). Hence, oceanic crust which was created 70 - 80 Ma ago at a spreading ridge crest has subsided by an average of 2900 ± 200 m. The sediment-corrected relief of the Alpha Ridge, 2900 ± 500 m, is quite comparable to the relief of currently active spreading ridges in these other oceans. However, Alpha Ridge is presently aseismic (Plate 2) which indicates that it is not now actively spreading.

Davis and Lister (1974) have shown that the subsidence, h, of the oceanic crust can be represented by

$$h = 2\alpha T \left(\frac{Kt}{H}\right)^{\frac{1}{2}}$$

where α is the effective thermal expansion coefficent, T is the intrusion temperature at the ridge crest, K is the thermal diffusivity and t is time. Values for these parameters are

$K = 8.0 \times 10^{-7} m^2/s$
$\alpha = 4.7 \times 10^{-5}\ ^oC^{-1}$
$T = 1300^oC$

from Parsons and Sclater (1977).

The above simple cooling relation predicts a subsidence of 500 m for oceanic crust created 2 Ma ago at a spreading ridge crest; for crust 40 Ma or 70 Ma old, the predicted subsidence is 2200 m or 2900 m, respectively. This subsidence would be the same as that predicted for a ridge crest about which spreading had stopped 2 Ma or 40 Ma, or 70 Ma ago (Sclater et al., 1971). Hence, the sediment-corrected relief, 2900 ± 500 m, cannot be explained as the result of the cessation of spreading 40 to 70 Ma ago. Either the ridge ceased spreading about 2 Ma ago and therefore has subsided by less than 500 m, or the spreading ridge hypothesis must be discarded.

Magnetic stratigraphy (on about 100 cores recovered from Alpha Ridge, Clark, 1970) has determined a pelagic sedimentation rate of between 1 to 3 mm/1000 a during the past 3 to 4 Ma (Steuerwold et al., 1968; Clark, 1969, 1970, 1975). This rate, however, accounts for only about the first 10 m of the 380 m to 1200 m of sediment that is believed (Hall, 1973) to be present on Alpha Ridge. Further, the recovery of a Late Cretaceous to Eocene silicoflagellate assemblage in tuffaceous

sediments (Ling et al., 1973; Clark, 1974) suggests that sediment has been accumulating on Alpha Ridge since Late Cretaceous time. Therefore, the possibility that the ridge ceased spreading within the past 2 Ma must be discarded. Hence, the spreading ridge hypothesis for the origin of the Alpha Ridge is not tenable.

REFERENCES

Beal, M.A., 1969. Bathymetry and structure of the Arctic Ocean. Ph.D. Thesis, Oregon State Univ., Cornwallis, 187 p., Appendix.

Clark, D.L., 1969. Paleoecology and sedimentation in part of the Arctic Basin. Arctic, 22, 233-245.

Clark, D.L., 1970. Magnetic reversals and sedimentation rates in the Arctic Ocean. Geol. Soc. Am. Bull., 81, 3129-3134.

Clark, D.L., 1974. Late Mesozoic and early Cenozoic sediment cores from the Arctic Ocean. Geology, 2, 41-44.

Clark, D.L., 1975. Geological history of the Arctic Ocean basin. in: Canada's Continental Margins, eds., C.J. Yorath, E.R. Parker and D.J. Glass, Can. Soc. Petrol. Geol. Mem. 4, 501-524.

Crary, A.P., and N. Goldstein, 1957. Geophysical studies in the Arctic Ocean. Deep-Sea Res., 4, 185-201.

Davis, E.E., and C.R.B. Lister, 1974. Fundamentals of ridge crest topography. Earth and Planet. Sci. Lett., 21, 405-413.

Hall, J.K., 1973. Geophysical evidence for ancient sea-floor spreading from Alpha Cordillera and Mendeleyev Ridge. in: Arctic Geology, ed. M.G. Pitcher, Am. Assoc. Petrol. Geol. Mem. 19, 542-561.

Herron, E.M., J.F. Dewey and W.C. Pitman III, 1974. Plate tectonics model for evolution of the Arctic. Geology, 2, 377-380.

Hunkins, K.L., 1961. Seismic studies of the Arctic Ocean floor. in: Geology of the Arctic, v. 1, ed. G.O. Raasch, Univ. Toronto Press, Toronto, 645-665.

Ling, H.Y., L.M. McPherson and D.L. Clark, 1973. Late Cretaceous (Maestrichtian?) silcoflagellates from the Alpha Cordillera of the Arctic Ocean. Science, 180, 1360-1361.

Ostenso, N.A., and R.J. Wold, 1977. A seismic and gravity profile across the Arctic Ocean basin. Tectonophysics, 37, 1-24.

Parsons, B., and J.G. Sclater, 1977. An analysis of the variation of ocean floor bathymetry and heat flow with age. J. Geophys. Res., 82, 803-827.

Pitman, W.C. III, and M. Talwani, 1972. Sea-floor spreading in the North Atlantic. Geol. Soc. Am. Bull., 83, 619-646.

Sclater, J.G., R.N. Anderson and M.L. Bell, 1971. Elevation of ridges and the evolution of the central eastern Pacific. J. Geophys. Res., 76, 7888-7915.

Steuerwold, B.A., D.L. Clark and J.A. Andrew, 1968. Magnetic stratigraphy and faunal patterns in Arctic Ocean sediments. Earth Planet. Sci. Lett., 5, 79-85.

Vogt, P.R., and N.A. Ostenso, 1970. Magnetic and gravity profiles across the Alpha Cordillera and their relation to Arctic sea-floor spreading. J. Geophys. Res., 75, 4925-4937.

Evolution of the Arctic Basin

J. F. Sweeney, E. Irving and J. W. Geuer

ABSTRACT

The relative positions of Laurentia and Eurasia have been reconstructed from the Jurassic to present time using the paleomagnetic data and major tectonic constraints. It is suggested that during the Jurassic the two continental masses were joined and the Arctic Ocean did not exist. In its place was northern Alaska and the Chukotsk Peninsula - the Arctic-Alaska plate (AA). During the Early Cretaceous the North Atlantic between Newfoundland and Britain began to open about a pivot point near northern Greenland. This gave rise to compression between northern Laurentia and eastern Eurasia which caused AA to rift off and rotate about 70° anticlockwise, thereby creating the Amerasia Basin. Continued longitudinal compression of AA in the Late Cretaceous may have caused folding in the Verkhoyansk zone, dextral motion along the Kaltag fault, and oroclinal buckling between the Brooks Range and the Chukotsk Peninsula. It is suggested that the structural lines of weakness that delineated AA, and ultimately formed its margins, were inherited features; the Laurentian margin was the site of the Franklinian foldbelt (Devonian) and the Eurasian margin the site of a possible Permian rift and subsequent Triassic zone of shear. The Alpha and Mendeleev Ridges within the Amerasia Basin may have been produced by buckling of young oceanic crust caused by continuing compression between the bordering continental blocks as Herron and colleagues have suggested, but they could also be continental fragments or volcanic accumulations created in the wake of the rotating Arctic-Alaska plate. The Eurasia Basin was initiated by spreading from the Nansen-Gakkel Ridge as early as Late Cretaceous time.

RÉSUMÉ

On a reconstruit les positions relatives de la Laurentie et de l'Eurasie entre le Jurassique et la période actuelle, à l'aide des données paléomagnétiques et des principaux éléments tectoniques. On suggère que pendant le Jurassique, les deux masses continentales étaient reliées, et que l'océan Arctique n'existait pas. A sa place, se trouvaient le Nord de l'Alaska et une portion de la Sibérie - la plaque Arctique Alaskienne (AA). Pendant le Crétacé inférieur, l'Atlantique du Nord a commencé à s'ouvrir entre Terre-Neuve et la Grande-Bretagne, par rapport à un centre de rotation situé dans le nord du Groenland. Il s'en est résulté un effet de compression entre la partie de nord de la Laurentie et de l'Eurasie, qui a provoqué la fracturation de la plaque AA, et sa rotation d'environ 70° en sens contraire des aiguilles d'une montre, et ainsi créé le bassin Amérasien. L'effet prolongé d'une compression longitudinale de la plaque AA au Crétacé supérieur a peut-être engendré un plissement dans la zone de Verkhoyansk, un déplacement dextre le long de la faille de Kaltag, et un orocline entre la chaîne Brooks et la péninsule de Chukotsk. On suggère que les lignes de faiblesse structurale qui délimitaient la plaque AA, et qui en ont finalement formé les limites, étaient des structures pré-existantes; la limit Laurentienne était le site de la zone de plissement Franklinienne (au Dévonien) et la marge Eurasienne le site d'un rift Permien et ultérieurement d'une zone de cisaillement dans le Triassique. Dans le bassin Amérasien, les dorsales Alpha

et de Mendeleev ont peut-être été engendrées par la flexion d'une croûte océanique jeune, sous l'effet d'une compression prolongée entre les blocs continentaux marginaux, comme l'ont supposé Herron et al., mais il pourrait aussi s'agir de fragments continentaux ou d'accumulations volcaniques subséquents à la rotation du bloc Alaskien Arctique. Le bassin Eurasien a commencé à se former par expansion de la dorsale de Nansen-Gakkel, dès le Crétacé supérieur.

INTRODUCTION

The main purpose of this paper is to describe, in necessarily tentative fashion, one possible way in which the Arctic Ocean may have evolved. The descriptions are made in the form of maps and cartoons showing the motions of the continental blocks bordering the Arctic Ocean. the reconstructions are based primarily on a compilation of paleomagnetic data from North America, Europe and northern Asia (Irving et al., 1976, 1977), including the most recent results from the USSR (Khramov, 1975), together with what we believe to be the major tectonic constraints.

Apparent polar wander (APW) paths can now be drawn for northern Eurasia and Laurentia (North America together with Greenland) back to the Carboniferous. The APW paths of figures 1 and 2 are obtained by first referring all the results to a scale of millions of years, and then by calculating overlapping averages. The statistics are given in Irving (1977). The mean standard errors are 3° for North America and 4° for northern Eurasia.

Average pole positions of figures 1 and 2 are used to set the continents in their correct latitude and azimuth relative to geographic north. The mean pole is assumed to be a good estimate of the geographic pole, the geomagnetic field averaging to an axial dipole. The problems associated with this assumption are discussed elsewhere (Wilson and McElhinny, 1974; Irving, 1977). Therefore in the first instance, these maps are an attempt to describe the motions of the continents relative to the earth's axis of rotation rather than relative to one another. However, the paleomagnetic results do provide certain constraints on the relative motions of continental blocks as will be shown later. Other constraints are provided by geology, by the shapes of the edges of the continental shelves and by the linear magnetic anomalies. For the northern end of the world these latter two sources of information are applicable to post mid-Cretaceous time. Prior to that time there are no magnetic anomalies to be used as guides to the size of oceans, and the form of the present continental shelves date only from the time of last opening of the Arctic and Atlantic. Prior to the Middle Cretaceous, therefore, the constraints that we have used are paleomagnetic and geological, with the additional assumption that relative motions during successive time intervals are held to a minimum.

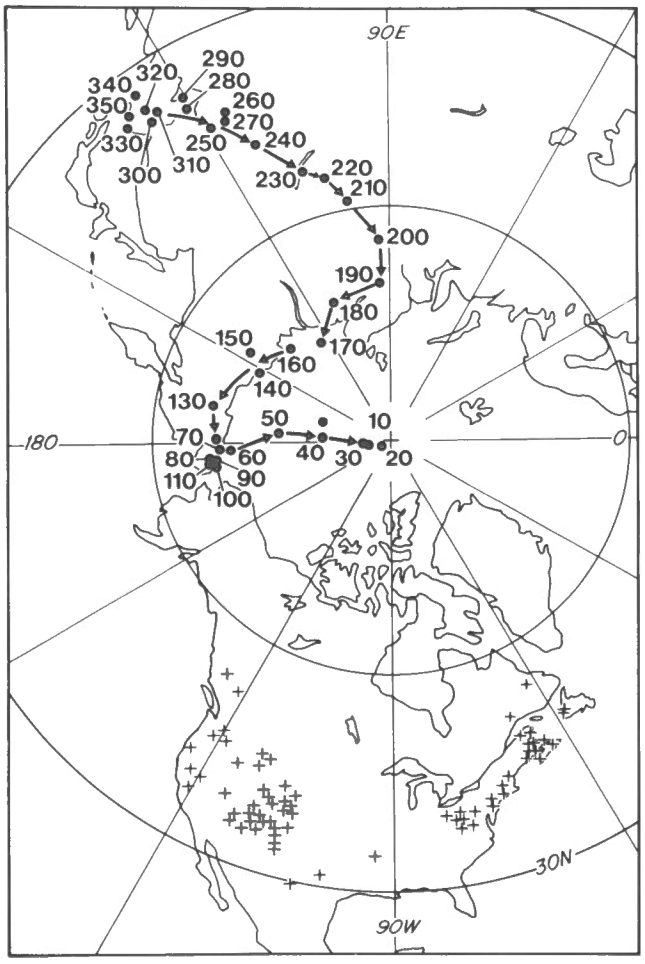

Figure 1. Apparent polar wander path for Laurentia. Redrawn from Irving (1977).

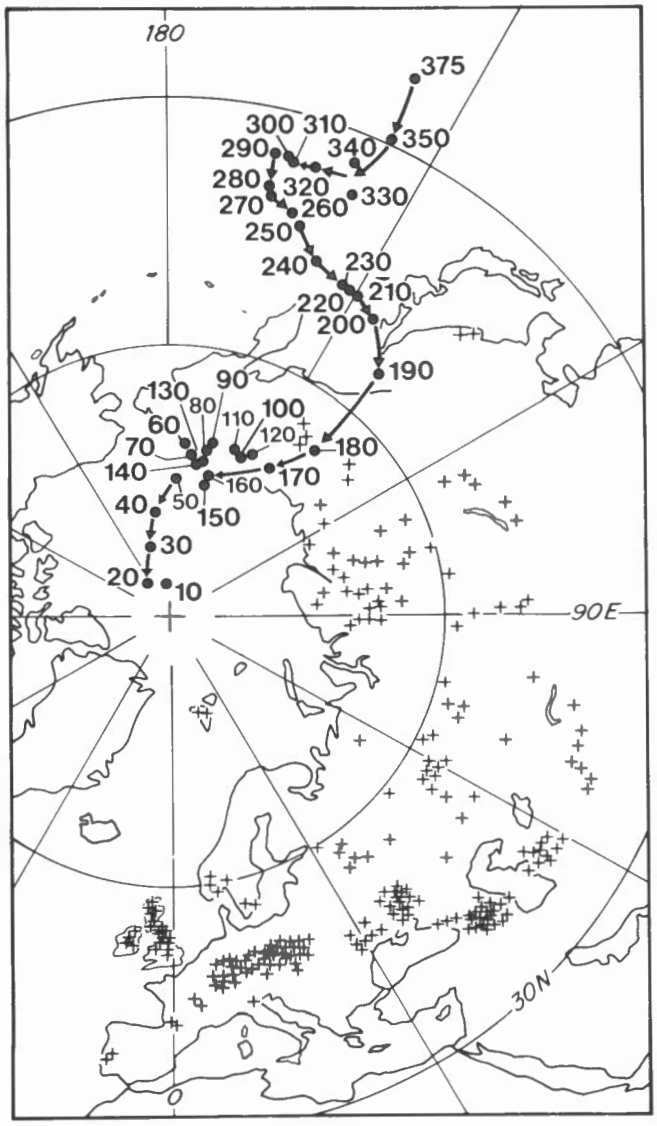

Figure 2. Apparent polar wander path for Eurasia. Redrawn from Irving (1977).

THE ARCTIC-ALASKA PLATE

The key feature of this account is the recognition that a tectonic block (the Arctic-Alaska plate (AA), a name introduced by Newman et al., 1977) was back-to-back against the Canadian Arctic Islands prior to the Cretaceous and was rotated into its present position in the Early Cretaceous, thereby opening the Arctic Basin. There are several lines of evidence that favour such an idea.

Figure 3 shows the main tectonic elements. In northeastern Siberia there are the Chukotsk Peninsula and the Kolyma block with the Anyui Suture between them. To the west there is the Cherskiy Range that may be the site of a suture, and beyond that the Verkhoyansk foldbelt (VK) and the edge of the Siberian Shield (ES). In northern Alaska the Brooks Range is tectonically continuous with the Chukotsk Peninsula to the west. To the south the Kaltag fault (KA) cuts across the Yukon Suture. Readers are referred to the sources used to compile figure 3 for further details (Nalivkin, 1962; Ziegler et al., 1977; Patton and Tailleur, 1977).

Recent paleomagnetic results from Carboniferous rocks of the Brooks Range have indicated a 70° anticlockwise rotation of the northern half of Alaska (Newman et al., 1977). But how much, if any, of northeastern Siberia has rotated with northern Alaska? It is possible that the Chukotsk Peninsula together with the Kolyma block may have been continuous with northern Alaska (Churkin, 1973a). Alternatively, Kolyma may have been welded onto Asia separately (McElhinny, 1973).

We are faced, therefore, with two choices. The first is that AA consists of northern Alaska and the Chukotsk Peninsula

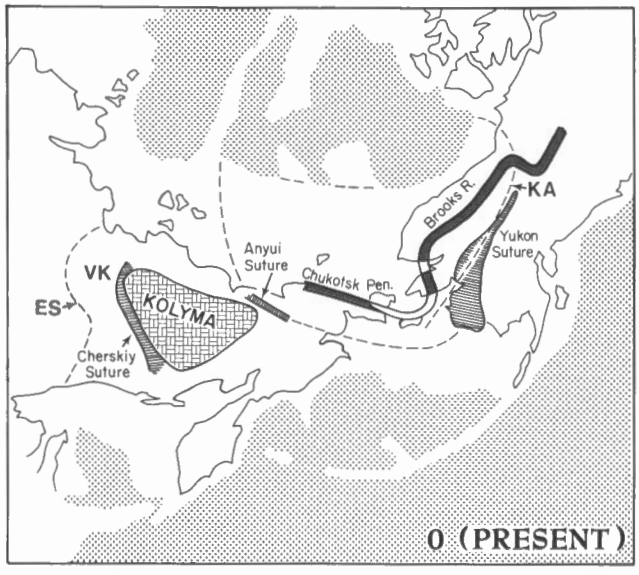

Figure 3. Tectonic elements. The Arctic-Alaska plate is outlined by the dashed line. (See caption figure 4 for symbols.)

and the Anyui Suture forms its margin. The second is that AA also includes the Kolyma block so that the Cherskiy Suture forms its margin. This ambiguity is not yet settled, but we favour the former for the reason given below.

This picture of two mini-plates (Kolyma, AA) that dominate the interaction between northern Eurasia and northern Laurentia during the Mesozoic may be too simple. Fujita (1978) has recently recognized several additional smaller plates in northeastern Siberia that may have participated in Mesozoic plate interactions.

Inspection of figures 1 and 2 shows that the positions of the mid-Cretaceous (~100 Ma) poles relative to Eurasia and Laurentia make it impossible to place the poles together without substantial overlap of the continental shelves. This does not by itself imply that AA has rotated, but it does indicate that the spatial relationships of AA and Laurentia and Eurasia in the Cretaceous were different from those at present.

The structural lines of weakness that delineated AA and ultimately formed its margins were, we suggest, inherited features (Fig. 4). At the close of the Early Paleozoic the Caledonide foldbelt (CA) of eastern Greenland and Norway, and the Franklinian (FR) and northern Uralian (UR) foldbelts were formed by the interaction of the Baltic (BA), Siberian (SB) and Laurentian (LA) Shields. Paleomagnetic evidence indicates that these shields were far apart during the Early Paleozoic and they approached one another and were apparently welded together in the Late Silurian and Devonian to form the supercontinent Laurasia (Morel and Irving, 1977). The relative positions of these three shields do not seem to have changed very much during the later Devonian and Carboniferous, but during the Permian a rift may have been formed (the boreal rift, NR) between Laurentia and Baltica and it followed the line of the Caledonide foldbelt (Irving, 1977).

Thus before Triassic times it is possible that AA was delineated by two potential zones of weakness - the Franklinian foldbelt along the Laurentian margin and the boreal rift along the Eurasian margin. The boreal rift was destroyed during the Early Triassic by the northward movement of Laurentia relative to Baltica (Roy, 1972). During the later Triassic this motion was reversed and the classical Pangea of Wegener achieved (Irving, 1977).

The time at which the rotation of AA occurred is uncertain. It could have occurred over a short interval of time, or there may have been several phases widely spaced in time. We believe that rifting may have been initiated in the Triassic but that the main opening phase was in the Early Cretaceous, and our reasons are now presented.

There are several rather loose constraints on the time of rotation. The evidence of Newman et al., (1977) referred to above show it to have occurred after the Devonian. The presence of Late Cretaceous (Maastrichtian) marine fossils from Alpha Ridge (Ling et al., 1973) and the presence of a submarine canyon leading into Canada Basin north of Alaska that is filled with about 1.4 km of what appear to be Late Cretaceous sediments (Collins and Robinson, 1967, in Churkin, 1973a) can be taken as evidence that the rotation was pre-Late Cretaceous. If, however, the Alpha Ridge is a continental fragment, the first piece of evidence provides no constraints on the time of rotation, and it is only the second that is relevant. Stronger evidence is cited by Newman et al. (1977) in the Prudhoe Bay area of northern Alaska where there are uppermost Jurassic or Early Cretaceous sandstones of northern provenance that appear to grade southward into shale and may be a product of regional arching and erosion during the initial stages of rifting and rotation. Additional evidence has recently been given by Forsyth et al. (1978) who have described the presence of major pull-apart structures of Early Cretaceous age in central Sverdrup Basin which may be a consequence of the initial stages of rifting along the Canadian Arctic margin.

If elements of Siberia have rotated with the Arctic-Alaska plate it should be evident from the paleomagnetic results. The region is tectonically complex and paleomagnetic data from pre-Cretaceous rocks are, as a consequence, fragmentary and difficult to interpret. There are two results that are particularly important. First, Triassic sediments from the Omolonsk massif in the centre of the Kolyma block yield a pole situated in North America (72°N, 72°W, Khramov, 1975), strongly divergent from the APW path for Eurasia as a whole (Fig. 2). A 70° anticlockwise rotation of this result about a pivot point near the Mackenzie delta (the northeastern margin of AA) yields a pole at 83°N,152°E that approaches the Eurasian path but is still 22° ± 10° from the expected Triassic position. In contrast, Lower and Middle Jurassic sediments from the

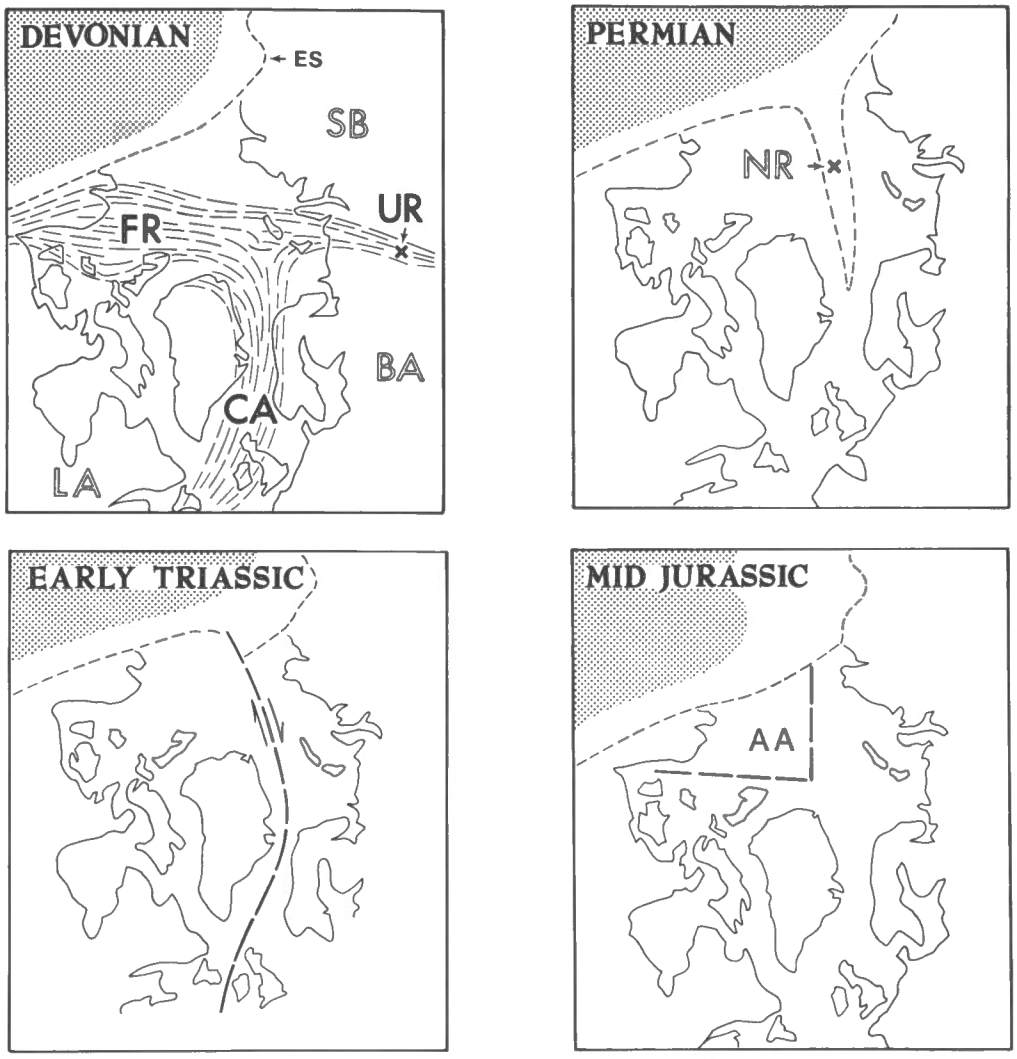

Figure 4. Cartoon of possible early tectonic framework of the Arctic regions. The abbreviations used throughout this paper are as follows:

AA - Arctic-Alaska plate
AL - Alpha and Mendeleev Ridges
AM - Amerasia Basin
BA - Baltica
BB - Baffin Bay
BR - Brooks Range
CA - Caledonide foldbelt
CB - Canada Basin
CH - Chukchi Plateau
CP - Chukotsk Peninsula
EA - Eurasia Basin
ES - Eastern edge of Siberian Shield
FR - Franklinian foldbelt
GS - Greenland Sea
KA - Kaltag fault
KB - Kolyma block
KC - Khrebet-Cherskogo fault system
LA - Laurentia
LO - Lomonosov Ridge
LS - Labrador Sea
MB - Makarov Basin
NA - North Atlantic Ocean
NR - boreal rift
NS - Nares Strait
PE - mean pole for Eurasia
PL - mean pole for Laurentia
SB - Siberia
SP - Sverdrup Basin
SV - Svalbard
UR - Ural foldbelt
VK - Verkhoyansk foldbelt

Omolonsk massif yield poles that are somewhat different from one another (80°N,168°E and 64°N,103°E) but are in approximate agreement with the APW path for Eurasia. This evidence can be viewed in two ways. It could be argued that the data are too fragmentary for interpretation. Alternatively, the evidence can be taken at its face value which then indicates that Kolyma was tectonically separate from both Eurasia and the Arctic-Alaska plate in the Triassic and that it was welded to Eurasia by about the Early Jurassic. We shall adopt the latter view.

In the Sverdrup Basin (SP) of Arctic Canada (Fig. 8) the rapid increase in subsidence and the cessation of sediment influx from northern sources in the Triassic indicates that limited rifting along the eastern polar margin of Laurentia may have been initiated during this time (Sweeney, 1977). However, further west, in what was later to become northern Alaska, the continued accumulation of Triassic sediments from sources on the opposite side of the rift (Churkin, 1973b) indicates that this early rifting did not proceed very far.

The above factors therefore appear to confine the age of the major opening of the Arctic Basin within the limits Jurassic and Early Cretaceous. In the description of maps below we tie the rotation of AA to the earliest opening of the North Atlantic between Newfoundland and western Europe. This opening began in the Early Cretaceous (Laughton, 1975). This is our reason for choosing, from within the wider limits set by the paleomagnetic and the geological evidence, the Early Cretaceous as the most likely time of the major opening of the Arctic Basin.

DESCRIPTION OF MAPS

Figures 5,6,7, and 8 are maps for 4 time intervals and are summarized in cartoon form in figure 9. During the Jurassic, Laurentia and Eurasia were joined to form Laurasia, and the Arctic Ocean did not exist. In its place was the Arctic-Alaska plate. In figure 5 two possible arrangements of AA are given. In the main map it consists of northern Alaska (BR) and the Chukotsk Peninsula (CP) only, and the Eurasian margin of AA will later form the eastern side of the Anyui Suture. The Kolyma block (KB) is shown welded to Eurasia. In the inset of figure 5 AA now includes KB and because of this northern Alaska has been pushed about 300 km southward relative to the main mass of Laurentia. This is regarded as less likely because the

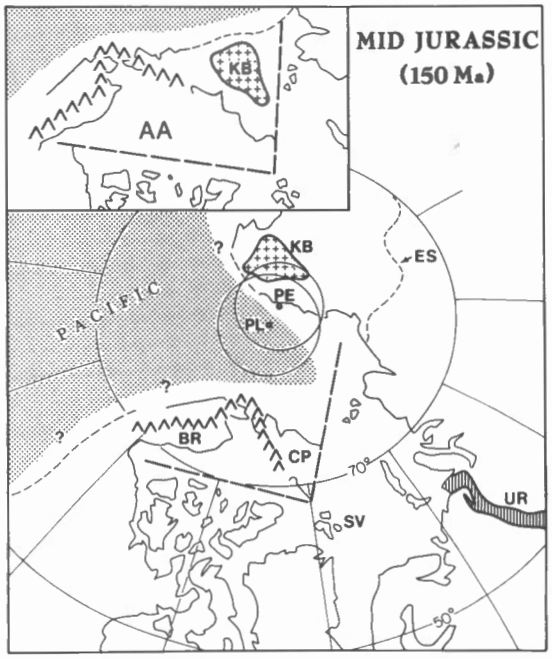

Figure 5. Proposed reconstruction for the mid-Jurassic, approximately - 150 Ma. The Arctic-Alaska plate (AA) is rotated back to close the Amerasia Basin. In the main map AA consists of the Chukotsk Peninsula (CR) and northern Alaska (BR). The Kolyma block (KB) is part of Eurasia. In the inset Kolyma is shown as part of AA. (See caption figure 4 for symbols.)

paleomagnetic evidence, taken at its face value, indicates that Kolyma had docked by the Middle Jurassic.

In the Late Cretaceous the pivot point for the opening of the North Atlantic was near northern Greenland (Pitman and Talwani, 1972) and we shall assume that this was its approximate position in the Early Cretaceous also. This assumption is central to our thesis. The consequence is that there is compression between northern Laurentia and eastern Eurasia which causes AA to rift off and to rotate about 70° creating the Amerasia Basin (AM) in its wake (Fig. 6).

In the Late Cretaceous, spreading in the North Atlantic extends into the Labrador Sea (LS) and Baffin Bay (BB) as Laurentia splits forming Greenland and present-day North America (Fig. 7). Compression directed longitudinally along AA continues, and may have caused folding in the Verkhoyansk

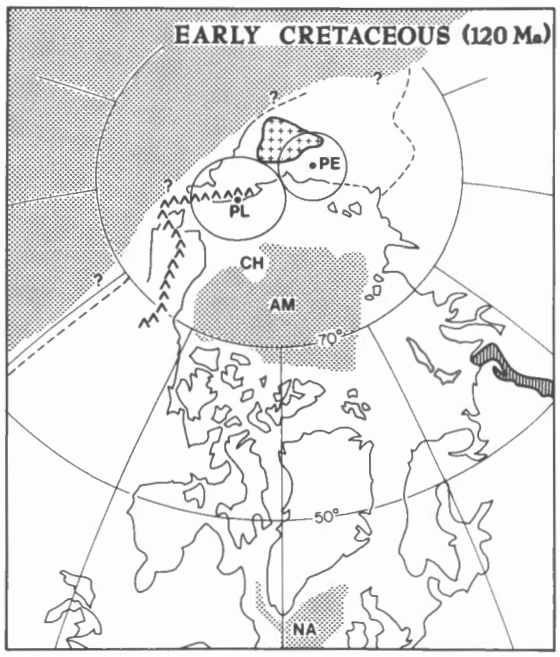

Figure 6. Proposed reconstruction for the Early Cretaceous, approximately 120 Ma. (See caption figure 4 for symbols.)

foldbelt (VK), during the earlier Cretaceous, the initiation of the Khrebet-Cherskogo fault system (KC) and dextral motion along the Kaltag fault (KA) during the Late Cretaceous. The Alpha and Mendeleev Ridges (AL), which separate Amerasia Basin into the Canada (CB) and Makarov (MB) Basins, may have been produced in the Cretaceous by buckling of the newly formed oceanic crust, or by short-lived subduction (Herron et al., 1974) as the bordering continents continue to approach one another. Alternatively, the ridges could be volcanic accumulations created behind AA as it receded from North America, or they could be continental material fragmented by the breakup and left in the wake of AA.

At the beginning of the Tertiary the pivot point about which North America and Eurasia rotate moves into northeastern Siberia (Pitman and Talwani, 1972) and a tensional regime is initiated in the Arctic Basin (Fig. 8). The North Atlantic rift extends into the Norwegian and Greenland (GS) Seas and into Eurasia Basin (EA) where spreading begins along what is to become the Nansen-Gakkel Ridge. The Lomonosov Ridge (LO) is severed from the Eurasian polar shelf as the spreading proceeds (Wilson, 1963).

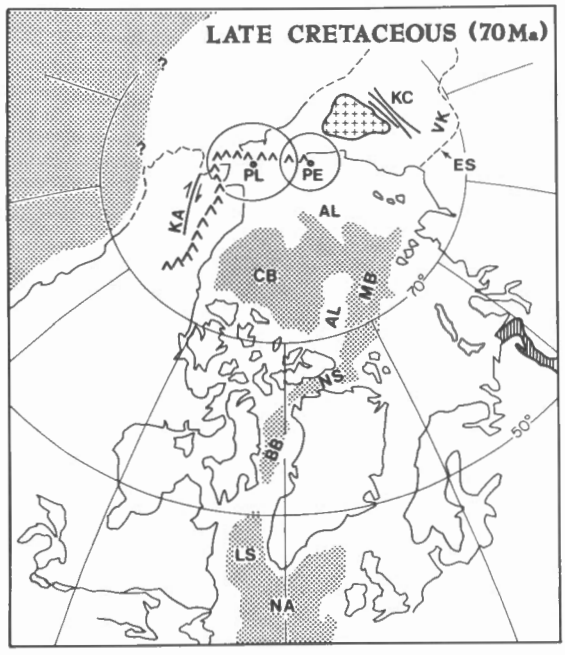

Figure 7. Proposed reconstruction for the Late Cretaceous, approximately 70 Ma. (See caption figure 4 for symbols.)

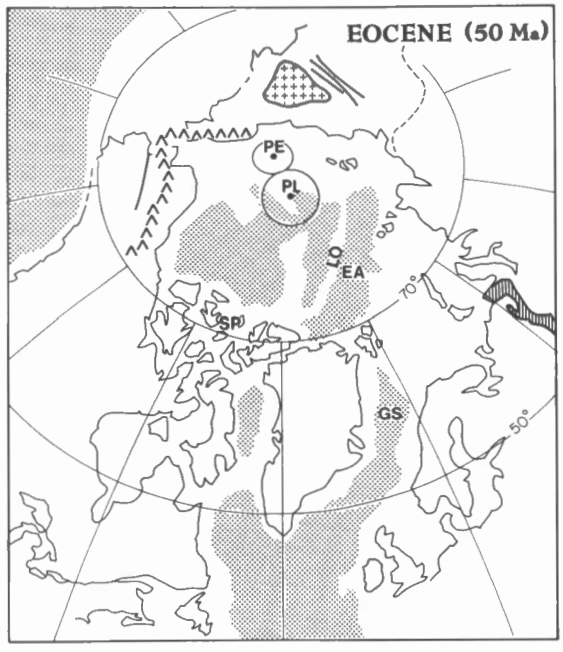

Figure 8. Proposed reconstruction for the Eocene, approximately 50 Ma. (See caption figure 4 for symbols.)

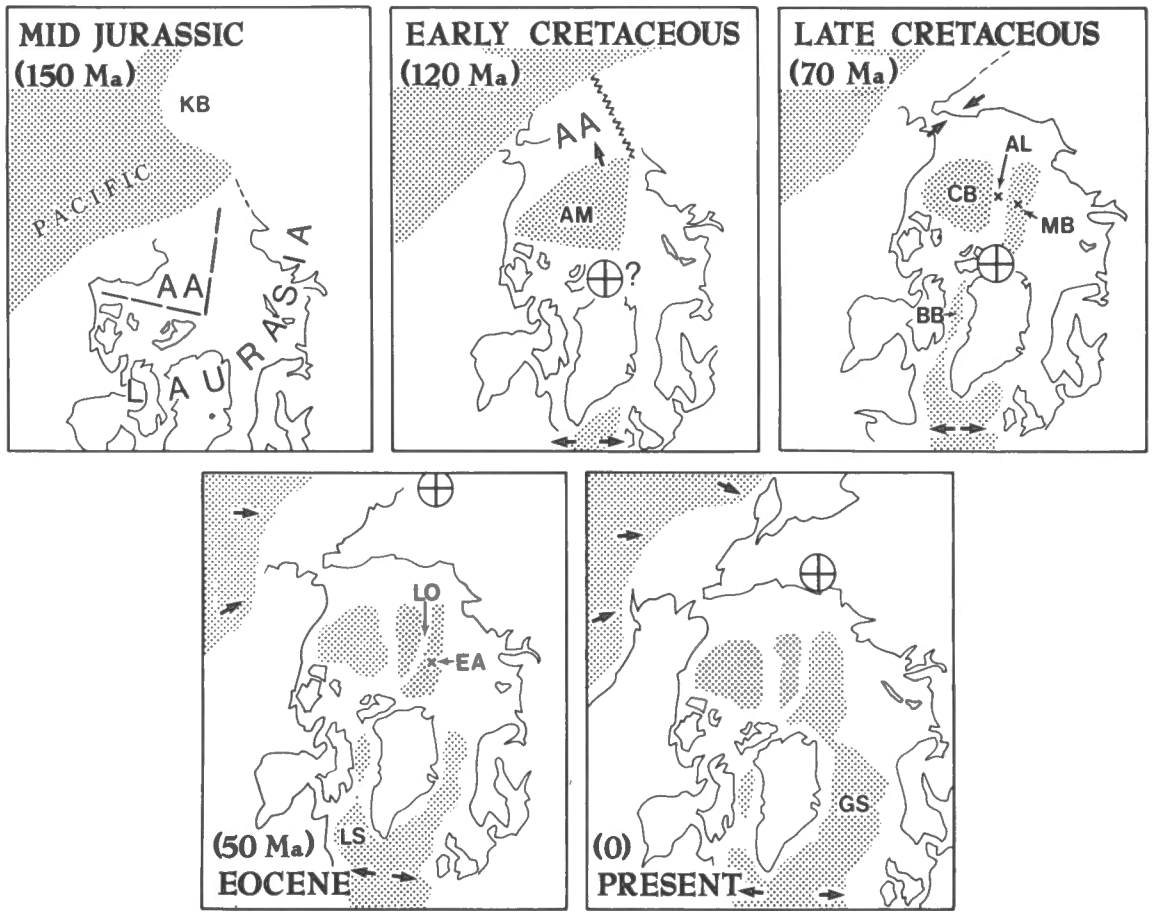

Figure 9. Cartoon of proposed evolution of the Arctic Ocean. (See caption figure 4 for symbols.) Poles of rotation for North America and Eurasia for opening of North Atlantic from Pitman and Talwani (1972) are marked. Note that the rotation pole for the Early Cretaceous is conjectural.

DISCUSSION

With some minor exceptions the various elements of the scheme summarized in figure 9 have already been suggested by other workers, - the rotation of AA by Carey (1955) and Tailleur (1969, 1973), the compressional nature of the Alpha and Mendeleev Ridges by Herron et al. (1974), and the opening of the Eurasia Basin by extension of the North Atlantic rift into the Arctic region by many workers. It is the combination of elements which is new, and which, we suggest, better accords with the available evidence. For example, according to Tailleur (1973), the rotation of Alaska produced the Canada Basin only and not the Makarov Basin as well, and Herron et al. (1974) regarded the submarine ridge complex (AL) as a compressional feature but rejected the rotation of Alaska.

The essence of our scheme is that during Cretaceous and Tertiary time compression followed by tension was produced in the Arctic regions as a result of the opening of the North Atlantic Ocean. The Arctic-Alaska plate was forced out in the Early Cretaceous and the Brooks-Chukotsk orocline and possibly also the Alpha and Mendeleev Ridges were formed by continuing compression in the Late Cretaceous. This compressional regime was replaced by tension in the Early Tertiary when the pivot moved to northeastern Siberia and the Eurasia Basin opened. The complexities of Arctic history arise in large measure from its close proximity to the pivot points of bordering major plates, and the two stage history of its opening is a consequence, we contend, of the migration of the pivot point between the Cretaceous and Early Tertiary.

Two factors in this scheme are uncertain. First is the assumption that the pivot point in the Early Cretaceous was near where it is thought to have been in the Late Cretaceous (Pitman and Talwani, 1972). Secondly, the paleomagnetic evidence, which ultimately will prove critical in this matter, is fragmentary; the Brooks Range study of Newman et al. is known only in abstract, and the paleomagnetic results from Kolyma for times prior to rotation are few. These are weak links in our chain of argument which underscore the speculative nature of our scheme. Nevertheless we believe that it does adequately explain the existing evidence.

ACKNOWLEDGEMENTS

We thank G.L. Johnson and J. Monger for a useful discussion of geological relationships, and R.L. Coles, J.M. DeLaurier and L.W. Sobczak for critical review of the manuscript. S. Cumyn drafted the figures.

REFERENCES

Carey, S.W., 1955. The orocline concept in geotectonics. R. Soc. Tasmania Papers and Proc., 89, 255-288.

Churkin, M. Jr., 1973a. Geologic concepts of Arctic Ocean basin. in: Arctic Geology, ed. M.G. Pitcher, Am. Assoc. Petrol. Geol. Mem. 19, 485-499.

Churkin, M. Jr., 1973b. Paleozoic and Precambrian rocks of Alaska and their role in its structural evolution. U.S. Geol. Survey Prof. Paper 740, 64 p.

Collins, F.R., and F.M. Robinson, 1967. Subsurface stratigraphic, structural and economic geology, northern Alaska. U.S. Geol. Survey Open File Rept., 252 p.

Forsyth, D.A., J.A. Mair and I. Fraser, 1978. Crustal structure of the central Sverdrup Basin. Can. J. Earth Sci. (in press).

Fujita, K., 1978. Pre-Cenozoic tectonic evolution of northeast Siberia. J. Geol., 86, 159-172.

Herron, E.M., J.F. Dewey and W.C. Pitman III, 1974. Plate tectonics model for evolution of the Arctic. Geology, 2, 377-380.

Irving, E., E. Tanczyk and J. Hastie, 1976. Catalogue of paleomagnetic directions and poles. 3rd (Paleozoic), 4th (Mesozoic) and 5th (Cenozoic) issues, Earth Phys. Br. Geomag. Series Nos. 5,6 and 10.

Irving, E., 1977. Drift of the major continental blocks since the Devonian. Nature, 270, 304-309.

Khramov, A.N., 1975. Acad. Sci. USSR Soviet Geophys. Commun. WDC 3, 1-43.

Laughton, A.S., 1975. Tectonic evolution of the northeast Atlantic Ocean; a review. Norges Geol. Unders., 316, 169-193.

Ling, H.Y., L.M. McPherson and D.L. Clark, 1973. Late Cretaceous (Maestrichtian?) silicoflagellates from the Alpha Cordillera of the Arctic Ocean. Science, 180, 1360-1361.

McElhinny, M.W., 1973. Paleomagnetism and Plate Tectonics. Cambridge Univ. Press, 358 p.

Morel, P., and E. Irving, 1977. Tentative paleocontinental maps for the early Phanerozoic and Proterozoic. J. Geol. (in press).

Nalivkin, D.V., 1962. Geology of the USSR. The Academy of Sciences USSR, Moscow (English translation by N. Rast, 1973, Oliver and Boyd, Edinburgh), eds. N. Rast and T.S. Westoll, Univ. of Toronto Press, Toronto, 855 p.

Newman, G.W., C.G. Mull and N.D. Watkins, 1977. Northern Alaska paleomagnetism, plate rotation, and tectonics (abs). Alaska Geol. Soc. Symposium, Anchorage, Alaska, 16-19.

Patton, W.W. Jr., and I.L. Tailleur, 1977. Evidence in the Bering Strait region for differential movement between North America and Eurasia. Geol. Soc. Am. Bull., 88, 1298-1304.

Pitman, W.C. III, and M. Talwani, 1972. Sea-floor spreading in the North Atlantic. Geol. Soc. Am. Bull., 83, 619-646.

Roy, J.L., 1972. A pattern of rupture of the eastern North America-western Europe paleoblock. Earth Planet. Sci. Lett., 14, 103-114.

Sweeney, J.F., 1977. Subsidence of the Sverdrup Basin, Canadian Arctic Islands. Geol. Soc. Am. Bull., 88, 41-48.

Tailleur, I.L., 1969. Rifting specualtion on the geology of Alaska's North Slope, Pt. II. Oil and Gas J., Sept 29, 128-130.

Tailleur, I.L., 1973. Probable rift origin of Canada Basin, Arctic Ocean. in: Arctic Geology, ed. M.G. Pitcher, Am. Assoc. Petrol. Geol. Mem. 19, 526-535.

Vogt, P.R., and O.E. Avery, 1974. Tectonic history of the Arctic Basins: Partial solutions and unsolved mysteries. in: Marine Geology and Oceanography of the Arctic Seas, ed. Y. Hermon, Springer-Verlag, New York, 83-117.

Wilson, J. Tuzo, 1963. Hypothesis of the Earth's behaviour. Nature, 198, 925-929.

Wilson, R.L., and M.W. McElhinny, 1974. Investigation of the large-scale nature of the paleomagnetic field over the past 25 million years. Geophys. J. R. Astr. Soc., 39, 570-586.

Ziegler, A.M., K.S. Hansen, M.E. Johnson, M.A. Kelly, C.R. Scotese and R. Van Der Voo, 1977. Silurian continental distributions, paleogeography, climatology and biogeography. Tectonophysics, 40, 13-51.

Arctic geophysical review — a summary

J. F. Sweeney, R. L. Coles, J. M. DeLaurier, D. A. Forsyth,
E. Irving, A. S. Judge, L. W. Sobczak and R. J. Wetmiller

ABSTRACT

Seismic refraction experiments, magnetotelluric soundings and analyses of the magnetic anomaly field indicate that the continental shelves bordering the Arctic Ocean are covered by sedimentary sequences that are 2 km to over 10 km thick. Similar data indicate that the Chukchi Plateau is a continental fragment composed largely of sedimentary material. The presence of thick sedimentary loads may be responsible for the free-air gravity anomaly highs and the low-level seismicity along parts of the North American polar margin. The Arctic abyssal plains are covered by a 0.5 to 6 km thick subhorizontally bedded sedimentary carpet. The seismically active Nansen-Gakkel Ridge is composed of a series of narrow peaks and troughs with up to 2.5 km of relief. Heat flow values over the ridge are typical of actively accreting margins but the associated magnetic anomaly amplitudes are less than expected. The magnetic anomaly pattern over the Greenland end of the ridge indicates that spreading rates have been slow (<10 mm/a) over the last 20 Ma with little evidence of transform offsets greater than a few kilometres. Seismic reflection results and magnetotelluric soundings together with heat flow and magnetic anomaly data suggest that the Lomonosov Ridge is composed of stratified sedimentary units. Magnetic anomalies over the Alpha Ridge are of high amplitude and the sediment-corrected relief of the ridge is 2900 ± 500 m. The Arctic Ocean basin originated during Early Cretaceous time when the Arctic-Alaska plate (northern Alaska and the Chukotsk Peninsula) rotated 70 degrees anticlockwise away from Arctic Canada and thereby opened the Amerasia Basin. This major rotation resulted from the compression between the Arctic-Alaska and Eurasia plates that was a consequence of the early opening of the North Atlantic about a pole in northern Greenland. The margins of the Arctic-Alaska plate developed along existing zones of weakness. This compressional regime could have produced the Alpha and Mendeleev Ridges by sea-floor buckling or by subduction. Alternatively, the ridges could be continental fragments or volcanic accumulations left in the wake of the rotating Arctic-Alaska plate. The present relief of the Alpha Ridge precludes it being a spreading centre during Late Cretaceous time. At this time sediments began to accumulate within the Amerasia Basin. In Late Cretaceous-Early Tertiary time the pole of rotation for the opening of the North Atlantic moved into northeastern Siberia. The Lomonosov Ridge is a fault block of continental crust rifted from the polar shelf of Eurasia as a new accreting margin developed. Sea-floor spreading activity has been intermittent, and the Nansen-Gakkel Ridge is the recent location of the accreting margin.

RÉSUMÉ

Des levés de réfractions séismiques ainsi que des sondages magnétotelluriques et des analyses du champ des anomalies magnétiques ont démontré que les plateaux continentaux le long de l'océan Arctique, sont couverts par des séries de couches sédimentaires, épaisses de 2 km à 10 km. Des données semblables ont aussi montré que le plateau Chukchi est une section continentale formée en grande partie de matériaux sédimentaires. Ces charges

sédimentaries épaisses peuvent être à l'origine des niveaux élevés des anomalies gravimétriques d'air libre et de la séismicité de faible intensité le long de certaines parties de la marge polaire nord-américaine. Un lit sédimentaire (de 0.5 à 6 km d'épaisseur) stratifié approximativement horizontalement, recouvre les plaines abyssales Arctiques. La dorsale Nansen-Gakkel qui présente une activité séismique, est formée d'une série de crêtes et de creux étroits possédant un relief qui peut aller jusqu'à 2.5 km. Les valeurs du flux thermique de cette dorsale sont typiques de marges en voie d'accroissement sédimentaire; mais les intensités des anomalies magnétiques sont moins élevés que prévues. Le groupement d'anomalies magnétiques pris de la fin de la dorsale au Groenland démontre que, pendant ces 20 derniers Ma, les vitesses d'expansion furent lentes (moins de 10 mm/a) et que les déplacements du type tranforme, ne dépassent pas quelques kilomètres. A l'aide des résultats de sondages à réflexion séismique, et magnétotelluriques ainsi que des données de flux thermique et d'anomalie magnétique, on pense que la dorsale Lomonosov se constitue d'unités sédimentaires stratifiées. Les anomalies magnétiques de la dorsale Alpha sont élevées et le relief corrigé en fonction des couches sédimentaires varie de 2900 ± 500 m. Le bassin de l'océan Arctique a son origine dans le Crétacé inférieur lorsque la plaque Arctique-Alaskienne a subi une rotation de 70 degrés dans le sens contraire des aiguilles d'une montre, ce qui l'éloigna de l'Arctique du Canada et ainsi engendra le bassin Amérasien. Cette rotation importante fut le résultat de la compression entre la plaque Arctique-Alaskienne d'une part, et la plaque Eurasienne d'autre part, et celle-ci, due au commencement de l'ouverture de l'Atlantique du nord autour d'un centre situé au nord du Groenland. Les marges de la plaque Arctique-Alaskienne s'accrurent le long de zones de faiblesses déjà présentes. Ce régime de compression aurait pu, d'une part, engendré les dorsales Alpha et Mendeleev par la flexion du fond marin ou par subduction. D'autre part, ces dorsales pourraient être des fragments continentaux ou des accumulations volcaniques laissés à la suite de la rotation de la plaque Arctique-Alaskienne. Le relief actuel de la dorsale Alpha écarte la possibilité qu'elle ait été un centre d'expansion pendant le Crétacé supérieur. Dans cette période, la sédimentation commença à remplir le bassin Amérasien. Autour du Crétacé supérieur et du Tertiaire inférieur, le centre de rotation pour l'ouverture de l'Atlantique du nord si déplaça vers le nord-est de la Sibérie. La dorsale Lomonosov est une masse faillée de croûte continentale qui fut séparée du plateau polaire de l'Eurasie pendant qu'une nouvelle marge d'accroissement se développait. L'expansion du fond marin a eu lieu par intervales, et la dorsale Nansen-Gakkel est maintenant le siège de la marge d'accroissement.

INTRODUCTION

The collection and discussion of the geophysical data assembled in this volume is presented with two purposes in mind. The first is to assess the present character of the major elements of the Arctic sea-floor and adjacent landmasses by reviewing the history of geophysical measurements made on and over them. The second is to reconstruct the development of the Arctic Basin using these measurements and the major tectonic relationships as constraints.

In this paper the major results of this effort are reviewed. First, the character of the present Arctic Basin is discussed by bringing together the evidence bearing on the nature of the continental shelves, the abyssal plains and the submarine ridges. Geophysical evidence collected over the past 25 years indicates that oceanic crust is present beneath the Amerasia Basin (e.g., Churkin, 1969). Discussion of the past begins with a brief review of ideas concerning the evolution of this crust and is followed by a synopsis of the Arctic Basin evolutionary model that is believed to be most consistent with the geophysical and geological data available at the present time.

THE PRESENT

Sediment distributions across the broad Eurasian polar shelf are poorly known because few published data exist. Available deep seismic sounding information suggests that relatively thick (up to 8 km) sedimentary sequences may underlie the inner shelf areas. These sequences presumably thin to the north as the higher velocity (>6.0 km/s) basement horizons generally shallow in that

direction (Forsyth, 1978, profiles R1, R2, R3). A seismic refraction experiment (Hunkins, 1965) indicates, however, that up to 6 km of sediments underlie the outer parts of the East Siberian Shelf. Magnetotelluric soundings along the outermost parts of the Chukchi and East Siberian Shelves indicate that sediment thicknesses there range from about 2 km to about 4 km (DeLaurier, 1978a). Sediments on the narrow North American polar shelf generally thicken seaward and are over 10 km deep in places (e.g., Sobczak, 1975; profiles A2, A3, Forsyth, 1978).

A series of elliptical free-air gravity anomaly highs occur along the North American polar shelf break (Plate 4). A similar pattern is observed along the Eurasian polar margin from Scandinavia to Svalbard. Observed gravity data are not available to the east along the northern Barents Shelf margin. The gravity pattern over the Beaufort Sea can be largely explained in terms of flexural bending of the lithosphere in response to the large sediment load present along that polar margin (Sobczak, 1975). It has been suggested (Basham et al., 1977) that low level seismicity associated with the flanks of two of the gravity highs along the Arctic margin of western Canada (Plate 2) could be produced by the release of crustal stresses built up by the concentration of sediment loads along the outer continental shelf.

Magnetotelluric sounding data suggest that the Chukchi Plateau is composed of up to 3.8 km of conducting sediments (DeLaurier, 1978a). Models of the magnetic anomaly field over the plateau indicate, however, that as much as 12 km of nonmagnetic materials (Shaver and Hunkins, 1964), presumably sediments or nonmagnetic crystalline rocks, may be present. Such sediment thicknesses support the notion that the Chukchi Plateau is a fragment of continental material.

The Arctic abyssal plains are covered with subhorizontal sedimentary sequences that range from 0.5 km to 1.5 km in Fletcher Plain (Crary and Goldstein, 1957; Ostenso and Wold, 1977) to between 3.5 km and 6 km in Wrangel Plain (Kutschale, 1966; Gramberg and Kulakov, 1975). Sediments in the Canada Basin are at least 2 km thick (Hall, 1970), whereas 2 km to 2.5 km of sediments are reported in the Fram Basin, and the axial portions of the Nansen Basin are covered by 3 km to 5 km of sediments (Gramberg and Kulakov, 1975). Heat flow measurements in Canada Plain are slightly higher (by 15 per cent) and far more uniform than measurements made on Arctic submarine ridges or continental shelves (Judge and Jessop, 1978). The free-air gravity anomaly field is generally negative over the deep basins (Plate 4; Sobczak, 1978) but a large positive anomaly is present over the centre of the Canada Plain. Maximum depth calculations indicate that the top of the anomaly source could be as deep as the mantle. Few measurements of the magnetic field have been made in this region (Coles et al., 1978, Fig. 2) with no clear evidence of a corresponding magnetic anomaly. For the northern parts of Canada Basin, the magnetic anomalies are sublinear but irregular and are generally of high amplitude, similar to the pattern observed over the Alpha Ridge, whereas in the southern parts of the basin they are more subdued and may reflect the presence of a thicker sedimentary sequence there.

The Eurasia Basin sea-floor has a magnetic anomaly pattern that is approximately symmetric with respect to the Nansen-Gakkel Ridge and is similar to that observed about mid-oceanic ridges associated with actively accreting plate margins (Coles et al., 1978). The ridge is seismically active (Plate 2). Fault plane solutions (Sykes, 1967) indicate that the seismicity is mainly produced by normal faulting. Surface seismic waves and heat flow values measured from the ridge are similar in character to measurements of these parameters at active spreading centres. Nansen-Gakkel Ridge is therefore considered to be an axis of active sea-floor spreading and Eurasia Basin the result of sea-floor accretion along this ridge over the last 63 Ma (Pitman and Talwani, 1972) or possibly the last 95 Ma (Sclater et al., 1977).

Several geophysical aspects of the Nansen-Gakkel Ridge, however, are not similar to those measured over other active spreading centres. There are the reduced magnetic anomaly amplitudes over the ridge, the absence, in places, of a prominent axial magnetic anomaly (Coles et al., 1978), and the greatly reduced scatter of seismic epicentres in Eurasia Basin relative to that observed in, for example, the North Atlantic (Plate 2). These characteristics are generally thought to be a consequence of low spreading rates (about 1.0 cm/a total) for the ridge (Coles et al., 1978; Vogt et al., 1978). Nansen-Gakkel Ridge may, in fact, have been only intermittently active (Karasik, 1973) during the Cenozoic and parts of the ridge may be presently inactive. The latter could be true for areas (for example, between 84°30'N and 86°30'N) in which the ridge exhibits a very reduced axial magnetic anomaly (Coles et al., 1978, Fig. 4) and

relatively reduced seismicity (Wetmiller and Forsyth, 1978; Plate 2).

The Nansen-Gakkel Ridge is less than 200 km wide, and is composed of a series of narrow ridges and troughs of high relief with a central rift which is over 5100 m deep in places (Sobczak and Sweeney, 1978). These bathymetric characteristics also are indicative of slow spreading rates (Rona, 1971), but the ridge has a modest average relief of 300 m to 500 m above the surrounding abyssal plains which does not provide the expected topographic profile associated with an active spreading centre (Sclater et al., 1971). There is, however, insufficient data to obtain a sediment-corrected profile for the ridge. The ridge apparently protrudes through the 2 km to 5 km thick sedimentary cover in the adjacent deep basins, and has a discontinuous veneer of sediment no more than 300 m to 400 m thick (Rassokho et al., 1967; Demenitskaya and Hunkins, 1970; Gramberg and Kulakov, 1975; Ostenso and Wold, 1977).

The Lomonosov Ridge rises sharply about 3 km above the adjacent abyssal plains (Plate 1). It is close to 200 km wide where it approaches the North American and Eurasian polar continental shelves but narrows to about 20 km at its midpoint close to the North Pole where the ridge appears to be dextrally displaced by about 80 km. Its relatively flat top and the steepness of its flanks indicate that it may be a fault block (Dietz and Shumway, 1961) rather than a volcanically constructed or an otherwise thermally generated feature. Several lines of geophysical evidence are consistent with this idea. The low amplitude of magnetic anomalies over much of the Lomonosov Ridge (Coles et al., 1978, Fig. 6) suggests either a weakly magnetic crystalline basement or a thick sediment pile beneath the ridge crest. Seismic refraction studies (Kiselev, 1970; Gramberg and Kulakov, 1975) indicate that the ridge is composed of two main structural units: a 1.8 to 2.0 km/s surface layer up to 1.0 km thick overlying a 3.0 to 4.0 km/s layer 2.5 to 3.0 km thick. Both units appear to be stratified. Rocks of the lower unit do not possess seismic properties similar to those either of crystalline basement or of oceanic layer 2 (Kiselev, 1970). There are, in fact, no seismic studies which indicate the presence of either continental or oceanic crustal thicknesses beneath the ridge (Forsyth, 1978). Magnetotelluric soundings (DeLaurier, 1978a) are consistent with the reported seismic interpretations and show that the ridge may be composed of up to 3.7 km of conducting sediments. The heat flux associated with the ridge (63 ± 15 mWm^{-2}) is slightly higher than heat flow values (50 to 57 mWm^{-2}) obtained from other aseismic submarine ridges, including those of the Arctic Ocean (Judge and Jessop, 1978). A ridge basement composed of continental-type material could account for this greater heat production. These data indicate that the Lomonosov Ridge is a continental fragment as Ostenso (1962) and Wilson (1963) first suggested.

The Alpha Ridge is the most prominent and least understood of the Arctic submarine ridges. The ridge crest varies between 1200 m and 2000 m below sea level and can be separated into three distinct subparallel components close to the North American margin (Plate 1). Three unreversed refraction profiles over the ridge indicate that it is covered by a mean thickness of 380 m of 2.0 km/s unconsolidated sediments (Hunkins, 1961). Hall (1973), using seismic reflection records obtained over the Alpha Ridge from T-3, reported that up to 1200 m of sediments cover a mountainous 4.4 km/s to 5.5 km/s basement. The Mendeleev Ridge is much narrower and has steeper slopes than the Alpha Ridge but the two may be joined (G.L. Johnson, personal communication, 1977). Bathymetric evidence for the connection, however, is uncertain (Sobczak and Sweeney, 1978).

Although the Alpha Ridge is presently aseismic (Plate 2), its relief, when corrected for sediment cover (2850 m), is similar to that of active spreading centres in the North Pacific, southeast Indian and South Atlantic Oceans (DeLaurier, 1978b). It has been previously suggested, primarily on the basis of magnetic evidence of linear sea-floor anomalies (Vogt and Ostenso, 1970; Hall, 1970, 1973; Ostenso and Wold, 1971), that the Alpha and Mendeleev Ridges may represent a spreading centre thought to have been active until about the end of Cretaceous time (Vogt et al., 1978). However, the crest of a thermally generated spreading ridge that ceased activity at the end of the Cretaceous (65 Ma) would have subsided by about 2.5 km since that time (Sclater et al., 1971; Parker and Oldenburg, 1973) so that virtually no relief should be presently observed for the Alpha Ridge. The present relief of the ridge therefore indicates that it was not a Mesozoic spreading centre. The presence of marine fossils of Maastrichtian age near the ridge crest (Ling et al., 1973; Clark, 1973, 1975) and the presence of significant thicknesses of sediments over the ridge preclude also a Cenozoic history of spreading (DeLaurier, 1978b).

Magnetic anomalies over the Alpha Ridge are of high intensity, twice that of typical spreading ridges. Although these anomalies tend to be sublinear, there are many irregularities, especially close to the North American margin where there is little evidence of symmetry in the anomaly pattern with respect to the ridge crest (Coles et al., 1978). The magnetic anomalies over the crestal area, including an apparent axial anomaly, appear to be related to ridge topography (Vogt et al., 1978). However, this relation does not appear to hold for the ridge flanks. The high amplitude of the magnetic anomalies over the Alpha Ridge cannot be adequately explained by oceanic magnetic crustal thicknesses or by the magnetic susceptibilities typically associated with an oceanic basement (Vogt and Avery, 1974). POGO satellite data over the Alpha Ridge (Langel et al., 1975) show a long wavelength (>1000 km) intense magnetic anomaly of a type that is similar to satellite anomalies (Regan et al., 1975) found over small continental shields such as in northern Greenland, India and western Australia as well as over submarine features thought to represent continental fragments such as the Seychelles and Saya de Malha Banks (Francis and Shor, 1966) and the Broken Ridge (Francis and Raitt, 1967) in the Indian Ocean.

The free-air gravity anomalies over the Alpha and Mendeleev Ridges are somewhat more positive than those over the adjacent abyssal plains (Plate 4). The low amplitudes indicate that the positive effect of the relief of the ridges is largely compensated at depth. Hall (1970, Fig. 23), following Talwani et al. (1965), accounted for this compensation in terms of a low density root in the mantle beneath the Alpha Ridge. If reduced mantle densities are, in fact, present beneath the Alpha and Mendeleev Ridges, they could have a thermal origin. But heat flow values (50 ± 7 mWm^{-2}, Judge and Jessop, 1978) measured on Alpha Ridge do not suggest elevated temperatures at present. Furthermore, elevated temperatures would likely produce a thin magnetic crust and this would be difficult to reconcile with the POGO satellite data (Coles et al., 1978). It is, however, conceivable that the reduced densities result from phases no longer in equilibrium, but remaining from an earlier high temperature regime. The Alpha and Mendeleev Ridges were not accreting margins, but the available data do not settle the question of what the ridges do represent. They may well be broad deposits of volcanic material that extruded upon the Amerasia Basin sea-floor in pre-Tertiary time, but the ridges could also represent a zone of buckled sea-floor, or a fossil subduction zone as Herron et al. (1974) have suggested. The possibility that the Alpha and Mendeleev Ridges could be continental fragments, however, cannot be discounted. In this case, a thermal regime to explain reduced densities is no longer required.

THE PAST

Carey (1955) suggested the opening of the Arctic Basin in post-Paleozoic time by a rotation of Alaska and Eurasia away from North America. Nowadays, this would imply sea-floor spreading in the Arctic Basin from an axis parallel to the North American margin. Others have rotated only Alaska during the Jurassic, and have confined the opening to the Canada Basin (Tailleur, 1969, 1973; Freeland and Dietz, 1973). Herron et al. (1974) inferred movement of the Kolyma block from eastern Asia into, and later out of, the region now comprising the Amerasia Basin, with associated spreading in the later stages about an axis parallel to the Canadian continental shelf, in pre-Laramide time. Herron et al. (1974) suggested that linear magnetic anomalies in the basin are absent because the spreading occurred during the Jurassic magnetic quiet interval (180 Ma to 150 Ma). Yorath and Norris (1975) also supported spreading parallel to the Canadian margin and contended that some of the magnetic profiles of King et al. (1966) indicated appropriately oriented linear magnetic anomalies in the Canada Basin. Correlations between fairly widely spaced profiles, however, can almost always be obtained. No unequivocal magnetic evidence for sea-floor spreading has been found in the southern Canada Basin.

The central theme for Amerasia Basin evolution presented here is the rotation of northern Alaska. Paleomagnetic evidence indicates a 70° anticlockwise rotation of an Arctic-Alaska plate, in post-Devonian time (Newman et al., 1977). The continuity of geologic structures between Alaska and the Chukotsk Peninsula of northeastern Siberia (Churkin, 1973; Patton and Tailleur, 1977) requires that this latter region be part of the Arctic-Alaska plate (Sweeney et al., 1978, Fig. 3). The paleomagnetically reconstructed relative positions of Laurentia and Eurasia from mid-Mesozoic to present time (Irving, 1977) provide timing constraints for the movements of this plate.

During Early Mesozoic time, Eurasia and Laurentia were joined in the north and the Arctic-Alaska plate occupied the site of the

present Arctic Ocean (Sweeney et al., 1978, Fig. 4). The earliest opening of the North Atlantic began in Early Cretaceous time (Laughton, 1975) about a pole assumed to be in northern Greenland (Sweeney et al., 1978), and this opening created a compressional regime between northern Eurasia and the Arctic-Alaska plate. Consequently, the Arctic-Alaska plate rotated away from Laurentia, and thereby opened the Amerasia Basin into which sediments began to accumulate. The margins of the Arctic-Alaska plate could have developed along the Franklinian foldbelt (a Devonian orogeny) and along a narrow Permian rift between present-day Greenland and Eurasia which later became a Triassic zone of shear (Irving, 1977). Although minor rotation of the Arctic-Alaska plate during Triassic and Jurassic time cannot be excluded, the major rotation is believed to have occurred during Early Cretaceous time. The occurrence of sedimentary deposits of Late Cretaceous age within Amerasia Basin (Collins and Robinson, 1967, reported by Churkin, 1973; Ling et al., 1973; Clark, 1975) and the proximity of northern Laurentia to eastern Eurasia during mid-Cretaceous (~100 Ma) time (Sweeney et al., 1978) require that the rotation of the Arctic-Alaska plate be completed by this time. The rotation pole for the latter plate may have been located in the northern Yukon region. The Alpha and Mendeleev Ridges could have formed during the rotation of the Arctic-Alaska plate. Their nature, however, is not limited by this evolutionary model nor can it be determined from existing information; a subduction zone (Herron et al., 1974), or sea-floor buckling, or volcanic accumulations, or continental fragments, are possibilities for future consideration.

In Early Tertiary time the rotation pole for the opening of the North Atlantic shifted into northeastern Siberia (Pitman and Talwani, 1972). As a consequence, the Lomonosov Ridge was rifted from the Eurasian polar continental shelf as a new accreting margin developed (Wilson, 1963). The Nansen-Gakkel Ridge is the recent location of this accreting margin in the Arctic Basin.

REFERENCES

Basham, P.W., D.A. Forsyth and R.J. Wetmiller, 1977. Sesimicity of northern Canada. Can. J. Earth Sci., 14, 1646-1667.

Bhattacharyya, B.K., 1968. Analysis of aeromagnetic data over the Arctic Islands and continental shelf of Canada. Geol. Survey Can. Paper 68-44, 14 p.

Carey, S.W., 1955. The orocline concept in geotectonics. R. Soc. Tasmania Papers and Proc., 89, 255-288.

Churkin, M. Jr., 1969. Paleozoic tectonic history of the Arctic Basin north of Alaska. Science, 165, 549-555.

Churkin, M. Jr., 1973. Geologic concepts of Arctic Ocean basin. in: Arctic Geology, ed. M.G. Pitcher, Am. Assoc. Petrol. Geol. Mem. 19, 485-499.

Clark, D.L., 1973. Arctic Ocean studies progress. Oil and Gas J., 71, 104-106.

Clark, D.L., 1975. Geological history of the Arctic Ocean basin. in: Canada's Continental Margins, eds. C.J. Yorath, E.R. Parker and D.J. Galss, Can. Soc. Petrol. Geol. Mem. 4, 501-524.

Coles, R.L., W. Hannaford and G.V. Haines, 1978. Magnetic anomalies and the evolution of the Arctic. in: Arctic Geophysical Review, ed. J.F. Sweeney, Pub. Earth Phys. Br. (this volume).

Collins, F.R., and F.M. Robinson, 1967. Subsurface stratigraphic, structural and economic geology, northern Alaska. U.S. Geol. Survey Open File Rept., 252 p.

Crary, A.P., and N. Goldstein, 1957. Geophysical studies in the Arctic Ocean. Deep-Sea Res., 4, 185-201.

DeLaurier, J.M., 1978a. Arctic Ocean sediment thicknesses and upper mantle temperatures from magnetotelluric soundings. in: Arctic Geophysical Review, ed. J.F. Sweeney, Pub. Earth Phys. Br. (this volume).

DeLaurier, J.M., 1978b. The Alpha Ridge is not a spreading centre. in: Arctic Geophysical Review, ed. J.F. Sweeney, Pub. Earth Phys. Br. (this volume).

Demenitskaya, R.M., and K.L. Hunkins, 1970. Shape and structure of the Arctic Ocean. in: The Sea, v.4, Part II, ed. Arthur E. Maxwell, Wiley-Interscience, New York, 223-249.

Dietz, R.S., and G. Shumway, 1961. Arctic Basin geomorphology. Geol. Soc. Am. Bull., 72, 1319-1330.

Forsyth, D.A., 1978. Review of Arctic crustal studies. in: Arctic Geophysical Review, ed. J.F. Sweeney, Pub. Earth Phys. Br. (this volume).

Francis, T.J.G., and R.W. Raitt, 1967. Seismic refraction measurements in the southern Indian Ocean. J. Geophys. Res., 72, 3015-3041.

Francis, T.J.G., and G.G. Shor Jr., 1966. Seismic refraction measurements in the northeast Indian Ocean. J. Geophys. Res., 71, 427-449.

Freeland, G.L., and R.S. Dietz, 1973. Rotation history of Alaskan tectonic blocks. Tectonophysics, 18, 379-389.

Gramberg, I.S., and Yu. N. Kulakov, 1975. General geological features and possible oil and gas provinces of the Arctic Basin. in: Canada's Continental Margins, eds. C.J. Yorath, E.R. Parker and D.J. Glass, Can. Soc. Petrol. Geol. Mem. 4, 525-529.

Hall, J.K., 1970. Arctic Ocean geophysical studies: The Alpha Cordillera and Mendeleyev Ridge. CU-2-70, Lamont-Doherty Geol. Obs., Palisades, New York, Tech. Rept. 2, 125 p.

Hall, J.K., 1973. Geophysical evidence for ancient sea-floor spreading from Alpha Cordillera and Mendeleyev Ridge. in: Arctic Geology, ed. M.G. Pitcher, Am. Assoc. Petrol. Geol. Mem. 19, 542-561.

Herron, E.M., J.F. Dewey and W.C. Pitman III, 1974. Plate tectonics model for evolution of the Arctic. Geology, 2, 377-380.

Hunkins, K.L., 1961. Seismic studies of the Arctic Ocean floor. in: Geology of the Arctic, v.1, ed. G.O. Raasch, Univ. of Toronto Press, Toronto, 645-665.

Hunkins, K.L., 1965. The Arctic continental shelf north of Alaska. in: Continental Margins and Island Arcs, ed. W.H. Poole, Geol. Survey Can. Paper 66-15, 196-205.

Irving, E., 1977. Drift of the major continental blocks since the Devonian. Nature, 270, 304-309.

Judge, A., and A. Jessop, 1978. Heat flow north of 60°N. in: Arctic Geophysical Review, ed. J.F. Sweeney, Pub. Earth Phys. Br. (this volume).

Karasik, A.M., 1973. Anomalous magnetic field of the Eurasian Basin of the Arctic Ocean. Dokl. Akad. Nauk. SSSR, 211, 86-89 (in Russian).

King, E.R., I. Zietz and L.R. Alldredge, 1966. Magnetic data on the structure of the central Arctic region. Geol. Soc. Am. Bull., 77, 619-646.

Kiselev, Yu. G., 1970. Some of the features of the present morphotectonic structure of the Lomonosov Ridge based on seismic data. Morskaya Geol. i Geofiz., 1, 123-128 (in Russian).

Kutschale, H.W., 1966. Arctic Ocean geophysical studies - the southern half of the Siberian basin. Geophysics, 31, 682-710.

Langel, R.A., S.J. Bensusen, R.D. Regan, W.M. Davis and J.C. Cain, 1975. High latitude magnetic anomaly maps (abs)., EOS, Trans. Am. Geophys. Union, 56, 356.

Laughton, A.S., 1975. Tectonic evolution of the northeast Atlantic Ocean; a review. Norges Geol. Unders., 316, 169-193.

Ling, H.Y., L.M. McPherson and D.L. Clark, 1973. Late Cretaceous (Maestrichtian?) silicoflagellates from the Alpha Cordillera of the Arctic Ocean. Science, 180, 1360-1361.

Newman, G.W., C.G. Mull and N.D. Watkins, 1977. Northern Alaska paleomagnetism, plate rotation, and tectonics (abs). Alaska Geol. Soc. Symposium, Anchorage, Alaska, 16-19.

Ostenso, N.A., 1962. Geophysical investigations of the Arctic Ocean basin. Geophys. and Polar Res. Center, Res. Rept. 4, Univ. of Wis., Madison, 124 p.

Ostenso, N.A., and R.J. Wold, 1971. Aeromagnetic survey of the Arctic Ocean: Techniques and interpretations. Marine Geophys. Res., 1, 178-219.

Ostenso, N.A., and R.J. Wold, 1977. A seismic and gravity profile across the Arctic Ocean basin. Tectonophysics, 37, 1-24.

Parker, R.L., and D.W. Oldenburg, 1973. Thermal model of ocean ridges, Nature Phys. Sci., 242, 137-139.

Patton, W.W. Jr., and I.L. Tailleur, 1977. Evidence in the Bering Strait region for differential movement between North America and Eurasia. Geol. Soc. Am. Bull., 88, 1298-1304.

Pitman, W.C. III, and M. Talwani, 1972. Sea-floor spreading in the North Atlantic. Geol. Soc. Am. Bull., 83, 619-646.

Rassokho, I.I., L.I. Sechura, R.M. Demenitskaya, A.M. Karasik, Yu. G. Kiselev and N.K. Timoshenko, 1967. The Central Submarine Arctic Ridge and its place in the ridge system of the Arctic Ocean. Dokl. Akad. Nauk. SSSR, 172, 659-662 (in Russian).

Regan, R.D., J.C. Cain and W.M. Davis, 1975. A global magnetic anomaly map. J. Geophys. Res., 80, 794-802.

Rona, P.A., 1971. Depth distribution in ocean basins and plate tectonics. Nature, 231, 179-180.

Sclater, J.G., R.N. Anderson and M.L. Bell, 1971. Elevation of ridges and the evolution of the central eastern Pacific. J. Geophys. Res., 76, 7888-7915.

Sclater, J.G., S. Hellinger and C. Tapscott, 1977. The paleobathymetry of the Atlantic Ocean from the Jurassic to the present. J. Geol., 85, 509-552.

Shaver, R., and K. Hunkins, 1964. Arctic Ocean geophysical studies: Chukchi Cap and Chukchi Abyssal Plain. Deep-Sea Res., 11, 905-916.

Sobczak, L.W., 1975. Gravity anomalies and passive continental margins, Canada and Norway. in: Canada's Continental Margins, eds. C.J. Yorath, E.R. Parker and D.J. Glass, Can. Soc. Petrol. Geol. Mem. 4, 743-761.

Sobczak, L.W., 1978. Gravity From 60°N to the North Pole. in: Arctic Geophysical Review, ed. J.F. Sweeney, Pub. Earth Phys. Br. (this volume).

Sobczak, L.W., and J.F. Sweeney, 1978. Bathymetry of the Arctic Ocean. in: Arctic Geophysical Review, ed. J.F. Sweeney, Pub. Earth Phys. Br. (this volume).

Sweeney, J.F., E. Irving and J.W. Geuer, 1978. Evolution of the Arctic Basin. in: Arctic Geophysical Review, ed. J.F. Sweeney, Pub. Earth Phys. Br. (this volume).

Sykes, L.R., 1967. Mechanism of earthquakes and nature of faulting on the mid-oceanic ridges. J. Geophys. Res., 72, 2131-2153.

Tailleur, I.L., 1969. Rifting speculation on the geology of Alaska's North Slope, Pt. II. Oil and Gas J., Sept. 29, 128-130.

Tailleur, I.L., 1973. Probable rift origin of Canada Basin, Arctic Ocean. in: Arctic Geology, ed. M.G. Pitcher, Am. Assoc. Petrol. Geol. Mem. 19, 526-535.

Talwani, M., X. LePichon and M. Ewing, 1965. Crustal structure of the mid-oceanic ridges, 2. Computed model from gravity and seismic refraction data. J. Geophys. Res., 70, 341-352.

Vogt, P.R., and O.E. Avery, 1974. Tectonic history of the Arctic basins: Partial solutions and unsolved mysteries. in: Marine Geology and Oceanography of the Arctic Seas, ed. Y. Hermon, Springer-Verlag, New York, 83-117.

Vogt, P.R., and N.A. Ostenso, 1970. Magnetic and gravity profiles across the Alpha Cordillera and their relation to Arctic sea-floor spreading. J. Geophys. Res., 75, 4925-4937.

Vogt, P.R., P.T. Taylor, L.C. Kovacs and G.L. Johnson, 1978. Detailed aeromagnetic investigation of the Arctic Basin. J. Geophys. Res. (in press).

Wetmiller, R.J., and D.A. Forsyth, 1978. Seismicity of the Arctic, 1908 - 1975. in: Arctic Geophysical Review, ed. J.F. Sweeney, Pub. Earth Phys. Br. (this volume).

Wilson, J. Tuzo, 1963. Hypothesis of the Earth's behaviour. Nature, 198, 925-929.

Yorath, C.J., and D.K. Norris, 1975. The tectonic development of the southern Beaufort Sea and its relationship to the origin of the Arctic Ocean basin. in: Canada's Contiental Margins, eds. C.J. Yorath, E.R. Parker and D.J. Glass, Can. Soc. Petrol. Geol. Mem. 4, 589-611.